INHIBITION OF TUMOURIGENICITY OF SMALL CELL LUNG CANCER BY SIMULTANEOUS SUPPRESSION OF ID1 AND ID3 EXPRESSION

THESIS SUBMITTED IN ACCORDANCE WITH THE REQUIREMENT OF THE UNIVERSITY OF LIVERPOOL FOR THE DEGREE OF DOCTOR IN PHILOSOPHY

BY

DANQING CHEN

JUNE 2014

To my Mother and Father

Learn from yesterday, live for today, hope for tomorrow. The important thing is not to stop questioning.

Albert Einstein

Inhibition of Tumourigenicity of Small Cell Lung Cancer by Simultaneous Suppression of Id1 and Id3 Expression

Danqing Chen

ABSTRACT

Inhibitor of DNA binding (Id) proteins are a group of transcription factors belonging to the basic helix-loop-helix (bHLH) family and play a wide range of roles in differentiation, proliferation and cell cycle progression. Id proteins act as negative dominant regulators of other bHLH factors by making dimers to these factors to prevent them from binding to E-box of DNA and, hence, to inhibit transcription of target genes.

In this work, we first established SCLC cell line N417-derived sublines expressing reduced levels of Id1 and Id3 by transfection of a single vector constructed to co-express two shRNAs simultaneously. Then we investigated the effect of either singly or jointly suppressed Id1 or Id3 on tumourigenicity of SCLC cells *in vitro* and *in vivo*. The molecular mechanisms involved in the functional roles of Id1 and Id3 were also assessed. Id1-suppressed cells and Id1 and Id3 double knockdown cells produced significant reductions in proliferation rate by more than 1.4- and 3.9-fold respectively when compared with the control. Soft agar assay showed the number of colonies produced by Id1-suppressed cells and Id1 and Id3 double knockdown cells were reduced by more than 13.7- and 233-fold respectively compared with the control. The suppression effect was also observed in the invasion assay which showed that Id1-suppressed cells and Id1 and Id3 double knockdown cells produced more than 1.7- and 4.6- fold reduction respectively in relative invasiveness. When tested in nude mouse, the average volume of tumours produced in the Id1-suppressed and Id1 and Id3 double knockdown groups was significantly reduced by 5- and 8.2-fold respectively. A similar reduction was observed by directly weighing the resected tumours at autopsy. The weight of tumours in the Id1-suppressed and Id1 and Id3 double knockdown groups was dramatically decreased by 4.1- and 6.8-fold respectively. The number of apoptotic cells in Id1-suppressed and Id1 and Id3 double knockdown transfectants increased by more than 1.6- and 2.5-fold respectively compared to the control. It was observed that the level of VEGF was reduced as the decreased levels of Id1 and Id3 in SCLC *in vitro* and *in vivo*. Conditioned medium

of the control strikingly promoted tube formation in the HUVEC angiogenesis assay, as well as human recombinant VEGF, with average score of 4.2 and 4.4 respectively. In contrast, N-Id1-1, N-Id1-5, N-Id1-Id3-1 and N-Id1-Id3-2 with average score of 2.6, 3.8, 1.4 and 2 respectively, significantly blocked the HUVEC cells forming branching networks.

In conclusion, suppressing both Id1 and Id3 can greatly inhibit the tumourigenicity of human SCLC cells *in vitro* and *in vivo*. The results also revealed that Id1 and Id3 may promote the malignant progression of SCLC cells through facilitating angiogenesis and suppressing apoptosis.

ACKNOWLEDGEMENTS

The present work has been conducted at the Molecular Pathology Laboratory, the University of Liverpool. I wish to thank my supervisor Professor Youqiang Ke for providing me the chance to study in this fruitful lab. I am grateful to Professor Youqiang Ke not only for his sober and careful attitude towards the scientific work, but also his warm support in the daily life and revision of the manuscript. I wish to thank Professor John Gosney for reviewing my paper.

I also sincerely appreciate all the help and assistance of Shiva Seyed Forootan throughout the work. I am so grateful to Shiva Seyed Forootan for sharing her knowledge and experience and for reviewing this manuscript. I am much obliged to Tim Dickinson, Patricia Gerard for the technical assistance. I owe deepest gratitude to Farzad Seyed Forootan, Majed Al Fari, Wassem Al-Jameel for providing a friendly working environment and keeping me optimistic. Outside the department, my warmest thanks belong to Lihui Wang, Alix Bee, Laleh Kamalian and Carol Beesley for doing their best to offer me suggestions and help me through confusion.

My special thanks go to my friend Chen Li for her accompany in Liverpool. During the last four years, she generously gave me all the advice, comfort and encouragement anyone could want. Chen Li is not only a dear friend, but also a sister to me. I wish to thank my friend Li Wen, Miao Li, Hongmiao Ren and Ola AL-Sanabra for their support that helped me through frustration.

I owe my deepest gratitude to my dear mother and father, Linning Ma and Zhiming Chen. Without your love and support, I could not possibly fulfil my dream of pursuing Phd study. My memory comes back to me the days and nights we discussed the difficulties in transfection experiment, in balancing two part-time jobs and my research progress and in searching for a proper job position. I greatly thank you for your understanding and patience. To you I dedicate this work.

ABBREVIATIONS

ACTH	Adrenocorticotropic hormone
ADD1	Adipocyte determination and differentiation factor-1
ADH	Antidiuretic hormone
Ago2	Argonaute 2
APS	Ammonium Persulfate
Apaf-1	Apoptotic protease-activating factor-1
Arnt	Aryl hydrocarbon receptor nuclear translocator
AS-C	Achaete-scute complex
Bad	BCL-2-associated death promoter
Bak	BCL-2 homologous antagonist / killer
Bax	BCL-2 homologous antagonist x
BCL-2	B-cell lymphoma 2
bFGF	Basic fibroblast growth factor
BH	BCL-2 homology
bHLH	Basic helix-loop-helix
BLP	B lymphocyte progenitor
BMP	Bone morphogenetic protein
bp	Base pair
BSA	Bovine serum albumin
bZIP	Basic-region leucine zippers
CDK2	Cyclin dependent kinase 2
CEPs	Circulating endothelial precursor cells
CHO	Chinese hamster ovary
CHOP	Cyclophosphamide, hydroxydaunorubicin, oncovin, prednisone
CT	Computed tomography
CI	Confidence interval
DAB	3, 3’ diaminobenzidine tetrahydrochlorate
DNA	Deoxyribonucleic acid
DMSO	Dimethyl sulphoxide
dsRNA	Double-stranded RNA
EBPβ	Enhancer-binding protein β
ECL	Enhanced chemiluminescence
ECM	Extracellular matrix
ED-SCLC	Extensive stage small cell lung cancer
EDTA	Ethylenediaminetetraacetic acid
EGF	Epidermal growth factor
EGFR	Epidermal growth factor receptor
EGR1	Early growth response gene 1
ELISA	Enzyme-linked immunosorbent assay
emc	Extramacrochaetae
EORTC	European organisation for research and treatment of cancer
EP	Etoposide
ERK	Extracellular signal-regulated kinases
EWS	Ewing sarcomas
FCS	Fetal calf serum
FHIT	Fragile histidine triad

GRP	Gastrin-releasing peptide
Gy	Gray, a derived unit of ionizing radiation dose
h-ASH-1	Human achaete-scute homolog-1
Hes1	Hairy enhancer of split 1
HGF	Hepatocyte growth factor
HGFR	Hepatocyte growth factor receptor
HH	Hedgehog
HIF-1α	Hypoxia-inducible factor-1α
HSP-90	Heat shock protein-90
HUVEC	Human umbilical vein endothelial cell
Id	Inhibitor of DNA binding/differentiation
IGF-1R	Insulin-like growth factor 1 receptor
IgH	Immunoglobulin heavy chain
IHC	Immunohistochemistry
INT1	Integration 1, the vertebrate homologue
IPGT	Isopropyl β-D-1-thiogalactopyranoside
kDa	Kilodalton
LB	Luria-Bertani
LRP	Low density lipoprotein receptor-related protein
LS-SCLC	Limited stage small cell lung cancer
MAPK	Mitogen activated protein kinase
MDD	Microquantity differential display
MIDA1	Mouse Id Associate 1
MITF	Microphthalmia transcription factor
MMP	Matrix metalloproteinase
MRI	Magnetic resonance imaging
mRNA	Messenger ribonucleic acid
mTOR	Mammalian target of rapamycin
MTS	(3-(4,5-dimethylthiazol-2-yl)-5-(3-carboxymethoxyphenyl)-2-(4-sulfophenyl)-2H-tetrazolium
MTT	Dimethylthiahiazo (-z-y1)-3, 5-di- phenytetrazoliumromide
Myc	Myelocytomatosis oncogene
NCAM	Neural cell adhesion molecule
NPC	Nasopharyngeal carcinoma
NSCLC	Non-small cell lung cancer
NSE	Neuron-specific enolase
PAI	Plasminogen activator inhibitor
PBS	Phosphate buffered saline
PCI	Prophylactic cranial irradiation
PDGF	Platelet derived growth factor
PET	Positron emission tomography
PI3K	Phosphatidylinositol-3-kinase
RAR β	Retinoic acid receptor β
RB	Retinoblastoma
RISC	RNA-inducing silencing complex
RNAi	RNA interference
ROS	Reactive oxygen species
RTK	Receptor tyrosine kinase
SBE	SMAD-binding element

SCF	Stem cell factor
SCL	Stem cell leukeamia
SCLC	Small cell lung cancer
SD	Standard deviation
shRNA	Small hairpin RNA
SIADH	Syndrome of inappropriate antidiuretic hormone secretion
siRNA	Small interfering RNA
SMAD	Mothers against decapentaplegic homolog
SOB	Super optimal broth
SOC	Super optimal broth plus glucose
TBE	Tris/borate/EDTA
TBST	Tris-buffered saline and tween 20
TCF	Ternary complex factor
TEMED	Tetramethylethylenediamine
TFE	Transcription factor E
TGF-α	Transforming growth factor-α
TGF-β	Transforming growth factor β
TNFα	Tumour necrosis factor α
TNM	Tumour node metastasis
TRAIL	TNF-related apoptosis-inducing ligand
TRAP	Telomeric repeat amplification protocol
TRT	Thoracic radiotherapy
VEGF	Vascular endothelial growth factor
WHO	World health organisation

LIST OF FIGURES

Chapter 1

Figure 1.1. Age-adjusted annual worldwide cancer incidence rates and mortality rates by cancer patterns/sex
Figure 1.2. Lung cancer incidence rate by sex, 1973-2008
Figure 1.3. Lung cancer, world age-standardised incidence rates
Figure 1.4. The diagnosis of SCLC by sex, 1973-2000
Figure 1.5. High-power view of a surgically resected small-cell lung cancer
Figure 1.6. Cell fate mediation by Id proteins

Chapter 2

Figure 2.1. RNA Interference mechanism
Figure 2.2. Nucleotide sequences of three siRNAs against Id1
Figure 2.3. Plasmid map of psiRNA-DUO

Chapter 3

Figure 3.1. Effect of knockdown Id1 by transient transfection of three siRNAs
Figure 3.2. Agarose gel electrophoresis of restriction enzymes digestion of plasmid DNA
Figure 3.3. Sequencing analysis confirmed insertion of siRNA.
Figure 3.4. Knockdown effect of stable transfection of shRNAs targeting either Id1 and Id3 or Id1 alone on levels of Id1 and Id3 or on that of Id1 expressed in N417 cells
Figure 3.5. The inhibition of the invasiveness in sh-Id1 and sh-Id1-Id3 sublines was determined by Boyden chamber assay
Figure 3.6. MTS standard curve for N417 cells
Figure 3.7. Proliferation assay of different transfected cells
Figure 3.8. Photographs of stained soft agar wells
Figure 3.9. Number of colonies produced by different transfected cells in soft agar
Figure 3.10. Testing tumorigenicity of different transfectant cells in nude mouse
Figure 3.11. The average tumour volume of different groups of nude mice
Figure 3.12. The average tumour weight of different groups of nude mice
Figure 3.13. Immunohistochemistry analysis of the expression status of Id1, Id3, VEGF and CD34 in tumours produced in mice
Figure 3.14. The numbers of microvessel in xenograft tumours produced by transfectants
Figure 3.15. Titration of cisplatin on induction of apoptosis of transfected cells
Figure 3.16. Expression level of VEGF in transfected cells
Figure 3.17. The standard curve of VEGF ELISA analysis
Figure 3.18. VEGF protein levels in conditioned medium of transfected cells
Figure 3.19. Measurement of biological activity of VEGF produced by different transfectant cells
Figure 3.20. Scoring network formation produced by different conditioned media

LIST OF TABLES

Chapter 1
Table 1.1. Frequency of presenting symptoms in SCLC
Table 1.2. Classification of bHLH proteins according to Murre *et al*
Table 1.3. Classification of bHLH proteins according to Atchley *et al*

Chapter 3
Table 3.1. Summary of cell count after 48 hours of invasion assay with transfected cells
Table 3.2. Summary of final cell count of MTS proliferation assay with transfected cells
Table 3.3. Summary of number of colonies formed by different cells in soft agar assay
Table 3.4. Summary of the average tumour volume calculated for each group of animals on the day 9, 12, 15 and 18
Table 3.5. Summary of the average tumour volume calculated for each group of animals on the day 21
Table 3.6. Summary of the average tumour weight of each group of nude mice on day 21
Table 3.7. Id1 protein expression levels in mice xenograft tumours which inoculated with Id1 shRNA, Id1 and Id3 shRNA or scramble RNA transfected cells.
Table 3.8. Id3 protein expression levels in mice xenograft tumours which inoculated with Id1 and Id3 shRNA or scramble RNA transfected cells.
Table 3.9. VEGF protein expression levels in mice xenograft tumours which inoculated with Id1 shRNA, Id1 and Id3 shRNA or scramble RNA transfected cells.
Table 3.10. Summary of the average apoptosis rate of transfected cells

TABLE OF CONTENTS

ABSTRACT I
ACKNOWLEDGEMENTS III
ABBREVIATIONS IV
LIST OF FIGURES VII
LIST OF TABLES VIII
TABLE OF CONTENTS IX
CHAPTER 1 INTRODUCTION 2
1.1. Small cell lung cancer 2
1.1.1. Overview 2
1.1.2. Epidemiology 3
1.1.3. Etiology 6
1.1.3.1. Smoking 7
1.1.3.2. Radon exposure 7
1.1.3.3. Asbestos 7
1.1.4. Molecular pathogenesis 8
1.1.4.1. Tumour suppressor genes 8
1.1.4.1.1. TP53 gene 8
1.1.4.1.2. Retinoblastoma (RB) gene 10
1.1.4.1.3. Intracellular Molecular Chaperones 11
1.1.4.2. Nonreceptor Oncogenes 12
1.1.4.2.1. BCL-2 12
1.1.4.2.2. MYC oncogenes 14
1.1.4.3. Receptor Tyrosine Kinases and Growth Factors 15
1.1.4.3.1. c-MET 15
1.1.4.3.2. c-KIT 16
1.1.4.3.3. Vascular endothelial growth factor (VEGF) and basic fibroblast growth factor (bFGF) 17
1.1.4.3.4. Insulin-like growth factor-1 receptor 20
1.1.4.3.5. Epidermal growth factor receptor (EGFR) 21
1.1.4.3.6. GRP 22
1.1.4.3.7. Matrix metalloproteinase (MMP) 23
1.1.4.4. Cell Surface Markers 24
1.1.4.4.1. NCAM (CD56) 24
1.1.4.4.2. Gangliosides 25
1.1.4.5. Chromosomal alterations 26
1.1.4.5.1. Chromosomal alterations 26
1.1.4.5.2. Telomerase 28
1.1.4.6. Signalling pathways 29
1.1.4.6.1. Phosphoinositide 3-kinase/AKT/mTOR 29
1.1.4.6.2. Hedgehog 31
1.1.4.6.3. Notch pathway 32
1.1.4.6.4. WNT 34
1.1.5. Clinical diagnosis 35
1.1.6. Staging 39
1.1.7. Prognosis 40
1.1.8. Treatment 41
1.1.8.1. Limited stage disease 41
1.1.8.2. Extensive stage disease 43

1.1.8.3. Progressive or relapsing disease 46
1.1.9 New Agents 47
1.1.9.1. Paclitaxel 47
1.1.9.2. Topoisomerase I inhibitors 48
1.1.9.3. Gemcitabine and vinorelbine 49
1.2. Id family protein 50
1.2.1. bHLH Family Introduction 50
1.2.1.1. Classifications of bHLH proteins 51
1.2.1.2. The structure of bHLH protein 56
1.2.1.2.1. The basic domain: E-box binding sites 56
1.2.1.2.2. The HLH domain 57
1.2.1.3. The function of bHLH protein 57
1.2.2. Id protein 58
1.2.2.1. Introduction 58
1.2.2.2. Structure of Id 59
1.2.2.3. Function of Id protein in biological conditions 61
1.2.2.3.1. Id proteins in differentiation, proliferation and cell-cycle control 61
1.2.2.3.2. Id proteins in developmental biology 64
1.2.2.3.2.1. *Drosophila* 64
1.2.2.3.2.2. Zebrafish 64
1.2.2.3.2.3. *Xenopus* 65
1.2.2.3.2.4. Mouse 65
1.2.2.3.3. Id proteins and apoptosis 66
1.2.2.3.4. Id proteins in angiogenesis 66
1.2.2.3.5. Id proteins in invasiveness 67
1.2.2.3.6. Id proteins in tumour biology 68
1.2.2.4. Mechanism of action of Id proteins 70
1.2.2.4.1. Id-bHLH protein interaction 70
1.2.2.4.2. Interactions with non-bHLH proteins 71
1.2.2.4.3. Regulation of Id expression and function 72
1.2.2.4.4. Promoter of Id 72
1.2.2.4.5. Signalling pathways in regulation of Id 73
1.2.2.4.5.1. TGFβ signalling pathway 73
1.2.2.4.5.2. MAPK/ERK pathway 75
1.2.2.4.6. Modification and degradation of Id 77
1.2.2.4.7. Dimerisation and localisation 78
1.2.3. Id and SCLC 78
1.2.4. Summary and Hypothesis 79
1.2.4.1. Summary 79
1.2.4.2. Hypothesis and objectives 80
CHAPTER 2 METHODS AND MATERIALS 83
2.1. Cell culture 83
2.1.1 Initiate cell culture from frozen stock 83
2.1.2 Subculture of suspension cells 84
2.1.3. Subculture of adherent cells 84
2.1.4. Cryopreservation of cells 85
2.2. RNAi technology 86
2.2.1. RNAi Overview 86
2.2.2 Transient transfection 87
2.2.2.1 siRNA design 87
2.2.2.2 Obtain mRNA sequence of target gene 88
2.2.2.3 siRNA delivery 89
2.2.2.4 Optimizing conditions of transient transfection 89
2.2.2.5 Transient transfection of Id1 90

2.3. Stable transfection 93
2.3.1. Design of shRNA 93
2.3.2. Vector 94
2.3.3. Making competent *E.coli* GT115 96
2.3.4. Construction of the vector expressing siRNA 97
2.3.4.1. Annealing the hairpin siRNA template oligonucleotide 97
2.3.4.2. Digestion of plasmid DNA 98
2.3.4.2.1. First step digestion to insert Id1 siRNA 98
2.3.4.2.2. Second step digestion to insert Id3 siRNA 100
2.3.4.3. Ligation reaction 100
2.3.4.4. Bacterial transformation 101
2.3.4.5. Confirmation of the presence of siRNAs 103
2.3.4.5.1. Agarose gel electrophoresis 104
2.3.4.5.2. Sequencing of the siRNA insert 105
2.3.5. Transfecting mammalian cells 106
2.3.5.1. General considerations before transfection 106
2.3.5.2. Transfection Procedure (To optimize the condition) 107
2.3.5.3. Optimisation of antibiotic-resistant selection 108
2.3.5.4. Transfection protocol 108
2.4. Cell lysis and protein extraction 109
2.5. Western blots 111
2.5.1. SDS –PAGE gel electrophoresis 111
2.5.2. Transfer of protein samples to membrane 111
2.5.3. Antibody staining 112
2.6. Invasion assay 113
2.6.1. Overview 113
2.6.2. Procedure 113
2.6.3. Analysis method 115
2.7. MTS assay 115
2.7.1. Overview 115
2.7.2. Standard curve 115
2.7.3. Procedure 116
2.8. Soft agar assay 117
2.8.1. Overview 117
2.8.2. Procedure 117
2.9. *In vivo* tumourigenicity assay 118
2.10. Immunohistochemistry 119
2.11. Apoptosis assay 121
2.12. Angiogenesis 122
2.12.1. Immunosorbent assay for VEGF (ELISA assay) 123
2.12.1.1. Preparation of standard 123
2.12.1.2. Procedure of VEGF ELISA assay 124
2.12.2. *In vitro* angiogenesis assay (tube formation assay) 125
2.12.2.1. Procedure of *in vitro* angiogenesis assay 125
2.12.2.2. Quantitation of tube formation 126
2.13. Statistical analysis 127
CHAPTER 3 RESULTS 129
3.1. Identification of the most effective suppressor against Id1 by transient transfection 129
3.2. Establishment of clones with reduced levels of Id1 and Id3 131
3.2.1. Confirmation of siRNA inserts 131
3.2.2. Establishment of stable SCLC cell lines expressing reduced Id1 and Id3 136
3.3. Effect of knockdown of Id1 alone or Id1 and Id3 jointly on invasiveness of SCLC cells

.....140
3.4. Effect of knockdown of Id1 alone or Id1 and Id3 jointly on proliferation of SCLC cells 143
3.5. Effect of knockdown of Id1 alone or Id1 and Id3 jointly on anchorage-independent growth of SCLC cells.....147
3.6. Inhibition of Id1 and Id3 greatly suppressed the tumour growth in nude mice.....150
3.7. Expression levels of Id1, Id3 and VEGF in xenograft tumours by immunohistochemistry.....158
3.8. Effect of Id1 and Id3 suppression on sensitivity of apoptosis induction 164
3.9. Effect of Id1 and Id3 suppression on angiogenesis.....167
3.9.1. Detection of VEGF protein expression in transfectant cells and conditioned medium.....167
3.9.2. Biological activity of VEGF produced by transfectants.....172
CHAPTER 4 DISCUSSION.....176
4.1. Establishment of Id1- and Id3-doubleknockdown or Id1-suppressed clones 176
4.2. MTS assay studying the cell growth of SCLC.....180
4.3. Soft agar assay studying the tumourigenicity of SCLC *in vitro* 181
4.4. Boyden chamber assay studying the invasiveness of SCLC *in vitro*.....182
4.5. Testing the tumourigenesis of SCLC *in vivo* 183
4.6. Apoptosis and angiogenesis 185
4.7. Future work.....189
4.8. Summary and conclusion.....191
REFERENCES 194
APPENDIX I. RECIPES OF SOLUTIONS AND REAGENTS.....229
APPENDIX II. LIST OF CHEMICALS AND BIOLOGICS.....233
APPENDIX III. LIST OF EQUIPMENTS 236
APPENDIX IX. RELEVANT PUBLICATIONS.....237

CHAPTER 1
INTRODUCTION

CHAPTER 1 INTRODUCTION

1.1. Small cell lung cancer

1.1.1. Overview

Small cell lung cancer (SCLC), one distinct subtype of lung cancers, accounts for approximately 15-25% of all lung cancers (1). Squamous cell carcinoma, adenocarcinoma and large cell lung cancer are grouped together as non-small cell lung cancer (NSCLC). These two major forms of cancers of the lung are treated differently due to their different biological and clinical characteristics.

The size of SCLC cell is relative tiny and thus SCLC is also named as oat cell cancer. Most cases of SCLC occur in the larger airways located between primary and secondary bronchi (2). The occurrence of early metastases is common in SCLC cases, in which cancer cells spread widely into the secondary sites in the liver, brain, bone, and lymph nodes. Due to the inappropriate secretion of hormones such as antidiuretic hormone (SIADH) and adrenocorticotropic hormone (ACTH) by the cancer cells, SCLC is frequently associated with a variety of paraneoplastic syndromes such as hypercalcaemia, hypernatraemia, anemia, cachexia and Cushing's syndrome, etc. (3). SCLC is characterised with rapid growth, early metastases, sensitivity to chemotherapy and radiotherapy. Thus chemotherapy and radiotherapy, not surgery, are optimal choices for SCLC treatment because SCLC usually has been widely disseminated by the time it is diagnosed. SCLC almost exclusively occurs in smokers.

1.1.2. Epidemiology

The incidence of lung cancer has been rising since the 1930's. Though lung cancer is the second most common malignancy in both men and women, it is the leading cause of cancer deaths among men since 1950's and in 1987 became the leading cause among women in the US (4). An estimated 1.61 million people throughout the world were diagnosed with lung cancer in 2008, accounting for 13% of the total cases of cancer (5). More people die of lung cancer than breast, prostate cancers combined together each year (**Figure 1.1**). Lung cancer was estimated to cause 160,340 deaths in 2012, accounting for 28 percent of all cancer deaths (6). Lung cancer is strongly correlated to the age factor (7). Around two thirds of people diagnosed with lung cancer are 65 or over, no more than 2% of all patients are younger than 45 (8). The average age at the time of diagnosis for lung cancer is about 71. The rate of incidence in 2008 showed that men developed lung cancer more often than women (70.2 and 50.5 per 100,000 respectively) (9). However, the rate of lung cancer incidence over the past 33 years has decreased 22% among men, while it has risen for women (106%). The rate of new cases for men peaked (102.1 per 100,000) in 1984 and then began to decline, whereas the rate of incidences for women increased further and did not peak until 1998 (52.9 per 100,000) and began to drop after a long period of rising (**Figure 1.2**) (9). The rates of lung cancer in the younger age groups are reducing, more prominent in men than women. Globally, the lung cancer incidence rate is the highest in Europe and Northern American and lowest in parts of Africa (**Figure 1.3**).

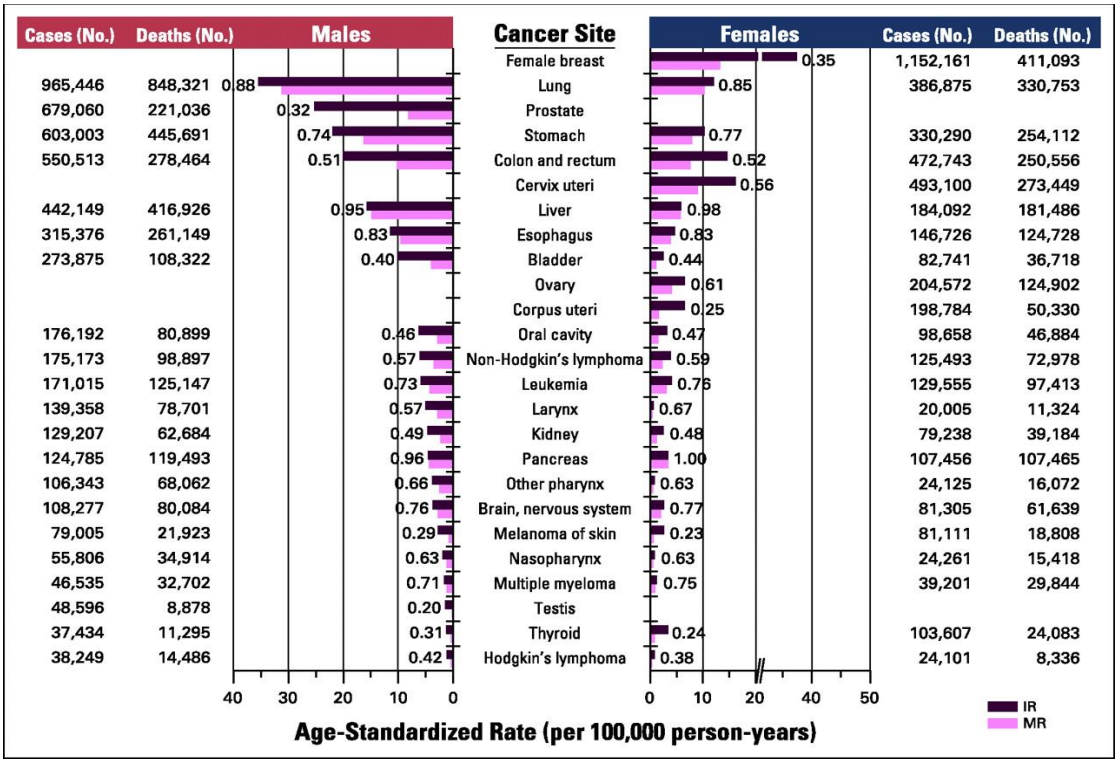

Figure 1.1. Age-Adjusted Annual Worldwide Cancer Incidence and Mortality Rates By Cancer Patterns/Sex (10).

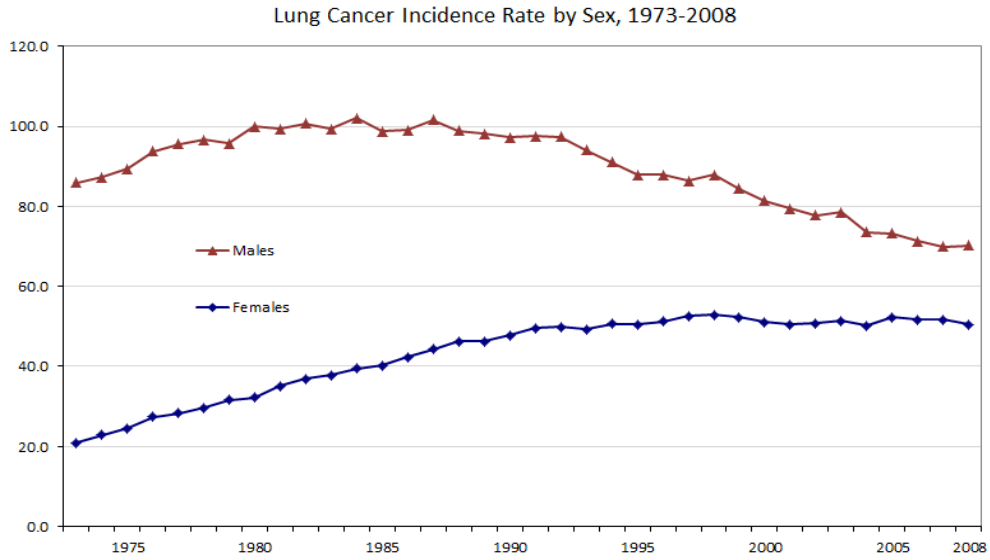

Figure 1.2. Lung Cancer Incidence Rate By Sex; 1973-2008. Source: Centres for Disease Control and Prevention. National Centre for Health Statistics.

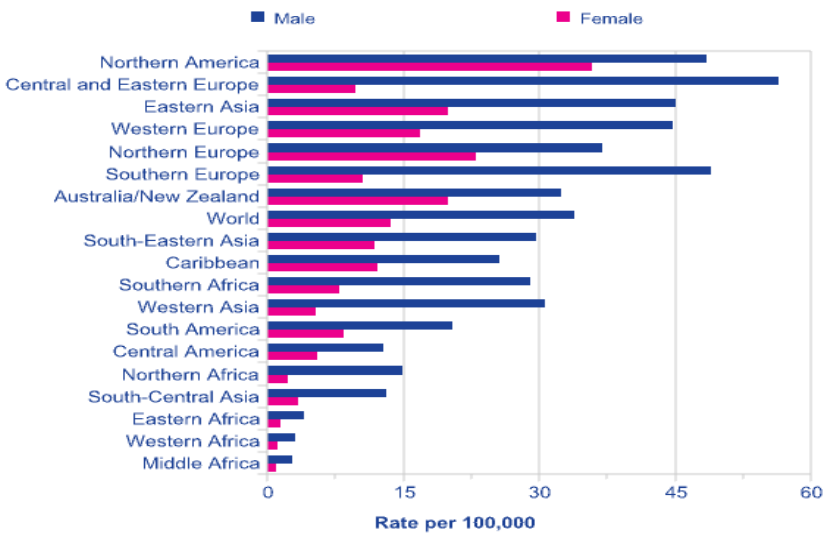

Figure 1.3. Lung Cancer, World Age-Standardised Incidence Rates, World Regions, 2008 Estimates. Sources: Cancer Research UK. Lung cancer incidence statistics

The incidence of SCLC has not been dramatically changed over the last few years. The incidence of SCLC was about 20-25% of all newly diagnosed lung cancers in the past. It currently accounts for approximately 15%. In 2002, SCLC comprised 12.95% of all lung cancers in the analysis of Surveillance, Epidemiologic, and End Results program of the National Cancer Institute (11). By 2010, 222,000 new cases of lung cancer were diagnosed, of which 16% were SCLC in the US according to the estimation of American Cancer Society. Some reports believed that the incidence of SCLC dropped recently, however one study suggested that this may be due to the change in classification (12). Same as the other histopathological types of lung cancer, most patients developed SCLC with age of 35-75 years; the peak of incidence is at around 55-65 years of age (13). An investigation to calculate the incidence of SCLC

over the past 30 years using Surveillance, Epidemiologic, and End Results database showed that although more male patients with SCLC in 1973 (72.37% of all patients with SCLC), the incidence has steadily decreased over the subsequent 20 years, and in 2002 the male to female ratio of patients with SCLC was reduced to 1 to 1 (**Figure 1.4**) (11).

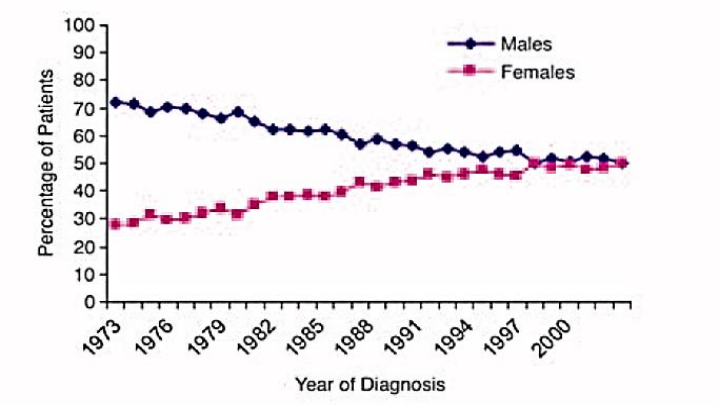

Figure 1.4. The Diagnosis of SCLC by sex, 1973-2000 (11).

In 2010 there were roughly 82,000 diagnosed incident cases of SCLC in the major regions worldwide, and approximately 100,400 diagnosed incident cases are predicted for 2020 (www.datamonitor.com). The number of incident cases of SCLC is expected to remain fairly stable throughout the forecast period.

1.1.3. Etiology

Tobacco use, radon exposure, and asbestos are known to be associated with an increased risk of SCLC.

1.1.3.1. Smoking

Tobacco smoking is the primary cause of SCLC and NSCLC. According to the data of American Cancer Society, tobacco smoking gives rise to 8 out of 10 cases of lung cancer. It is possible that this number is higher for SCLC (14). Smokers have a 20-fold increase in the risk of lung cancer compared to non-smokers, and SCLC rarely occurs in never-smokers (15). Cigar and pipe smoking have a similar risk as the tobacco smoking, and the same pattern holds true for low-tar cigarette smoking (16). Nearly 98% of SCLC patients have a smoking history. The longer of the time a patient smoked and the heavier of the smoking, the greater the risk to develop SCLC. Ceasing smoking even after the patients diagnosed with SCLC can still contribute to improved survival rates (17).

1.1.3.2. Radon exposure

Radon is an inert gas that is generated from uranium decay in soil and rocks. Radon is colourless, odourless, and tasteless. A number of degraded products of radon can cause DNA damage to the cells of respiratory epithelium. Exposed to radon has been observed with high risk of SCLC, but much lower than smoking. Cigarette smoking and radon exposure have been documented to increase risk of SCLC in a synergistic manner (18).

1.1.3.3. Asbestos

Asbestos is a well-established occupational carcinogen, which causes great health problems among the miners of asbestos. The prolonged inhalation of asbestos fibres

has been noted to increase the risk of SCLC. Like radon, asbestos and cigarette smoking are two independent cancer-leading causes, but in combination they enhance the risk of SCLC (19).

1.1.4. Molecular pathogenesis

A variety of disorders at molecular level have been observed in SCLC including activation of oncogenes, loss or inactivation of tumour-suppressor genes and autocrine growth loops, however, what remains unclear is to what extent the alterations become causative in tumourigenicity of SCLC.

1.1.4.1. Tumour suppressor genes

The retinoblastoma (RB) gene is located on chromosome 13 (13q14), and it was found that RB messenger ribonucleic acid (mRNA) cannot be detected in 60% of SCLC (20). This high frequency of inactivation of a tumour suppressor gene suggests that it may be an important step in the molecular pathogenesis of SCLC. Mutations of the TP53 tumour suppressor gene are commonly found in both SCLC and NSCLC, but their precise role in pathogenesis is not clear. Tobacco smoking and radon exposure are associated with TP53 gene mutations (21).

1.1.4.1.1. TP53 gene

TP53 gene, which located on chromosome 17 (17p13.1) in human, encodes a nuclear protein P53 which has been known as a crucial tumour suppressor in multicellular organisms. P53 plays multiple roles in maintaining genomic stability, inducing apoptosis and inhibiting proliferation and angiogenesis. TP53 gene alterations have

been frequently observed in most human cancer tissues and cell lines. Generally, wild type P53 protein only expresses in a low level in the normal tissues and cell lines, whereas mutant P53 is commonly up-regulated in cancer cells because of the prolonged half-life. Abnormal levels of P53 protein were detected in approximately 40–70% of SCLC (22).

Mutations of TP53 are suggested as a high risk factor in a wide spectrum of early-onset malignancies. The types of TP53 mutation include missense substitutions (75%), frame-shift insertions and deletions (9%), nonsense mutations (7%), silent mutations (5%) (23). Although a high rate of missense mutation in TP53 is commonly detected, other tumour suppressor genes tend to alter by truncating mutations. A study showed that G to T transversions on the non-transcribed strand was the frequent mutations in SCLC, and suggested that TP53 mutation may be related to cigarette smoking (21). Inactivation of TP53 was found in nearly 90% of SCLC, the typical missense mutations in the DNA binding domain was more liable to occur comparing to homozygous deletions (24). The difference of TP53 gene expression between normal and SCLC cells provides a mechanism basis for vaccine therapy in SCLC. A prior study showed that a vaccine composed of dendritic cells transduced with a human wild type P53 (DC-Ad-P53) can lead to antitumor response (25). The efficacy of the vaccine has undergone examination of a phase I/II clinical trial. Extensive stage SCLC patients were treated with this vaccine after completed first-line platinum based chemotherapy. The trial confirmed the vaccine was safe, and increase of objective response was observed only after salvage chemotherapy was administered. However, when similar vaccine was used to treat 29 patients who had relapsed extensive stage of SCLC, only one patient showed positive response to the vaccine therapy (26). High

rate of objective responses to chemotherapy (61.9%) followed vaccination was observed. Hence, the vaccine therapy was supposed to be used as an adjunct to chemotherapy, rather than a primary treatment. Another dendritic cell-based P53 vaccine, delivered via adenovirus vector, was evaluated in patients with extensive stage SCLC after standard platinum-etoposide chemotherapy in a phase I/II trial (27). A randomized phase II clinical trial was also underway by using this vaccine in patients with SCLC (28).

1.1.4.1.2. Retinoblastoma (RB) gene

Loss of both alleles of the Rb gene, located on chromosome 13q14.11-q14.2, would inactivate the Rb and lead to retinoblastoma cancer. Rb protein has been associated with cell cycle progression regulation. It prevents cell cycle transition from G1 (first gap phase) into S (synthesis phase) via inactivation of members of the E2F transcription factor family (29, 30). Hypophosphorylated Rb suppresses the transcription factors E2F1, E2F2 and E2F3, which are required in the G1/S transition (29). The hypophosphorylated Rb binds to the inactive form of E2F and hence stall cell cycle in the G1 phase. When cyclin D1/CDK4 complex phosphorylates Rb, E2F is capable of releasing and being activated to allow cell to enter into S phase. Phosphorylation of Rb is under the control of cyclin E and CDK2 during S phase (30, 31). However, when Rb is mutated, E2F binding fails to occur and E2F activity will lose control (23). Moreover, phosphorylated Rb also inhibits apoptosis by repressing other pro-apoptotic target genes, including apoptotic protease activating factor-1 (Apaf-1) and caspases (32).

SCLC is mostly characterized by loss of Rb expression (~90%). Small deletions of Rb

and chromosomal loss including the Rb locus account for approximately 80%-90% of changes, and other Rb mutations account for nearly 20%-30% of changes in SCLC (33). Besides the deletion and chromosomal loss, other types of mutations include nonsense mutations and splicing abnormalities (34). Drugs were developed to target cells of inactivated or deleted Rb in SCLC patients. The drugs under development include heat shock protein-90 (Hsp90) inhibitors (35).

1.1.4.1.3. Intracellular Molecular Chaperones

Heat shock protein (Hsp)-90 belongs to a highly conserved protein family of molecular chaperones, which is essential for viability in eukaryotes under all conditions. This protein was initially isolated from the cells stressed by heating, dehydration or by other means that can cause the proteins in cells to denature. This implied that heat shock proteins are able to protect cells when stressed. Molecular chaperones Hsp90 are necessary for conformational maturation of proteins, stabilization of various proteins such as steroid receptors, and protein degradation. Hsp90 has been implicated in regulation of signalling factors, assembly and disassembly of transcriptional complexes (36) and immunogenic peptide processing (37). Hsp90 protein is constitutively expressed in normal cells, whereas increased in tumour cells due to the presence of mutated and deregulated proteins, oxidative damage, hypoxia or a low nutrient environment (38). Hsp90 client proteins include a number of oncogenic proteins, such as Akt, MET, Bcl-2, telomerase, survivin and Apaf-1. Hsp90 can increase survival, growth and metastases of tumour cells by promoting protein translation and cellular proliferation (35). Hsp90 also drives signal transduction and proliferation of multiple oncogenic kinases involved in growth of

lung cancer cells, therefore Hsp90 inhibitors have been investigated as anticancer drugs. Hsp90 has been considered as a crucial inhibitor of apoptosis in SCLC, which is distinct from other cellular systems (19). Preclinical data showed that Hsp90 regulates apoptosis in SCLC by inhibiting Apaf-1 and mediating the PI3K/Akt pathway (35).

Several inhibitors of Hsp90 have entered clinical trial such as geldanamycin analogs, 17-AAG, 17-DMAG, as well as IPI-504, a reduced derivative of 17-AAG (39, 40). A pre-clinical study for 17-AAG showed that RB-dependent G1 arrest caused by Hsp90 inhibitors exerted different mechanisms driving apoptosis in Rb-containing and Rb-null cell lines. Majority of tumour cells underwent a G1 blockage, presumably due to Rb-mediated regulation when treated with the 17-AAG. In contrast, when cells lacking Rb were treated with 17-AAG, they progressed through G1 and arrested in M phase instead, where they went through immediate apoptosis (41). Other types of HSP-90 inhibitors being evaluated in early phase trials include purine scaffold inhibitors such as CNF2024, and diarylpyrazole compounds such as diarylisoxazole NVP-AUY922/ VER-52296 and SNX5422 (39).

1.1.4.2. Nonreceptor Oncogenes

1.1.4.2.1. BCL-2

Bcl-2 (B-cell lymphoma 2) is a member of protein family that regulates cell death such as apoptosis, necrosis and autophagy (42). Located on the chromosome 18, BCL-2 is one of the well-established proto-oncogenes. Members of Bcl-2 family share one or more of four conserved Bcl-2 homology (BH) domains designated BH1, BH2,

BH3, and BH4 (43). Deletion of BH domains has an impact on survival/apoptosis rates (44). The Bcl-2 family has dual functions as it is comprised of anti-apoptotic proteins (Bcl-2, Bcl-x and Mcl-x) and pro-apoptotic proteins (Bax, Bak and Bad) (45). Hence Bcl-2 family can be classified into two groups according to promoting or inhibiting apoptosis. The family can be further classified by whether they contain multiple BH domains or only BH3 domain (46). More studies are needed to fully understand the effect of structural features of these proteins on their pro- or anti-apoptotic function.

There is an 'intrinsic' pathway of apoptosis initiated by mitochondria-dependent mechanism through caspase (proteolytic enzymes) activation. Cells undergo apoptosis when they receive stimuli such as DNA damage (caused by irradiation or anticancer drugs), growth factor deprivation, and ER stress (47). Caspase activation in this pathway can be triggered by cytochrome c released from mitochondria to cytoplasm. Release of cytochrome c results in activation of initiator caspase-9 which then activates effector caspases (48). Bcl-2 exerts the anti-apoptotic effect by inhibiting the release of cytochrome c from mitochondria. Another caspase cascade is called 'extrinsic' pathway since it can be activated by interaction of death receptors (such as Fas/CD95 or TNFR-1) and the recruitment of caspase-8. The interaction of Fas ligand and its receptor leads to trimerisation and clustering of death domain, then binding to cofactor such as Fas-Associated via Death Domain (FADD) and Tumour Necrosis Factor Receptor-1-Associated Death Domain (TRADD). Fas and FADD form a complex called death inducing signalling complex (DISC), which initiates apoptosis via recruitment and cleavage of procaspase-8 (49). Nevertheless, activation of caspase-8 also requires the engagement of the intrinsic pathway via cleavage of Bid

and a Bcl-2 family protein (50). The crosstalk between extrinsic and intrinsic pathway is necessary to activate the cell death program effectively when caspase-8 signal is faint or caspase cascade is inhibited by inhibitor of apoptosis (IAP) proteins (51).

Overexpression of anti-apoptotic Bcl-2 protein has been demonstrated in a variety of malignancies including SCLC cell lines and tumours. While up-regulation of Bcl-2 has been presented in 75%-95% of SCLC, low expression of Bax has been identified in SCLC (52). The dysregulation of Bcl-2 in SCLC is correlated with resistance to anticancer drugs. Therefore, Bcl-2 has long been involved in anticancer therapy as a potential therapeutic target. It has been demonstrated that suppression of Bcl-2 inhibits tumour activity in both SCLC cell lines and xenograft models (53). One of the agents developed for clinical application is oblimerson, an 18-base antisense phosphorothioate oligonucleotide targeting a region encodes the first six amino acids of BCL-2 mRNA (54). Preclinical and clinical studies have proved that intravenous administration of oblimerson can reduce the production of Bcl-2 protein (55). However, one study of the treatment with a combination of oblimerson and paclitaxel on 12 SCLC patients failed to show any positive effect (56). The reason may be due to that dosage of drugs given to patients was below routine usage. In 2004, another test yielded promising result in 16 extensive stage SCLC patients who were given a treatment which combined oblimersen with etoposide and carboplatin (57). Further study on the effect of treatment of antisense molecules of Bcl-2 is still ongoing.

1.1.4.2.2. MYC oncogenes

The MYC oncogene family encodes three nuclear DNA binding proteins, c-MYC, N-MYC and L-MYC. Myc family plays a role in regulating transcription activity, cell

growth, and cell cycle progression (58). The Myc protein interacts with other proteins by forming heterodimers. The over-expression of Myc has been observed in numerous types of cancer. It is suggested that Myc plays a role in development of neoplastic diseases by enhancing proliferation and losing control of terminal differentiation. Over-expression of Myc has been reported in 16–32% of SCLC and in 40% of cell lines established from patients with SCLC progression after chemotherapy (59). Such over-expression is largely due to the amplification of MYC gene, over 50 copies of c-MYC, N-MYC, or L-MYC can be identified in each SCLC cell (60, 61). This amplification can adversely impact survival rate of SCLC patients. c-MYC is more commonly detected in relapsed tumours than untreated tumours, and its over-expression in SCLC usually indicates a poorer prognosis (62). Amplification of C-MYC in SCLC implies resistance to therapy and a worse prognosis (63). It has been found that treatment with MYC antisense DNA and tretinoin can inhibit c-MYC expression and slow down the cell growth of SCLC (66). The amplification of L-Myc family, however, cannot be identified in any tumour samples of SCLC. Although it is postulated that Myc expression is not an initial event in the developing of SCLC, the role of the Myc family in the pathogenesis of SCLC has not been fully understood to date.

1.1.4.3. Receptor Tyrosine Kinases and Growth Factors

1.1.4.3.1. c-MET

The receptor tyrosine kinase (RTK) c-MET has been identified as a proto-oncogene and encodes a protein known as hepatocyte growth factor receptor (HGFR). c-MET is

a high-affinity receptor for its natural ligand hepatocyte growth factor (HGF). Phosphorylation of specific tyrosine residues on c-MET can activate HGF/c-MET signalling pathway. Activation of the HGF/c-MET signalling pathway results in various cellular responses including increased proliferation, scattering (cell-cell repulsion), motility, migration, invasion, angiogenesis and metastasis of solid tumours (64). c-MET alterations, including over-expression and mutations, have been observed in many different kinds of tumours such as papillary renal cancer, gastric cancer, and hepatocellular carcinoma (65). Over-expression of c-MET and mutations of c-MET have also been detected in SCLC (66). Recently, a number of studies investigated the expression of c-MET in SCLC through mutational and function alteration analyses (67). Novel somatic missense mutations were identified in both SCLC cell lines and tumour tissue samples. The mutations included two different c-MET missense mutations, one Sema domain missense mutation and two-base-pair insertional mutations (72). Other splicing isoforms of c-MET (such as exon 10) were identified in SCLC as well (68). It was also found that the expression level of c-MET did not show any significant relation to the mutations of c-MET in the SCLC cell lines (68). Another study found that c-Met can be activated by HGF. When localized to the nucleus, the phosphorylated c-Met can interact with topoisomerase-I and the transcription factor Pax 5 (69). A specific inhibitors against c-Met has been identified and it has been applied on Phase I clinical trials. Therefore, c-Met receptor tyrosine kinase may be a crucial therapeutic target in SCLC.

1.1.4.3.2. c-KIT

The receptor tyrosine kinase c-Kit can be activated by its ligand stem cell factor (SCF).

c-Kit has been found in multiple cell types, including hematopoietic progenitor cells, mast cells, germ cells, melanocytes and interstitial cells of Cajal (70). Studies showed that c-Kit played a key role in cell survival, proliferation, and differentiation. Recently, the aberrant expression of c-KIT was implicated in the pathogenesis of human neoplastic diseases, such as SCLC (71), as well as prostate cancer (72), and acute myeloblastic leukaemia (73). However, the mechanism of this aberrant expression has not been elucidated in most types of the neoplasms. In SCLC, phosphorylated wild-type c-Kit was over-expressed in the presence of stem cell factor and this was associated with autocrine and paracrine signalling loops (74). This finding indicated that the inhibitory drugs which block the wild-type c-Kit receptors may play a role in SCLC. However, several trails conducted in clinic with imatinib were not shown any improvement in SCLC patients with c-Kit over-expression (75). One of the putative reasons of the inactivity of imatinib in SCLC was that the origin cells of SCLC are not as hematopoietic stem cells which dependent on c-KIT in the development (76). Another reason may be the SCLC patients lack of activating mutations in c-Kit exon 11 which accounts for imatinib activity in gastrointestinal stromal tumours (77).

1.1.4.3.3. Vascular endothelial growth factor (VEGF) and basic fibroblast growth factor (bFGF)

Angiogenesis is a crucial factor during the development of malignancy. Mutations allow the cancer cells grow out of control, but these cells are not able to grow beyond certain size due to lack of essential nutrients, such as oxygen. Therefore tumour induces angiogenesis by secreting growth factors such as VEGF and bFGF. These growth factors enhance capillary growth into the tumours and facilitate tumour

expansion.

VEGF is a family consisting of five isoforms which are VEGF-A, VEGF-B, VEGF-C, VEGF-D and VEGF-E (78). Their biological activities are regulated by binding to type III receptor tyrosine kinases (RTKs) VEGFR-1 (Flt-1), VEGFR-2 (KDR/Flk-1) and VEGFR-3 (Flt-4) (79). VEGF is a key factor of two distinct processes: vasculogenesis and angiogenesis (80). Vasculogenesis is vascular development triggered by hematopoietic precursor cells during embryogenesis. Angiogenesis is the vessel formation from the pre-existing vessels throughout the whole life of an organism both in the physiological and pathological conditions. The VEGF signalling pathway also promotes tumour angiogenesis by enhancing the proliferation, migration, and invasion of endothelial cells (21). Over-expression of VEGF was observed in SCLC patients and implicated with tumour progression, resistance to chemotherapy and poor prognosis (81). There are a few ways to target angiogenesis in SCLC such as external inhibitors, endogenous inhibitors and miscellaneous agents. The expression of VEGF, VEGF-C, and their receptors, VEGFR-2 and VEGFR-3 was identified in five SCLC cell lines, and was associated with tumour growth and invasion (79). ZD6474, a VEGFR-2 or EGFR kinase inhibitor, was proved to be effective in suppressing VEGF signalling and thereby angiogenesis, resulting in decreased proliferation and increased apoptosis in SCLC xenografts in a preclinical trial (28). Bevacizumab, a recombinant monoclonal antibody, was approved to be used in treatment of certain metastatic cancers by inhibiting angiogenesis through blocking VEGF-A. Reports showed that following carboplatin and irinotecan treatment, bevacizumab can increase the response rate, survival rate and safety rate of patients with limited stage SCLC (82). In the future, large randomized phase III trials are needed to study the exact effect of

bevacizumab in SCLC. Positive result of ZD6474 was demonstrated in non-small cell lung cancer patients, and efficacy of sunitinib and sorafenib was tested in the treatment of gastrointestinal stromal tumours and renal cancer patients (83). Sunitinib as a multi-targeted TK inhibitor (such as VEGF1, 2, 3) was used in the treatment of SCLC on a small scale (84).

The fibroblast growth factor (FGF) receptor family of tyrosine kinases includes four isoforms (FGFR 1-4). Upon binding of fibroblast growth factors (FGFs) to the FGFR, the receptor interacts with a number of signalling factors and activates the Ras/Raf/MEK/ERK1,2 and PI3K-AKT signalling pathways (85). Basic fibroblast growth factor (bFGF), also known as fibroblast growth factor-2, is a secreted cytokine which functions as a stimulator of angiogenesis. High levels of bFGF were detected in serum samples of 103 SCLC patients (86). It was suggested that the high level of serum bFGF at diagnosis was related to the poor outcome in SCLC by promoting active angiogenesis. Basic fibroblast growth factor also stimulates the growth of SCLC and results in resistance to chemotherapeutic drugs (87). PD173074, a selective FGFR inhibitor, can inhibit the development of SCLC *in vitro* and *in vivo*, and significantly promote response when prescribed with cisplatin (69). Moreover, PD173074 induced complete responses can last more than six months in xenografts (69). These responses may be regulated through decreasing intratumoral proliferation and increasing apoptosis. Thalidomide (a glutamic acid derivative) which inhibits the expression of VEGF and bFGF and exerts anti-angiogenic activity, has been studied in two randomized phase III clinical trials (70,71). In those studies, chemotherapy as maintenance treatment was administered with or without thalidomide for two years. It was not observed any improvement in outcome in either of the treatment but greater

side effects (70,71). Inhibitors of FGF-R including XL228, which actives against IGF1-R, SRC, BCR-ABL, were entered the early phase clinical trials (www.clinicaltrials.gov)(28).

1.1.4.3.4. Insulin-like growth factor-1 receptor

The insulin-like growth factor-1 receptor (IGF-1R) belongs to the insulin receptor family of receptor tyrosine kinase. IGF-1R can be activated by the ligands Insulin-like growth factor 1 (IGF-1) and Insulin-like growth factor 2 (IGF-2). The tyrosine kinase activity of IGF-1R regulates downstream signalling through Ras/Raf/mitogen activated protein kinase (MAPK) pathway and PI3K/Akt pathway. Insulin has been identified to be the potent growth stimulators for SCLC (88), but it was detected only in less than 10% of SCLC cell lines in a survey of peptide hormone secretion (89). A report showed that the mitogenic effect of insulin was not regulated by the insulin receptor in *Escherichia coli,* and this process can be inhibited by polyclonal anti-insulin receptor antibodies which were able to block ligand binding to the insulin receptor (90). Thereafter, the IGF-1R was revealed as the mediator in mitogenic effect of insulin in human fibroblasts. Over-expression of IGF-1R and its ligand, IGF-1, has been identified in SCLC cell lines. IGF-1 protein was elevated in more than 95% of SCLC and was implicated in up-regulation of survivin expression (91). The IGF-1R signalling pathway was suggested to play a potential role in the development, as well as resistance to chemotherapy of SCLC (81). A number of monoclonal antibodies has been confirmed to inhibit the IGF-1R pathway, including IMC-A12 and AMG479, as well as receptor tyrosine kinase inhibitors, such as NVP-ADW742, BMS-554417 and AG1024 (28). IMC-A12 can inhibit growth and increase chemosensitisation in SCLC

cell lines when PI3K/Akt signalling was blocked (92). NVP-ADW742 alone can exert antitumor activity to a certain extent and there was a synergic effect in proliferation inhibition and apoptosis induction in SCLC when combined with AG1024 and AG1296, inhibitors of IGFR-1 and c-Kit, respectively (93).

1.1.4.3.5. Epidermal growth factor receptor (EGFR)

The epidermal growth factor receptor is a member of the ErbB family of receptor tyrosine kinases (RTKs), which consist of four receptor tyrosine kinases: EGFR (ErbB-1), HER2/neu (ErbB-2), Her 3 (ErbB-3) and Her 4 (ErbB-4) (94). EGFR is found on specific cell surface in metazoans and regulates protein tyrosine kinase (PTK) activity that leads to division of cells (95). EGFR is associated with increased proliferation, decreased apoptosis, enhanced tumour cell motility and neo-angiogenesis (96). Abnormally high level of EGFR was observed in different types of cancer (97). Up to date, 11 EGFR mutant-positive SCLC patients have been identified in total. They were more likely to be non-smokers and combined with adenocarcinoma. Recent studies found that the SCLC patients with EGFR mutation responded to gefitinib treatment. Gefitinib, an EGFR tyrosine kinase inhibitor, has been demonstrated to inhibit EGFR signalling in SCLC cell lines. After treated with gefitinib, it was showed that tumours regressed in advanced stage SCLC patients (98). This evidence suggested that the drug targeting EGFR in SCLC may play a promising role to inhibit this tumour. However, another study showed that among the 76 SCLC specimens examined, only 2 (2.6%) EGFR mutations were detected and both of them were deletions in exon 19 (99). There was no improvement observed when one of the patients was treated with gefitinib. This study cannot confirm the valid effect of

gefitinib in treating SCLC patients. This finding may be consistent with the fact that EGFR is weakly expressed in SCLC. The importance of HER2/neu expression in SCLC has not been elucidated. Over-expression of HER2/neu has been detected in approximately 29.5% of patients with advanced stage SCLC using immunohistochemistry (100). It is further reported that the up-regulated HER2/neu was related to a poor prognosis of SCLC patients (101). It is suggested that trastuzumab (an anti-HER2/neu monoclonal antibody) may play a potential role in treating SCLC.

1.1.4.3.6. GRP

Gastrin-releasing peptide (GRP) is a gut hormone originally isolated from porcine non-antral gastric tissue, whose amphibian homolog is thought to be a tetradecapeptide: bombesin (102). Bombesin and its counterpart GRP2 in human belong to a family of brain-gut peptides. This kind of peptide probably acts in an autocrine manner to stimulate the growth of the tumour cells, through bombesin receptors expressed on the membranes of these cells (103). Bombesin-like immunoreactivity has been detected in various types of tissues and cell lines, such as brain, gut, fetal bronchial epithelium, human pulmonary carcinoids, and human SCLC or SCLC-derived cell lines (104). Over-expressed GRP receptors have been determined in a large variety of human tumours, including NSCLC, prostate cancers, breast carcinomas, as well as renal cell carcinomas (105).

It was expected that detection of serum GRP in patients can facilitate the diagnosis of SCLC, however, GRP’s serum levels was difficult to determine because of the instability of GRP in blood (106). To resolve this issue, a radioimmunoassay system

has developed for pro-gastrin-releasing peptide (ProGRP). ProGRP, a more stable precursor of GRP, has been regarded as a specific tumour marker of SCLC (107). In addition, an enzyme-linked immunosorbent assay (ELISA) system which is a more convenient assay system has been established to detect ProGRP (108). Neuron-specific enolase (NSE) has been preferentially selected as a marker of SCLC; however, there are some disadvantages of NSE, such as low positive rates in patients with limited stage SCLC (109). In a large scale study with SCLC, NSCLC, and various benign pulmonary diseases, elevation of both ProGRP and NSE was determined as a poor prognostic factor (110). ProGRP and NSE play complementary roles due to the fact that ProGRP is more sensitive than NSE for SCLC diagnose, while NSE is superior to ProGRP as a prognostic indicator (111).

1.1.4.3.7. Matrix metalloproteinase (MMP)

Matrix metalloproteinases (MMPs) are a family of highly homologous zinc-endopeptidases that cleave and degrade the extracellular matrix and basement membranes (112). Up until now 23 MMP genes have been found in human, and they play a central role in various biological activities, such as embryogenesis, normal tissue remodelling, wound healing, and angiogenesis (113). Aberrant expression of these proteinases has been identified in a number of cancer types as well as SCLC. Over-expression of MMP was identified as a negative predictor of SCLC due to the association with poorer survival rates and higher relapse rates (114). In IHC analysis, 60 to 70% of SCLC cells stained positive for MMP-1 and -9, positive signals of MMP-11, -13, and -14 were identified in 70 to 100% of SCLC cells. Extracellular matrix degradation is a key factor in metastasis process. Protease inhibitors may

hinder extracellular matrix proteolysis and hence interfere with tumour invasion. Thus inhibitor of MMPs seems to be an attractive therapeutic target (115).

Marimastat is a synthetic, orally administered, broad spectrum inhibitor of MMPs. It was used in a large randomized trial to test whether it can prolong survival rate of SCLC patients who responded to chemotherapy (116). MMP family member MMP-11 and MMP-14 were confirmed to be independent negative prognostic factors for Marimastat (114). A study with 532 SCLC patients who were randomly selected to administrate 10 mg oral marimastat or placebo twice a day for two years has not shown significant improvement on survival rates (117). It was suggested that this result may be because the role of MMP system in angiogenesis and tumourigenesis has not been fully understood or MMPs has limited function in advanced cancers.

1.1.4.4. Cell Surface Markers

1.1.4.4.1. NCAM (CD56)

The neural cell adhesion molecule (NCAM) is a cellular adhesion molecule in membrane, initially isolated in the study of its role in neural cell adhesion (118). NCAM has been implicated with the immunoglobulin family and modulates neuroendocrine differentiation, cell growth, and migration (119). NCAM is expressed on natural killer cells, cardiomyocytes, neuroendocrine glands, central and peripheral nervous system (120). NCAM can be found in almost 100% of SCLC (119). CD56 is an isoform encoded by the NCAM gene and has been suggested to be a useful tool for SCLC diagnosis (121). It was shown that NCAM positive carcinomas were more aggressive than NCAM negative carcinomas, and NCAM was investigated as a target for anti-cancer therapy (119). When NCAM signalling pathway was studied in the

malignant cells, it was found that NCAM ligands or antibodies may inhibit tumour progression (122). N901, an anti-CD56 monoclonal antibody, can link to a ricin molecule and bind to SCLC tumours and cell lines (123). Although previous studies on N901 showed promising result, it has potentially fatal side effects by inactivating immune response (124). To overcome the side effects of N901, another antibody was produced and named as BB-10901 or huN901-DM1. A phase I clinical trial was conducted in patients with relapsed and other neuroendocrine tumours using BB-10901 (125). Studies of this compound demonstrated the efficacy and safety.

1.1.4.4.2. Gangliosides

Ganglioside molecules are glycosphingolipids containing a variable number of sialic acids linked on the sugar chain. Gangliosides modulate cell signal transduction events on cell plasma membrane, particularly in central nervous system (126). Elevated expression of these antigens was demonstrated in SCLC (126). Fucosyl GM-1 was originally identified as a selective tumour-associated marker of SCLC in 1986 (127). FucGM-1 ganglioside was shed from SCLC cells *in vitro* and *in vivo* and this antigen can also be detected in serum samples from SCLC patients. In a study, FucGM-1 ganglioside was found to be expressed in 75% of SCLC specimens, and rarely in normal tissue, NSCLC and other tumours (128). Another study showed that the presence of FucGM-1 was detected in 90% of the SCLC cases as compared to 12% positive cases observed in other lung cancers by immunohistochemistry analysis of frozen tissue sections (127). Detection of these antigens in serum may provide an aid for diagnosis and follow-up of SCLC (129). Polysialic acid (polySia) is a large glycan of more than twenty negatively-charged alpha 2-8 linked sialic acid. PolySia was

expressed in low level and attaches to the protein scaffold neural cell adhesion molecule (NCAM) (130). PolySia is best known for its proposed role in modulating neuronal development and cell motility (131). Expressions of other gangliosides including GM-2 and Globo-H are also found in multiple tumours. The development of a tetravalent vaccine with antigens fucosyl GM1, GM2, Globo H and polysialic acid is currently ongoing (132).

1.1.4.5. Chromosomal alterations

1.1.4.5.1. Chromosomal alterations

Multiple chromosomal aberrations found in SCLC reflect the genomic instability during the SCLC initiation and development (133, 134). Loss of the short arm of chromosome 3, which can result in inactivation of three putative tumour suppressor genes, was consistently observed in SCLC (135). In majority of SCLC, it was found the deletions in multiple chromosomal sites including recurrent losses at 3p, 5q, 13q and 17p, which are loci with tumour suppressor genes such as p53 (133). Using comparative genomic hybridization analyses, it was revealed that a large number of SCLC harbour gains of 1p, 2p, 3q, 5p, 8q and 19p, which are regions encoding well-known oncogenes such as MYC and KRAS (28). Amplifications of 1p, 2p and 3q and deletion of 18q in SCLC cell lines are associated with a more aggressive phenotype of the disease (133). Allele loss on chromosome 3p occurs in more than 90% of SCLC and was implicated to be an early event in lung carcinogenesis (134). Distinct areas of loss that have been determined include 3p21.3, 3p12, 3p14.2 and 3p24 (21). A number of genes of these regions have tumour suppressor activity and

loss of their expression was frequently detected.

Tumour suppressor genes on the 3p21 include RASSF1A, FUS1, SEMA3B and SEMA3F. RASSF1A gene is located within a 120 k base pair region of chromosome 3p21.3 which also contains the FUS1, SEMA3B and SEMA3F loci (136). RASSF1A encodes a protein similar to Ras effector proteins and can be inactivated by tumour-acquired promoter hyper-methylation in 90-100% of SCLC samples (137). RASSF1 has been involved in cell cycle regulation, apoptosis and microtubule stability (138). TGFBR2, located at 3p21.3.22, encodes the transforming growth factor β (TGF-β) type II receptor. Deletion of TGFBR2 was also reported in SCLC (139). The nonsense mutation of TGFBR2 leads to the synthesis of a truncated receptor related to exposure to benzo[a]-pyrene (an element of cigarette smoke) (139). FUS1, a novel tumour suppressor gene, was found in the human chromosome 3p21.3 region where allele losses and genetic alterations occur frequently at the early stage of various human cancers (140). The absence and reduction of FUS1 protein expression were detected in the majority of lung cancers as well as premalignant lung lesions. Particularly, the FUS1 protein lost its expression in 100% of SCLC cases (141). Wild type FUS1 was related to induction of G1 arrest and apoptosis through the intrinsic mitochondrial and Apaf-1-dependent pathways, as well as through inhibition of the activities of tyrosine kinases including EGFR, PDGFR, AKT, c-Abl, and c-Kit (134). The restoration of wild-type FUS1 in 3p21.3-deficient NSCLC cells has significantly suppressed tumour cell growth by promoting apoptosis and changing cell cycle kinetics (142). Loss of fragile histidine triad (FHIT, located at 3p14.2) can lead to DNA synthesis and proliferation stimulated by diadenosine tetraphosphate (143). FHIT, an important tumour suppressor gene, regulates death receptor genes and was

involved in the pathogenesis of lung cancer (22). Homozygous deletion of FHIT occurs in 100% of SCLC (22). Preclinical studies identified that transfection of wild-type FHIT into lung cancer cells can induce apoptosis (144). Retinoic Acid Receptor Beta (RAR-β) is located on chromosome 3p24 (145). Retinoic acid regulates lung development and differentiation via its nuclear receptors RAR-β primarily. It was reported that RAR-β was able to modulate the growth of epithelial cells and suppress the tumourigenicity (146). Loss of heterozygosity of RAR-β2 and RAR-β4 was observed in almost all cases of SCLC. Methylation of the promoter region of these two isoforms could be the reason for the silencing of RAR-β in SCLC (146).

1.1.4.5.2. Telomerase

Telomerase, a ribonucleoenzyme which is an RNA-dependent DNA polymerase, compensates for telomere shortening during cell division by synthesizing nucleotide sequence repeats TTAGGG at the end of the chromosomes (147). DNA sequence repeats TTAGGG are also known as telomeres, which are genetic elements present at the ends of linear chromosomes to protect stabilising chromosomes from degradation and cell death (148). The functional unit of telomerase consists of an RNA subunit hTR, and a catalytic subunit hTERT. Telomerase activity is silenced during the terminal differentiation of cells. However, reactivating telomerase can result in immortality by compensating for the loss of telomeric repeats (148). This mechanism may support the inhibition of telomerase in the somatic tissues of humans, and this telomerase suppression can provide protections against carcinogenesis (149). Up-regulation of hTR and telomerase activity was detected in 98% of human SCLC in a study (150). Another similar study showed that increased telomerase activity can be

found in all SCLC specimens (147). Using telomeric repeat amplification protocol (TRAP) assay which can investigate telomerase activity, the signal of TRAP was identified in 14 of 15 (93%) SCLC, 7 of 8 (87%) large-cell neuroendocrine carcinomas, and only 1 of 15 (7%) typical carcinoid tumours (151). The loss of telomerase activity was related with absence of P53, BCL-2, c-KIT, and CDK4 expression and presence of RB. Conversely, telomerase positive tumours usually displayed a consistent immunophenotype of gene alterations including over-expression of P53, BCL-2, and c-KIT, and loss of RB and were characterized by a high proliferative index. A number of agents have now entered in early phase clinical trials targeting telomerase, such as GV1001 (a synthetic peptide vaccine, hTERT), telomelysin (OBP-301, telomerase specific oncolytic virus) and GRN163L (antagonist of RNA template region of hTR) (152).

1.1.4.6. Signalling pathways

1.1.4.6.1. Phosphoinositide 3-kinase/AKT/mTOR

The family of phosphoinositide 3-kinases (PI3Ks) comprises three different classes, I, II, and III. PI3Ks are able to phosphorylate the 3′-OH group in inositol lipoids and regulate cellular functions such as cell proliferation, survival, motility, adhesion and differentiation (21). PI3Ks can translate signals from multiple growth factors and cytokines into intracellular messages by creating phospholipids in response to the stimulation of tyrosine kinase receptors and G-protein coupled receptors. This process thereafter activates the downstream pathways, such as Akt (a serine/threonine protein kinase) which is involved in insulin-mediated glucose uptake and in cell motility,

invasion, metastasis of cancer (153). One of the crucial downstream mediators of the PI3K/Akt pathway is mammalian target of rapamycin (mTOR), which belongs to a serine/threonine kinase of PI3K-related kinase family. It was firstly identified in yeast *Saccharomyces Cerevisiae*. Molecule mTOR harbours a COOH-terminal catalytic domain with a high sequence similarity to PI3K (154). Protein mTOR regulates protein synthesis by targeting ribosomal protein S6 kinase 1 (S6K1) and eukaryotic translation initiation factor 4E-binding protein 1 (4EBP1) (155). Moreover, mTORC1 negatively regulates autophagy, a non-apoptotic form of cell death, which can influence the sensitivity of tumours to various types of therapies (156). PTEN, a dual specificity lipid/protein, is the primary negative regulator that antagonizes network signalling of PI3K (157). The PI3K/Akt/mTOR pathway is essential for integrin-mediated regulation of cell proliferation and survival (158). Over-activation of this pathway was found to be able to reduce apoptosis and increase proliferation in various cancers, therefore this pathway plays key roles in tumorigenesis and therapeutic resistance (159). In SCLC, it was detected that the PI3K/Akt/mTOR signalling was aberrant such as PI3K and PTEN mutations, constitutive action of PI3K, over-expression of mTOR, S6K1 and phosphorylated 4EBP1. Phosphorylation of Akt was found in 70% of SCLC patients (160). Those alterations are involved in reduction of survival rate and development of chemotherapy resistance in SCLC (161).

Wortmannin and LYS294002, two specific PI3K inhibitors, can induce changes in cell growth rate and apoptosis in SCLC (162). RAD001, a rapamycin derivative, can be used to antagonize mTOR and hence inhibit the tumour growth of SCLC both *in vitro* and *in vivo* (163). Synergic effect of LYS294002 and RAD001 was reported to enhance the pro-apoptotic activity induced by etoposide (164). Inhibitors of the

PI3K/Akt/mTOR pathway have also been entered the evaluation phase of early clinical trials. In a randomized, phase II study, temsirolimus (CCI-779) failed to show any improved outcomes in 87 patients with extensive stage of SCLC after standard first line chemotherapy (165). Everolimus (RAD001) was well tolerated when administered to 40 previously treated SCLC patients; however limited efficacy was shown in an unselected population (166). A phase Ib trial is underway to evaluate the effect of cisplatin, etoposide and everolimus in extensive stage SCLC patients who have not been previously treated (www.clinicaltrials.gov). Furthermore, multiple PI3K inhibitors (e.g., XL147, CAL-101, PK-866, GDC-0941, BKM-120), dual inhibitors of PI3K and mTOR (e.g., BEZ235, BGT226, XL765, SF1126, GSK1059615), Akt inhibitors (e.g., perifosine, VQD002, MK2206), and mTOR inhibitors (e.g., AP23573, AZD8055, OSI1027) are all undergoing early phase clinical trials (157, 167).

1.1.4.6.2. Hedgehog

The Hedgehog (HH) pathway, a conserved embryonic signalling cascade, was initially found as a mediator of segment polarity in the fly (168). Study has shown that HH pathway is essential in early lung formation and development through epithelial-mesenchymal interactions (169, 170). Sonic Hedgehog (SHH), Indian Hedgehog (IHH) and Desert Hedgehog (DHH) are three known ligands of this pathway in human. This signalling pathway is initiated by HH binding to a twelve transmembrane protein Patched-1 receptor (PTCH-1) (171). In the absence of HH ligand, PTCH-1 can suppress the transmembrane protein Smoothened (SMO), thus inhibit activity of this signalling pathway (186). When HH ligand binds to PTCH-1, thereafter SMO relieves and activates a protein complex which regulates downstream

transcription of HH targets in the nucleus, including transcriptional activator GLI-1 and PTCH-1 (172). The aberrant HH pathway activation caused by inactivating mutation in PTCH was related to medulloblastoma, therefore it was suggested that HH pathway may play a role to control the behaviour of malignant cells (173). Loss of HH can lead to severe lung defects, which was implicated in the failure of branching morphogenesis (174). HH signalling pathway may determine progenitor cell fates and regulate differentiation in some regenerating mammalian epithelia and hence repair epithelial airway (175). Activation of Hedgehog signalling can lead to an intraepithelial cell population to expand during airway regeneration induced by naphthalene injury (170). In SCLC, ligand-dependent activation of the Hedgehog pathway was observed when adjacent cells expressing SHH in a juxtacrine fashion (169, 170). Cyclopamine, a steroidal alkaloid Hedgehog antagonist, can inhibit development of SCLC in both *in vitro* and *in vivo* studies (176). The dependency of chemotherapy resistant progenitor cell of SCLC on Hedgehog developmental pathway requires further study. IPI-926 (Infinity Pharmaceuticals, Inc.), a cyclopamine analogue, and LDE225 (Novartis Oncology) are inhibitors of SMO and currently being evaluated in the phase I testing (28). GDC-0449, another inhibitor of SMO, is being studied in a randomized phase II clinical trial in SCLC patients with extensive stage (28). Furthermore, XL139 (Bristol-Myers Squibb Company and Exelixis, Inc.) and PF-04449913 (Pfizer), which are also inhibitors of Hedgehog pathway, has entered in phase I clinical trials (28).

1.1.4.6.3. Notch pathway

Notch pathway is a highly conserved cell signalling system throughout multicellular

organisms (177). Notch signalling is known as a mediator in the differentiation, development, proliferation and death of cells (178). More importantly, Notch pathway preserves uncommitted, multi-potential functions in development and adult tissue (179). The Notch pathway is critical in regulation of the airway epithelial development, specifically, has been implicated in determination of cellular neuroendocrine and non-neuroendocrine differentiation (180). In mammals, there are four transmembrane Notch receptors (Notch 1-4) which can be activated by three Notch ligands (Delta1, Jagged 1 and Jagged 2) (170). Both the Notch receptor and its ligands are transmembrane proteins with large extracellular domains, which consisted of primarily of epidermal growth factor (EGF)-like repeats (181). Two proteolytic cleavage events are promoted when the ligands bind to the Notch receptor. In this process, the first cleavage is catalysed by ADAM-family metalloproteases (181). The second is regulated by γ-secretases (an enzyme complex) which are composed of presenilin, nicastrin, PEN2 and APH1. The enzyme γ-secretase releases the Notch intracellular domain (Nicd) which transfers to the nucleus. Nicd then inactivates the DNA-binding protein CSL (named after CBF1, Su(H) and LAG-1) and its co-activator Mastermind (Mam) to promote transcription. Notch signalling may lead to the activation of transcriptional targets such as Hairy enhancer of split 1 (Hes1), which are known as the inhibitory factors (182). Hes-1 can inhibit the transcription of human achaete-scute homolog-1 (h-ASH-1), which is required for the development of neuroendocrine cells in the lung (180). Up-regulation of murine ASH-1 in neuroendocrine cells and down-regulation in Clara cells was discovered in the lungs of Hes-1 knockout mice (61). In SCLC, high expression of h-ASH-1 was correlated with inactivation of Notch-1 (180), and the over-expression of Notch receptors led to

cell cycle arrest and growth inhibition of SCLC (183). Therefore, it was suggested that activation of Notch pathway may be an effective therapeutic strategy in SCLC.

1.1.4.6.4. WNT

The WNT gene was originally discovered from activation of INT1 (integration 1, the vertebrate homologue) in breast tumours of mice infected with virus (MMTV) by Roeland Nusse and Harold Varmus in 1982 (184). The name of WNT is derived from Int and Wg (wingless, the Drosophila melanogaster segment-polarity gene) in *Drosophila* (185). The WNT signalling pathway is a highly conserved signal transduction cascade. WNT pathway plays a critical role in embryonic development, tissue regeneration, and a host of other biological processes such as survival, differentiation, proliferation, cell motility and apoptosis (186) There are three key cascades in WNT signalling pathways. The first is canonical WNT pathway (or WNT/β-catenin pathway). The canonical WNT pathway functions as transcriptional co-activator of TCF/LEF family via transferring the accumulated β-catenin from cytoplasm to nucleus (187). The second pathway acts via activation of calmodulin kinase II and protein kinase C (WNT/Ca^{2+} pathway), which counterbalances the canonical pathway (188). The third, the planar cell polarity (PCP) pathway functions through small GTPases, such as RhoA and Jun Kinase (JNK). PCP pathway was associated with cytoskeletal rearrangements and cell polarity (188). It was suggested that WNT signalling was necessary for normal epithelial-mesenchymal interactions during lung morphogenesis (189). The activation of WNT signalling pathway led to cell proliferation and tumour growth when bronchial cells were exposed to cigarette smoke (190). Over-expression of WNT proteins (such as, WNT1 and WNT2) and

decreased expression of WNT regulators (such as WIF) were observed in NSCLC specimens (191). Activation of the WNT signalling was found in RB/P53 mutant SCLC cells (192). The nuclear localization of β-catenin was increased in early lesions, fully-grown tumours, and mouse primary SCLC cells. Therefore, it was concluded that the WNT/β-catenin pathway, unlike its oncogenic role in various tumours, may play a tumour suppressor role in SCLC development and maintenance. These identifications provide a novel therapeutic strategy to treat SCLC.

1.1.5. Clinical diagnosis

The most common presenting symptoms in SCLC are persistent cough, dyspnoea, chest pain, and haemoptysis (**Table 1.1**). SCLC tends to be centrally located, with hilar masses, hilar and mediastinal adenopathy. If the tumour invades local tissues, patients can exhibit chest pain or dyspnoea secondary to pleural and pericardial effusions. Severe pericardial effusions lead to cardiac tamponade and that can be considerable lethal. When the tumour located high on the right chest, it can generate superior vena cava syndrome including facial swelling and dyspnoea as well. Horner's syndrome, unilateral facial ptosis, miosis, and anhidrosis, can be observed if the sympathetic nerves are affected. These patients are possible to have hoarseness of the voice if the recurrent laryngeal nerve is influenced. Metastatic disease is common during the time of diagnosis. Disease can spread to bone, liver, brain, lymph node, the central nervous system, adrenal glands, subcutaneous tissue, and pleura (193). Common symptoms of metastatic disease include pain, headache, seizures, malaise, fatigue, anorexia, and weight loss.

Symptom or sign	Frequency,%
Local	
Cough	50
Dyspnoea	40
Chest pain	35
Haemoptysis	20
Hoarseness	10
Distant	
Weight loss	50
Weakness	40
Anorexia	30
Paraneoplastic syndromes	15
Fever	10

Table 1.1: Frequency of presenting symptoms in SCLC (3)

Paraneoplastic syndromes are frequently associated with SCLC as these tumours produce ectopic hormones or neural antigen to destruct immune-mediated tissues. The syndromes of inappropriate antidiuretic hormone secretion (SIADH) and cachexia are developed in nearly 40% of SCLC cases (194). The incidence of hypernatremia is secondary to elevated levels of ADH. Patients may suffer from nausea, malaise, confusion, irritability, confusion and poor mental status. Increased levels of immunoreactive adrenocorticotropic hormone in serum and tissues can result in Cushing syndrome. Patients may present with centripetal obesity, easy bruisability, diabetes, muscle wasting, bone pain, and a hypokalemic metabolic alkalosis. Lambert-Eaton myasthenic syndrome has also been regarded as one of the paraneoplastic neurologic syndromes. Patients may predominantly present with weakness of proximal muscles of the lower and upper extremities. Affection of the

respiratory and bulbar muscles is occasionally occurred. In contrast to patients with other myasthenic syndromes, Lambert-Eaton myasthenic syndrome generates much less prominent eye signs. Furthermore, patients with Lambert-Eaton syndrome may also have post-exercise facilitation which allows the improvement of the motor strength after exercise, subsequently weakening if activity is sustained. Cerebellar degeneration is another paraneoplastic syndrome that caused by an immune-mediated mechanism in patients with an underlying malignancy. The related symptoms include loss of coordination, truncal and limb ataxia, nystagmus and dysarthria, whereas encephalomyelitis can present as limbic, brainstem, or focal encephalitis in combination with subacute sensory and autonomic neuropathy (195). Hypercalcemia can also occur in patients either from bone metastases or from the release of parathyroid hormone-related peptides. Symptoms consist of neuropsychiatric problems, nephrolithiasis, and abdominal pain.

Diagnosis is typically made by histological analysis of a bronchoscopy biopsy sample, or by cytological study of percutaneous or transbronchial fine-needle aspiration samples (196). In the WHO 1999 classification system, SCLC is defined as “a malignant epithelial tumour consisting of small cells with scant cytoplasm, ill-defined cell borders, finely granular nuclear chromatin, and absent or inconspicuous nucleoli. The cells are round, oval, and spindle-shaped and nuclear moulding is prominent. The mitotic count is high” (**Figure 1.5**) (197). Patients with SCLC typically undergo haematological and serum chemistry tests, CT scan of the chest in addition to the physical examination. Imaging of the chest can assess the intrathoracic diseases such as the presence of pleural effusion, lobar collapse, hilar and mediastinal adenopathy, and contralateral parenchymal disease. Fiberoptic bronchoscopy can facilitate the

initial diagnosis in the airway, abnormality can be detected in more than 90% of cases (198). Any clinical symptoms of neurological abnormality should prompt MRI or CT of the brain and MRI of the spinal cord. Metastases in central nervous system can be identified in 80–90% of patients (199). Patients with bony pain should be subjected to a radionuclide bone scan. After the chest CT scan, this examination should be conducted in other tissues such as liver and adrenal glands owing to the frequency of liver metastases. Follow-up biopsy of hepatic or adrenal lesions should be performed if these tissues are the only potential metastasis sites. Bone marrow biopsy should be considered, if the patient with an abnormal complete blood count or peripheral blood smear cannot be explained. The role of positron emission tomography (PET) scan with fluorodeoxyglucose is proved for SCLC. Up until now, the investigation has shown that SCLC can take up fluorodeoxyglucose, and this imaging modality can identify metastatic lesions in patients who are regarded as limited stage SCLC disease by standard staging methods (200). After the PET scan, bone scan is not necessary but brain scan is still required. The SCLC is initially not easy to be recognized; therefore the invasion of the tumour has been started by the time it is diagnosed. Other methods to find out pathogenesis of SCLC include immunologic cross-reactivity between tumour-associated antigens and P/Q–type voltage gated calcium ion channels (Lambert-Eaton myasthenic syndrome), anti-Purkinje cell antibodies (cerebellar degeneration), and anti-Hu antibodies (encephalomyelitis) (201). The neurologic syndromes usually appear to be progressive and run their own course independently to predict the outcomes of cancer therapy.

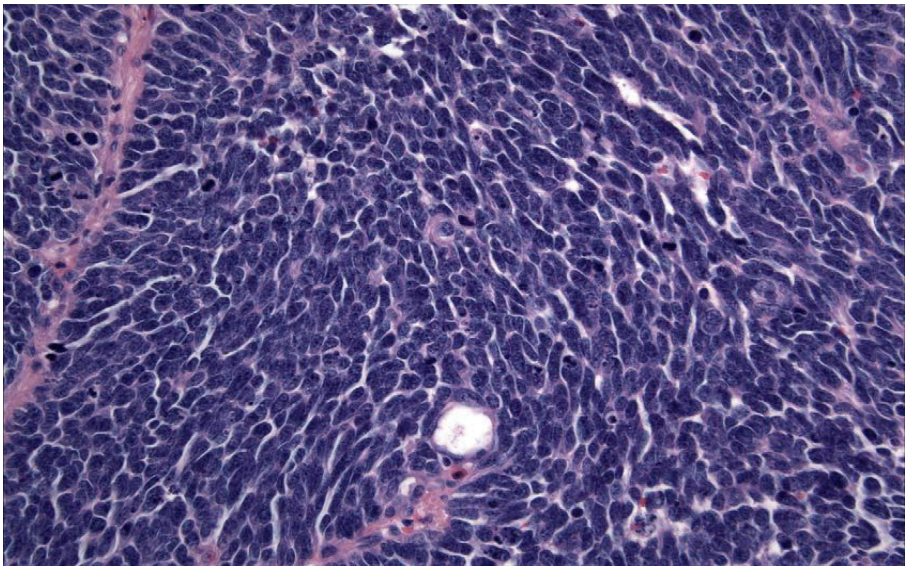

Figure 1.5. High-power view of a surgically resected SCLC, showing typical scant cytoplasm, increased mitotic index, spindling, and prominent nuclear moulding (3).

1.1.6. Staging

The purpose of staging is to identify the extent of SCLC through the patients presenting symptoms, as well as through the most likely sites of metastasis (202). The prognostic and therapeutic implications will thereby determine the treatment. According to the TNM staging system, there are four stages in both NSCLC and SCLC (203). In stage I and II, the lung cancer is limited within the lung or in the lung and the hilar lymph nodes. In stage III, the lung cancer has spread to the mediastinal lymph nodes. In stage IV, spread of lung cancer can be detected in the opposite lung or in other parts of the whole body. TNM staging system, which is generally used in diagnosis of NSCLC, can hardly be applied in SCLC because the patients with SCLC rarely present with disease that is sufficiently localised for surgical resection. Instead, Veterans Administration Lung Study Group system has been typically used during the

staging process which classifies patients as having either limited stage or extensive stage disease (204). At the limited stage of SCLC, the disease is limited to one hemi-thorax, with hilar and mediastinal lymph nodes that can be encompassed within one tolerable radiotherapy portal (23, 205). In terms of the TNM staging system, limited stage consists of stage I, II and III. Nearly 25-30% of all patients with SCLC possess limited disease by the time of diagnosis (206). A SCLC case is considered to be limited if the cancer is detected only in the lung itself, or in the hilar or mediastinal lymph nodes. The definition of extensive stage of SCLC refers to any disease beyond those boundaries; usually cancer has spread to other parts of body such as brain, bones, liver, adrenal glands, pleura or other parts of the body. Extensive stage consists of stage IV in terms of the TNM staging system. When the cancer has spread to the pleura, the excess fluid will form and retain in the pleural cavity. The excess accumulation of fluid in the pleural cavity can lead to shortness of breath and sometimes a cough. Those are usually regarded as extensive stage SCLC patients even the metastasis region only within the pleura or cancer cells can only be detected in the pleural fluid. For those showed signs of the presence of micrometastatic SCLC cells in the blood stream; and this usually implies that the cancer may have spread to other parts. It is estimated that more than 65% of SCLC patients are under the extensive disease at the time of diagnosis (13).

1.1.7. Prognosis

Most (65-70%) of SCLC patients present with disseminated or extensive stage disease. For the untreated cases, those patients with extensive disease have median survival of

7–12 months and the 5-year survival rate is 2%. Among the patients with a limited stage disease (localized disease), the median survival is about 20 months and the 5-year survival rate is 12–17% (3). After treated with multiple-agent chemotherapy and multimodality therapy, the survival rates of patients with SCLC are as follows: those patients with extensive disease had a median survival of 12 months and the 2-year survival rate was 1.5% in 1973; the 2-year survival rate was 4.6% in 2000. Among the patients with limited stage disease (localized disease), the median survival was about 23 months and the 2-year survival rate was 20% (207). The poor prognostic factors include age, relapsed disease, weight loss, and performance status (208). Patients who suffer from weight loss of more than 10% in 6 months and reduction of 50% of their waking hours indicate a worse prognosis. Elevated serum lactic dehydrogenase level, low serum sodium, and high level of alkaline phosphatase are also considered to confer a poor prognosis (209).

1.1.8. Treatment

1.1.8.1. Limited stage disease

Approximately 30% of patients with SCLC have a limited stage disease at the time of diagnosis (206). The combination of concurrent radiotherapy and chemotherapy is the currently used standard treatment regimen. Surgery treatment in SCLC was largely abandoned from the 1970s due to the fact that SCLC had an early haematogenous spread feature and the 5 year survival rate was less than 5%. In a prospectively randomized trial of the Lung Cancer Study Group, pulmonary resection from limited stage SCLC patients partially showed response to chemotherapy combine by

following thoracic radiotherapy (TRT) and prophylactic cranial irradiation (PCI) (210). The potential benefit of the resection in SCLC was observed only in patients who diagnosed with TNM stage I disease. If the patients can tolerate the surgical treatment, it is also recommended for the patients with disease of clinical stage I with peripheral lesions but no hilar or mediastinal nodal involvement. Patients who undergo resection should receive adjuvant chemotherapy, while the patients with hilar or mediastinal involvement should be considered to take modality therapy and chemotherapy. The combination of modality therapy and chemotherapy showed a significant improvement in survival. A former study showed that compared to those receiving chemotherapy alone, an increased 3-year survival rate for 5% patients was achieved when they received a combination of chemotherapy and radiation (211).

Several chemotherapeutic agents including vincristine, doxorubicin, methotrexate, cyclophosphamide, etoposide, cisplatin, and carboplatin, have been used in patients with SCLC. The combination regimens yield remarkable response and superior survival compared to the treatment of single agent. The initial chemotherapy regimens were based on cyclophosphamide. The combination of doxorubicin and vincristine became more widely used by the late 1970s. Now, the regimen has been replaced with a combination of etoposide and cisplatin. This combination treatment had a median survival of 14.5 months compared with 9.7 months for limited stage SCLC patients treated by cyclophosphamide, epirubicin, and vincristine in a large randomised trial (212). The regimen is helpful due to less haematological toxicity and easier combination with chest radiotherapy (213). The etoposide and cisplatin regimen is typically administered every 3 weeks for a total of four to six cycles. For day 1, 2 and 3, etoposide is administered intravenously at 80–120 mg/m^2 and cisplatin is given

intravenously at 60–90 mg/m^2 (213). However, the therapy that lasted more than six cycles failed with the increased toxicity and no prolonged survival for limited stage SCLC patients in various studies (214, 215).

Modest doses of TRT (45-50 Gy) are administered in daily fractions of 1.8 to 2.0 Gy because the SCLC is radiosensitive. The concurrent chest radiotherapy and the first or second cycle of chemotherapy exhibited a superior effect to sequential radiotherapy (216). For those limited stage SCLC cases assigned to chemotherapy and radiotherapy, a further of 5% patients were alive after 2 and 3 years; This was in contrast with the chemotherapy alone in a meta-analyses of prospective, randomised trial (211). It is observed that twice-daily chest radiotherapy to a dose of 45 Gy plus etoposide and cisplatin is favoured over once-daily chest radiotherapy to 45 Gy (a 10% absolute survival benefit at 5 years) (217). Therefore, for the limited stage disease SCLC patients, the current recommendation is four to six cycles of chemotherapy with etoposide and cisplatin, combined with twice-daily radiation in the first or second cycle (3).

1.1.8.2. Extensive stage disease

The basic treatment of extensive stage SCLC is the combination chemotherapy. Although routine use of chest radiotherapy does not prolong survival, it can be used as the palliative treatment of lobar collapse, prevention or treatment of brain metastases, symptomatic bone metastases or superior vena cava syndrome in patients who fail to respond to chemotherapy and have not received radiotherapy to those sites (218).

The current standard chemotherapy for extensive stage SCLC is cisplatin and etoposide. Most patients respond to this regimen, with a median survival time of 7 to 9

months, only 2% of patients can survive for 5 years. The regimen, including dose intensity and density, schedule, and duration of chemotherapy has been assessed to improve the results. Etoposide is typically administered intravenously for 3–5 days in a 21-day cycle. The optimal efficacy of this drug is achieved by assigning on a 3–5 day schedule than on a single day (219). Attempts to alter this schedule failed to generate less toxicity or survival advantage. In a randomized study, etoposide was compared to carboplatin and etoposide in 147 patients with limited stage and extensive stage disease (220). Though no significant difference was observed in response rate or median survival time, less toxicity of carboplatin was reported. The incidence of myelosuppression was less but diarrhoea happened more in patients who were assigned to irinotecan plus cisplatin treatment than those assigned to etoposide plus cisplatin (221). There was a significant survival advantage with irinotecan in patients with extensive stage SCLC in a study, in which etoposide plus cisplatin were compared with irinotecan plus cisplatin in Japan (222). However, the topoisomerase inhibitors failed to show any benefit in subsequent trials in the USA and Europe. In an American study, there was no significant difference in response rate (48% vs 44%), median time to progression (4.1 vs 4.6 months), median survival (9 vs 10 months), or 1-year survival (35% vs 37%) (194). Furthermore, no improved efficacy was showed in a trial carried in a European population when comparing oral topotecan and cisplatin with intravenous etoposide plus cisplatin. The median survival and 1-year survival were similar in both study groups, and time to progression favoured etoposide plus cisplatin (223).

Other agents also have been tested to compare with the standard regimen of etoposide plus cisplatin in large randomised trials. In one study, etoposide, cisplatin with or

without ifosfamide were given to patients (224). A study compared etoposide, cisplatin, cyclophosphamide, and epirubicin with the standard regimen (225). Though the regimen with three or four drugs showed more survival benefits, the greater toxicity was also generated. Trials also have been carried to investigate the benefit of higher doses of chemotherapy with platinum-based regimens. No survival difference was shown between the standard-dose and high-dose group in a study of 90 patients with extensive stage disease (226). In two phase II trials, high-dose therapy showed encouraging results in patients with autologous bone marrow transplantation (227), but no difference in median survival in the completed phase III group study (228). Therefore, the higher doses of chemotherapy are not the choice of routine use, and are still under investigation.

For those SCLC patients who have been successfully treated, the risk of central nervous system metastasis remains 35% to 60% in 2 years (229). Prophylactic Cranial Irradiation (PCI) was initially introduced for responsive limited stage SCLC patients who have a complete response to chemotherapy. PCI is used prophylactically. The radiation is typically administered in doses of 24–46 Gy in 8 to 15 fractions (194). A meta-analysis including 847 patients with limited stage SCLC and 140 patients with extensive stage SCLC showed a complete remission with chemotherapy. All patients took part in 7 trials with or without thoracic radiotherapy exhibited a 25.3% decrease in cumulative incidence of brain metastasis in 3 years with PCI. There was also an absolute increase in overall survival of 5.4% for 3 years (230). Study suggested that the neurotoxicity of PCI was more frequent and severe when it was given concurrently with or before chemotherapy, or radiation fractions were greater than 2.5 Gy, or total radiation dose was more than 30 Gy (231). A randomized study showed that PCI not

only reduced the incidence of symptomatic brain metastases, but also prolonged disease free period and overall survival of patients with extensive stage SCLC (232). The Radiation Oncology and Lung Cancer group of European Organisation for Research and Treatment of Cancer (EORTC) carried a randomized study on 286 patients with extensive stage SCLC. Those patients responded to 4-6 cycles of chemotherapy when received PCI (dose ranging from 20 Gy/5 fractions to 30 Gy/12 fractions) or no PCI. The 1-year cumulative incidence of symptomatic brain metastasis in the PCI group was 14.6% (95% CI, 8.3%-20.9%) compared with 40.4% (95% CI, 32.1%-48.6%) in the control group. After 1 year, the survival rate in the PCI group was 27.1%, and that was 13.3% in the control group (232). According to the previous studies, the National Comprehensive Cancer Network recommended PCI for both patients who have limited stage disease and those who have extensive stage disease after they achieved a complete response.

1.1.8.3. Progressive or relapsing disease

Most of the patients with SCLC relapse within a year after treatment. The effect of the subsequent therapy can be judged from the response to previous therapy and the duration of drug-free interval. The patients who respond to the previous treatment and relapse after longer than 3 months are judged as sensitive, and those patients who failed to response to the previous treatment or relapse within 3 months are regarded as refractory. With the disease recurrence, the overall median survival for patients is only 2 to 3 months. If relapse occurs within 3 months of primary treatment, only 10% response rates can be attained for the further chemotherapy. If relapse occurs more than 3 to 4 months after initial treatment, then 40% response rates can be attained,

whereas if relapse occurs more than 8 months, long term survival is possible. For the patients with sensitive disease, second-line regimens such as single-agent topotecan or the combination of cyclophosphamide, doxorubicin, and vincristine can be used to achieve a response rate around 20%, with median survival times of about 25 weeks (233). For those with refractory disease, single agent topotecan only showed a response rate about 8% (234), whereas the combination chemotherapy based on topotecan or irinotecan for relapsed SCLC generated more promising result. A study of topotecan plus cisplatin in 110 patients with relapsed disease found response rates of 29.4% in sensitive disease and 23.8% in relapsed disease (235). Topotecan was as effective as cyclophosphamide, doxorubicin, and vincristine for patients with relapsed disease, and improving dyspnoea, fatigue, and anorexia were found in a multicenter randomized trial (233). Combination chemotherapy regimens based on irinotecan, etoposide, or paclitaxel have documented response rates of 71% in small scale studies (236). Larger randomised clinical trials with the regimens for SCLC relapsed disease are needed to identify the best options.

1.1.9 New Agents

1.1.9.1. Paclitaxel

Paclitaxel has been studied in patients with limited diseases, extensive diseases, as well as in those patients with relapsed SCLC. The drug has been applied as a single agent and in combination with other agents. In 1993, paclitaxel was first introduced and tested by the Eastern Cooperative Oncology Group and North Central Cancer Treatment Group in previously untreated SCLC with response rates of 34% and 53%,

respectively (237). A study reported that when assigned with the combination of paclitaxel and etoposide/cisplatin, the patients with extensive disease showed a response rate of 94% (238). In addition, there was a 96% response rate (39% complete response rate) in patients with limited disease, when received the above regimen along with thoracic radiotherapy in a phase I/II study (239). A study investigated paclitaxel and docetaxel combined carboplatin/etoposide in patients with limited or extensive disease (240). A 98% response rate was reported in patients with limited disease and an overall response of 91% in all patients. However, only a response rate of 25% was observed when docetaxel was given to 28 patients with SCLC in a study (241). The function of paclitaxel in SCLC requires further study.

1.1.9.2. Topoisomerase I inhibitors

Camptothecin, topotecan and irinotecan (CPT-11) are three major topoisomerase I inhibitors. Camptothecin, which inhibits topoisomerase I, is an important new class of anticancer agents against SCLC. Two other analogues of camptothecins (topotecan and irinotecan) have been applied in clinical chemotherapy. Topotecan has been widely investigated in both primary and secondary treatment regimens. A 38% response rate in patients with sensitive disease compared to a 6% response rate in patients with relapsed disease (234, 242). A study in patients with extensive disease who received topotecan as first-line single-agent therapy showed a 39% response rate (214). More promising results were found in sensitive diseases rather than patients with relapsed disease. Topotecan has also been applied in combination with other cytotoxic agents in patients with relapsed disease (233). There was a response rate of 29% and 17% for patients with sensitive and relapsed diseases, respectively.

Irinotecan was studied either as a single agent or in combination with other chemotherapies in patients with limited, extensive, and relapsed disease. In one study, the response rate in the previously patients with SCLC was 37% (243). Another study showed that a similar response rate (47%) was observed from patients with relapsed SCLC treated in a Phase II trial (244). Irinotecan had been combined with other cytotoxic agents when applied as chemotherapy. A study of irinotecan combining cisplatin was conducted in patients with both limited and extensive stage diseases in a phase II trial (245). Patients with limited stage disease were also given thoracic radiotherapy. For those patients, a response rate of 84%, 29% complete remission and a median survival of 14.3 months were reported. In a phase III trial, the standard etoposide/cisplatin regimen was compared with irinotecan/cisplatin regimen in patients with extensive disease. There was a significant improvement of response rate (67% versus 89%, respectively) and median survival (9.4 months versus 12.8 months, respectively) between the former and the latter (222).

1.1.9.3. Gemcitabine and vinorelbine

Gemcitabine, a nucleoside analogue closely related to cytarabine (Ara-C), was applied so far as a single-agent therapy. A 27% response rate was observed when gemcitabine was given to the untreated patients (246). Vinorelbine, a vinca alkaloid, was shown to inhibit the tubulin polymerization. This drug has also been studied in a single-agent therapy. There was a better response rate in those patients with sensitive disease versus those with relapsed diseases (247).

1.2. Id family protein

1.2.1. bHLH Family Introduction

The basic helix-loop-helix (bHLH) proteins belong to a family of transcription factors that have been well characterized in mammalian systems, in which considerable structural, functional, and phylogenetic analyses have been conducted (248, 249). The bHLH proteins are essential regulatory components in transcriptional networks, regulating a wide diversity of biological processes such as cellular differentiation, proliferation and lineage commitment (250). The bHLH family is defined by its domain, which consists of 60 amino acids with two functionally distinct regions (251). The basic domain, at the N-terminal end, is correlated with DNA binding and consists of 15 amino acids (252). The HLH domain, located at the C-terminal end, acts as a dimerization region and comprises two amphipathic-helices separated by a loop region of variable sequence and length (253). The helix parts in bHLH protein pack together and exhibit strong van der Waals interactions that stabilize the structure of the homodimer (254). Except of the conserved bHLH domain, proteins show considerable sequence divergence (255).

The DNA sequence motif that can be recognized by the bHLH proteins is a consensus sequence called E-box 5'-CANNTG-3' (256). Numerous types of E-boxes have been discovered so far, the most canonical and common one is the palindromic G-box 5'-CACGTG-3'. Certain bHLH factors such as bHLH-PAS family can bind to non-palindromic sequences, which are closed to E-box (256). Some conserved amino acids located at the basic region of bHLH facilitate recognise DNA sequence, while the other residues in this domain control the specificity for the E-box binding (257).

Moreover, the nucleotides outside of the DNA core sequence also have an effect on binding specificity (255).

1.2.1.1. Classifications of bHLH proteins

The bHLH motif was initially found in murine E12 and E47 (252). As more other bHLH proteins identified, they were classified into six groups according to the specific DNA binding, dimerization potential and distributions of particular tissue (258) (**Table 1.2**).

Class I of HLH proteins are ubiquitously expressed proteins, and are capable of forming homo- or heterodimers and binding to DNA (252). Members of this group of proteins include El2, E47, E2-2 and daughterless. E12, E47 and E2-2 may play key roles in regulating lineage specification of numerous cells such as B cell, myocyte, neural and pancreatic cell (259). HEB can form a hetero-oligomer with myogenic regulatory proteins such as E12 protein, and hence modulate the DNA-binding specificity of those proteins (260). The daughterless is an important gene product that controls neurogenesis, oogenesis and sex determination in *Drosophila* (261, 262).

Class II HLH proteins are expressed in restricted type of tissues. This class of proteins includes MyoD, myogenin, MYF5 and the achaete-scute complex. To function properly, the Class II HLH proteins have to form heterodimers with Class I HLH proteins. MyoD, myogenin and MYF5 belong to a family of proteins known as myogenic regulatory factors (MRFs), and have been involved in the regulation of muscle differentiation (263). The achaete-scute gene family encodes for proteins involved in the determination of the neuronal precursors in the peripheral and central

nervous systems of *Drosophila* (264). Achaete-scute complex can resemble other members of the Myc family of transcription factors.

Class III HLH proteins contain Myc family of transcription factors such as c-Myc, N-Myc and L-Myc. This class of protein has been involved in growth control (265). Transcription factor E3, which is encoded by the TFE3 gene in human, also belongs to Class III HLH proteins. The basic helix-loop-helix leucine zipper (bHLH-Zip) members are MITF, TFE3, TFEB and TFEC from the microphthalmia transcription factor/transcription factor E (MITF-TFE) family (266). The TEF3 protein can activate transcription through binding to the muE3 motif of the immunoglobulin heavy-chain enhancer (267). To function properly, this group of transcription factors needs to specifically recognise and bind to E-box sequences 3'-CANNTG-5'. Capability of DNA-binding needs dimerisation with TFE3 itself or with other MIT/TFE family members (266). TFEB supports T-cell-dependent antibody responses to activate CD4 (+) T-cells and thymus-dependent humoral immunity, because it can induce the expression of CD40L in T-cells (268).

Class IV of HLH proteins include Mad, Max and Mxi. Those proteins have been identified to be capable of dimerising with the Myc proteins or with one another (269, 270). When Mad binds to Max, they can form a sequence-specific protein complex which recognises the Myc core sequence 5'-CAC[GA]TG-3' (269). Hence Mad acts as transcriptional repressor antagonise Myc transcriptional activity by competing for Max.

Class V of HLH proteins is a family of molecules, including Id and emc. This group of proteins lacks a DNA binding domain, and plays a negative role to regulate bHLH transcription factors when dimerise with other bHLH proteins (271, 272). Id proteins

are key regulators to prevent premature differentiation and promote proliferation (273). The gene emc is associated with the development of sensory organ by inhibiting the neurogenic activity of the achaete-scute complex (AS-C) (274).

Class VI HLH proteins are characterised by the presence of a proline in the basic region. Class VI proteins consist of the *Drosophila* proteins hairy and enhancer of split. The hairy protein is required for proper embryonic segmentation (275). The enhancer of split has been identified that can transcriptionally control the intestine stem cell in the *Drosophila* (276).

Classification	Examples of classified proteins
I	E12, E47, E2-2, HEB, daughterless
II	MyoD, Myogenin, MYF5, AS-C
III	TFE3, TFEB, Myc
IV	Mad, Max
V	Id, emc
VI	Hairy, Enhancer of split

Table 1.2 Classification according to Murre *et al* (258)

Recently, bHLH proteins were classified by an evolutionary approach. The bHLH family was divided into six groups (A-F) based on the E-box binding, other conservation of residues of the motif, and the presence or absence of additional domains (248) (**Table 1.3**). An analysis of phylogenetic tree derived from 122 sequences pointed out that it is highly possible that ancestral HLH sequence came from group B (248). The group B proteins are the most prevalent type of bHLH proteins in animals, as well as the *Arabidopsis* genome, in which the G-box-binding bHLH proteins (part of group B) are the most abundant group (251).

Based on the evolutionary classification shown in **Table 1.3**, among all the additional domains the most common are PAS, orange and leucine-zipper domains (277). The PAS domain found in PAS-domain-containing bHLH (bHLH-PAS) proteins, is 260-310 amino acids long, and located in the C-terminal of the bHLH region within transcriptional activation domains (278). The PAS domain is named after three proteins: *Drosophila* Period (Per), the human aryl hydrocarbon receptor nuclear translocator (Arnt) and *Drosophila* Single-minded (Sim) (279). The domain comprises two repeats of approximately 50 amino-acid residues (known as PAS A and PAS B) separated by about 150 residues which are poorly conserved (280). bHLH-PAS functions as dimeric DNA-binding protein (280). PAS domains are common in phylogenetic group C.

The orange domain is found in the phylogenetic group E, specifically *Drosophila* proteins Hesr-1, hairy, and enhancer of split. The orange domain, a 30-residue sequence, is also located in the C-terminal to the bHLH region and separated by a short, variable length of sequence (277). It is proposed that the molecular function of orange domain is to regulate specific protein-protein interaction between hairy and scute, as well as specificity and transcriptional repression (281).

Many bHLH proteins have a leucine-zipper domain, especially phylogenetic group B. Leucine zippers are parallel alpha-helical coil motifs with the most representative member: basic-region leucine zippers (bZIP) (282). The leucine zipper is one of the most widely known mediators of protein-protein interaction (283). Max is one of bHLH proteins that contain leucine-zipper domain, and is important in the network of bHLH transcription factors. Max binds to group B proteins Myc, Mad, Mnt and Mga to form homodimers and heterodimers, which are characterised by sequence specific

DNA binding and transcriptional functions (284). The position of the bHLH and additional domains within the protein varies widely between different families. This variable pattern of domain positioning suggested that bHLH proteins have undergone modular evolution by domain shuffling, a process that involves domain insertion and rearrangement (285).

Phylogenetic group	Description	Classification according to Murre *et al*. [12]	Examples of classified proteins
A	Bind to CAGCTG or CACCTG	I, II	MyoD, Twist, Net
B	Bind to CACGTG or CATGTTG	III, IV	Mad, Max, Myc
C	Bind to ACGTG or GCGTG. Contain a PAS domain		Single-minded, aryl hydrocarbon receptor nuclear translocator (Arnt), hypoxia-inducible factor (HIF), Clock
D	Lack a basic domain and hence do not bind DNA but form protein-protein dimers that function as antagonists of group A proteins	V	Id
E	Bind preferentially to N-box sequences CACGCG or CACGAG. Contain an orange domain and a WRPW peptide	VI	hairy
F	Contain an additional COE domain, involved in dimerization and DNA binding		Coe (Col/Olf-1/EBF)

Table 1.3 Classification of bHLH proteins according to Atchley *et al* (248)

1.2.1.2. The structure of bHLH protein

1.2.1.2.1. The basic domain: E-box binding sites

The E box binding sites were initially identified in the immunoglobulin heavy chain (IgH) gene enhancer, which regulates the transcription of IgH gene (286). Five E-box elements: μE1, μE2, μE3, μE4, and μE5 have been found in the IgH gene enhancer. These elements share a motif of the consensus hexanucleotide sequence, CANNTG, and are thereafter called E boxes (287). The E box binding sites was initially found by *in vivo* methylation protection assay, which were only observed in B cells but not in nonlymphoid cells (287). The immunoglobulin kappa light chain enhancer also includes three canonical E boxes, designated κkE1, κE2, and κE3. E-box sites were subsequently found in B-cell-specific promoter and enhancer elements, including a subset of Ig light-chain gene promoters, the IgH and Ig light-chain 3' enhancers, and the λ5 promoter (286, 288). E-box elements were detected in both promoter and enhancer that control muscle-, neuron-, and pancreas- specific gene expression (250). For example, in muscle, the muscle creating kinase gene acetylcholine receptor genes α and δ, and the myosin light-chain gene all require E-box elements for full activity (289). Quite a few genes whose expression is limited to the pancreas also require E-box sites for proper expression. The insulin and somatostatin genes, which contain E-box sites, are sufficient to mediate pancreatic β-cell-specific gene expression when multimerised (290). More recently, E-box regulatory sites were identified in a variety of neuron-specific genes, including the opsin, hippocalcin, beta 2 subunit of the neuronal nicotinic acetylcholine receptor, and muscarinic acetylcholine receptor genes (291).

1.2.1.2.2. The HLH domain

It has been investigated that the HLH domain is a dimerisation domain by using electrophoretic mobility shift assay. Crystal structures of six members in bHLH family have been studied, which are MAX, E47, MyoD, USF, PHO4, and SREBP (292, 293, 294). Max, which can be dimerised with proto-oncogene Myc, was first confirmed by the presence of HLH motif. The three-dimensional structure of bHLH domain of Max/Myc has been shown by X-ray crystallography at 2.9A resolution (293). Max, a parallel, left-handed, four-helix bundle protein, can bind to E-box recognition site CACGTG as a homodimer (295). Each subunit of the homodimer contains two α-helical segments separated by a loop. The two α-helical segments consist of the basic region, helix 1, helix 2 and the leucine repeat (292). The conserved hydrophobic amino acids of helix 1 and helix 2 in Max pack together to stabilize the structure of homodimer under the van der Waals interactions between hydrophobic residues (254). A glutamate in the basic region of each subunit interacts with the adenine and cytosine in the E-box (250). An adjacent arginine residue plays a role to stabilize the position of the glutamate. Both the glutamate and the arginine residues are conserved within the bHLH family and they facilitate specific DNA binding (248, 252, 293). It is assumed that all 242 HLH proteins share the similar structure as Max (254).

1.2.1.3. The function of bHLH protein

The bHLH proteins interact with heterogeneity of DNA sequences and thereby regulate a variety of biological activities. There are two basic groups in the bHLH family: cell specific and widely expressed proteins. The cell-type-specific members

have been linked with the determination of various types of cell lineages and the process such as myogenesis, neurogenesis, cardiogenesis and hematopoiesis (277). Four bHLH proteins myogenin, MyoD, MYF5 and MRF4 are involved in the differentiation of myogenic lineage (296). Another bHLH member-Id has been identified as a negative regulator of MyoD. Daughterless, a *Drosophila* HLH protein, is involved in neurogenesis and sex determination (261). In vertebrates, Mash-1, Math-1 and neurogenins are crucial for the initiation of the neurons, and NeuroD2, Math-2 also participate in differentiation (297). Studies have showed that dHAND (Heart- and neural crest derivatives-expressed protein) and eHAND are related to the development of cardiac organ in vertebrates (298). The stem cell leukemia (SCL) protein is essential for hematopoietic specification. The gene encoding SCL is the target of chromosomal translocations in T-cell acute leukemia (299). The Myc family is one of widely expressed bHLH proteins that regulate activation of translation. In addition Myc proteins can either activate the expression of certain genes or inhibit transcription. In the normal cells, Myc plays a role in a large variety of biological activities such as proliferation and differentiation (300). Myc is also regarded as an essential transcriptional oncogenic switch, and up-regulation of Myc has been found in many types of cancer (301).

1.2.2. Id protein

1.2.2.1. Introduction

Id proteins are also known as inhibition of DNA binding or inhibition of differentiation proteins. Id proteins play a role in a variety of cellular processes, and Id

genes encoding these proteins were identified in 1990 (271). The Id protein, which belongs to the bHLH family of transcription factor, does possess a helix-loop-helix domain but lack a DNA-binding domain. The DNA-binding domain is a region of basic residues close to the HLH domain, which facilitates homo- or hetero-dimerisation. This domain also assists the bHLH protein binding to E-box (CANNTG), N-box (CACNAG), or Ets-site (GGAA/T) in the promoter region of target genes. Therefore, the members containing a DNA-binding domain can positively regulate transcription. The Id protein, however, lacks the DNA-binding domain and only can form dimmers with other transcriptional regulators, mainly the bHLH protein. Thereby the Id protein acts as the negative regulators of bHLH proteins.

1.2.2.2. Structure of Id

There are four known members (designated Id1-Id4) in Id family and in human they all locate on separate chromosomes, 20q1, 2p25, 1p36 and 6p21-22 respectively (302, 303). In addition, the Id family members are more closely related to one another than the other members of bHLH family. At least two splice forms for each member has been found, whereas the biological relevance of these isoforms has not been established (304). Different members of Id family genes all share a similar genomic organization of exon-intron boundaries within their coding regions, consistent with evolution from a common ancestral Id gene (303). It was identified there are alternative open reading frames in the Id1 and Id3. The open reading frames produce variant Id proteins with distinct C-termini by read-through of a small intron closed to the 3' end of the coding region (305).

The Id1 and Id3 protein with hetero-dimerisation properties have been largely studied, but the relevant biological significance still needs to be clarified. Id protein is one distinct subfamily of bHLH proteins and all members in the Id family have similar size (13-20 kDa) (306). The Id proteins contain a highly conserved HLH domain which comprises two amphipathic helices (each 15-20 residues) separated by an intervening loop like the other members in bHLH family (307). Each HLH monomer packs to form a four-α-helix bundle structure which can be stabilized through a combination of electrostatic and polar interactions at the monomer interface (252). The HLH domain can regulate homo- or hetero-dimerisation, and hence regulate DNA binding and transcription of target genes. However, the Id protein lack this domain and it can inhibit both DNA binding and transcription when binds to other bHLH proteins as homodimers or heterodimers (**Figure 1.6**) (308). A large number of proteins that interact with Id protein have been identified, but the most compelling are E-proteins. The most common complexes are Id1–E-protein, Id1–Ets and Id2–Rb interactions (307). The best characterised interaction of Id-protein is also with the E-protein, for instance E12, E47, E2-2 and HEB binding of Id protein in B cells as homodimers (309). The loop region of Id proteins, which varies on the basis of length and sequence, may play a role in the hetero-dimerisation.

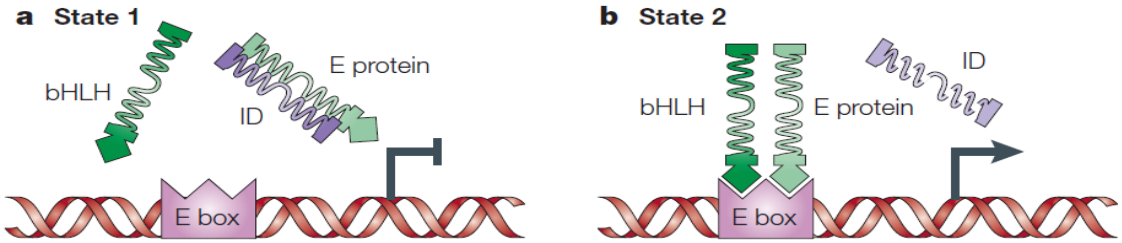

Figure 1.6. Cell fate mediation by Id proteins. Cells are maintained in "state 1" by bHLH inhibitor: Id proteins, which lack the basic DNA binding domain, are the negative regulators of bHLH transcription factors. The E-proteins activate transcription (state 2) by binding to promoter of E box as dimerised with other bHLH members except Id proteins (308).

1.2.2.3. Function of Id protein in biological conditions

1.2.2.3.1. Id proteins in differentiation, proliferation and cell-cycle control

Id proteins have a role to negatively regulate the cell differentiation, and positively regulate the cell proliferation and growth. Id proteins are necessary for cell cycle progression in cell lines. The loss- and gain- of-function study demonstrated that mutants of emc in *Drosophila* can inhibit the functions of daughterless and achaete-scute bHLH proteins, and hence play a role in sex determination and neurogenesis (310). Interestingly, down-regulation of Id expression was observed in various differentiated cell lines, and over-expression of Id proteins can inhibit differentiation in keratinocytes, myoblasts, myeloid precursor cells, mammary epithelium, and pre-adipose cells under proper conditions (311). It was found that the

over-expression of Id protein in normal cell lines led to extended proliferation, the similar phenomenon happened in tumour cells (312). Using oligonucleotide antisense of Id genes, the elevated levels of Id proteins were reduced. The down-regulation of Id can inhibit the proliferation in a variety of carcinomas (313, 314). The blocked proliferation can lead to subsequent inhibition of the malignant behaviour of cancer cells. It was suggested that the proliferation of tumour cells depend, at least in part, on high levels of Ids (311). It is generally known that the Id expression is high in proliferating cells and low or undetectable in quiescent or terminally differentiated cells (307). A notable exception is Id2, which is over-expressed during monocyte-macrophage differentiation (315).

In most of the cell lines, Id expression is rapidly increased following mitogen/growth factor stimulation, with an expression peak occurring in 1-3h, and then the Id expression level is sustained throughout the G1 phase (316, 317). This is a typical fluctuation of early-response genes. After a decline, there is a second peak of expression prior to the onset of S phase. The induced expression of Id proteins can persist throughout the S phase. The core issue involved in cell cycle control is the correlation of Id protein and p16. There are two distinct ways which can regulate the cell cycle machinery during the late G1 phase. One of them involves intriguing reactions between Id2 and the retinoblastoma proteins (Rb) or the related pocket proteins in Rb family (p107 and p130) (311). Id2 and probably Id4 can bind to the pocket protein of Rb family, and inhibit their anti-proliferation function (307). The genetic correlation has been determined between Id2 and Rb in which the loss of Id2 can rescue $RB^{-/-}$ mice at E14.5, and the lethality was absent in $RB^{-/-}$ $Id2^{-/-}$ mice. It is speculated that there is an existed pathway of Rb-Id2-p16. Down-regulation of Rb

family proteins can lead to the elevated level of Id2, which can consequently restrain Ets2 and reduce the expression of p16 (318). Moreover, the targets of Id2 such as bHLH, Ets and E2F family are very important in Rb regulated cell cycle arrest (319). On the other hand, Id1 and Id3 can suppress the expression of the Rb by inhibiting Ets-regulated transcription of cyclin-dependent kinase inhibitors such as p16 INK4a. This suppression effect is regulated by the Ras pathway, and can lead to Rb phosphorylation (320). It was observed that the over-expression of Id1 in cell lines can reduce the expression of the gene encoding p16, and the disruption of Id1 and Id3 or Id1 alone can increase p16 in mouse brain at embryonic day 11.5 (320, 321). These evidences lend great credibility to Id1 or Id1 plus Id3 that their regulated suppression of p16 plays at least in part in cell cycle progression. Another mechanism is that Id1 inhibits expression of CDK inhibitor p21, which is regulated by E2A bHLH transcription factor. Suppressing p21 promoted the activity of cyclin dependent kinase 2 (CDK2) (322), which can lead to phosphorylation of Rb. The phosphorylated Rb can dissociate from E2F-DP1 complexes, and thereby activate genes involved in the progression to S phase (307). One study also reported that over-expression of Id1 was related to the down-regulation of the CDK2 inhibitor p27 (323). Besides the above discovery, the phosphorylation is another issue that raises concern during cell cycle progression and proliferation. Though the specific phosphorylation sites and their binding affinity of bHLH transcription factors have been identified, their importance is still unclear. Id2, Id3 and Id4 (but not Id1) have been found to be subjected to CDK2-dependent phosphorylation during late G1 or early S phase (324, 325). The mutated Id proteins that lack CDK2 phosphorylation sites can lead to S phase arrest and then cell death (324).

1.2.2.3.2. Id proteins in developmental biology

1.2.2.3.2.1. *Drosophila*

In *Drosophila*, there is an Id-like locus, extramacrochaetae (emc), encodes an Id-like protein (272, 274). To avoid the embryonic lethal when two emc loci were absent in the *Drosophila*, several partial emc mutants were generated through loss- and gain-of-function strategy. This model was used to study the role of emc in modulating cell lineage commitment, differentiation and proliferation (326). During the process of cell fate determination, the balance between the relative levels of emc protein and its bHLH target played an essential role (307). The emc locus was also indicated in sensory organ development and wing morphogenesis in *Drosophila* (307). It was shown that factors in the Ras signalling pathway can cooperate with emc in cell proliferation, but antagonize emc in differentiation (327). The Norch signalling pathway regulates the response to the developmental signals throughout cell development, and has also been associated with the mediation of emc during wing morphogenesis (328).

1.2.2.3.2.2. Zebrafish

The zebrafish homologue of Id was isolated and named as Id6, due to the fact that five members of Id family had been detected in vertebrates (329). The HLH domain of Id6 was suggested to have a high similarity to vertebrate Ids and *Drosophila* emc. Using Northern blot analysis, the expression of Id6 was found in the oocyte, and that in zygote was started after the midblastula transition (330). The Id6 expression remains nearly constant during the rest of embryonic period. The Id6 can suppress the activation of transcription regulated by ZfE12 with and without Zash l/b in a

dose-dependent manner (329). Therefore, function of Id6 is similar as its vertebrate homologues to antagonise bHLH by *in vitro* assay.

1.2.2.3.2.3. *Xenopus*

The Id genes have been isolated and three cDNA XIdIa and XIdIb and XIdII have been characterised in *Xenopus* embryos (331). The expression of Id gene was at a low level in the oocyte, and at a high level in midblastula stage (332). XIdI has been found to interfere with MyoD transactivation of a reporter gene driven by an E-box enhancer in the oocyte (331). Ids can be detected in a large number of embryonic tissues. In myogenesis, Id expression is high in proliferating but low in differentiation myoblasts. Id in *Xenopus* has not only been linked to myogenesis, but also suggested to modulate differentiation, cell fate determination and cell cycle as in higher vertebrates (307).

1.2.2.3.2.4. Mouse

Id expression boosts upon gastrulation and declines at embryogenesis process in mouse (333). The mammalian Id genes can antagonize bHLH proteins to inhibit differentiation and promote proliferation, and was involved in various developmental processes, such as trophoblast development (334), myogenesis (335), myelopoiesis (336), lymphopoiesis (337), bone morphogenesis (338), as well as kidney glomerular mesangial cell development (339). The expression profile of different Id genes was determined by in situ hybridisation analysis. Id1, Id2, Id3 genes are widely expressed in many tissues related with mesenchymal-epithelial interactions during organogenesis (340). However, Id4 is only expressed during early development of neuronal tissues and stomach, and in couples of tissues of more advanced stage of differentiation (340). Therefore, it is suggested that Id4 may be distinct from other members of the Id family

during mouse embryogenesis (376).

1.2.2.3.3. Id proteins and apoptosis

Id proteins influence apoptosis in two different ways, and whether it behaves as pro-apoptotic or anti-apoptotic factor depends on the cell context. A number of investigations suggest that Id proteins can induce apoptosis under the physiological conditions while inhibit apoptosis under the pathological circumstance. Id1 was found to induce apoptosis in dense mammary epithelial cell cultures, neonatal and adult cardiac myocytes (341, 342), Id3 can trigger apoptosis in B-lymphocytes (343) and Id4 has been involved in generating apoptosis in an astrocyte-derived cell line (344). In general, over-expression of Id proteins promotes cancer cell proliferation and resistance against apoptosis. Id1 functions as an anti-apoptotic factor in malignant cells to protect them from undergoing programmed cell death when treated with chemotherapeutic agents (345). Over-expression of Id1 in prostate cancer cells prevents cancerous cells from apoptosis (346). However, elevated Id3 allowed the MG-63 sarcoma cells to be more sensitive to cis-Diamminedichloroplatinum-induced apoptosis, through activation of ROS and caspase-3 (347). Suppression of Id1 and Id3 proteins can promote cell cycle arrest and apoptosis in breast and ovarian cancer cells (348).

1.2.2.3.4. Id proteins in angiogenesis

One of the features of the highly malignant tumour is the invasion to adjacent tissues and metastasis to distant sites. The angiogenesis process provides the tumour cells with unlimited nutrients and space. An increasing number of studies demonstrated the

crucial role of Id proteins in the angiogenesis of tumours. The mutant mice lacking both Id1 and Id3 genes was embryonically lethal at day E13.5 (306). Before death, the embryos of mice suffered haemorrhage in the forebrain (313). These mice also possessed angiogenic defects. Mice lacking single or multiple Id1 and/or Id3 alleles were unable to support growth of tumour due to the poor vascularization, and hence induced necrosis of tumour tissues (321). Tumours in animals with down-regulated Id1, Id2 and Id3 have a profound loss of vascular integrity (308). One of the explanation may be that Id proteins control the expression of matrix metalloprotease 2 (MMP2), a target of αvβ3 integrins on endothelial cells during induction of angiogenesis in the tumour (349). Tumours produce chemocytokines (such as VEGF) that can promote recruitment of endothelial cells and bone marrow-derived endothelial precursor cells (CEPs) to the site of angiogenesis (350). VEGF-induced activation of Ids may be one of the critical molecular factors that promote mobilization of bone marrow precursors (350). However, transplantation of wild type CEPs expressing VEGF receptors can functionally rescue tumour angiogenesis in Id mutant mice, suggesting other targets of Id family may play a regulatory role in this system (351). It has been reported that thrombospondin-1 may be a major regulator of Id1 in angiogenesis and other downstream effectors of Id1 (352).

1.2.2.3.5. Id proteins in invasiveness

Angiogenesis is very important during the development of tumours. Genetic alterations drive the normal cells to highly malignant cells. However, the tumours are unable to grow beyond certain size due to lack of essential nutrients and oxygen. Therefore invasion or metastasis facilitates the expansion of malignant cells by

providing oxygen and nutrient. The most representative example of regulation of invasiveness by Ids lies on the studies conducted in mammary epithelial cells. Suppression of Id1 not only promoted differentiation, inhibited proliferation, but also stopped the cells migrating and invading (353). In contrast, over-expression of Id1 in mammary epithelial cell conferred the ability to invade the basement membrane to other non-tumorigenic cells by secreting a 120 kDa gelatinase (354). Elevated Id1 has been identified in the most aggressive breast cancer cell lines and as well as primary tumours, it promoted metastasis when the breast cells were injected into animals (313). Furthermore, migration of B6RV2 lymphoma can be largely inhibited when the mice lacking a single Id1 allele (321). Specifically, $Id1^{+/-}$ mutant animals that implanted with Lewis lung carcinoma cells were survived twice longer than wild-type animals, and produced significant reduction in metastasis (349).

1.2.2.3.6. Id proteins in tumour biology

Deregulation of Id proteins has been reported in numerous human primary malignancies, including pancreatic cancer (312), astrocytic tumours (355), high-grade neural tumour endothelial cells (321), invasive breast carcinoma (313), seminomas (356), colorectal adenocarcinoma (307), multiple myeloma (307), squamous cell carcinomas of the head and neck (357), etc. Examination showed that the expression status of Ids can facilitate the determination of histological grade and prognosis. High level of Id1 has been reported to correlate with the feature in prostate cancer and is associated with poor prognosis (358). Elevation of Id1 was more frequently associated with poor prognostic outcome of breast cancer (359). Id1 was suggested as an independent marker for tumour progression in cervical cancer, and elevated Id1

expression was correlated with poor or moderate histological grade in epithelial ovarian tumours and also with poor prognostic outcome (360). Over-expression of Id2 can predict poor outcome in children with neuroblastoma, irrespective of other clinical and biological variables (314). Elevation of Id2 in thymocytes can lead to polyclonal lymphomas (361). However, different studies showed controversial role for Id2 in other cancers. A study showed that high level of Id2 were related to better patient outcome and indicated reduced invasiveness in breast cancer (362). The expressions of all four Ids were found up-regulated in testicular seminomas (356). In addition, elevated expressions of Id genes were identified in a large number of tumour cell lines by Northern blot and Western blot analysis, including lung tumour cells, astrocytic tumour cells, colon cancer cells, Ewing sarcoma cells, and chondrosarcoma cells (311, 363).

The role of Id proteins in the molecular events of physiological and pathological condition has been studied. Over-expression of mutant P53 has been linked with elevated Id1 in colon carcinoma (364). In one study, Id1 functioned as a transcriptional target of Kaposi's sarcoma herpesvirus-associated genes in human endothelial cells (365). The activation of Id1 promoter was correlated with loss of histone deacetylase transcriptional repressor complex in metastatic breast cancer (366). High level of Id2 was found in Ewing sarcomas (EWS), and Id2 promoter was identified as a transcriptional target of EWS-Ets fusion proteins (363). Elevated Myc family members and high level of EWS-Ets proteins can up-regulate the Id2 promotor/enhancer directly, such up-regulation is vital for Myc-regulated transformation of fibroblasts (318). In neuroblastoma, over-expression of N-Myc transcription factors can directly bind to the Id2 promoter and hence regulate its

transcription. The elevated expression of Id2 finally inactivates Rb tumour suppressor pathway (318). Furthermore, Id proteins have been identified as downstream targets of proliferation and anti-proliferation signalling pathways associated with the development of cancer. Id1, Id2 and Id3 expression can be induced by mitogenic signals driven by estrogens, insulin growth factor-2 and T-cell receptor respectively (313, 367, 368). The extracellular signalling pathway Ras/ERK/MAPK cascade and the PI3K pathway were suggested to regulate the expression of Ids (367, 368). On the other hand, the progesterone and TGFβ initiated the antimitogenic pathways can inhibit the expression of Id proteins (313, 318).

1.2.2.4. Mechanism of action of Id proteins

1.2.2.4.1. Id-bHLH protein interaction

bHLH transcription factors can be broadly classified into two categories. Class A proteins (E2A gene products E12 and E47, E2-2, HEB) are expressed generally ubiquitously, whereas class B proteins (myogenic regulatory factors: MyoD, myogenin, RAS5, and MRF4/MYF6 and the hematopoietic factors: SCL/TAL-1, TAL-2, and LYL-1) are relatively more tissue/lineage restricted (316). Ids have been found as a mediator in the formation of class A-class B complexes. Whereas Ids bind to the proteins of class A with high affinity, they dimerise with class B proteins poorly but in a way of much broader range of interactions (271). All Id proteins interact with four E proteins of class A, however individual Id protein has specific preference for E protein target (369, 370). It is found that Id1 and Id2 interact strongly with MyoD and MYF5, and weakly with myogenin and MRF4/MYF6. Id3 interacts weakly with all

four MRFs. There was no interaction can be detected between the Ids and hematopoietic factors in a study (369). Id proteins have been suggested to modulate the functions of class B bHLH proteins through sequestration of their class A and E protein partners (316). It was identified that single Id protein was enough to disrupt the activity of E protein-MyoD complexes *in vivo* (369).

1.2.2.4.2. Interactions with non-bHLH proteins

Mouse Id associate 1 (MIDA1) was isolated and implicated in the regulation of cell growth. The antisense oligonucleotide of MIDA1 can suppress growth of murine erythroleukemia cells but does not interfere with erythroid differentiation (371). It was demonstrated that Id1-Id3 can interact with the ternary complex factor (TCF), and the TCF subfamily members of ETS-domain proteins regulated immediate-early gene expression in response to mitogenic stimulation (372). *In vivo*, the Id proteins suppressed the transcriptional activity regulated by the TCFs and hence inhibited MAPK signalling, because TCFs were direct targets of MAPK signal transduction cascades (411). The interaction between Id2 and pRb was observed in the human osteosarcoma cell line U2OS (373). When Id2 was up-regulated in U2OS, it was observed that the cellular proliferation can be stimulated by shortening the doubling time and increasing the percentage of cells in S phase. Additionally, Id2 expression was able to reverse the inhibition of cellular proliferation and the block in cell cycle progression regulated by the product of the retinoblastoma tumour suppressor gene pRb. Therefore, Id2 was demonstrated as an antagonist involved in cell cycle and growth control. The adipocyte determination and differentiation factor-1 (ADD1)/sterol regulatory element-binding protein 1c (SREBP-1c) is a member of the

basic HLH-leucine zipper family of transcription factors. ADD1/SREBP-1c controlled the expression of several key genes during lipogenesis and also interacted with Id2 and Id3 (374). When Id2 or Id3 binding to promoters of ADD1/ SREBP-1c, the transcription activity was then inhibited. Therefore Id proteins are associated with regulating ADD1/SREBP-1c transcriptional activity, and thereby lipogenesis in adipocytes.

1.2.2.4.3. Regulation of Id expression and function

The expression of Id genes has been found highest in a number of undifferentiated and proliferating cells, lowest in terminally differentiated cells, in agreement with their roles to inhibit cell differentiation and promote cell proliferation (333, 375). Id1, Id2, and Id3 are expressed ubiquitously, whereas Id4 is expressed predominantly in testis, brain, and kidney (376). In diverse mammalian cell lineages, Id expression responds to extracellular growth factors/mitogens, ligand-receptor interactions, like other early response genes involved in cell fate determination (316). A biphasic expression pattern of Id1 was identified after serum stimulation, these two peaks corresponded to the early G1 phase and the G1-S transition during the cell cycle progression. This expression pattern of Id1 was found in a number of human cell lines (317, 339). Id2 can be induced in a different manner, depending on the cell types (377). Id3 was expressed in the early phase after mitogen stimulation (378).

1.2.2.4.4. Promoter of Id

It was found that the regulation of Id expression was determined at the promoter region in several studies. The upstream regions of mammalian Id genes harbour

numerous conserved, *cis*-regulatory sequences which are typical in early-response genes, whose expression is associated with mitogenic third-messenger signalling cascades (316). It was found that Id1 promoter can be regulated by a functional EGR1/KROX24-binding site of 210-bp enhancer element. The EGR1/KROX24-binding site of enhancer is serum-responsive, and can be induced immediately prior to activation of Id1 (379). This EGR1/KROX24-binding site is also shared by the Id3 and Id4 genes (303, 380). As for the Id2 promoter, there is a serum-responsive, 300-bp enhancer at the upstream of Id2 promoter in U87Y glioma cells (381). Some regions of the promoter can bind to repressor proteins in serum starved cells but not in proliferating cells. It was found the Id2 promoter was regulated by interacting with both serum and protein kinase C, and Id2 can be activated when bind to ATF-like transcription factors in muscle C2 cells (382). In the development of B cells, an 8-bp pro-B-cell-specific enhancer, which is downstream of the Id1 gene, bound to two pro-B-cell-specific complexes. All of the pro-B-cell-specific complexes contain CAAT/enhancer-binding protein β (C/EBPβ) complexes (383). Suppression of Id during B-cell maturation was supposed to be controlled by CHOP, the negative regulator C/EBPβ (384). Besides, it was shown that expressions of Ids can be induced by a large number of factors including nerve growth factor (385), insulin-like growth factor-I (368), and estrogen (313). The signalling pathways that regulate Id expressions are still under careful investigation (see below).

1.2.2.4.5. Signalling pathways in regulation of Id

1.2.2.4.5.1. TGFβ signalling pathway

The transforming growth factor β1 (TGFβ1) (343) and bone morphogenic proteins

BMP-2/4/7 (338, 386, 387, 388) have been shown that can induce the expression of Id genes. TGFβ superfamily ligands can bind to a heterodimeric receptor which exhibits serine and threonine kinase activity (389). The heterodimeric receptor recruits and phosphorylates cytoplasmic signalling molecules mothers against decapentaplegic homolog 2 (SMAD2) and SMAD3. They interacted with SMAD4 and SMAD7 in the TGF-β/activin pathway, or SMAD1/5/8 in the bone morphogenetic protein (BMP) pathway. TGFβ1 signalling pathway is essential in regulation of diverse biological effects such as cell growth, differentiation and fate determination. TGFβ1 can interact with transcription factors so that to modulate the expression of target genes (389).

During embryogenesis, the expression of the Id genes overlapped with the expression of BMP2 and BMP4 in a variety of sites, and the deregulation of BMP4 can induce ectopic expression of Id3 (390). It was shown that BMP treatment can induce the expression of Id1, Id2 and Id3 in the embryonic stem cells (386). Additionally, BMP up-regulated the Id genes and hence regulated the activities of neuronal and myogenic cell. Induction of Id1 and Id3 by exposing to BMP2 resulted in failing to undergo neurogenesis of neural progenitors (387). It was shown that BMPs can direct up-regulate Id1. SMAD-binding elements (SBEs) and a GC-rich region of Id1 promoter were regarded as potential BMP-responsive elements that facilitated the interaction of BMP and Id1 (391, 392). The similar components have also been found in the Id3 promoter. It was indicated that BMP-induced SMADs co-ordinately regulated expression of Id1 and Id3 gene (391). Id1 was up-regulated in response to TGFβ in hepatocytes (393). Id3 transcription was rapidly induced by TGFβ treatment in B-lymphocyte progenitors (343). There were controversial observations regarding the expression of Id2 regulated by TGFβ. TGFβ inhibited the Id2 expression in mouse

embryonic fibroblasts and other cell types (318). Another study reported that TGFβ1 induced the expression of both Id2 and Id3. While Id3 induction was more prominent at the pro- and pre-B-cell stages, the Id2 expression was more robust in mature B cells (394). In contrast, Id1, Id2 and Id3 were down-regulated in a number of epithelial cells lines treated with TGFβ, though BMP induced the Id1 gene expression in epithelial cells (309). ATF3, a transcriptional repressor in the ATF/CREB family, is required for TGFβ-specific SMAD2–SMAD3 to repress the Id1 promoter. TGFβ but not BMP induced the synthesis of ATF3, which co-operated physically with TGFβ-responsive SMAD3 (395). The biphasic response exhibited by endothelial cells in response to different concentration of TGFβ showed that TGFβ can act either as an activator or inhibitor of endothelial cells (396). The mechanism is that, when ALK1 signalling activated by low concentrations of TGFβ through BMP-responsive SMAD5, can promote migration and proliferation of endothelial cells by induction the Id1 expression (396). At high doses of TGFβ, ALK5 inhibits endothelial-cell migration and proliferation through up-regulation of plasminogen activator inhibitor (PAI) and perhaps through down-regulation of Id1 (396).

1.2.2.4.5.2. MAPK/ERK pathway

Mitogen-activated protein kinases (MAPK) pathway was originally called extracellular signal-regulated kinases (ERK) involved signalling pathway. MAPK/ERK pathway is the major signal transduction system, which transduces the signal from the receptor on cell membrane to nucleus. It is also known as the Ras/Raf/MEPK/ERK pathway. The MAPK/ERK pathway regulates cell growth, proliferation, differentiation and death (397). Deregulation of MAPK cascades can

contribute to cancer and other diseases in normal developmental processes. In the MAPK/ERK cascade, a number of regulatory components may be phosphorylated to modulate the efficiency and the duration of the signal transduction through the pathway. Generally, the extra-cellular mitogen such as platelet derived growth factor (PDGF) and epidermal growth factor (EGF) binds to the ligand of membrane and activates Ras small GTPase. Ras small GTPase then activates the Raf serine/threonine kinases. Raf phosphorylates and activates the MAPK/ERK kinase (MEK)1/2 dual-specificity protein kinases, which then activate ERK1/2. It was found that the key components of MAPK/ERK pathway can be mutationally activated and/or overexpressed in a wide range of human cancers.

It was implicated that Id1 can facilitate human primary fibroblasts escaping senescence through MAPK/ERK pathway (398). In human prostate cancer cells, activation of MAPK/ERK pathways was vital for Id1-induced serum independent cell proliferation, while the ectopic Id1 expression was identified can induce the expression of immediate early growth response gene 1 (EGR1) (399). Over-expression of Id1 was found in nasopharyngeal carcinoma (NPC), and ectopic expression of Id1 in NPC cells contributed to increased cell proliferation (400). In addition, Id1 played a part against chemodrug-induced apoptosis in NPC cells, and this function of Id1 was exerted via activation of the MAPK/ERK pathway (401). It was shown by the previous study that EGR1 was a major regulator of Id1 gene expression in myoblasts and fibroblasts (379). Recent experiments showed that the thymocytes with increased mRNA level of EGR1 were sensitive to a pharmacological inhibitor of MAPK pathway (367).

The activation of MAPK/ERK pathway can also be regulated by T cell receptor during

T cell maturation. This process is known as positive selection. It was found that there is a positive feedback loop between MAPK/ERK and Id3 expression. The MAPK/ERK pathway can be induced by Id3 via EGR1 (367). Elevation of EGR1 via the MAPK/ERK pathway resulted in an up-regulation of Id3 levels, a down-regulation of E-protein DNA binding activity, and hence promotion of thymocyte maturation. It was also demonstrated that Id3 gene expression was regulated by the MAPK/ERK kinase pathway, resulting in a significant reduction in DNA binding activity of the HLH transcriptional regulators E2A/HEB. The suppression of DNA binding activity then promoted the differentiation of the thymocyte (367).

1.2.2.4.6. Modification and degradation of Id

The Id proteins are also regulated by modification at the post-translational level. The potential phosphorylation sites for protein kinase A, protein kinase C, cdc2 kinase, and casein kinase II have been identified in Id proteins. In the previous study, phosphorylation activities of Id1, Id2, and Id3 were found in all above protein sites but casein kinase II sites *in vitro* (402). Phosphorylation found in Id family however, does not affect the ability of these proteins to heterodimerize with bHLH factors or the binding of bHLH homodimers to DNA (402). Id1 and Id2 can be phosphorylated by cAMP-dependent protein kinase *in vitro*. Id2 and Id3 can be phosphorylated by cdc2, cyclin E/cdk2 and cyclin A/cdk2 (324, 325). All three Ids (Id1, Id2, Id3) can be phosphorylated by protein kinase C (402). Taken together, it was suggested that phosphorylation of Id proteins can regulate the cell differentiation but not dimerization and DNA binding (402).

1.2.2.4.7. Dimerisation and localisation

The intracellular levels of Id proteins are regulated by ubiquitin-proteasome degradation pathway (403). Like other proteins encoded by early response genes, Id proteins can rapidly turn over. Id proteins have a relatively short half-life around 1 hour, which may be varied in different cell types (403, 404). Id4 was found much less sensitive to inhibitors of the 26S proteasome pathway. The reason may be that degradation of Id4 was regulated by other pathways besides ubiquitin-activating enzyme activity (403). Id proteins can extend half-life by hetero-dimerisation with bHLH proteins and thereby are less susceptible to degradation through the 26S proteasome pathway (403, 404). In the state of heterodimer, subcellular localisation of Id proteins can be regulated through the nuclear localisation signals of their bHLH protein partners (404).

1.2.3. Id and SCLC

The link between Id protein and SCLC was established by our group recently. We initially screen the possible candidates which may be implicated in the tumourigenicity of SCLC using microquantity differential display (MDD) developed in our laboratory (10). Over-expression of Id1 was found in a malignant SCLC cell line Lu-165 when compared with the benign bronchial epithelial cell line Beas-2B. To further investigate the expression level of Id family, Western blotting was used to determine the levels of Id proteins in SCLC cell lines, while immunohistochemical analysis was performed in SCLC tissues and their normal counterparts. The expressions of Id1 in 8 out of 10 SCLC cell lines were up-regulated in comparison

with the benign Beas-2B cells. Similarly, increased expression of Id2 and Id3 was detected in these SCLC cell lines. Using immunohistochemical staining analysis, over-expression of all four Id proteins was identified in cytoplasm of the malignant tissues. The nuclear staining was increased for Id2, Id3 and Id4 but not Id1. Also, in this study the high levels of cytoplasmic Id2 expression in biopsy specimens were correlated with longer survival time of SCLC patients.

Recently, it was found that suppression of Id3 can inhibit tumourigenicity of a SCLC cell line, GLC-19, by using the RNA interference technique (405). Id3-siRNA tranfectant cells produced significant reductions in proliferation rates and in numbers of colonies formed in soft agar assay. When both Id3-siRNA and control transfectant cells were inoculated subcutaneously into nude mice, although there was no difference in tumour incidents among groups, the size and weight of the tumours were significantly decreased compared to the control. Upon induction of apoptosis by cytotoxin camptothecin, the percentage of apoptotic cells in Id3-siRNA transfectants were significantly higher than that in parental cells.

Overall, the role of Id family in the tumourigenicity and progression of SCLC are still unclear. The knowledge of Id family in other malignancies is served as clues for the putative characters and functions of that in SCLC. However, SCLC is such a distinct carcinoma in both clinical and biological features, therefore to elucidate the role of Id proteins in SCLC is of great importance.

1.2.4. Summary and Hypothesis

1.2.4.1. Summary

Lung cancer is a predominant fatal neoplasm. SCLC accounts for 15% of all lung tumours, and is the most aggressive subtype with highest growth fraction, shortest doubling time and early widespread metastases. The efficient detection at early stage and effective therapies are blank until now. Due to the relapse of the disease, it is estimated that only 3-8% of all patients with SCLC can survive beyond 5 years despite treatment

Evidence has showed that dysregulation of Id proteins can induce oncogenic transformation and render cells malignant. The role of Id proteins has been explored in several biological settings such as embryonic development, cell cycle control, differentiation, proliferation, angiogenesis, migration and invasiveness. However, the molecular mechanism responsible for aberrant Id expression in specific cancer type (such as SCLC) has not been elucidated. In addition, the activities of upstream and downstream target that regulated by Ids are still not clear.

The previous investigation performed has suggested a link between Id proteins and SCLC. Over-expression of Id proteins (Id1, Id2 and Id3) has been observed in numerous malignant SCLC cell lines compared with the non-malignant bronchial epithelial cell line Beas-2B. Similar results have been found in SCLC tissues. Suppression of Id3 by Id3 siRNA inhibited the tumourigenicity of SCLC both *in vitro* and *in vivo*. In this study, we intend to simultaneously suppress Id1 and Id3 expression to study the role of Id proteins in SCLC.

1.2.4.2. Hypothesis and objectives

Id1, Id2 and Id3 were highly over-expressed in SCLC in our previous work, it is not known what exact roles they may play in SCLC cells and whether they can be used as

a joint or separate treatment targets for tumour suppression. In this study, we hypothesised that simultaneous suppression of Id1 and Id3 can jointly inhibit the tumourigenicity of SCLC.

To achieve the aim of testing this hypothesis, we set the following sub-objectives step by step so that we can track progress of the whole project.

1. Screen for the most effective silencer for Id1
2. Establishment of SCLC cell lines with reduced expression levels of Id1 and Id3
3. To study the effect of suppressing both Id1 and Id3 on tumourigenecity in SCLC
4. To explore the role of Id1 and Id3 in regulating angiogenesis and apoptosis

CHAPTER 2

METHODS AND MATERIALS

CHAPTER 2 METHODS AND MATERIALS

2.1. Cell culture

2.1.1 Initiate cell culture from frozen stock

For long-term storage, all cell lines had been frozen down and preserved in liquid nitrogen. To initiate a new cell culture, vials were collected from liquid nitrogen storage and immersed into 37^{o}C water bath for 1-2 minutes by continuously swirling to quickly thaw the cells. While holding the tip of the vial, the outside of vial should be carefully cleaned with 70% ethanol before transferring to cell culture dish. As dimethyl sulphoxide (DMSO) in the cryoprotectant has been identified to induce differentiation, thawed cells were diluted in 20 ml of fresh culture media. After a centrifuge at 900 rpm for 3 minutes, the supernatant was decanted gently, cells were resuspended in 10 ml of fresh culture media and plated in a 25 cm^2 flask. An aliquot was removed for cell count. Cells were placed in the incubator at 37 ℃ with 5% of CO_2 before proceeding with other experimental manipulations. Culture media was replaced when necessary. Variant human SCLC cell line N417 and normal bronchial epithelial cell line Beas-2B were grown in RPMI-1640 (Life Technologies), supplemented with 10% (v/v) FCS (Biosera), 2 mmol/l L-glutamine,100 U/ml penicillin and 100 μg/ml streptomycin (Lonza). Human Umbilical Vein Endothelial Cells (HUVECs) were cultured with EndoGRO reduced-serum medium (Millipore).

2.1.2 Subculture of suspension cells

N417 is a suspension cell line and should be subcultured in the exponential growth phase when they appear bright, round, refractile under the microscope. Media including phenol red should be pinky orange in colour but not yellowish. A small amount of culture cells was removed to determine cell density and viability with hemocytometer after trypan blue staining. According to the viable cell density and desired final volume of the flask, the appropriate volume of pre-warmed culture medium and required number of cells were transferred to the new flask. Culture vessels were placed in the 37℃ incubator with 5% CO_2. Cells were daily checked under the microscope to ensure they were healthy. Subculture was repeated as required to avoid overgrowth.

2.1.3. Subculture of adherent cells

Beas-2B and HUVEC cells are adherent cells. They were microscopically viewed and split when reached 80-90% confluency. Used medium was removed by using sterile pipette. Subculturing demands rupture of intercellular and cell-to-substrate connections by introducing proteolytic enzymes such as trypsin. To reduce the concentration of divalent cations and proteins that inhibit trypsin action, attached monolayer cell was washed 1 or 2 times with PBS without Ca^{2+}/Mg^{2+} prior to trypsinisation. The volume of the PBS used should be approximately half of the culture medium. Appropriate volume of trpsin/versene (1 ml per 25 cm^2 of surface) was transferred to the flask with monolayer cell. Gently rotated the flask to make sure trpsin/versene covered the entire surface areas. Flask with monolayer cell was incubated at 37℃ for 3 minutes or until cells were detached. Cautiously tapping on

one side of the culture vessel can help release the cells. After dissociation, double volume of culture medium was added to deactivate the enzyme. The medium and cells were centrifuged to remove the trpsin/versene, and cell pellet was resuspended in fresh medium. Cell culture disk containing cells and fresh medium was return in the incubator. This process was repeated as required by the growth properties of the cell line.

2.1.4. Cryopreservation of cells

Healthy cultures have to be frozen in late log phase growth for the cryopreservation of cell lines. Monolayers of the adherent cells should be detached from the tissue culture vessel by using trypsin/versene. After dissociation, cells were resuspended in growth medium and counted to determine percentage viability and total number of cells. Suspention cells can be directly subjected to perform a cell count. Ideally viability of cells should be in excess of 90% in order to achieve a successful cell recovery after the frozen state. Thereafter, cells were resuspended with freezing medium at a concentration of 2-4$\times 10^6$/ml, 1ml of cells was pipetted into each cryovial which had been properly labelled with cell line name, cell concentration, passage number, and date. Cryovials containing cells were placed in cryobox to be frozen at a slow controlled rate, decreasing the temperature approximately 1℃ per minute. During the freezing process, DMSO in the freezing media was absorbed into the cell membranes to prevent ice crystal formation for preservation of cell viability. Cryobox was stored at -80℃ overnight before transferring to liquid nitrogen for long term storage.

2.2. RNAi technology

2.2.1. RNAi Overview

RNA interference (RNAi) possessing an evolutionarily conserved feature, and it is a naturally existed mechanism to inhibit gene expression. RNAi has been developed into a powerful approach for the studies of loss-of-function in eukaryotic organisms. RNAi was initially discovered in *Petunias* (406), a couple of years later observed in *C. elegans* when another group of scientists demonstrated the double-stranded RNA (dsRNA) triggered gene-silencing effect. It is suggested that RNAi play a role as a defence mechanism against invaders such as RNA viruses or transposons. The double-strand form of invaders can trigger RNAi to inactivate their genes.

After entering the cell, the long dsRNA is cleaved by ribonuclease III-like enzyme (Dicer) into short double stranded molecules called small interfering RNAs (siRNAs) in an ATP-dependent reaction (**Figure 2.1**). siRNA is 21-23 nucleotides fragments in length containing 2 nucleotide overhangs on the 3' end. Every single siRNA duplex consists of a guide (antisense) strand and a passenger (sense) strand. Catalyzed by endonuclease Argonaute 2 (Ago 2), the siRNA duplex becomes unwound. The passenger strand is released, while the guide strand binds to the RNA-inducing silencing complex (RISC). Under the guidance of the remaining strand, RISC directs degradation of complementary mRNA by endonucleolytic cleavage of the target mRNA.

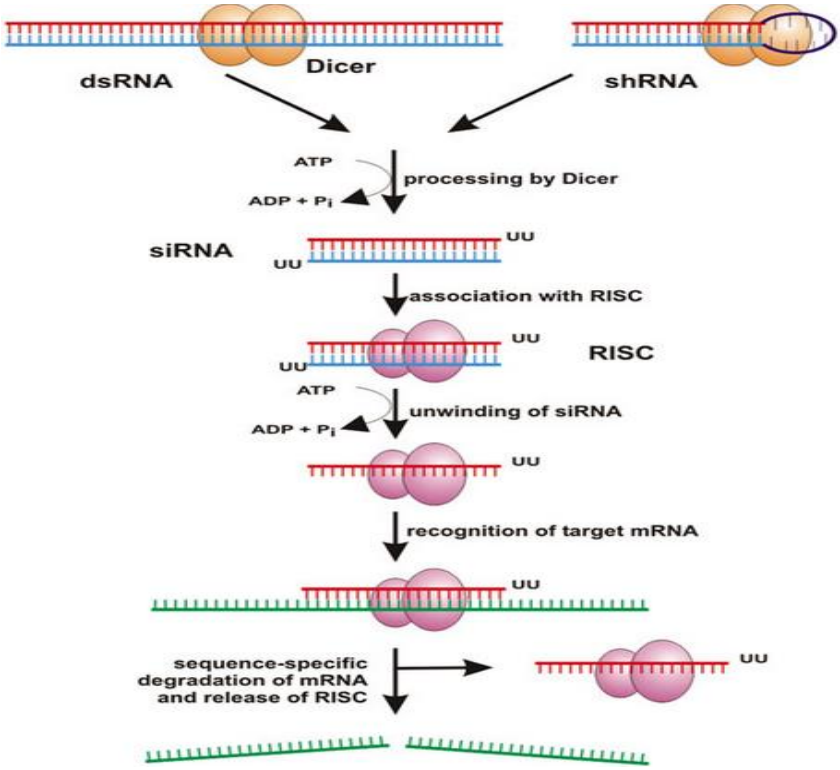

Figure 2.1. RNA Interference mechanism. The RNA interference pathway: when long double-stranded RNA (dsRNA) or small hairpin RNA (shRNA) enters the cell, it's processed by Dicer to yield small interfering RNA (siRNA). Duplex siRNA is accompanied by RNA-induced silencing protein complex (RISC) and regulates target sequence specificity for subsequent mRNA cleavage leading to gene silencing. Source: RNAi Database sample wiki.

2.2.2 Transient transfection

2.2.2.1 siRNA design

To optimize the gene knock down effect, several factors that can influence siRNA result should be considered for siRNA design. There are several important principles

to guide how to select siRNA targets on mRNA sequences: 1) target sequences locate 50-100 nt downstream of the start codon (ATG); 2) siRNAs with 3' overhanging UU dinucleotides are the most effective sequences; 3) the optimum of G+C content in the target sequences should between 30-52%; 4) avoid more than three consecutive same bases appear; 5) avoid 5'URT (5'-untranslated region) and 3'UTR (3'-untranslated region); 6) avoid sequences that share more than 16-17 contiguous base pairs of homology with other related or unrelated genes.

2.2.2.2 Obtain mRNA sequence of target gene

Before screening for the siRNA target on the gene of interest, the mRNA or cDNA sequence of corresponding gene is required and can be retrieved from a nucleic acids database such as the NCBI Gene database (http://www.ncbi.nlm.nih.gov/gene/) by entering gene name and the desired organism. It is preferred to choose RefSeq which is the unique accession number starting with NM or XM. There are many different programs online to search for candidate siRNA targets. In this study, tool on the website of the Whitehead Institute has been applied to select siRNAs. Additionally a mandatory BLAST search is available for this siRNA finder to reduce off-target effects. Three different siRNA molecules were commercially synthesized in order to test the most effective suppressor among the multiple candidates. To validate the siRNA experiment, Silencer® Select Negative Control (Life Technologies) was chosen as the negative control. This commercially available negative control was designed not to target any gene in human, rat, mouse cells. Therefore, no detectable silencing should be found in the cells treated with this control. The negative control or non-targeting siRNA was served to evaluate non-specific knock-down effects in the

RNAi experiments.

2.2.2.3 siRNA delivery

The siRNA is transported into the eukaryotic cell by using lipid based methods. Conventional lipid-mediated delivery relies on the formation of liposomes. Liposomes mediate the fusion of negatively charged nucleic acids and cationic lipid complex with the plasma membrane (407). Current lipofection regents, however, supply nonliposomal lipids which combine the nucleic acids to form a complex. This complex can entry the cell through the endocytic route and release the exogenous nucleic acids into the cytoplasm. Nonliposomal lipids perform efficiently on a wide range of cells even in the presence of serum and display significantly reduced cytotoxic effects. Owing to these two essential elements, nonliposomal lipids have been more widely used than the conventional liposome-based delivery method. This nonliposomal lipid method can be used universally in both transient and stable transfection (408).

2.2.2.4 Optimizing conditions of transient transfection

To obtain the ideal concentration of the factors participating in the transient transfection, it is prerequisite to optimize the conditions before the formal experiment. On the whole, siRNA effect can be observed within five hours and lasts for 24 to 48 hours. Transfection efficiencies of nonliposomal lipid delivery are usually considered high, but may vary between different cell types. In general, suspension cells are believed to be more stubborn than adherent cells. In this study, the suspension N417

cell line was initially used in optimization experiment following the manufacture's instruction. However, RNAi effects were faint and hardly be detected by Western blot analysis. Afterwards, HELA cells (monolayer cells which have been widely used in the transfection experiment) were introduced in the optimization process to confirm the effect of siRNA and the efficiency of transfection reagent. However, the same conditions were failed to produce optimal results on N417 cell. Then increased amount of siRNA and transfection reagent was tested with N417 cells, and showed Id1 and Id3 suppression effect. All the following transient transfection tests on N417 cells were conducted using these conditions.

2.2.2.5 Transient transfection of Id1

The sequence of 21 nt of mRNA with 40-60% GC content were recorded as optimal targeted region to perform the RNA interfering assay. Three siRNA target sequences (**Figure 2.2**) were selected by running the siRNAext program on the website of The Whitehead Institute for Biomedical Research (http://jura.wi.mit.edu/siRNAext). We initially screened all three siRNA candidates and anticipated to choose the best suppressor by using Western blotting. To minimise the siRNA off-targeting effects, all chosen siRNAs have been tested with nucleotide BLAST (http://blast.ncbi.nlm.nih.gov/Blast.cgi). The proper siRNA sequence for Id3 has been confirmed by the previous study (405). Sequences used for Id1 siRNA assay were as follows:

Sequence 1 for Id1	
sense strand	5’: CGCCAAGAAUCAUGAAAGU UU
antisence strand	5’: ACUUUCAUGAUUCUUGGCG UU
Sequence 2 for Id1	
sense strand	5’: CUAGUCACCAGAGACUUUA UU
antisence strand	5’: UAAAGUCUCUGGUGACUAG UU
Sequence 3 for Id1	
sense strand	5’: CGCAUCUUGUGUCGCUGAA UU
antisence strand	5’: UUCAGCGACACAAGAUGCG UU

Three siRNA sequences against Id1 were manufactured (Life Technologies). A Silencer® Select Negative Control (Life Technologies) was purchased commercially and used to monitor all factors which may affect the result such as toxicity of transfection reagent or siRNA itself.

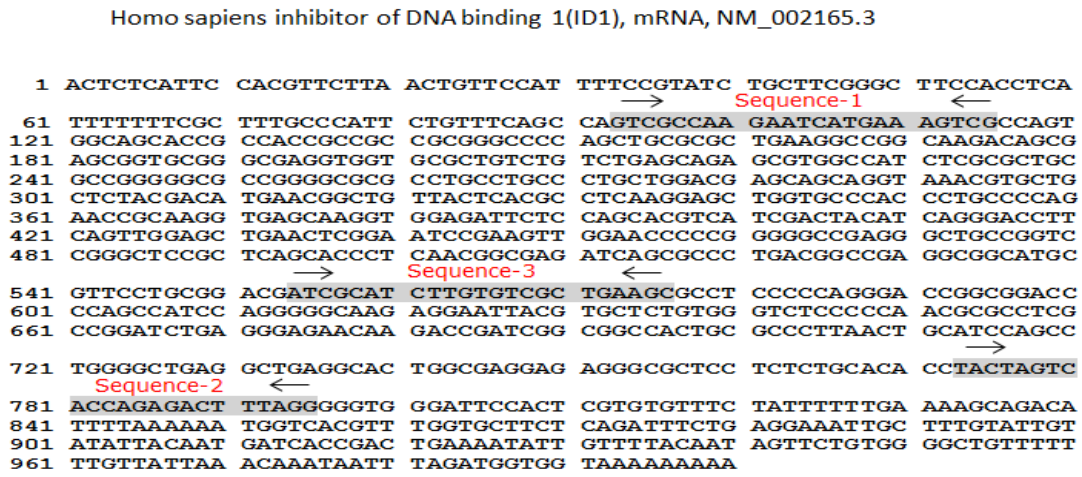

Figure 2.2. Nucleotide sequences of three siRNAs against Id1. The sites where three sense strand sequences of siRNAs located were lightly shadowed in Id1 cDNA. The siRNAs targeting Id1 were selected through Whitehead library, for screening the most effective suppressor of Id1. Silencers examined were not validated previously.

To avoid adverse effect of the antibiotics and sera for the transfection efficiency, cells were washed twice with PBS and resuspended in normal growth medium without antibiotics. Cell suspension was adjusted to 1×10^5 cells /ml and added to the siRNA/transfection reagent mixture. Transient transfection was performed within 6-well plates. Two wells were set up as negative control. One well contained cells, scramble RNA and transfection reagent, another well contained cells and transfection reagent to rule out the cytotoxicity of transfection reagent. Eight μg siRNA duplex was diluted in 100 μl of Opti-MEM I Reduced Medium (Life Technologies), the contents were mixed by gentle pipetting. Forty μl of X-tremeGENE siRNA Transfection Reagent (Roche) was diluted in 100 μl of Opti-MEM I Reduced Medium. Diluted

siRNA should be combined with transfection reagent within 5 minutes. The complex was mixed gently and incubated 15-20 minutes at room temperature. The diluted cells (2 ml) were transferred to each well containing siRNA/transfection reagent complex, and the wells were swirled cautiously to ensure distribution over the entire plate surface. Cells were harvested after 24, 48, 72 hours respectively and subjected to evaluation assay to check the effect of gene knockdown. In this study, the suppression effect of the Id1-siRNA was identified with Western blotting.

2.3. Stable transfection

2.3.1. Design of shRNA

After transient transfection, the most effective Id1-siRNA sequence which caused the greatest reduction in expression level of target gene was chosen for short hairpin RNAs (shRNAs) construction. Two shRNAs insert consisted Id1 and Id3 siRNA were designed using tools online (http://www.sirnawizard.com), and cloned respectively into the psiRNA-DUO vector (InvivoGen) which was capable of expressing two shRNA simultaneously. Two scrambled RNA sequences were cloned into the same plasmid as control. N417 cells were transfected with a vector containing Id1 and Id3 shRNA or a vector containing scramble RNA molecules using X-tremeGENE HP DNA transfection reagent (Roche). A separate construct containing shRNA against Id1 only was also transfected in parallel. To isolate single colony from the suspended cells, stable transfectants were selected after cells were cultured for 4 weeks with a semisolid ClonaCell-TSC (StemCell Technologies) selective medium containing 75

μg/ml Zeocin (Life Technologies).

2.3.2. Vector

RNA interference (RNAi) has emerged as a powerful tool to study gene functions in mammalians. RNAi leads to target gene silencing by the cleavage of long dsRNA into small interfering RNA (siRNA) and formation of RNA induced silencing complex. The double stranded siRNA is 21-23 nucleotides in length with 2 nucleotide overhangs on the 3′ ends, or 43-51 nucleotides in length containing a hairpin structure, which is also called small hairpin RNA (shRNA). Degradation of target gene by using RNAi technique is extensively used in both biomedical studies and clinical trials. However, the RNAi response initiated by siRNA is transient due to the short lifespan of RNAs. To overcome this limitation, a variety of vectors have been produced to deliver the RNAs to the host cells. InvivoGen has designed a plasmid vector that facilitates the stable production of two siRNAs within the cell (**Figure 2.3**).

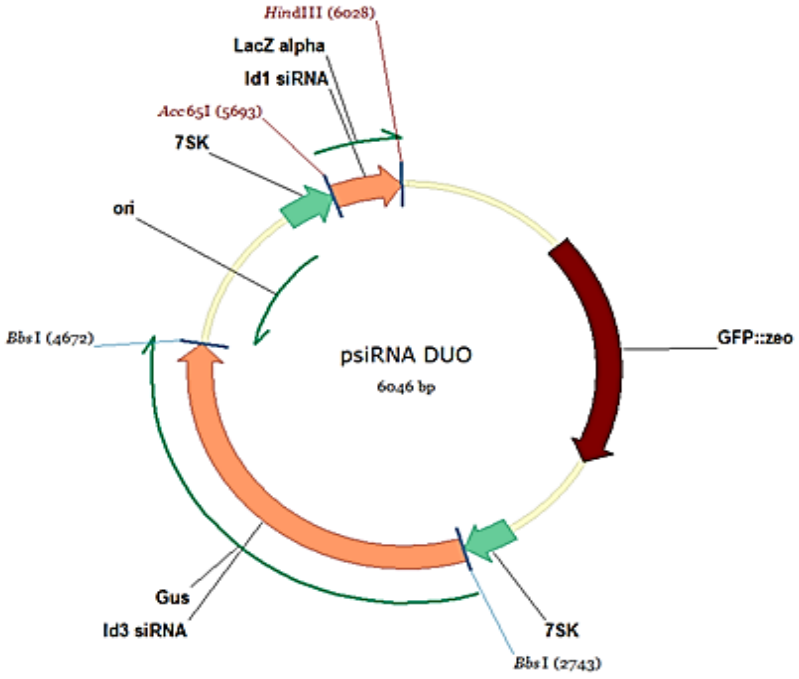

Figure 2.3. Plasmid map of psiRNA-DUO, a dual RNA PolIII cassette vector for the expression of two shRNAs.

psiRNA-DUO, a duet vector, is designed for the cloning and expression of two short hairpin RNAs (shRNAs) in a single plasmid vector to knockdown two target genes simultaneously. psiRNA-DUO contains two expression units for siRNA inserts, two human 7SK RNA polymerase III promoters and multiple restriction enzyme sites. Both inserts are cloned downstream of the 7SK promoter, and each of the siRNA insert is controlled by a separate 7SK promoter.

psiRNA-DUO plasmid carries a lacZ gene which codes for ß-galactosidase and a ß-glucuronidase fusion gene. In the blue-white screening, chromogenic substrate known as X-Gal or X-Gluc is added to the agar plate. In the first step of transformation, IPTG, an analogue of galactose, is used along with X-Gal to induce the expression of lacZ gene. Due to the ß-galactosidase secreted by non-recombinant

cells can catalyse the hydrolysis of X-Gal to produce blue pigment, the colonies formed by non-recombinant cells are blue while that by recombinant cells are white in colour. In the second step of transformation, the non-recombinant cells which can hydrolyse X-Gluc to generate blue pigment form blue colonies while recombinant cells form white colonies. This blue-white screening allows the discrimination between blue parental clones and white recombinant clones in *E. coli*. psiRNA-DUO also contains a Zeocin resistance fusion gene, which facilitates selection of transformed *E. coli* cells and stable clones of mammalian cells.

2.3.3. Making competent *E.coli* GT115

Generally DNA cannot pass through the membrane of a bacterial cell, because DNA is a hydrophilic molecule. The bacteria are initially made "competent" to take up DNA so that plasmid DNA can be transferred into the bacterial cells. Tiny holes are created in bacterial cells by suspending them in a solution with high concentration of calcium. Using heat shock technique, DNA can be transported into the cells. One vial of *E. coli* GT115 was incubated on ice for 5 minutes, then 1ml of sterile water was added into the tube. *E. coli* cells were gently homogenised and further incubated for 30 minutes on ice. Bacteria (100 µl) were dissolved in 10 ml of autoclaved LB without antibiotic and incubated overnight at 37℃ and 225 rpm in a shaking incubator. One ml of the overnight bacterial culture was transferred into 100 ml of SOB medium containing 1ml of 2M magnesium salts solution. This mixture was incubated at 37℃ and 225 rpm in a shaking incubator for approximately 90 minutes. OD value was examined with spectrophotometer which has been set on 550 nm and calibrated with SOB when

the OD550 reached 0.4. The culture was dispensed into 8 universal tubes and incubated on ice for 10 minutes. Cells were spun at 2,500 rpm for 10 minutes at 4℃, resuspended in a total of 66 ml of RF1 and left on ice for 10 minutes. Cells were spun again as the previously mentioned and resuspended in a total of 16 ml of RF2 buffer. Samples were pooled together and dispensed into 1ml aliquots into cryovials. The aliquots of competent cell were flash frozen in liquid nitrogen and transferred immediately to the -80℃ freezer for long term storage.

2.3.4. Construction of the vector expressing siRNA

2.3.4.1. Annealing the hairpin siRNA template oligonucleotide

The forward and reverse oligonucleotides were dissolved with nuclease-free water at a concentration of 100 μM. After that, oligonucleotides were further diluted to obtain the concentration of 25 μM. The annealing solution was prepared by mixing the following components in a 0.5 ml tube:

Component	Volume
Forward oligonucleotide (25 μM)	2 μl
Reverse oligonucleotide (25 μM)	2 μl
0.5 M NaCl	6 μl
H_2O to a final volume of	30 μl

The above mixture was incubated for 2 minutes at 80℃. Then the tube was maintained in water bath until the temperature reached 35℃ with heating switched off.

The annealed siRNA insert was then stored at -20 ℃ for further use.

2.3.4.2. Digestion of plasmid DNA

2.3.4.2.1. First step digestion to insert Id1 siRNA

A 200 µl reaction was set up a as follows (double digestion):

Component	Volume
Plasmid DNA	10 µl
10 × buffer 2	20 µl
100 × BSA	2 µl
Nuclease water	148 µl
*Acc*65I	10 µl
*Hin*dIII	10 µl

The above components were mixed by tapping and subjected to a brief centrifuge to remove bubbles. The tube was incubated at 37 ℃ in water bath for 2 hours. To guarantee the transformation efficiency, the restriction enzyme was heat inactivated by incubating the tubes at 80 ℃ for 20 minutes. The digested plasmid DNA was loaded on a 0.8 % low melting temperature agarose gel. Low melting temperature agarose powder (0.8 %) was dissolved in 40ml 0.5 ×TBE. Solution was microwaved with lid not screwed on tight. Time was initially set for 1 minute and then further 30 seconds until completely melted. After cooling the solution to about 55 ℃, safeview, a flourescent dye was added to the gel (final concentration of 5 µl/ml) to facilitate visualization of DNA. The agarose solution was poured into a casting tray with a

sample comb and allowed to solidify at room temperature for about 30 minutes. Samples were loaded to all wells except the first lane for DNA marker. The gel ran at 80 voltages for 1 hour. This gel was visualized on a U.V. trans-illuminator to check the digestion of plasmid DNA.

The large fragment (5711 bp) was cut after running a low melting temperature gel, and agarose DNA was cleaned up using PCR cleanup kit (Promega). The weight of the agarose gel was measured and membrane binding solution was added at a ratio of 10 µl of solution per 10 mg slice of agarose gel. The tube containing gel and membrane binding solution was incubated at 65℃ for 10 minutes and was shaken several times until all agarose gel was melted. The dissolved gel mixture was transferred to the SV minicolumn assembly and incubated for 1 minute at room temperature. The SV minicolumn assembly was centrifuged at 14,000 rpm for 1 minute. The flow through liquid in the collection tube was discarded. Then the column was washed by adding 700 µl of Membrane Wash Solution. The SV minicolumn assembly was centrifuged for 1 minute at 14,000 rpm. After spin, the collection tube was emptied as before. Washing was repeated with 500 µl of Membrane Wash Solution and the SV minicolumn assembly was centrifuged for 5 minutes at 14,000 rpm. The collection tube was carefully emptied as before. To allow evaporation of any residual ethanol, the collection tube was recentrifuged for additional 1 minute with the microcentrifuge lid open. The SV minicolumn was then placed to a clean 1.5ml microcentrifuge tube. nuclease-free water (50µl) was transferred directly to the center of the column without touching the membrane. After the incubation for 5 minutes at room temperature, the column was centrifuged for 1 minute at 14,000 rpm. The flow-through solution containing the eluted DNA was stored at –20℃.

2.3.4.2.2. Second step digestion to insert Id3 siRNA

A 200 µl digestion was set up as follows:

Component	Volume
Plasmid DNA	10 µl
10 × buffer 2	20 µl
100 × BSA	2 µl
Nuclease water	158 µl
*Bbs*I	10 µl

The above components were mixed by tapping and subjected to a brief centrifuge to remove bubbles. The tube was incubated at 37 ℃ in water bath for 2 hours. To guarantee the transformation efficiency, the restriction enzyme was heat inactivated by incubating the tubes at 65 ℃ for 20 minutes. The digested plasmid DNA was loaded on a 0.8 % low melting temperature agarose gel.

2.3.4.3. Ligation reaction

The vector was ligated with the insert by using T4 ligase. A 20 µl ligation reaction was set up as follows:

Component	Volume
Digested psiRNA DNA	100 ng
Annealed siRNA insert	1 µl
Nuclease water	15 µl
10 × buffer	1 µl
T4 ligase	1 µl

All the components were transferred into a sterile tube and mixed well by pipetting. Then the tube was centrifuged for 5 seconds. The reaction was incubated overnight at 16 ℃. The next day, the reaction was stopped by placing the tube in -20 ℃. Ligation reaction aims to join together two DNA molecules: digested plasmid DNA and siRNA insert. The ligation reaction is usually catalysed by T4 DNA ligase, which is the DNA ligase enzyme most commonly used in the cloning engineering to ligate 'sticky' or blunt ends (409). To achieve the optical ligation result, the two component of the reaction should be equimolar and around 100 μg/ml. The siRNA inserts have been predesigned with restriction enzyme sites at two ends, which were ready to be ligated into the digested plasmid, and proceeded to bacterial transformation. The insert to vector ratio has a vital effect on the outcome of the ligation and subsequent transformation. The ideal molar ratios for ligating insert to vector vary from 1:1 to 10:1. The insert amount can be calculated with the following formula: Insert Mass in ng = 6 × $\left[\frac{\text{Insert Length in bp}}{\text{Vector Length in bp}}\right]$ × Vector Mass in ng.

2.3.4.4. Bacterial transformation

Transformation protocol in this project was in two-step to clone the two siRNA inserts into the plasmid separately. An aliquot of frozen competent *E. coli* GT 115 cells was thawed out on ice. After mixing gently, 200 μl of the competent *E. coli* cell suspension was transferred into a sterile falcon 2059 tube. No more than 50 ng of the plasmid DNA in a volume of 10 μl or less was added for plasmid amplification, 10 μl of ligation product was required for recombinant plasmid transformation. Then the tube containing the mixture was swirled gently for a few seconds by finger flicking and

incubated on ice for further 30 minutes. In this set of experiment, plasmid was designed to be taken into the *E. coli* cells by heat shocking. After 30 minutes' incubation on ice, tube was placed in a 42 ℃ water bath and incubated for exactly 90 seconds without shaking. Tube was immediately replaced onto ice and kept for 2 minutes. To recover the transformed cells, 800 µl of SOC (preheated at 42 ℃) was added to the tube and it was incubated at 37 ℃ for 1 hour with shaking at 225 rpm. LB agar powder (10.5 g) was weighed out and dissolved with 300 ml of distilled water and pH was adjust to 7.5. The solution was autoclaved for 20 minutes, allow it to cool around 55 ℃ or until the bottle can be picked up with bare hands. To prepare the plates for the first step transformation, 75 µl of Zeocin (25 µl/ml) was added to LB agar solution with supplement of X-gal and IPGT. The jar was swirled to make the component well distributed. For the second step of transformation, X-Gluc plates were prepared with Fast-Media Zeo X-Gluc following the manufacture's instruction (InvivoGen). Approximately 25 ml of LB agar was poured out into each sterile Petri plate. It should take 20 minutes to allow each plate to set until it was ready for transformation.

Two types of agar plates have been prepared with and without Zeocin. Alongside the transformation reaction, plasmid alone was also transformed into *E. coli* cells as a control. The transformed reaction (100 µl) was plated out on both LB agar plates with or without Zeocin. The *E. coli* cells alone were plated out on both LB agar plates and LB agar antibiotic plates to ensure that the competent cells are alive. The following table shows how each plate was prepared.

The plates for transformation were set up as:

NO. of plate	Zeocin	Volume of plasmid transformation alone	Volume of transformation (ligation reaction)	*E. coli* GT115 alone
1	25 µg/µl	--	50 µl	--
2	25 µg/µl	--	100 µl	--
3	25 µg/µl	--	200 µl	--
4	--	--	100 µl	--
5	25 µg/µl	100 µl	--	--
6	--	100 µl	--	--
7	25 µg/µl	--	--	100 µl
8	--	--	--	100 µl

Plates were left to settle for 10 minutes and then inverted to incubate overnight at 37℃. The next day, plates were examined for bacterial growth. Six single colonies (the first step transformation) and five single colonies (the second step transformation) were picked up with an inoculating loop. Every single colony was inoculated in 10 ml of LB containing the antibiotic and incubated in the shaking incubator at 300 rpm over night at 37℃ until the solution becomes quite turbid. The next day, 3 ml of the overnight culture was removed and the plasmid DNA was extracted using the plasmid mini-prep kit (QIAGEN).

2.3.4.5. Confirmation of the presence of siRNAs

2.3.4.5.1. Agarose gel electrophoresis

To confirm presence of siRNA, the extracted plasmid DNA was digested with different restriction enzymes and examined by running on a mini agarose gel. The presence of the Id1 siRNA insert was confirmed on a 0.8% agarose gel after digestion with *Cla I* and *Nde I* restriction enzymes (2 hours at 37℃). The presence of the Id3 siRNA insert was confirmed on a 0.8% agarose gel after digestion with *Psp1406 I* and *Nsi I* restriction enzymes (2 hours at 37℃).

Samples for agarose gel electrophoresis were prepared as following:

Component	Volume
DNA	1 μg
6 × DNA loading buffer	2 μl
add water to	12 μl

Agarose solution (0.8 %) was made up with 40 ml 0.5×TBE. Solution was microwaved with lid not screwed on tight. Time was set for 1 minute first and then further 30 seconds until agarose was completely melted. After cooling the solution to 55℃, safeview, a florescent dye was added to the gel (final concentration 5 μl/ml) to facilitate visualization of DNA. The agarose solution was poured into a casting tray with a sample comb and allowed to solidify at room temperature for around 30 minutes. Samples were loaded to wells with first lane for DNA marker. The gel was electrophoresed at 80 voltages for 1 hour. This gel was visualized on a U.V. trans-illuminator to check the insertion of the siRNA.

2.3.4.5.2. Sequencing of the siRNA insert

The successful construction of the plasmid DNA checked by agarose gel was sent for sequencing (Cogenics) to confirm the presence and orientation of the insert. This was performed in two steps as following:

1) The first step: the positive clones were sequenced to verify the insert for Id1-shRNA.

Primer	MW	Tm	Sequence
OL178 (forward)	6090 g/mol	57.3 ℃	5’ TCTTTTCTACGGGGTCTGAC 3’ (20 mer)
OL408 (reverse)	6141 g/mol	55.3 ℃	5’ GCGTTACTATGGGAACATAC 3’ (20 mer)

2) The second step: the positive clones were sequenced to verify the insert for Id3-shRNA.

Primer	MW	Tm	Sequence
OL906 (forward)	7184 g/mol	60.6 ℃	5’ CAAGTAGAGGCTTGATTTGGAGG 3’ (23mer)
OL176 (reverse)	6144 g/mol	57.3 ℃	5’AGCCTATGGAAAAACGCCAG 3’ (20 mer)

To obtain the large quantity of DNA of the positive colony, 25 µl of the overnight culture was transferred into 250 ml of LB containing antibiotic and incubated in the shaking incubator over night at 37 ℃ at 300 rpm until the solution becomes cloudy. The bacterial cells were harvested by centrifugation at 6000 ×g for 15 min at 4 ℃ and

then resuspended the bacterial pellet in 4 ml buffer P1. Four ml buffer P2 was added to the cells and mixture was mixed thoroughly by vigorously inverting the sealed tube 4–6 times, and incubated at room temperature for 5 minutes. After transferring 4 ml of chilled buffer P3 and mixing immediately and thoroughly by vigorously inverting 4–6 times, the tube was placed on ice for 15 minutes. The solution was centrifuged at 20,000×g for 30 minutes at 4℃. Then the supernatant containing plasmid DNA was centrifuged again at 20,000×g for 15 minutes at 4℃. Buffer QBT (4 ml) was applied to a QIAGEN-tip 100 to run through the column, after this allow the supernatant containing DNA enter resin by gravity flow. When the supernatant finished, the QIAGEN-tip was washed twice with 10 ml of buffer QC. DNA was eluted with 5ml of buffer QF and precipitated by adding 3.5 ml room-temperature isopropanol. The solution was pipetted and centrifuged at ≥15,000×g for 30 minutes at 4°C. DNA pellet was washed with 2 ml of room-temperature 70% ethanol, and centrifuged at ≥15,000×g for 10 minutes. Then the pellet was air-dried for 5–10 minutes, and the DNA was dissolved in 50 µl of nuclease free water.

2.3.5. Transfecting mammalian cells

2.3.5.1. General considerations before transfection

The suspension cells (1×10^5/ml) were resuspended in 2 ml of culture medium. For best results, DNA purity was determined using a 260 nm/280 nm ratio (the optimal ratio is 1.8). The plasmid DNA solution was prepared using sterile TE (Tris/EDTA) buffer or sterile water at a concentration of 0.1 to 2.0 µg/µl. High quality DNA preparation kits was used to obtain endotoxin-free DNA. Culture cells that remain

untransfected and cells transfected with scramble RNA were used as the negative control.

2.3.5.2. Transfection Procedure (To optimize the condition)

X-tremeGENE HP DNA Transfection Reagent (Roche), DNA and Opti-MEM medium (Life Technologies) were allowed to equilibrate to +15 to +25 ℃. The X-tremeGENE HP DNA Transfection Reagent vial was briefly swirled before use. The recombinant DNA with sh-Id1-Id3 insert was diluted with Opti-MEM medium. All the solution was mixed gently. Two hundred µl of diluents containing 8 µg DNA was placed into each of three sterile tubes labelled 1:1, 2:1, and 3:1. The X-tremeGENE HP DNA Transfection Reagent (8, 16, 24 µl) was pipetted directly into the medium containing the diluted DNA without contacting with the walls of the tubes. All the solution was mixed gently. The transfection reagent/DNA complex was incubated for 15 minutes (up to 30 minutes) at +15 to +25 ℃. The transfection complex was added to the cells in a dropwise manner. The six-well plate was gently swirled to ensure even distribution over the entire plate surface. Following transfection, cells were incubated for 18-72 hours before measuring protein expression.

Culture vessel	Volume of Plating Medium (ml)	Amount of transfection complex(µl)	DNA (µg) using 1:1	Transfection Reagent(µl) using 1:1 Ratio	Transfection Reagent(µl) using 2:1 Ratio	Transfection Reagent(µl) using 3:1 Ratio
6-well plate	2	200	8	8	16	24

2.3.5.3. Optimisation of antibiotic-resistant selection

The concentration of Zeocin was recommended from 50 to 1500 µg/ml. Fifty µg/ml is a good start point. The viable cells were examined for every 2 days. The lowest Zeocin concentration that begins to give massive cell death for parental cells was identified in approximately 7-9 days, and that kills all parental cells within 2 weeks. This concentration was used to select transfected cells containing siRNA after transfection.

2.3.5.4. Transfection protocol

X-tremeGENE HP DNA Transfection Reagent, DNA and Opti-MEM medium were allowed to equilibrate to room temperature. The X-tremeGENE HP DNA Transfection Reagent vial was briefly vortexed before use. The reconstruct plasmid DNA with si-Id1-Id3 insert was diluted with Opti-MEM medium. All the solution was mixed gently. Two hundred µl of diluents containing 8 µg DNA was placed into a sterile tube. Eight µl of X-tremeGENE HP DNA Transfection Reagent was pipetted directly into

the medium containing the diluted DNA without contacting with the walls of the plastic tubes. All the solution was mixed gently. The transfection reagent: DNA complex was incubated for 15 minutes (up to 30 minutes) at +15 to +25℃. The transfection complex was added to the cells in a dropwise manner. The six-well plate was gently swirled to ensure even distribution over the entire plate surface. To isolate single colony from the suspended cells, stable transfectants were selected 4 weeks after cells were cultured in a semisolid ClonaCell-TSC (StemCell Technologies) selective medium containing 75 μg/ml Zeocin (Life Technologies).

2.4. Cell lysis and protein extraction

Firstly, the cells were counted with haemocytometer and treated differentially regarding their growth manners (Adherence/Suspension). For adherent cells, growth medium was removed, cells were washed with PBS and resuspended in lysis buffer celLytic-M (Sigma). For suspension cells, culture was centrifuged for 3 minutes at 900 rpm and supernatant was decanted. Cells were washed with PBS and resuspended in lysis reagent. Approximately 10^6-10^7 cells were pelleted and can be stored in -20℃ if the cells were not been used in short time. Cells can be stored in the freezer before extracting protein for two months. To dissolve the cells, 125 μl lysis buffer was added per 10^6-10^7 cells in general. Cells and lysis reagent were mixed by pipetting up and down, and transferred to a 1.5 ml mircotube. To avoid protein degraded, 10 μl/ml of protein inhibitor (Sigma) was added to each tube. This mixture was incubated for 15 minutes on a shaker. Lysed cells were centrifuged at 12, 000×g for 10 minutes to pellet the cellular debris. Supernatant was transferred to a pre-chilled 1.5 ml mircotube.

Lysate preservation may be kept in -20 ℃ freezer for 1-2 day, however -80℃ is recommended for long term storage.

The Bradford assay was used to determine the total protein concentration in solutions to ensure equivalent loading of samples on the gel. When proportional protein molecules in protein samples binding to Coomassie Blue G-250 dye under acidic conditions, Coomassie Blue G-250 dye convert from red form into its blue form (410). The protein-dye complex results in spectral shift of the dye absorption from 465 nm to 595 nm. The optical absorbance of the solution with proteins can be detected at a wavelength of 595 nm. The elevated amount of absorption at this wavelength reflects the proportionally increased protein present in the given solution. In addition, this proportional correlation is linear within a particular range. To measure the concentration of unknown samples, a regression curve should be derived from the standards using bovine serum albumin (BSA). The procedure of standard Bradford assay was carried out as follows. Dye reagent was diluted in four times of distilled water and filtered through filter sheet. To construct a BSA calibration curve, 0, 0.625, 1.25, 2.5, 5 µl of BSA standard solution (Sigma-Aldrich, 0.4 mg/ml) was added to each of 1.5 ml labelled microtubes. Complement with distilled water to reach 50 µl/well. Using new microtubes, 5 µl of unknown sample was diluted with 45 µl distilled water. Each standard and protein sample was incubated by adding 1 ml of diluted dye respectively for 20 minutes at room temperature. All standard and protein samples were measured in duplicate at 595 nm. To analyse the result, the curve of absorbance of each BSA standard had been plotted and the linear equation given as a function of theoretical concentration: y=ax+b, where y=absorbance at 595 nm, x=protein concentration. The protein concentration of the sample can be simply

calculated using the linear equation of the curve.

2.5. Western blots

2.5.1. SDS –PAGE gel electrophoresis

Once sample preparation was completed, proteins were separated on a SDS-PAGE gel electrophoresis. Each SDS-PAGE gel was prepared with 10 ml 12.5% NEXT GEL® (Amresco), 60 µl APS (10%) and 6 µl TEMED. Calculated from the targeting protein density, 20 µg sample combined with 2×loading buffer containing 0.5% 2-beta-mercaptoethanol, was loaded into each lane. Prior to loading, samples were boiling at 95℃ for 5 minutes. Then all samples were briefly vortexed, centrifuged for 1 minute at the maximum speed, and back on ice for 5 minutes to cool down. Ten µl of protein colour marker (Prosieve) and 10µl of 2×loading buffer were loaded in the first well. The gel was run at 150V for 1 hour or until migration front (dye molecule) ran off the bottom of the gel.

2.5.2. Transfer of protein samples to membrane

Following electrophoresis, proteins were electrotransferred from SDS-PAGE gel to a PVDF membrane using Bio-Rad Mini-PROTEAN 3. Six pieces of 3MM filter sheets were cut to the size of 7×10 cm, while the PVDF membrane was cut to the dimensions of 6×9 cm. PVDF membrane was rinsed in methanol, washed with distilled water and consequently equilibrated in cold 1×transfer buffer (25 mM Tris, 192 mM glycine, 20% methanol, pH 8.3) for 15 minutes. The transfer sandwich was created from bottom to

top: black saran wrap, fibre pad, 3 pieces of filter sheets, gel, membrane, 3 pieces of filter sheets, fibre pad, clear saran wrap (Bio-Rad mini trans blot instruction). This sandwich was inserted into the transfer apparatus between two electrodes. Transfer was conducted for 1 hour at 400 mA. The protein migrated out of the gel towards the (+) electrode and stuck to the PVDF membrane when an electric field applied. After transfer, the gel was stained with Coomassie blue for 2 hours to check if the protein had moved out of the gel. Alternatively, the membrane can be stained with 0.1% (w/v) Ponceau S solution to confirm the transfer efficiency.

2.5.3. Antibody staining

To block the membrane, 1×TBST was prepared from 10×TBS plus 0.1% Tween-20. The membrane was initially blocked with 5% skimmed milk in 1×TBST for 1 hour on a roller. Then membrane was incubated with primary antibody overnight at 4℃. The dilution of antibody for Id1 (Abnova) was 1:4,000, Id3 (Abnova) was 1:500, VEGF (Thermo Scientific) was 1:500. Afterwards, membrane was washed in 1×TBST three times, for 5 minutes each time. The secondary antibody used for Id1, Id3 (rabbit anti-mouse horseradish peroxidase-conjugated, HRP, Dako) and VEGF (swine anti-rabbit horseradish peroxidase-conjugated, HRP, Dako) was diluted 1:10,000 in 1×TBST. This incubation lasted for 1 hour at room temperature. Then membrane was washed as previously described. Membrane was drained from the wash buffer and incubated with ECL (Amersham) for 5 minutes, then was transferred to cassette to expose to the film. The membrane was covered by a piece of film at various exposure time points in accordance with the protein type. To check the protein loading, this

membrane was then subjected to incubation with anti-β-actin (1:50,000). The secondary antibody used for checking beta-actin was also diluted 1:10,000 in 1×TBST.

2.6. Invasion assay

2.6.1. Overview

One of the hallmarks of the metastatic process is the ability of malignant tumour cells to invade. During this process the tumour cells modulate the detachment from the primary tumour, the degradation of the surrounding extracellular matrix and migration into the neighbouring tissue. To investigate the mechanisms how tumour cells achieve the metastatic phenotype, a number of *in vitro* assay has been established. The most classical *in vitro* invasion assay is Boyden chamber assay, where cells migrate along a chemoattractant gradient from an upper compartment through microporous membrane into a lower compartment. The membrane coated with an extracellular matrix (ECM) can be used to mimic the basal lamina to study the invasive potential of the tumour cells. This protocol outlines the steps to conduct a cell invasion assay through BioCoat™ Matrigel™ Invasion Chamber (BD), containing 12 well culture inserts with an 8 μm polycarbonate membrane. The membrane has been coated with a layer of ECM to prevent noninvasive cells from going through the membrane.

2.6.2. Procedure

Cell culture was maintained according to standard cell culture procedures. Cells were

harvested and resuspended in serum-free culture medium prior to adjustment to a final concentration of 2×10^5 per ml. The foil bag containing invasion chamber was removed from -20℃ and allowed to come to the room temperature. Around 0.5 ml of pre-warmed (37℃) culture medium was transferred to the interior of the inserts. The chamber was rehydrated for 2 hours in a humidified tissue culture incubator at 37℃, 5% CO_2 atmosphere. After rehydration, the medium in the inserts was carefully removed without disturbing the layer of GFR Matrigel ™ Matrix™ on the membrane. An equal number of control inserts (no ECM coating) were prepared by using sterile forceps to transfer them to empty wells of the 24 well Plate. Culture medium (600 μl) with 20% FCS was added to each well of the 24 well plate (lower chamber). Cell suspended in culture medium without FCS (200 μl) was added to the pre-coated inserts and the control inserts. The pre-coated and control inserts was transferred by using the sterile forceps to the wells. To prevent air bubbles trapped beneath the membranes, the inserts were tipped at a slight angle. Each cell line including the control has been tested in triplicate. The invasion chambers and controls were incubated for 48 hours in a humidified tissue culture incubator at 37℃, 5% CO_2 atmosphere. After incubation, the inserts containing non-invading cells were removed from the wells. As the suspension cells cannot adhere to the membrane, the invasive cells migrated through the membrane and fall down to the bottom wells. The invasive cells in the bottom wells were resuspended in 30 μl of culture medium and counted with cytometer. On each filter, three random fields were countered.

2.6.3. Analysis method

Data is explained as the percentage of invaded cells through the GFR Matrigel™ Matrix™ membrane relative to the migration through the control membrane, using the following formula:

$$\%\text{Invasion} = \frac{\text{Mean of cells invading through GFR Matrigel insert membrane}}{\text{Mean of cells migrating through control insert membrane}} \times 100$$

2.7. MTS assay

2.7.1. Overview

MTS assay is a colorimetric assay to measure mitochondrial activity of the cells, and it has been widely used to reflect the viable cell numbers. (3-(4,5-dimethylthiazol-2-yl)-5-(3-carboxymethoxyphenyl)-2-(4-sulfophenyl)-2H-tetrazolium) (MTS) tetrazolium compounds can be bioreduced by dehydrogenase inside living cells to coloured formazan product, which was soluble in culture media and can be quantified by using microtiter plates and spectrometer. The quantity of formazan can be reflected by the intensity of the absorbance output signal, which is directly proportional to the number of living cells in culture.

2.7.2. Standard curve

To establish a standard curve, both parental cells and transfectants were serially diluted at density ranging from 5×10^3 to 8×10^4 cells per well in a volume of 100 µl and distributed into 96-well plate. For each cell line, the experiment was performed in triplicate. One well contained only culture medium was set up as the blank. MTS

assay was performed by adding 20 µl of MTS solution to each well, incubating for 4 hours at 37 ℃, 5% CO_2 and 95% humidity and recording the absorbance at 490 nm with spectrophotometer (BioTek). A standard curve was drawn between the optical density of formazan and the number of cell. From the standard curve, the linear correlation between the two variables was analysed and regression equation was established. The cell viability of different cell lines can be determined with this standard curve.

2.7.3. Procedure

All transfected, parental and scramble cells were seeded in the 96-well plate in culture media in triplicates, at a density of 5,000 cells per 100 µl. Make sure that the cells were evenly distributed in the wells, not clump in the centre or periphery of the wells. This experiment was carried out in a 8-day period, therefore the cells were subjected to MTS assay on day 2, 4, 6 and 8. The culture plates were gently transferred to the incubator. On each day for MTS assay, the CellTiter 96® AQueous One Solution Reagent (Promega) was thawed for 90 minutes at room temperature prior to use. MTS working solution was prepared by mixing 20 µl of the CellTiter 96® Aqueous One Solution Reagent with 100 µl of cell suspension in each well of the 96-well plate. The culture plates were incubated for 4 hours at 37 ℃ in a humidified, 5% CO_2 atmosphere to allow full colour development. After 4 hours incubation, the viability of different cells were determined by measuring the absorbance at 490nm using a spectrophotometer. The cell viability of different transfected cells and controls was calculated corresponding to the standard curve. The mean value of triplicate wells for

transfected cells was compared with that of the parental cell line by Student *t*-test.

2.8. Soft agar assay

2.8.1. Overview

Soft agar assay has been extensively used in cancer research. This assay measures the ability of cells to divide and proliferate in absence of underlying substrate. The ability of cells to form colonies without adhesion are considered to be anchorage independent. Anchorage independent growth of cells in soft agar is one of the hallmark characteristics of cellular transformation and tumorigenic cell growth. In contrast, the normal cells are unable to grow in semisolid matrices. Therefore the soft agar assay is considered as the most accurate and stringent *in vitro* method to monitor the malignant transformation of cells. The positive result of this assay is assumed as potential indication of *in vivo* carcinogenesis.

2.8.2. Procedure

Two-layer soft agar assay is routinely used in the soft agar assay, and this experiment was carried out in 24-well plate in triplicate for each cell line. A bottom layer was prepared with 0.7% low melting temperature agarose to devoid of cells. The base layer can prevent the contact of cells to substratum. The equal volume of 1.4% melted low melting agar and cell culture media (2×) containing 20% FCS, 2mg/ml Zeocin and 4mM/l L-glutamine at 37℃ was mixed. The mixture (0.5ml) was quickly placed into each well of the 24-well plate. The plate was left for 30 minutes at room temperature

to allow the agar to solidify. N417 cells and the transfected cells were harvested and resuspended in 2× culture medium prior to adjustment to a final concentration of 2×10^4 per ml. The upper layer of 0.4% agar was mixed by using the equal volume of 2×culture medium that contain cells and 0.8% of low melting temperature agarose. Then 0.5ml of the mixture was quickly placed over the bottom layer and incubate at room temperature for 1 hour to ensure the wells completely set. The plates were transferred to 37℃ incubator with 5% CO_2 and 95% humidity for 4-6 weeks for the appearance of colonies. The cells were fed with 0.1ml of cell culture media once a week. When the proper colonies formed, they were stained by adding 100 μl of MTT (5mg/ml) to each well and incubated at 37℃ for 4 hours before quantitate on an automated scanner (Oxford Optronix Gelcount).

2.9. *In vivo* tumourigenicity assay

Tumourigenicity of the transfected SCLC cell lines was examined by subcutaneous (s.c.) inoculation of control and transfected cells in 5-week-old male Balb/c nude mice (Harlan). Five cell lines were used for this experiment: (1) Id1 highly suppressed cells; (2) Id1 moderately suppressed cells; (3) Id1 and Id3 highly suppressed cells; (4) Id1 and Id3 moderately suppressed cells and (5) scramble control cells. They were collected separately and centrifuged at 900 rpm for 3 minutes. Then the cells were resuspended in ice cold PBS. Matrigel was thaw on ice at 4℃ overnight. All the pipettes, tips and bijous were pre-cooled. Cells were mixed with Matrigel at a ratio of 1:1. The cell mixtures were kept on ice when transporting to the animal house. Cell mixtures (0.2 ml) were injected using 26G needle to both flanks of each nude mouse

(2×10^6 cells/site) subcutaneously. The injection was completed rapidly to prevent the Matrigel from solidifying. Growth rates were determined by measuring three dimensions (length, width and depth) of tumours with calipers twice a week. After 3 weeks, mice were sacrificed with a CO_2 chamber. Volumes of tumours were calculated according to the formula: Volume=$\pi/6(H \times W)^{3/2}$ 0.67 (411). All animal experiments were conducted under UKCCCR guidelines with Home Office Project Licence PPL 40/2270 to Prof Y. Ke.

2.10. Immunohistochemistry

Tumours produced in nude mice were surgically removed after the mice were sacrificed in a CO_2 chamber, fixed in 10% buffered formalin for 24 hours, and embedded in paraffin wax. Then the tissue samples were cut to a thickness of 5μm with a microtome. The paraffin sections were placed on Apex ™ superior adhesive slides (Leica). The glass slides were then transferred in a 37℃ oven to dry for 12-24 hours and kept in slide cardboards at room temperature. Histological sections were deparaffinised in two changes of xylene for 5 minutes, rehydrated in two changes of 100% ethanol, for 5 minutes each. Slides were immersed into 3% hydrogen peroxide in 100% methanol for 15 minutes at room temperature to quench endogenous peroxidase. Then the slides were rinsed in running tap water for at least 1 minute. The fixation and processing steps of tissues can often result in loss of immunoreactivity of antigens. This can be reversed by the use of antigen retrieval by microwaving tissue sections for 15 minutes in 10 mM sodium citrate solution buffer (pH 6.0), then standing in the microwave for another 15 minutes. The sections were rinsed in running

tap water and Tris-buffered saline with Tween 20 (TBST, pH 7.6). For the primary antibody incubation, slides were transferred to sequenza casstte (Shandon). In order to block non-specific binding of antibody, each tissue section was applied 100 μl of 5% bovine serum albumin in TBS and allowed to remain for 10 minutes, followed by rinsing in TBST for 5 minutes.

Each primary antibody (rabbit polyclonal anti-human Id1, Id3 antibody, Santa Cruz; anti-human VEGF antibody, Thermo Scientific) was diluted in TBST at v/v ratio of 1/100, and anti-CD34 antibody (Dako) was diluted in TBST at v/v ratio of 1/50. Sections were covered with 200 μl of TBST as negative control. The positive control for Id1 and Id3 was tissues of a malignant prostate carcinoma with high Gleason score. For VEGF antibody staining, the normal lung tissue was implied as positive control. Both positive and negative controls ran routinely with each assay to help ensure proper performance. The slides were incubated at room temperature for 1 hour and washed with TBST three times for 5 minutes each. Then the slides were incubated in 200 μl of anti-rabbit HRP-conjugated polymer (Dako) for 30 minutes at room temperature followed by washing with 3 changes of TBST for 5 minutes each. To detective the conjugation of primary and secondary antibody, 100 μl of DAB substrate solution at ratio of 1:50 was applied to each section for 10 minutes at room temperature and rinsed in distilled water for 5 minutes to stop colour development. Slides were removed from the sequenza cassettes and counterstained with haematoxylin (Mayer’s) for 2 minutes following by rinsing in running tap water for a few minutes. Then slides were differentiated in 1% acid-alcohol, blued in ammonia water, finally rinsed in running tap water. The tissue slides were dehydrated through 2 changes of 100% ethanol, 2 minutes each. Then sections were cleared in 3 changes of

xylene and coverslipped with DPX synthetic resin (Bios Europe). The mounted slides were observed under microscope for antibody staining.

Slide evaluation was performed independently by two investigators. In case of different results between observers, consensus was reached at joint evaluation. All slides were examined and scored by using multiple-headed microscope (Nikon). The intensity of the staining was observed under microscope and scanned with ScanScope (Aperio Technologies) image scanner. Nucleic staining was scored by combining the stain intensity with percentage of cells stained. The intensity of staining was assessed by examining approximately 10 fields at 40× magnifications and was divided into 4 categories (no stain = 0, weakly stained = 1, moderately stained = 2, strongly stained = 3). The scores of percentage staining were also classified into 4 categories according to the percentages of the stained cells (0% = 0, 1–30% = 1, 31–69% = 2, 70-100% = 3). The final score (with points from 0-9) of immunohistological staining of a tissue section was obtained by multiplying the intensity score with the percentage score. Thus the nuclear staining was finally rated as follows: 0, negative staining; 1-3, weak staining; 4-6, moderate staining; 7-9, strong staining. Cytoplasmic staining was categorized as negative, weak, moderate and strong staining according to the intensities. The classification for VEGF staining was slightly different as follows: negative, very weak, weak, and moderate staining.

2.11. Apoptosis assay

Annexin V-PE detection kit ((BioVision) was used to measure the percentage of cells that were undergoing apoptosis. During the apoptosis, the membrane phospholipid

phosphatidylserine (PS) is translocated from the cytoplasmic face of the plasma membrane to the outer leaflet. The appearance of PS on the cell surface is a universal parameter of the early phase of cell apoptosis. Annexin V, a calcium-dependent phospholipid-binding protein, preferentially binds to negatively charged phospholipids such as PS and therefore can be used as probe to determine apoptosis. Annexin-V can be conjugated to a variety of different fluorochromes including FITC and PE. The conjugation of PE enables apoptotic cells to be identified and quantified by flow cytometry. In this study, the apoptosis of SCLC cells was induced by cisplatin (Sigma-Aldrich), which is the first-line chemotherapy in treatment of SCLC.

All transfected cells were cultured in six well plates at a concentration of 5×10^5. Each cell line was incubated in triplicate with varying concentrations (0, 25, 50, 75, 100 and 125 μM) of cisplatin (Sigma) in 37°C incubator for approximately 24 hours. Then 2×10^5 cells were counted, washed twice with PBS and resuspended in 500 μl of 1× Binding Buffer provided in the kit. PE solution (5 μl) was added into the cells and incubated at room temperature for 10 minutes, protected from light. The fluorescence intensity of Annexin V-PE was measured with a FACS Calibur (BD biosciences) flow cytometer using the phycoerythrin emission signal detector (FL2 channel).

2.12. Angiogenesis

Angiogenesis, or neovascularization, is the process of generating new capillary blood vessels involved in multiple steps: endothelial cell relocation, migration, proliferation and tube formation. Angiogenesis is a key factor in the progression of cancer. Tumour growth and metastasis depend on angiogenesis triggered by chemical signals from

tumour cells (412). A number of proteins have been identified as angiogenic activators, including vascular endothelial growth factor (VEGF), basic fibroblast growth factor (bFGF), transforming growth factor (TGF)-α, TGF-β, tumour necrosis factor (TNF)-α, and etc. The VEGF family and their receptors (VEGFR) are receiving more attention in the field of neoplastic vascularisation (413).

2.12.1. Immunosorbent assay for VEGF (ELISA assay)

The expression of secreted VEGF in supernatant of N-Id1 or N-Id1-Id3 transfected cells was measured with RayBio Human VEGF ELISA assay kit. This assay is based on the quantitative sandwich enzyme immunoassay technique. A specific VEGF antibody has been pre-coated onto a 96-well plate. Samples are added to the wells and the VEGF present in the sample will be bound to biotinylated anti-human VEGF antibody. Following a wash to remove the unbound reagent, the HRP-conjugated streptavidin is added to the wells. After washing away the unbound substance, 3',3',5',5'-Tetramethylbenzidine(TMB) is transferred to the wells and colour develops in proportion to the amount of bound VEGF. The intensity of the colour is determined at 450 nm when colour development stopped.

2.12.1.1. Preparation of standard

The recombinant human VEGF was briefly spun down and recombined with 640 µl of 1×Sample Diluent Buffer as the 50 ng/ml standard. VEGF powder was dissolved thoroughly by a gentle mix. Then 60 µl of 50 ng/ml VEGF standard was transferred into a tube with 440 µl of 1× Sample Diluent Buffer to prepare a 6,000 pg/ml stock

standard solution. Seven sterile tubes in total were labelled. To prepare the dilution series, 400 µl of 1× Sample Diluent Buffer was added to each of seven tubes. From the stock standard solution, 200 µl was transferred into the second tube. The solution was mixed thoroughly by pipetting. Then the same amount of solution was transferred to the third tube. The transfer was repeated until the sixth tube to create six standard solutions containing 6000, 2000, 666.7, 222.2, 74.97, 24.69 and 8.23 pg/ml VEGF. The seventh tube was filled with 300 µl 1× Sample Diluent Buffer serves as the zero standard (0 pg/ml).

2.12.1.2. Procedure of VEGF ELISA assay

Transfected cells were seeded to six-well plate at 1×10^6 per well and cultured in 2 ml phenol red-free RPMI 1640 medium containing 10% charcoal stripped FCS for 24 hours. After 24 hours incubation, cell culture was collected and centrifuged. Supernatant of each transfected cell line and VEGF standard (100 µl) were added to VEGF microplate wells. The wells were covered with an adhesive plastic and incubated at 4℃ with gentle shaking. The cell culture supernatant was completely removed on the next day and washed 4 times with 1×Wash Solution. After decanting any remaining wash buffer, 100 µl of biotinylated secondary antibody was added to each well and incubated for one hour at room temperature with gentle shaking. Solution was thoroughly removed from wells. The plate was then washed as described above. Streptavidin-HRP Working Solution (100 µl) was added to each well and incubated for 45 minutes at room temperature with gentle shaking. All the wells were washed as mentioned above. Then 100 µl of TMB One-Step Substrate Reagent was added to each well and incubated for 30 minutes at room temperature with gentle

shaking, protected from light. Finally, 50 µl of Stop Solution was pipetted to each well and gently mixed by tapping the side of plate. The optical density was determined by using a micro-plate reader set to 450 nm immediately. The mean value of optical density for both standards and samples was calculated. Background (the average zero standard) absorbance was then subtracted from all data point prior to plotting. The standard curve was plotted and best fit straight line was drawn through the standard points. The expression of VEGF in supernatant of each transfected cell can be determined according to the standard curve.

2.12.2. *In vitro* angiogenesis assay (tube formation assay)

2.12.2.1. Procedure of *in vitro* angiogenesis assay

The *In Vitro* Angiogenesis Assay Kit (Millipore) was used to assess if the secreted VEGF protein of N-Id1 or N-Id1-Id3 transfected cells can affect the ability of endothelial cells to form three-dimensional structures (tube formation). This kit utilizes ECMatrix™ (extracellular matrix gel), which prepared from Engelbreth–Holm–Swarm (EHS) mouse tumour cells. Thus the kit can evaluate the tube formation of endothelial cells such as human umbilical vein cells (HUVEC) in a 96-well format. On the extracellular matrix gel, endothelial cells can align and form tube-like structures in 4-8 hours. Consequently the endothelial cell tube formation assay is a powerful tool for examining the anti- or pro-angiogenic substances on cultured cells by premixing inhibitor or stimulator with the endothelial cell suspension.

ECMatrix™ Gel Solution and ECMatrix™ Diluent Buffer were thawed in a 4℃ frost-free refrigerator overnight prior to the *in vitro* angiogenesis assay. One hundred

μl of 10× Diluent Buffer was pipetted to 900 μl of ECMatrix™ solution in a sterile pre-cooled microfuge tube. The solution was mixed well and placed on ice to prevent solidification. To avoid air bubbles, 50 μl of solution was carefully transferred into each well of pre-cooled 96-well plate. Then the plate was incubated at 37 ℃ for 1 hour to allow the matrix solution to gel. Cryopreserved HUVEC was thawed and cultured in 75cm^2 culture flasks with pre-warmed EndoGRO reduced-serum medium (Millipore). Flasks were placed in incubator at 37℃ 5% CO_2. HUVEC cells were passaged or frozen as the method described in Section 2.1 when they reached to 80-100% confluency. The HUVEC cells were harvested and resuspended in pre-warmed EndoGRO reduced-serum medium. One hundred μl HUVEC cells were seeded at 5×10^3 cells per well onto the surface of the polymerized ECMatrix™ with 100 μl conditioned medium derived from each transfected cell line. To test the effect of VEGF on tube formation, same amount of HUVECs was also incubated with human VEGF antibody. HUVECs with human VEGF (10 ng/ml) and growth medium only were set as the positive control and negative control respectively. For each test there were triplicate wells to allow for statistical analysis of the data. The 96-well plate was then incubated at 37 ℃, 5% CO_2 in the cell culture incubator for 6 hours. Once tube structure was observed, tubes were stained with 50 μl of MTT (5mg/ml) for 10 minutes and quantified and photographed under inverted microscope in 40× magnification.

2.12.2.2. Quantitation of tube formation

For a better understanding of the data of cellular networks, various methods can be used to quantitate the network. One of simple visual assessment is the pattern

recognition quantitation method, which provides an accurate assessment of tube formation network with detectable key parameters as the table below (Millipore). Each pattern is allocated a numerical value. The numerical value is related to the degree of angiogenesis progression. Five random view-fields per well were assessed and the values averaged.

Pattern	**Value**
Individual cells, well separated	0
Cells begin to migrate and align themselves	1
Capillary tubes visible. No sprouting	2
Sprouting of new capillary tubes visible	3
Closed polygons begin to form	4
Complex mesh like structures develop	5

2.13. Statistical analysis

The continuous variables were expressed as means±SD. Statistical significance was determined by two-tailed Student's *t*-test. IHC data were statistically analysed according to their final score which is categorical variables. IHC data were analysed using Chi-Square tests. The error bars represent the standard deviation of the mean when the experiment has been repeated. In all the tests, $P<0.05$ was considered as statistically significant. The statistical analyses of two-tailed Student's *t*-test were performed using GraphPad software. IHC data were statistically analysed using standard statistical software online (http://www.quantpsy.org).

CHAPTER 3
RESULTS

CHAPTER 3 RESULTS

3.1. Identification of the most effective suppressor against Id1 by transient transfection

The 3 selected siRNAs were subjected to transient transfection to test their capability of silencing of Id1 and Id3 in SCLC cell line N417 and to identify the optimal silencer. The effect of Id1 suppression produced by the 3 siRNAs was shown in **Figure 3.1**. At 24h after the transient transfection, all 3 siRNAs produced a reduction in Id1 level (**Figure 3.1A**), but both scramble RNA and transfection reagent controls did not significantly change the Id1 expression level. When the Id1 level in the parental cells was set at 1, the levels produced by transfections with siRNA1, siRNA2 and siRNA3 were significantly reduced to 0.26, 0.27 and 0.39, respectively (**Figure 3.1B**, $P<0.0001$). Although further suppression was obtained at 48h after the transient transfection with siRNA1 and siRNA2, the suppression caused by siRNA3 was reversed partially (**Figure 3.1C**). While Id1 levels at 48h after the transient transfection with siRNA1 and siRNA2 were reduced to 0.18 and 0.13 respectively, the level of Id1 after siRNA3 transient transfection was reduced to 0.62 (**Figure. 3.1D**, $P<0.0001$). Thus combined the suppression effects in both experimental time points (24h and 48h), siRNA2 which produced a 3.9- and 7.7-fold reduction respectively, was chosen as the optimal siRNA sequence and used for further study. The optimal Id3 siRNA was previously selected in a similar manner (405).

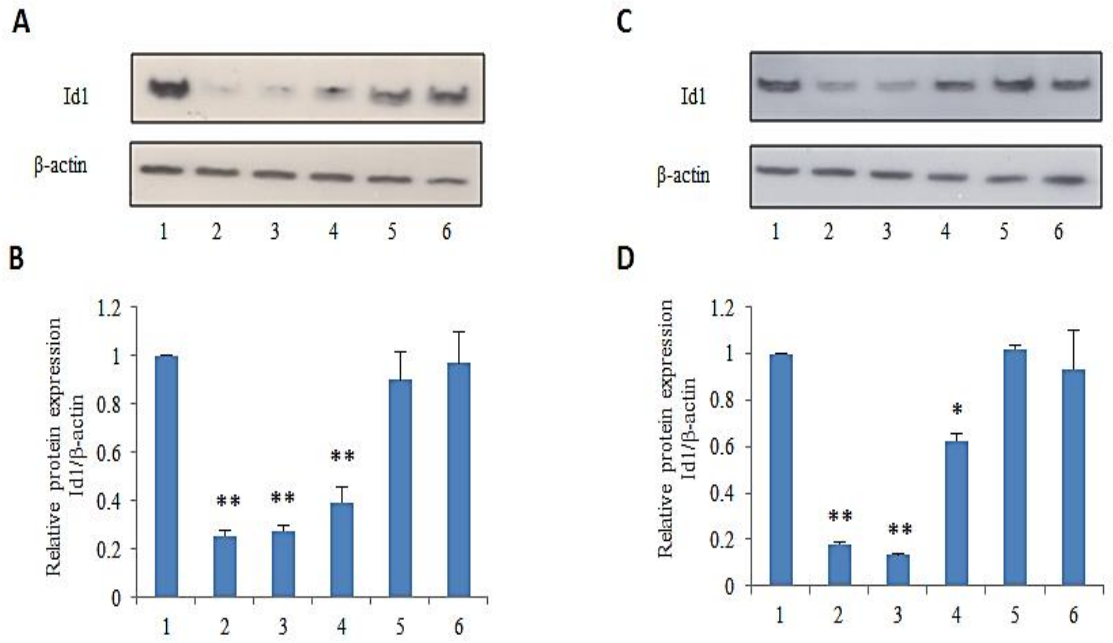

Figure 3.1. Western blot analysis of the knockdown effect of 3 candidate siRNAs on Id1 expression at protein level. SCLC cell line N417 was used as RNA recipient cells. The levels of Id1 expressed were measured in control cells and in cells transiently transfected with different siRNAs: 1, untreated N417 cells; 2, N417+ siRNA1; 3, N417+ siRNA2; 4, N417+ siRNA3; 5, N417+ scramble RNA; 6, N417+ transfection reagent. An antibody against β-actin was also incubated with the blot to normalize the possible loading errors. A. Western blot analysis of Id1 expressed in the control cells and in the cells transfected transiently with different RNAs for 24 hours. B. Quantitative analysis of Id1 levels detected with Western blot. The level of Id1 protein expressed in the parental N417 cells was set at 1; levels of Id1 expressed in cells after 24 hours of different transient transfections were calculated by relating to that in the parental cells. C. Western blot analysis of Id1 expressed in the control cells and in the cells transfected transiently with different RNAs for 48 hours. D. Quantitative analysis

of Id1 levels detected with Western blot. The level of Id1 protein expressed in the parental N417 cells was set at 1; levels of Id1 expressed in cells after 48 hours of different transient transfections were calculated by relating to that in the parental cells. Id1 protein relative expression levels after either 24 or 48 hours were quantified by scanning the intensity of band areas on the blot through densitometry and normalized to β-actin. The results were obtained through 3 separate measurements and the statistical difference was determined by 2-tailed Student's *t*-test (**P<0.0001).

3.2. Establishment of clones with reduced levels of Id1 and Id3

3.2.1. Confirmation of siRNA inserts

Digestion of the plasmid DNA with restriction enzymes was shown in **Figure 3.2.** The DNA of psiRNA-DUO was firstly digested by *Hin*dIII and *Acc*651 restriction enzymes (**Figure 3.2A**) to insert Id1 siRNA which flanked by *Hin*dIII and *Acc*651 restriction recognition sites. In the plasmid DNA, enzyme sites *Hin*dIII and *Acc*651 were designed between *Cla*I and *Nde*I. Because the part of the plasmid DNA was replaced by Id1 siRNA or scramble siRNA (they are the same size), the band size of the original plasmid and recombinant plasmid DNA were different when digested with *Cla*I and *Nde*I restriction enzymes. If the insertion was correct, a band approximately 520 bp can be detected in the agarose gel electrophoresis. Agarose gel electrophoresis showed that recombinant plasmid DNA digested with *Hin*dIII and *Acc*651 restriction

enzymes produced fragments of 520 bp, while the band of original plasmid DNA was approximately 980 bp (**Figure 3.2B-C**). Secondly, the DNA of psi-Id1 was digested by *Bbs*I restriction enzyme (**Figure 3.2D**) to insert Id3 siRNA. In the psiRNA-DUO DNA, two *Bbs*I enzyme sites were designed between *Psp*1406I and *Nsi*I restriction enzymes. The part of the plasmid DNA between two *Bbs*I enzyme sites was replaced by Id3 siRNA or scramble siRNA (they are the same size). If the insertion was correct, a band approximately 340 bp can be detected. Agarose gel electrophoresis showed that *Psp*1406I and *Nsi*I digestion of recombinant plasmid DNA produced fragments of 340 bp, while the band of original plasmid was 2215 bp (**Figure 3.2E**). DNA sequencing confirmed the presence of Id1 siRNA and Id3 siRNA within the recombinant plasmid DNA (**Figure 3.3**).

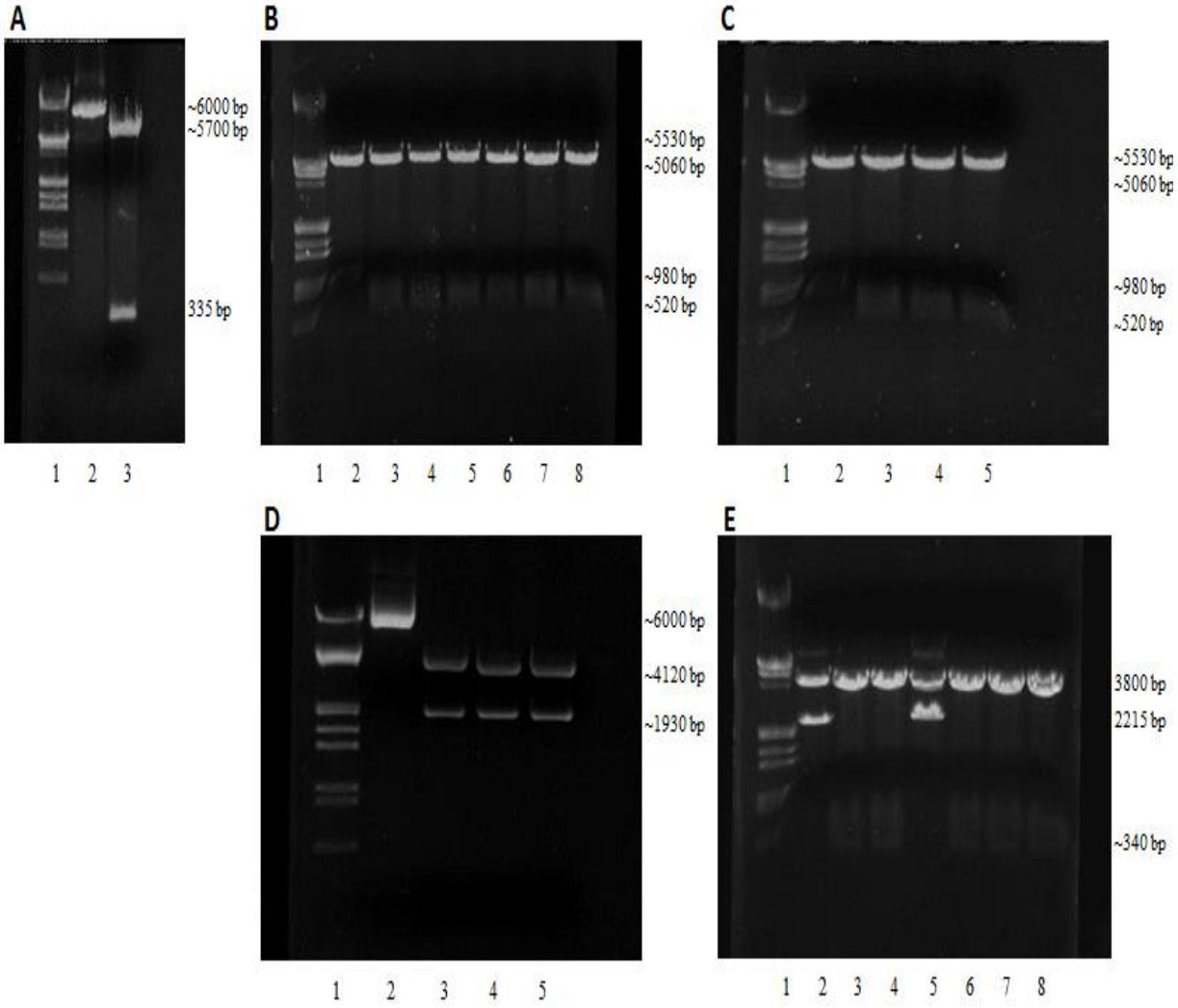

Figure 3.2. Agarose gel electrophoresis of restriction enzymes digestion of plasmid DNA. A. Enzymatic double digestion of psiRNA-DUO. Column 1, DNA marker; column 2, undigested psiRNA-DUO plasmid; column 3, psiRNA-DUO digested with *Hin*dIII and *Acc*651 which was prepared for Id1 insertion. B. Plasmid DNA extraction of *E. coli* GT115 cells transformed with Id1 siRNA. Column 1, DNA marker; column 2, psiRNA-DUO double digested with *Cla*I and *Nde*I which showed a fragment of 980 bp; column 3-8, Id1 siRNA contained recombinant plasmid DNA of six clones double

digested with *Cla*I and *Nde*I which showed fragments of 520 bp. C. Plasmid DNA extraction of *E. coli* GT115 cells transformed with scramble RNA. Column 1, DNA marker; column 2, psiRNA-DUO double digested with *Cla*I and *Nde*I which showed a fragment of 980 bp; column 3-5, scramble RNA contained recombinant plasmid DNA of three clones double digested with *Cla*I and *Nde*I which showed fragments of 520 bp. D. Enzymatic digestion of psi-Id1. Column 1, DNA marker; column 2, undigested psiRNA-DUO plasmid; column 3, psiRNA-DUO digested with *Bbs*I which produced a band of 1930 bp; column 4, psi-Id1 digested with *Bbs*I which produced a band of 1930 bp; column 5, digestion of the plasmid contained Id1 scramble RNA with *Bbs*I also produced a band of 1930 bp. E. Plasmid DNA extraction of *E. coli* GT115 cells transformed with Id1 and Id3 siRNAs. Column 1, DNA marker; column 2, psiRNA-DUO double digested with *Psp*1406I and *Nsi*I which showed a fragment of 2215 bp; column 3, digestion of the plasmid contained scramble siRNA with *Psp*1406I and *Nsi*I produced a band of 340 bp; column 4, 6-8, recombinant plasmid DNA of five clones contained Id1 and Id3 siRNA double digested with *Psp*1406I and *Nsi*I which showed fragments of 340 bp; column 5, a clone did not contain Id3 siRNA insert.

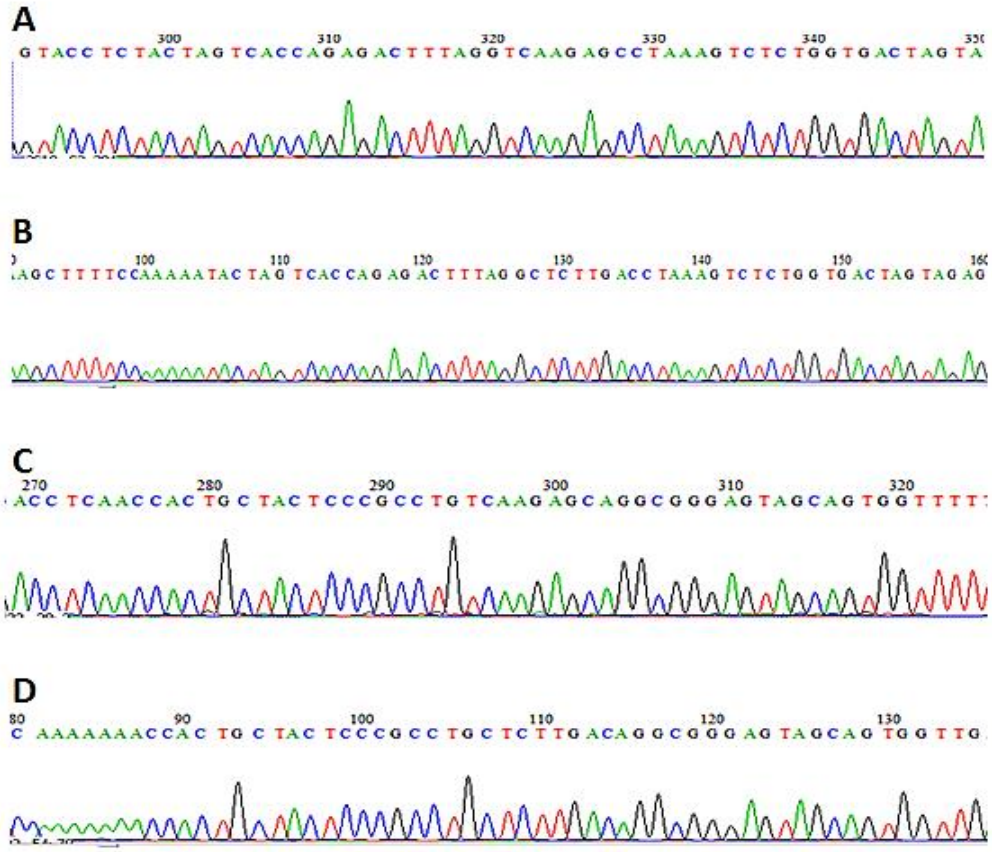

Figure 3.3. Sequencing analysis confirmed insertion of siRNA targeting of Id1 and Id3 into psiRNA-PUO. A. Forward sequence of Id1 siRNA; B. Reverse sequence of Id1 siRNA; C. Forward sequence of Id3 siRNA; D. Reverse sequence of Id3 siRNA.

3.2.2. Establishment of stable SCLC cell lines expressing reduced Id1 and Id3

The expression of Id1 and Id3 was respectively knockdown either singly or jointly in the 5 sublines established from each of transfectant groups. The expression levels of Id1 and Id3 in the 2 transfectant groups (each had 5 sublines) were measured by Western blot and was shown in **Figure 3.4**.

The Id1 expression levels were reduced unevenly amongst the five Id1 shRNA transfectant cell lines in comparison with the parental N417 cells (**Figure 3.4A**). When the Id1 level in the N417 cells was set at 1, the Id1 levels in N-Id1-1, N-Id1-2 and N-Id1-5 were significantly reduced to 0.1, 0.12 and 0.45, respectively (**Figure 3.4B**, $P<0.0001$). The relative expression of Id1 in N-Id1-1 and N-Id1-2 was reduced to levels similar to that expressed in the benign Beas-2B cells (0.12). Comparing to that in the parental cells, Id1 protein levels in N-Id1-3 and N-Id1-4 were decreased to 0.75 and 0.84 respectively. Id1 protein level in scramble control was 0.94 and did not show any significant difference when compared with the parental cells. The Id3 expression in all Id1 shRNA transfectant cell lines was detected with Western blotting (**Figure 3.4C**) and its relative levels in those cells were ranged from 0.85 to 1.24, which was not significantly different from the parental N417 cells (**Figure 3.4D**) ($p>0.05$). Id3 protein level in scramble control was 1.01 and did not show significant difference when compared with the parental cells.

Likewise, the Id1 levels in five Id1 and Id3 double knockdown cell lines were all inhibited, but with a degree of difference (**Figure 3.4E**). While the levels of Id1

protein in N-Id1-Id3-1, N-Id1-Id3-2 and N-Id1-Id3-4 were high-significantly suppressed to 0.16, 0.35 and 0.58, respectively (**Figure 3.4F**, $P<0.0001$) in comparison to the control, the Id1 relative level in N-Id1-Id3-5 and in N-Id1-Id3-3 was only slightly reduced to 0.62 and 0.95, respectively. The level of Id1 in N-Id1-Id3-1 cells was similar to that in the benign Beas-2B cells (0.13). Id1 protein level in scramble control was 0.97 and did not show any significant difference when compared with the parental cells. Although levels of Id3 were greatly reduced in 2 double knockdown transfected cell lines, there were nearly no RNAi silencing effect on other 3 cell lines (**Figure 3.4G**). The relative levels of Id3 protein in N-Id1-Id3-1 and N-Id1-Id3-2 were further reduced to 0.27 and 0.44 ($P<0.0001$), even lower than that in Beas-2B (0.55) (**Figure 3.4H**). However, the Id3 relative level in N-Id1-Id3-5, N-Id1-Id3-4 and N-Id1-Id3-5 was 1.11, 1.08 and 0.96 respectively, they were similar to that of the parental cells. Id1 protein level in scramble control was 1.14 and did not show any significant difference when compared with the parental cells. To assess the effect of suppression of Id1 and Id3 on SCLC tumourigenicity, one highly suppressed cell line (N-Id1-1, N-Id1-Id3-1) and one moderately suppressed cell line (N-Id1-5, N-Id1-Id3-2) from each group of transfectant cell lines were selected for further analysis.

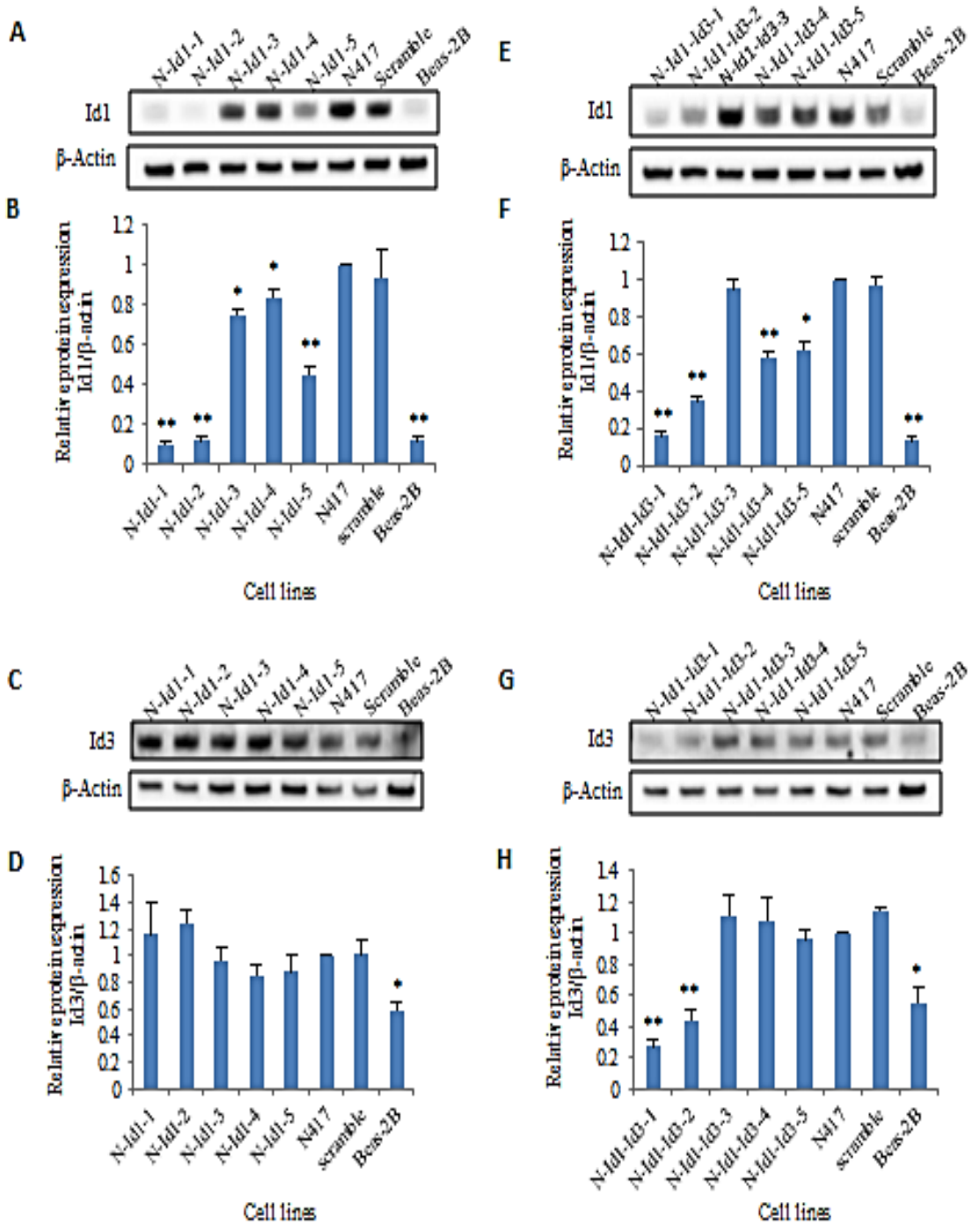

Figure 3.4. Knockdown effect of stable transfection of shRNAs targeting either Id1 and Id3 or Id1 alone on levels of Id1 and Id3 or on that of Id1 expressed in N417 cells. Five individual sublines were generated from five different individual shRNA

transfectant clones. The parental benign Beas-2B bronchial epithelial cells and the transfectants generated by a plasmid harbouring scramble RNA only were used as controls. A. Western blot analysis of Id1 expression in five sublines generated from clones of Id1-shRNA transfectants. B. Relative Id1 levels in the five Id1-shRNA -transfected sublines. C. Western blot analysis of Id3 expression in the five Id1-shRNA-transfected sublines. D. Quantitative analysis of relative Id3 levels in the five Id1-shRNA-transfected sublines. E. Western blot analyses of levels of Id1 expression in the five sublines established from separate clones of Id1- and Id3-shRNA transfectants. F. Relative levels of Id1 expressed in the five Id1- and Id3-shRNA- transfectant sublines. G. Western blot analysis of Id3 expression in the five Id1- and Id3-shRNA- transfectant sublines. H. Relative levels of Id3 expressed in the five Id1- and Id3- shRNA- transfectant sublines. For all quantitative measurements, the level of Id1 or Id3 expressed in control N417 cells was set at 1; levels in other transfectant lines were calculated by relating to that expressed in the control cells. Results were presented as the means and SD from three independent experiments. Statistical difference was determined by 2-tailed Student's *t*-test (**P<0.0001, *P<0.05).

3.3. Effect of knockdown of Id1 alone or Id1 and Id3 jointly on invasiveness of SCLC cells

To study the effect of Id1 and Id3 expression on SCLC cell invasiveness, we assessed invasion abilities of transfected cells with modified Boyden chamber assay. The invaded cells crossed the membrane and were found in the lower chamber but not surface of the membrane. The average number of invasive cells from different cell lines are summarised in **Table 3.1**. Notably more parental and scramble control cells passed through the pores in presence of 20% FCS as an attractant. The number of invaded cells from the control group was 9 ± 2, which was similar to that of the scramble control (8.33 ± 1.53). The average number of invasive cells in N-Id1-1, N-Id1-5, N-Id1-Id3-1 and N-Id1-Id3-2 was decreased to 4 ± 1, 5.33 ± 0.58, 0.67 ± 0.58 and 2 ± 1 respectively. The relative invasion rate of different transfectant cells was shown in **Figure 3.5**. When the percentage rate of the invaded parental N417 cells was set as 1, the relative invasion rate of N-Id1-1 and N-Id1-5 was significantly reduced to 0.44 and 0.59 respectively (**Figure 3.5**, $p<0.04$). The relative invasiveness in double knockdown transfectant cells N-Id1-Id3-1 and N-Id1-Id3-2 was further significantly reduced to 0.07 and 0.22 respectively (**Figure 3.5**, $p<0.007$). The relative invasiveness of scramble control (0.9) was not significantly changed from that of the parental cells ($p=0.78$).

Cell line	Average number of cells invaded (mean ± SD)
N417	9 ± 2
Scramble control	8.33 ± 1.53
N-Id1-1	4 ± 1
N-Id1-5	5.33 ± 0.58
N-Id1-Id3-1	0.67 ± 0.58
N-Id1-Id3-2	2 ± 1

Table 3.1. Summary of cell count after 48 hours of invasion assay with sh-Id1 and sh-Id1-Id3 transfected N417 sublines.

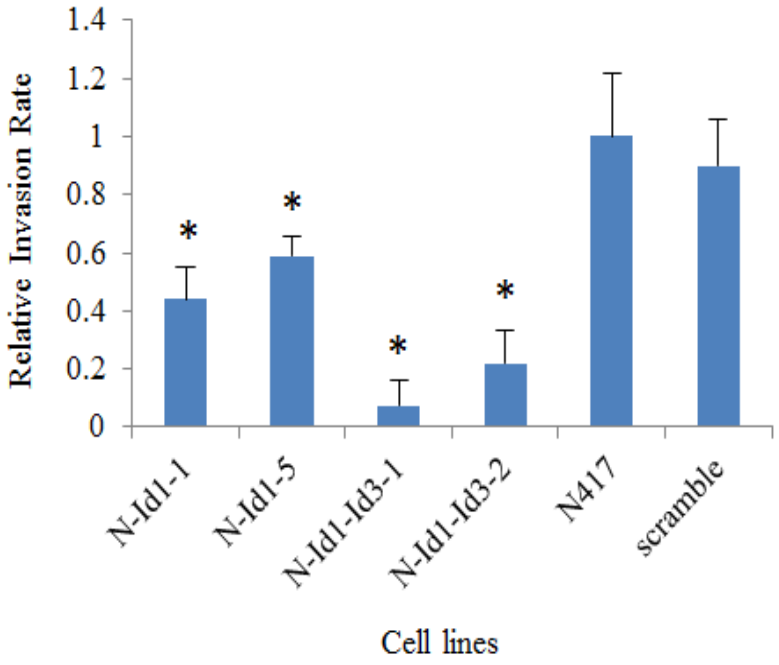

Figure 3.5. The inhibition of the invasiveness in sh-Id1 and sh-Id1-Id3 sublines was determined by Boyden chamber assay. The invasiveness in N-Id1-1, N-Id1-5, N-Id1-Id3-1 and N-Id1-Id3-2 cells was assessed by ability to invade trough polycarbonate membrane. Graphs showed quantification of relative invade rate of relevant cells when invasiveness of the control N417 cells was set at 1. Results were presented as the mean ± SD of three individual experiments. Statistical difference was determined by two-tailed Student's *t*-test (*P<0.05).

3.4. Effect of knockdown of Id1 alone or Id1 and Id3 jointly on proliferation of SCLC cells

To identify the cell number in the MTS assay, standard curves were generated to correlate optical density of formazan with cell number. The data indicated that a good linear correlation (R^2 = 0.996) between absorbance signal and cell number can be established at a cell density ranged from 0 to 1.6 × 10^6 cells (**Figure 3.6**). Thus from the range tested, the values of absorbance at 490 nm showed a strong correlation with the number of cells seeded. Then 5,000 cell count was determined as the optimal start for proliferation assay among N417 cell population. Likewise, the standard curves were drawn for other transfected sublines and similar results were obtained, figure not shown.

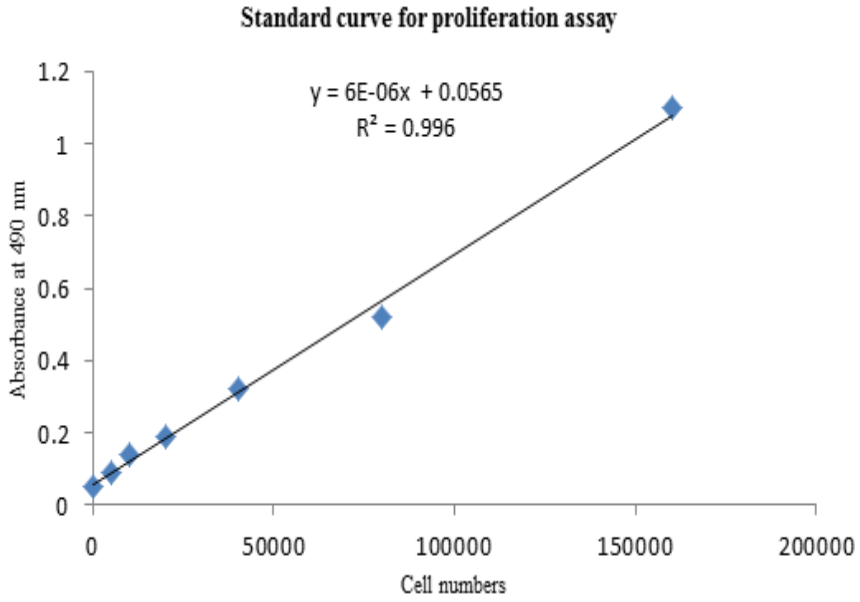

Figure 3.6. MTS standard curve for N417 cells. The curve equation and regression value of the curve were determined.

MTS assay was performed to reflect the effect of reduced Id1 and Id3 expression on the proliferation ability of N417 cells. Proliferation rates of different transfectant cells were indicated by a MTS assay and results were shown in **Figure 3.7**. With the same cell number (5,000) in all transfectants and parental cells at the beginning, though the viable cell numbers in all different groups increased progressively, the parental cells and scramble control exhibited significant elevations in viability relative to the N-Id1 and N-Id1-Id3 transfectants.

The average number of cells from different transfectants and parental cells was summarised in **Table 3.2**. On day 2, the cell number of N-Id1-1, N-Id1-5, N-Id1-Id3-1 and N-Id1-Id3-2 was reduced to 3216±382, 4958±548, 1986±623 and 3453±430 respectively, compared with that of the parental control (5846±303). On day 4, the

numbers of cells in N-Id1-1, N-Id1-5, N-Id1-Id3-1 and N-Id1-Id3-2 were 5833±936, 11542±1617, 3420±467, 3772±549 respectively, compared with that of the parental control (13987±1976). While numbers of cells from N-Id1-1, N-Id1-5, N-Id1-Id3-1 and N-Id1-Id3-2 on day 6 were only 10467±782, 18607±2585, 5233±411 and 7382±850, a 3-, 1.7-, 5.9- and 4.2-fold significant reduction ($p<0.002$) respectively, in comparison with that of the parental control. Further changes were observed on day 8. Numbers of cells reduced to 24483±797, 36269±1206, 8100±1175, and 13463±834 in N-Id1-1, N-Id1-5, N-Id1-Id3-1, and N-Id1-Id3-2, a further reduction of 3.1-, 1.4-, 6.4- and 3.9-fold respectively ($P<0.003$). No significant difference between parental cells and scramble controls was detected either on any time points throughout the period of 8 days ($p=0.11$, $p=0.06$, $p=0.07$, $p=0.56$).

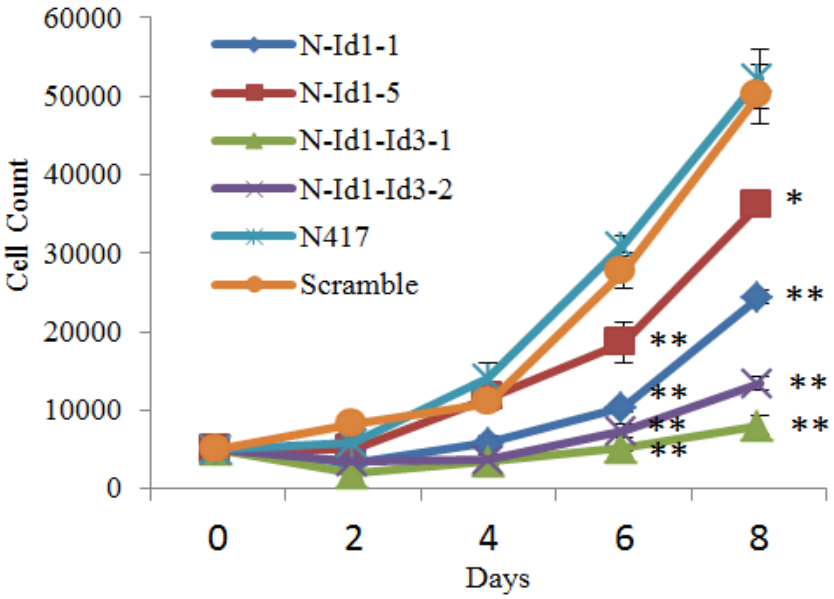

Figure 3.7. MTS assay of N-Id1-1, N-Id1-5, N-Id1-Id3-1, N-Id1-Id3-2, scramble RNA transfectant cell lines and the parental N417 cells. Number of relevant cells

cultured in 96-well plates was detected by MTS assay for a period of eight days. Results represented the data as mean and SD from triplicate wells (**P<0.0001, *P<0.05).

Day	Average number of cells (mean±SD)					
	N-Id1-1	N-Id1-5	N-Id1-Id3-1	N-Id1-Id3-2	N417	Scramble
0	5000	5000	5000	5000	5000	5000
2	3216 ±382	4958 ±548	1986 ±623	3453 ±430	5846 ±303	8228 ±805
4	5833 ±936	11542 ±1617	3420 ±467	3772 ±549	13987 ±1976	10895 ±418
6	10467 ±782	18607 ±2585	5233 ±411	7382 ±850	31055 ±1089	27597 ±2090
8	24483 ±797	36269 ±1206	8100 ±1175	13463 ±834	52228 ±3779	50281 ±3821

Table 3.2. Summary of cell count of MTS assay with N-Id1 and N-Id1-Id3 transfected N417 cell lines.

3.5. Effect of knockdown of Id1 alone or Id1 and Id3 jointly on anchorage-independent growth of SCLC cells

To test anchorage-independent growth of Id1-shRNA, Id1 and Id3-shRNA transfectants, soft agar assay was performed. The results of the anchorage-independent growth capability of the cells (as an indication of tumourigenicity) on soft agar assay were shown in **Figure 3.8**. Average number of colonies produced by different transfectants and parental cells was summarised in **Table 3.3**. Although the low growth rate of Id1 and Id3 supressed cells may have an effect on length of colony formation, the assay was conducted for a period of 4-6 weeks due to the limited growth conditions for colonies produced in the control group. After 6 weeks, the number of colonies produced by N-Id1-1 and N-Id1-5 was dramatically decreased to 4±0.57 and 34±1.76 respectively, as compared with the parental cells (466±36.12) ($P<0.0001$). Impressively, very small, and similar numbers of colonies were produced by the N-Id1-Id3-1 and N-Id1-Id3-2 cells (1±0.57 and 2±0.57, respectively). Numbers of colonies produced by N-Id1-1, N-Id1-5, N-Id1-Id3-1 and N-Id1-Id3-2 were largely decreased, a 117-, 14-, 466- and 233-fold reduction respectively in comparison with that of the parental control. The number of colonies produced by scramble control was 470±43.64. No significant difference was observed between the parental and scramble controls ($P=0.743$). The soft agar dishes of all groups in triplicate were shown in **Figure 3.9**.

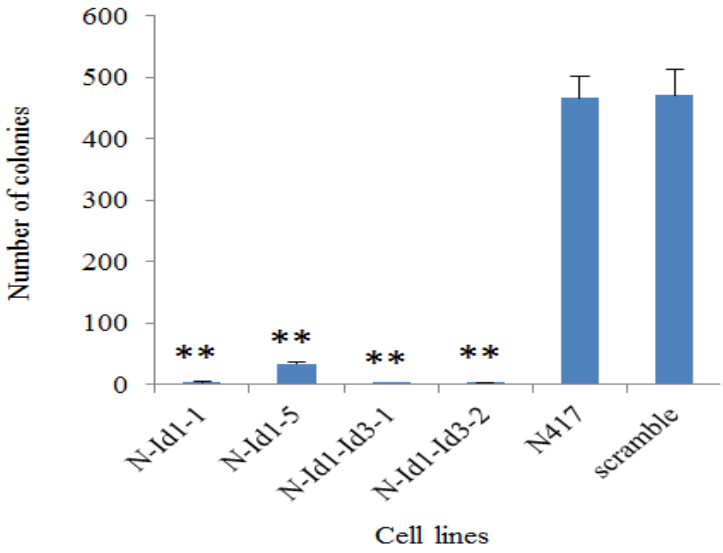

Figure 3.8. Number of colonies produced by Id1 and Id3-shRNA or Id1-shRNA transfected N417 cells in soft agar after six weeks. Quantitative analyses of colony numbers were graphed. Results represented the data as mean and SD from triplicate wells (**P<0.0001).

Cell lines	Average number of colonies (mean ± SD)
N417	466.33 ± 36.12
Scramble	470.33 ± 43.64
N-Id1-1	4 ± 0.57
N-Id1-5	34.33 ± 1.76
N-Id1-Id3-1	1 ± 0.57
N-Id1-Id3-2	2 ± 0.57

Table 3.3. Summary of number of colonies from all cell lines in soft agar assay.

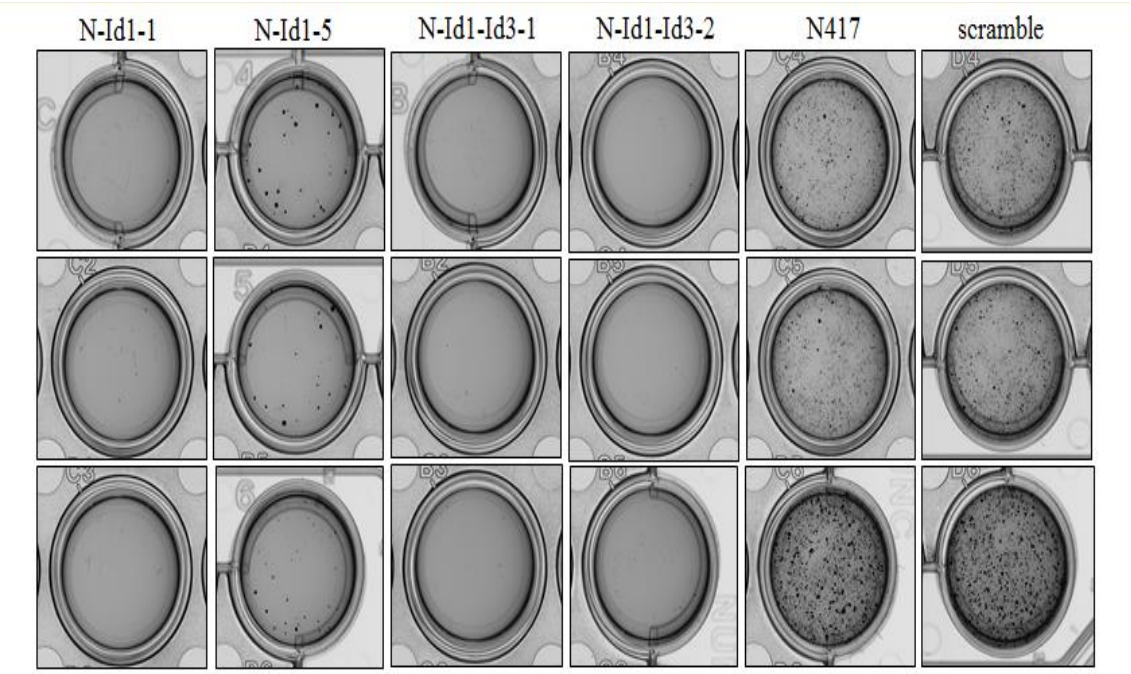

Figure 3.9. Soft agar assay were performed to compare the effect of the Id1 and Id3-shRNA or Id1-shRNA on clonogenicity of N417 cells in anchorage independent environment. The soft agar wells were stained with MTT for 4 hours. Photographs showed the stained soft agar wells when terminated at the end of 6 weeks.

3.6. Inhibition of Id1 and Id3 greatly suppressed the tumour growth in nude mice

To test the effect of inhibiting Id1 and Id3 expression in SCLC, Id1- and Id3-shRNA transfectant cells was inoculated in nude mice and the tumours produced by different transfectants was measured at different time points and resected at autopsy. Tumours

resected from different groups of mice and tumour-bearing mice were shown in **Figure 3.10**. Nude mice in all groups gained weight over the course of the study. All tumours were visualized 8 days after the inoculation thus no significant difference was seen on lengths of latent period. The scramble RNA transfected cell group elicited more rapid tumour growth than the N-Id1 and N-Id1-Id3 groups. In N-Id1-1 group, 1 mouse failed to produce tumours in either of the 2 flanks. In N-Id1-Id3-1 group, 1 mouse failed to produce tumour in the left flank. As a whole, no significant differences in tumour incidences were tested between the control and each of the testing groups (P=0.48, P=1).

As shown in **Figure 3. 11**, the average sizes of tumours produced by the control group on day 9, 12, 15, 18 and 21 respectively were all significantly larger than those produced by N-Id1-1, N-Id1-5, N-Id1-Id3-1 and N-Id1-Id3-2 groups at the same time-points (P<0.0001). On day 9, 12, 15 and 18, the average of tumour volume from different groups of nude mice was summarized in **Table 3.4**. After an 8-day latent period, the control cells grew much faster than N-Id1 and N-Id1-Id3 transfectant cells in nude mice. The average of tumour volume from different groups of nude mice on day 21 was summarized in **Table 3.5**. At autopsy, the average volumes of tumours produced by N-Id1-1, N-Id1-5, N-Id1-Id3-1 and N-Id1-Id3-2 were 63±32, 98±49, 60±14 and 40±28 mm^3 respectively; 7.8-, 5-, 12.3- and 8.2-fold significant reduction (p<0.0001) in compared with that produced by the scramble control (490±241 mm^3).

At the end of the experiment, the average weight of tumours produced in N-Id1-1, N-Id1-5, N-Id1-Id3-1 and N-Id1-Id3-2 groups was 55±34, 87±56, 33±16 and 53±32 mg, significantly reduction (p<0.002) of 6.6-, 4.1-, 10.9-, and 6.8-fold; respectively, in

comparison with that produced by the control group (360±164 mg) (**Figure 3. 12**). The average of tumour weight from different groups of nude mice on day 21 was summarized in **Table 3.6**.

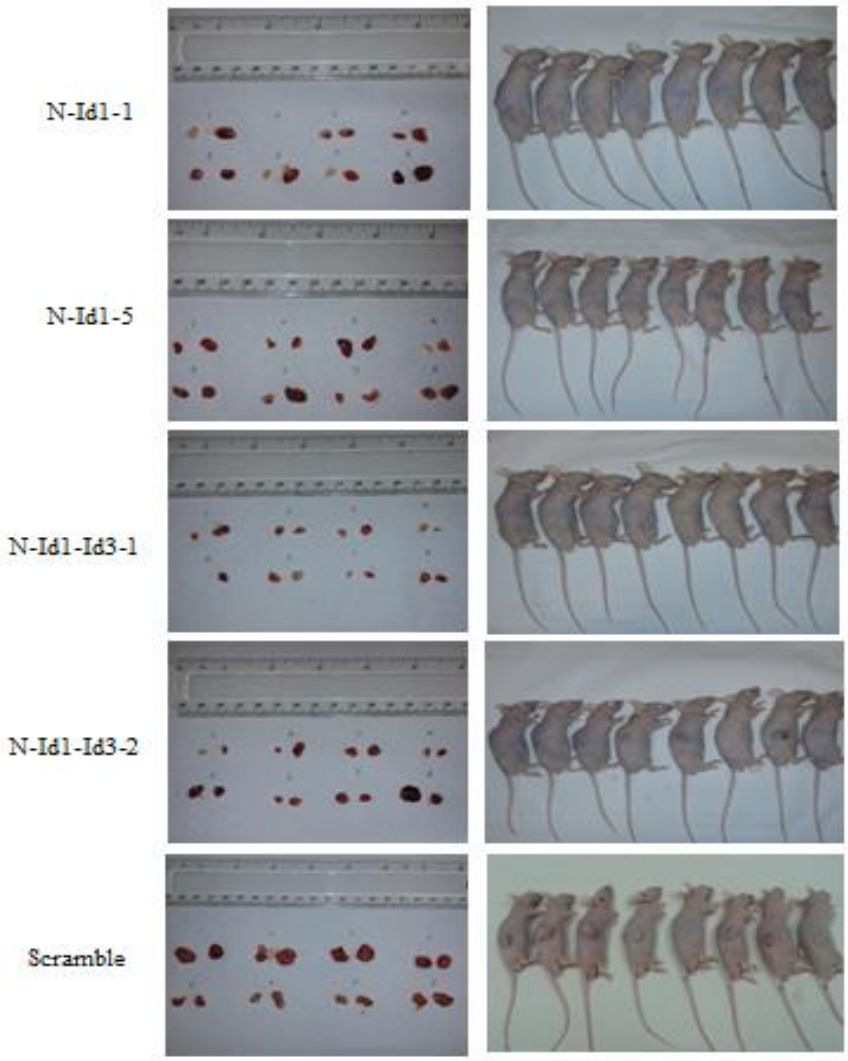

Figure 3.10. Testing tumorigenicity of different transfectant cells in nude mice. Transfectant cells N-Id1-1, N-Id1-5, N-Id1-Id3-1, N-Id1-Id3-2 and the control (scramble RNA transfected) cells were inoculated into both flanks of male BALB/c nude mice to produce tumours. Tumour produced in control and each of the 4 testing

groups. Left panel: tumours resected at autopsy (21 days after the initial inoculation); Right panel: different groups of mice that bear tumours with different sizes (21 days after the initial inoculation).

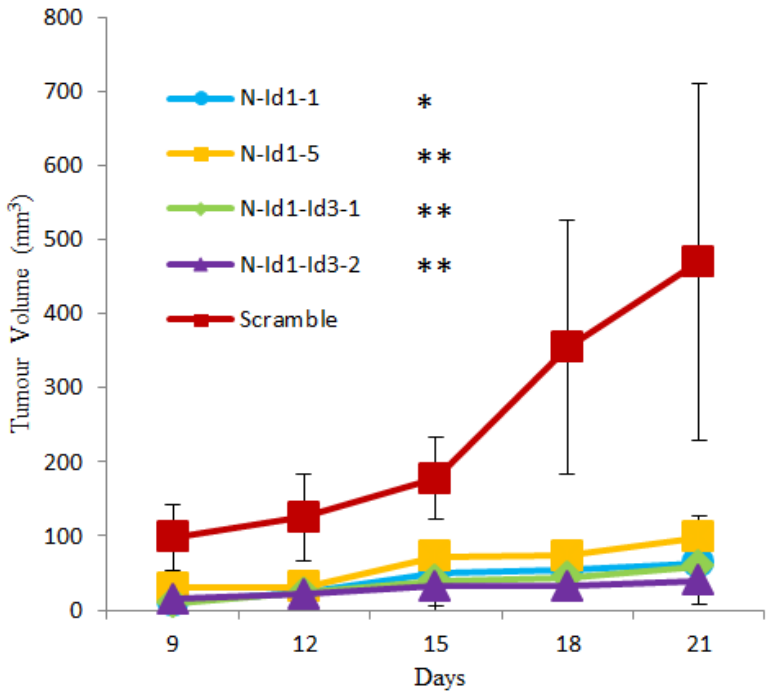

Figure 3.11. The average tumour volume of different groups of nude mice. Tumour started appearing after an 8-day latent phase in all five groups. Growth curves of tumours derived from the indicated groups over a period of three weeks. Data were presented as the mean and SD from independent groups (n=8, **P<0.0001, *P<0.05).

Day	Average tumour volume (mm^3, mean ± SD)				
	N-Id1-1	N-Id1-5	N-Id1-Id3-1	N-Id1-Id3-2	Scramble
9	11.34 ±9.37	30.17 ±10.64	9.65 ±2.28	15.11 ±8.24	97.75 ±44.98
12	23.17 ±3.75	30.99 ±15.04	21.27 ±2.1	22.86 ±3.66	125.49 ±58.61
15	50.59 ±33.71	72.06 ±21.84	31.63 ±8.82	39.19 ±9.43	177.63 ±54.94
18	54 ±20.92	73.06 ±36.94	32.16 ±11.84	44.05 ±13.24	353.93 ±171.18

Table 3.4. Summary of the average tumour volume calculated for each group of animals on the day 9, 12, 15 and 18, the average volume of tumours was represented as mean ± SD.

Animal group	Average tumour volume on day 21 (mm^3, mean ± SD)
Scramble control	359.94 ± 183.94
N-Id1-1	54.69 ± 33.96
N-Id1-5	87.14 ± 55.53
N-Id1-Id3-1	33 ± 16.34
N-Id1-Id3-2	52.81 ± 31.35

Table 3.5. Summary of the average tumour volume calculated for each group of animals on the day 21, the average volume tumours of different groups was represented as mean ± SD.

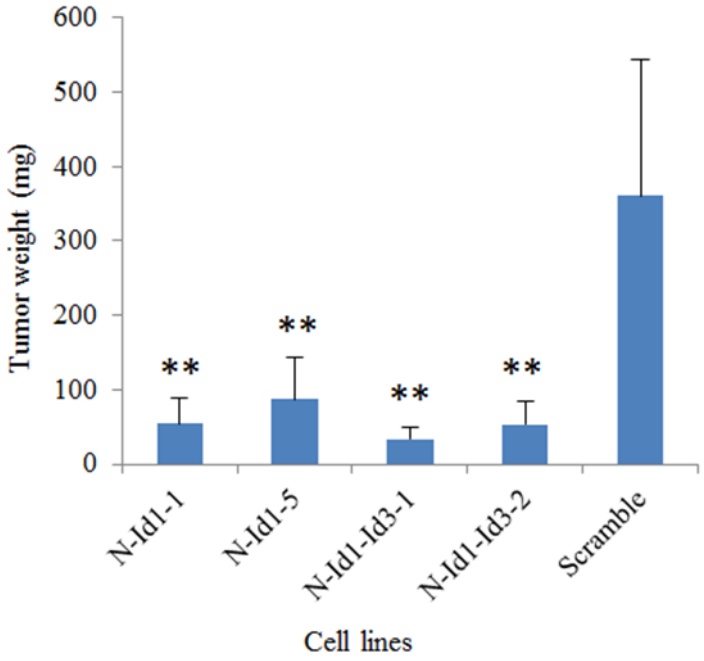

Figure 3.12. The average tumour weight of nude mice groups inoculated with different transfected cell lines. Tumour weight was quantified 21 days after transplantation. Data were presented as the mean and SD from independent groups (n=8, **P<0.0001).

Animal group	Average tumour weight on day 21 (mg, mean ± SD)
Scramble control	359.94 ± 183.94
N-Id1-1	54.69 ± 33.96
N-Id1-5	87.14 ± 55.53
N-Id1-Id3-1	33 ± 16.34
N-Id1-Id3-2	52.81 ± 31.35

Table 3.6. Summary of the average tumour weight of each group of nude mice inoculated with Id1- and Id3-shRNA, Id1 shRNA or scramble RNA molecules transfectants on day 21. The average tumour weight was shown as mean ± SD.

3.7. Expression levels of Id1, Id3 and VEGF in xenograft tumours by immunohistochemistry

Id1, Id3 and VEGF protein expression levels in xenograft tumours were analysed by immunohistochemistry (**Figure 3.13**). Tissue sections were evaluated by two investigators independently and results of Id1, Id3 and VEGF expression were summarized in **Table 3.7-3.9**. On control tissue sections, both cytoplasmic and nuclear staining were observed when Id3 were used, only cytoplasmic staining was observed for Id1 and VEGF.

Moderate staining (8 of 13, 62%) and weak staining (5 of 13, 38%) of Id1 were observed in control nude mice, and 2 of 7 (29%) samples and 5 of 7 (71%) samples in N-Id1-5 group were moderately and weakly stained with Id1 antibody respectively. In N-Id1-1 and N-Id1-Id3-1 groups, the Id1 staining was negative in cytoplasm and in N-Id1-Id3-2 group all samples were weakly stained. In most cases, Id1 staining in scramble control was much stronger than those in xenograpts produced by N-Id1 and N-Id1-Id3 cells ($P<0.004$).

When stained with antibody against Id3, 11 of 13 (85%) samples and 2 of 13 (15%) samples exhibited moderate and weak cytoplasmic staining respectively in control group, 7 of 9 (78%) samples and 2 of 9 (22%) samples in N-Id1-Id3-2 were respectively stained weakly and negatively. Cytoplasmic Id3 staining of N-Id1-Id3-1 group was negative. In the nuclei, 3 of 13 (23%) samples and 10 of 13 (77%) samples exhibited strong and moderate staining respectively in control group. All sections

from N-Id1-Id3-2 group were moderately stained, 1 of 9 (11%) samples and 8 of 9 (89%) samples from N-Id1-Id3-1 group were moderately and weakly stained respectively. Significantly decreased levels of Id3 were detected in both cytoplasm and nucleus of N-Id1-Id3 groups as compared with that produced by control cells ($P<0.02$). The expression of Id3 in N-Id1 groups was similar to that in control (results not shown).

The expression of VEGF was relatively faint in all tissue samples. In the control group, 11 of 13 (85%) samples and 2 of 13 (15%) samples were moderately and weakly stained respectively in the cytoplasm, whereas 6 of 7 (86%) samples and 1 of 7 (14%) samples were weakly and very weakly stained in N-Id1-5 group. All samples from N-Id1-1 group were stained very weakly for VEGF, and in groups of N-Id1-Id3-1 and N-Id1-Id3-2 the VEGF staining was negative. The cytoplasmic staining of VEGF in samples from scramble control group was significantly stronger than that in N-Id1 and N-Id1-Id3 groups ($P<0.002$). CD34 was used to quantify the microvessel numbers of the xenograft tumours and the results were shown in **Figure 3.14**. The average number of microvessel produced by N-Id1-1, N-Id1-5, N-Id1-Id3-1 and N-Id1-Id3-2 were 2.33 ± 0.57, 3.66 ± 0.57, 0.33 ± 0.28 and 1.66 ± 0.57 respectively; 4.1-, 2.6-, 29.2- and 5.8-fold significant reduction ($p<0.0001$) in compared with that produced by the scramble control (9.66 ± 1.15).

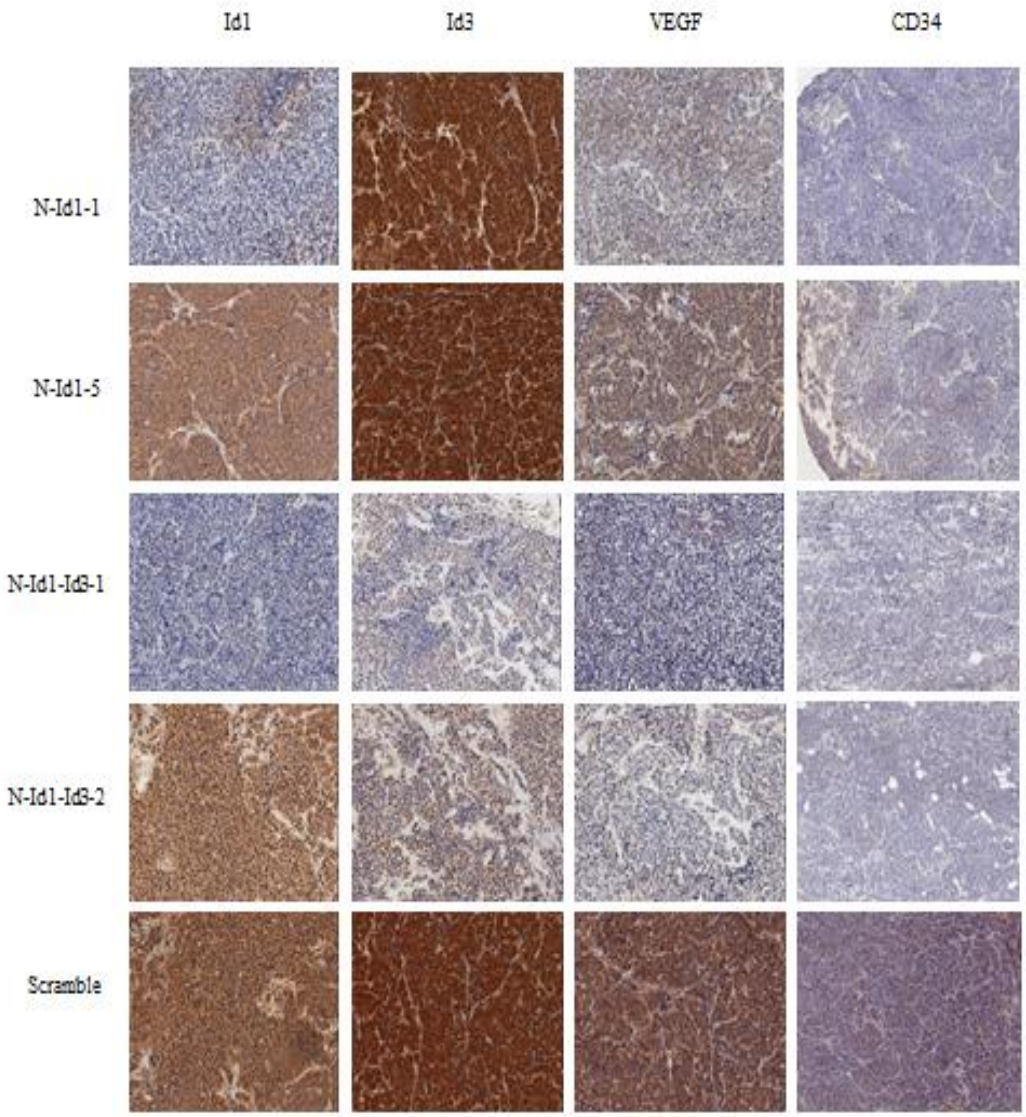

Figure 3.13. Immunohistochemistry analysis of the expression status of Id1, Id3, VEGF and CD34 in tumours produced in mice. Sections of tumour samples from each group were immunohistochemically stained with antibodies against Id1 (column 1), Id3 (column 2), VEGF (column 3) and CD34 (column 4), respectively. The staining intensities with different antibodies were scored by analysing ten fields per slide. Original magnification: 10×.

Animal group	No. of samples	Cytoplasmic stain intensities		Nuclear stain intensities & percentage score	
Scramble Control	**13**	0	**0**	**1-3**	**11**
		+	**5**	**4-6**	**2**
		++/+++	**8**	**7-9**	**0**
N-Id1-1	**7**	0	**7**	**1-3**	**7**
		+	**0**	**4-6**	**0**
		++/+++	**0**	**7-9**	**0**
N-Id1-5	**7**	0	**0**	**1-3**	**7**
		+	**5**	**4-6**	**0**
		++/+++	**2**	**7-9**	**0**
N-Id1-Id3-1	**9**	0	**9**	**1-3**	**9**
		+	**0**	**4-6**	**0**
		++/+++	**0**	**7-9**	**0**
N-Id1-Id3-2	**9**	0	**0**	**1-3**	**9**
		+	**9**	**4-6**	**0**
		++/+++	**0**	**7-9**	**0**

Table 3.7. Id1 protein expression levels in xenograft tumours which inoculated with Id1 shRNA, Id1 and Id3 shRNA or scramble RNA transfectants. Results based on immunohistochemistry analysis. The cytoplasmic intensity of staining was scored as: no stain = 0, weakly stained = +, moderately stained = ++, strongly stained = +++. The nuclear staining was obtained by multiplying the intensity score with the percentage score and finally rated as follows: 0, negative staining; 1-3, weak staining; 4-6, moderate staining; 7-9, strong staining.

Animal group	No. of samples	Cytoplasmic stain intensities		Nuclear stain intensities & percentage score	
Scramble Control	**13**	0	**0**	**1-3**	**0**
		+	**2**	**4-6**	**10**
		++/+++	**11**	**7-9**	**3**
N-Id1-Id3-1	**9**	0	**9**	**1-3**	**8**
		++	**0**	**4-6**	**1**
		++/+++	**0**	**7-9**	**0**
N-Id1-Id3-2	**9**	0	**2**	**1-3**	**0**
		+	**7**	**4-6**	**9**
		++/+++	**0**	**7-9**	**0**

Table 3.8. Id3 protein expression levels in xenograft tumours which inoculated with Id1 and Id3 shRNA or scramble RNA transfectants. The tumour tissues of Id1 shRNA transfected cells expressed similar level of Id3 as the control. Results based on immunohistochemistry analysis. The cytoplasmic intensity of staining was scored as: no stain = 0, weakly stained = +, moderately stained = ++, strongly stained = +++. The nuclear staining was obtained by multiplying the intensity score with the percentage score and finally rated as follows: 0, negative staining; 1-3, weak staining; 4-6, moderate staining; 7-9, strong staining.

Animal group	No. of samples	Cytoplasm			
		negative	very weak staining	Weak staining	moderate staining
Control	13	0	0	2	11
N-Id1-1	7	0	7	0	0
N-Id1-5	7	0	1	6	0
N-Id1-Id3-1	9	9	0	0	0
N-Id1-Id3-2	9	7	2	0	0

Table 3.9. VEGF protein expression levels in xenograft tumours which inoculated with Id1 shRNA, Id1 and Id3 shRNA or scramble RNA transfectants. Results based on immunohistochemistry analysis.

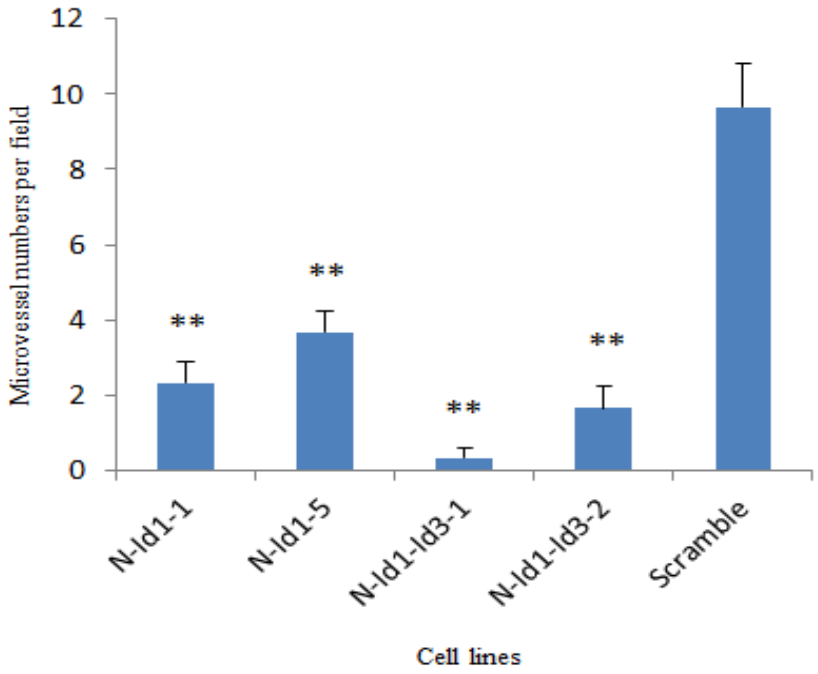

Figure 3.14. The numbers of microvessel in xenograft tumours produced by transfectants. Sections of tumour samples in each group were immunohistochemically stained with antibody against CD34. The microvessel numbers were quantified by analysing ten fields per slide. Original magnification: 10×. Results were presented as the mean and SD from independent groups (**P<0.0001).

3.8. Effect of Id1 and Id3 suppression on sensitivity of apoptosis induction

The effect of suppressing Id1 and Id3 jointly or Id1 alone on sensitivity of apoptosis induction of SCLC was determined by Annexin V-PE staining and flow cytometry. The percentages of apoptotic cells in different cultured cell lines under the treatments

with different doses of cisplatin (a first line drug used for chemotherapy) were shown in **Figure 3.15**. Summary of the average apoptosis rate of all transfectants was shown in **Table 3.10**.

The percentages of cells undergoing apoptosis in the scramble control cells were 0.92%, whereas that in N-Id1-1, N-Id1-5, N-Id1-Id3-1, N-Id1-Id3-2 was 4.25%, 2.86%, 8.43% and 5.74% respectively. When treated with different dosages of cisplatin, the number of cells undergoing apoptosis was increased in a dosage-dependent manner in all treated cell lines. A low dose (25 μM) cisplatin treatment caused 3.3-10.7% of cells undergoing apoptosis in the control and other transfectant cells. Apoptotic cells increased as the increasing doses of cisplatin. The percentages of apoptotic cells in 50μM cisplatin group increased to 9.58%, 7.05%, 15.98% and 11.39% in N-Id1-1, N-Id1-5, N-Id1-Id3-1, and N-Id1-Id3-2 respectively, in comparison with that of the scramble control (4.89%). The effect of 75 μM cisplatin treatment was similar as that of 50μM cisplatin treatment. The percentages of cells undergoing apoptosis were 10.03%, 8.75%, 17.91% and 12.72% in N-Id1-1, N-Id1-5, N-Id1-Id3-1, and N-Id1-Id3-2 respectively, in comparison with that of the scramble control (6.87%). A higher dose (100μM) cisplatin treatment further increased the percentages of apoptotic cells to 13.63%, 11.27%, 23.67% and 18.37% in N-Id1-1, N-Id1-5, N-Id1-Id3-1, and N-Id1-Id3-2 respectively, compared to that of the scramble control (8.72%). When the highest dose of cisplatin (125 μM) was used, the percentages of the apoptotic cells remarkably induced to 17.06%, 14.69%, 32.94%, and 23.76% in N-Id1-1, N-Id1-5, N-Id1-Id3-1 and N-Id1-Id3-2 respectively, in comparison with that of the scramble control (9.34%). Thus the number of apoptotic

cells increased 1.6-3.6-fold in N-Id1 and N-Id1-Id3 transfectants compared to the control ($P < 0.005$).

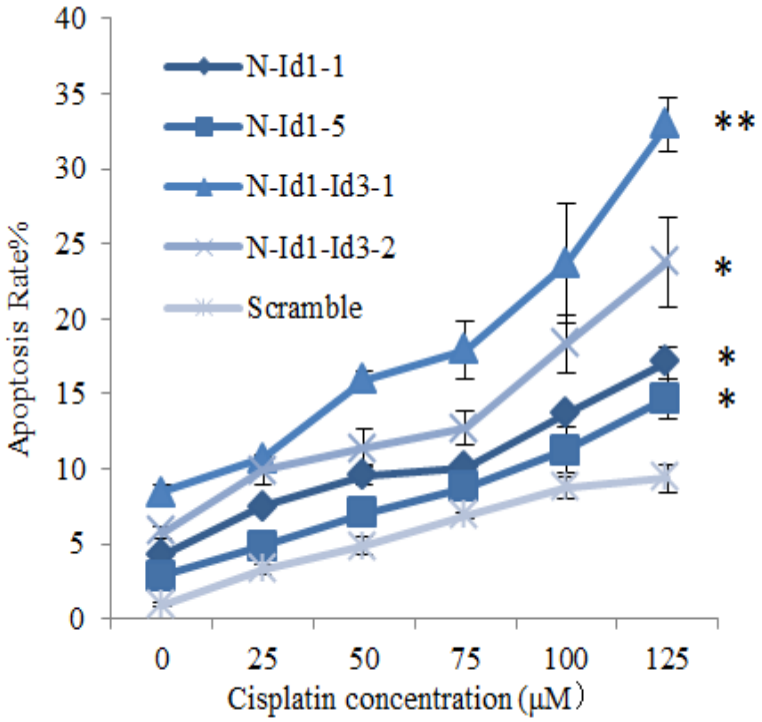

Figure 3.15. Titration of cisplatin on induction of apoptosis of Id1 shRNA, Id1 and Id3 shRNA or scramble RNA transfectants. Treatment of all indicated cells with 0, 25, 50, 75, 100, 125 μM cisplatin for 24 hours. After exposure to cisplatin, all cell lines were stained with Annexin V-PE. The apoptosis rate was assessed by flow cytometry. Results were shown as mean ± SD. Statistically significant was compared with the control **P<0.0001, *P<0.05.

Cell line	Apoptosis rate %					
	0μM	25μM	50μM	75μM	100μM	125μM
Scramble	0.92	3.3	4.89	6.87	8.72	9.34
N-Id1-1	4.25	7.52	9.58	10.03	13.63	17.06
N-Id1-5	2.86	4.89	7.05	8.75	11.27	14.69
N-Id1-Id3-1	8.43	10.71	15.98	17.91	23.67	32.94
N-Id1-Id3-2	5.74	9.9	11.39	12.72	18.37	23.76

Table 3.10. Summary of the average apoptosis rate of Id1 and Id3-shRNA, Id1-shRNA or scramble RNA transfectants. The average of apoptosis rate was calculated from three independent experiments.

3.9. Effect of Id1 and Id3 suppression on angiogenesis

3.9.1. Detection of VEGF protein expression in transfectant cells and conditioned medium

To assess the effect of changed expression levels of Id1 and Id3 on VEGF expression, Western blot and ELISA were conducted to detect VEGF expressed in the transfectant cell lines and that secreted into the culture medium. Results of Western blotting were

shown in **Figure 3.16A**. Relative VEGF levels of all transfected cell lines were quantified using densitometry and the values were normalised against β-actin (**Figure 3.16B**). The VEGF expression levels in N-Id1-1, N-Id1-5 were mildly reduced to 0.6 and 0.83 respectively, while that in N-Id1-Id3-1 and N-Id1-Id3-2 were markedly reduced to 0.11 and 0.36 respectively when compared with the control which was set at 1 ($p<0.0004$).

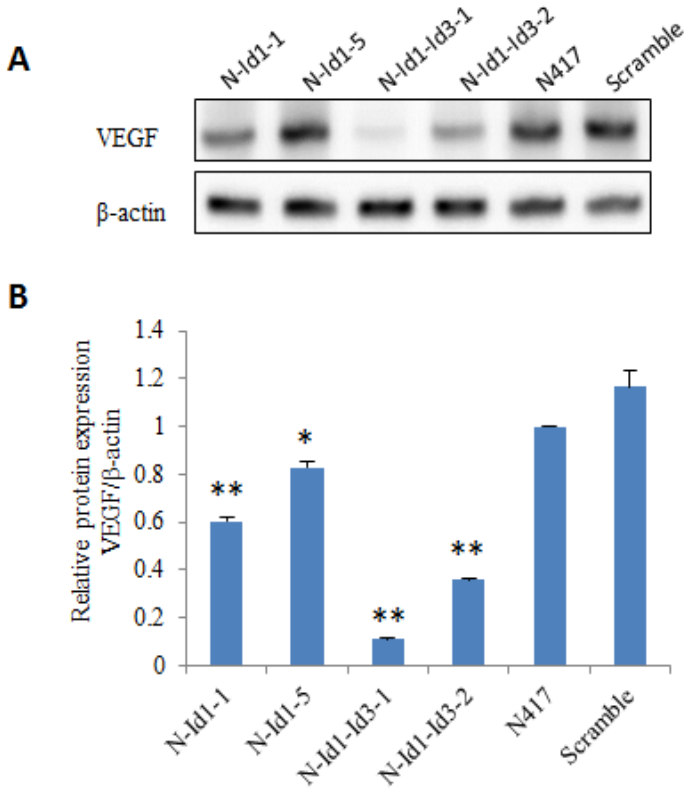

Figure 3.16. Expression level of VEGF in Id1 shRNA, Id1 and Id3 shRNA or scramble RNA transfectant N417 cells. A. Western blot analysis of VEGF proteins in N-Id1-1, N-Id1-5, N-Id1-Id3-1, N-Id1-Id3-2, scramble RNA transfected and N417 cells. B. Quantitative analysis of relative VEGF protein expression. The results were

shown as mean ± SD. of three individual experiments. Statistical difference was determined by two-tailed Student's *t*-test (**P<0.0001, *P<0.05).

To determine the VEGF amount in conditional medium of all samples, the recombinant human VEGF was used as VEGF standard. A standard curve was generated by plotting the optical density of each standard concentration on the vertical (Y) axis vs. the corresponding human VEGF concentration (pg/ml) on the horizontal (X) axis. The results of VEGF standard showed a good regression (R^2 = 0.9966) between absorbance signal and VEGF concentration (**Figure 3.17**). Therefore, the VEGF amount in medium of samples may be calculated by using the standard curve. ELISA was performed to assess VEGF levels in conditioned medium of cell culture and results of ELISA were shown in **Figure 3.18**. The amount of VEGF in conditioned medium of cell culture collected from N-Id1-1, N-Id1-5, N-Id1-Id3-1 and N-Id1-Id3-2 was 1190±143, 2655±218, 297±28, and 554±30 pg/ml respectively versus that in control (3415±155 pg/ml). The significant difference was detected between scramble control and the other transfectants (P<0.008).

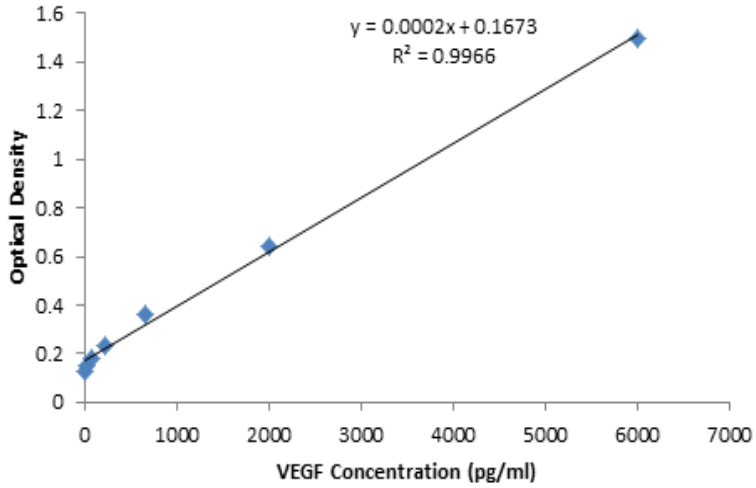

Figure 3.17. The standard curve illustrated how to calculate VEGF concentrations of unknown samples in VEGF ELISA analysis. The readings of samples subtracted the zero standard optical density and the best fit curve was graphed via regression analysis. The curve equation and regression value of the curve were determined.

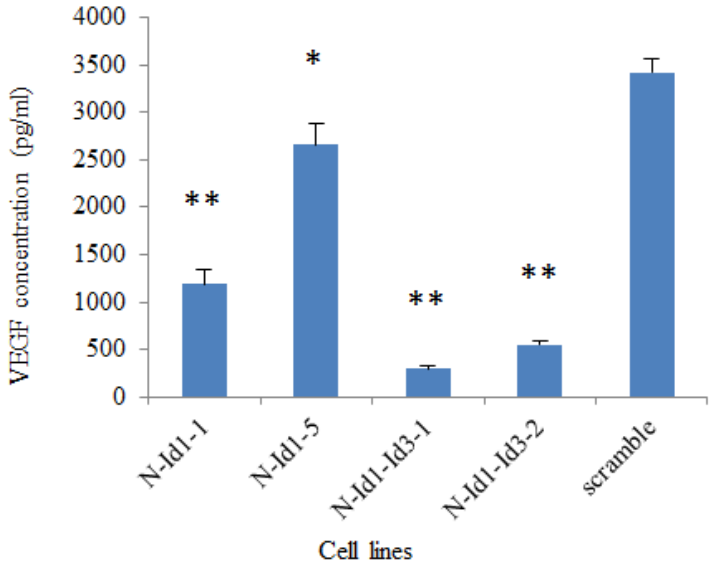

Figure 3.18. Analysis VEGF protein level in conditioned medium of Id1 shRNA, Id1 and Id3 shRNA or scramble RNA transfectants. VEGF protein concentrations in the conditioned medium of indicated cells were analysed by ELISA. The data were shown as mean ± SD. of three individual experiments. Statistical difference was determined by two-tailed Student's *t*-test (**P<0.0001, *P<0.05).

3.9.2. Biological activity of VEGF produced by transfectants

To test whether the VEGF produced by different cells is biologically active, a tube-like formation assay was performed to exam the conditional media and the results of the network formations were shown in **Figure 3.19**. VEGF secreted by transfectants into the conditional medium was collected to test whether it can affect the endothelial cells forming tube-like structures. The HUVEC cells aligned and developed capillary tubes when they were seeded onto Matrigel. As shown in **Figure 3.19**, the representative photos from different transfectant cells showed that the culture media of transfectants largely inhibited tube-like formations of HUVECs. Capillary tubes were evaluated through pattern recognition quantitation following the manufacture's instruction. The network formation scores were shown in **Figure 3.20**. Conditioned medium of scramble control strikingly promoted endothelial tube formation, as well as human recombinant VEGF, with average score of 4.2 and 4.4 respectively. In contrast, the average score of N-Id1-1, N-Id1-5, N-Id1-Id3-1 and N-Id1-Id3-2 was 2.6, 3.8, 1.4 and 2 respectively. Thus N-Id1-Id3-1 and N-Id1-Id3-2 significantly blocked the HUVECs forming branching networks ($P<0.0001$).

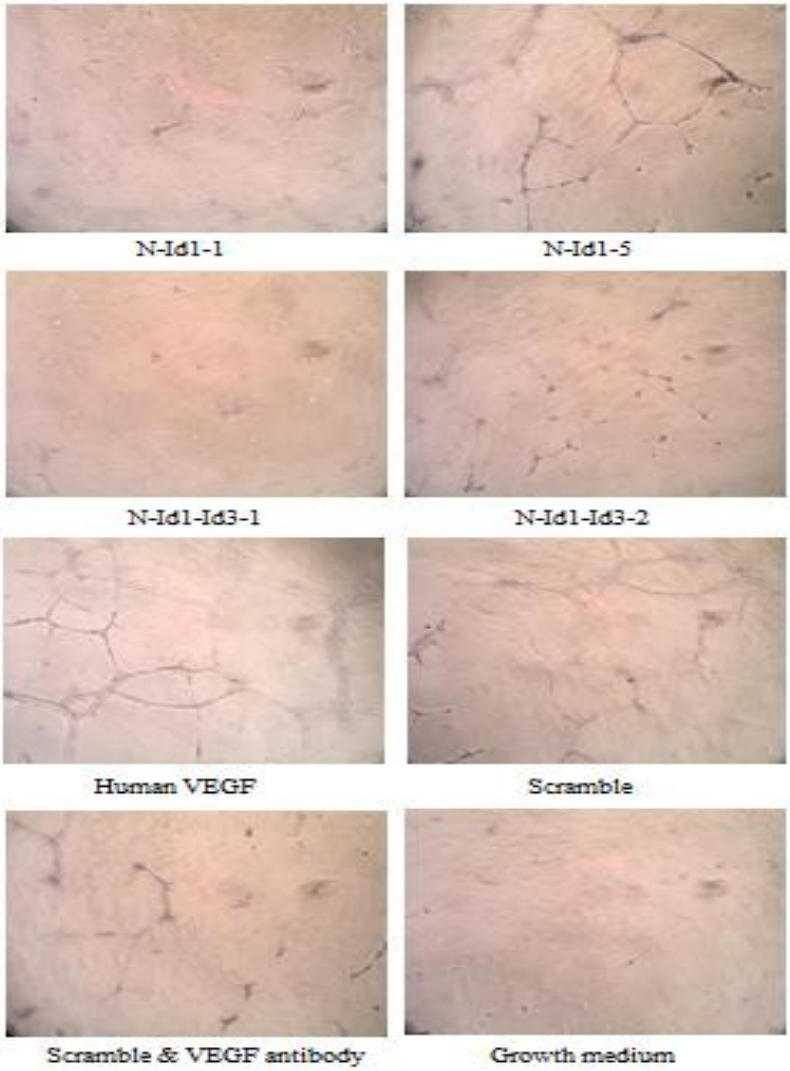

Figure 3.19. Measurement of biological activity of VEGF produced by different transfectant cells. Representative photographs of matrigel-coated culture of HUVEC cells after incubation with conditioned medium of indicated cells. Network formation was observed by inverted microscope in 40× magnification. Five randomly selected microscopic fields of each cell line under same condition were evaluated.

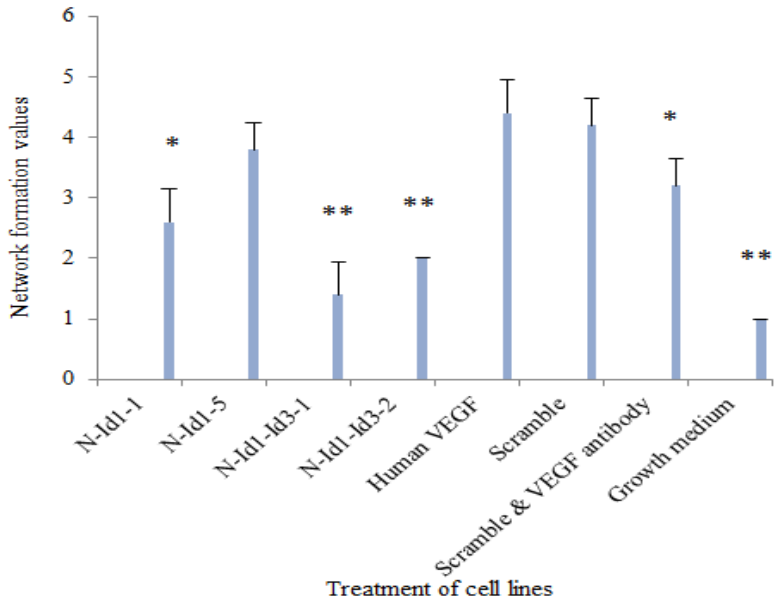

Figure 3.20. Scoring network formation produced by different conditioned media. Five randomly selected microscopic fields of each cell line under same condition were evaluated. Each column displays average number of tubes formed by different groups in three independent experiments (mean ± SD, **P<0.0001, *P<0.05).

CHAPTER 4
DISCUSSION

CHAPTER 4 DISCUSSION

4.1. Establishment of Id1- and Id3-doubleknockdown or Id1-suppressed clones

Increased expression of Id1 and Id3 was detected in both SCLC cell lines and tissues in our previous work (414). According to Id1 and Id3 expression profile in 10 SCLC cell lines, malignant SCLC cell line N417 overexpressed both Id1 and Id3 in comparison with benign Beas-2B cells. To clarify the roles of Id proteins in SCLC, RNAi technique was used in a way of two-step evaluation system. For selection of the most effective silencer against Id1, three siRNA candidates were initially retrieved from Whitehead library and compared for their knockdown effects by transient transfection. Generally, transient transfection only takes less than three days to conduct and remains one of the most efficient ways for knockdown efficiency monitoring. Secondly, we introduced a single duet shRNA expression vector that facilitated the double knockdown of Id1 and Id3. The advantages of cloning two shRNA into a vector relied on minimizing the risks of transfection, which is especially important for the stubborn cells (with low transfection efficiency). Then the optimal suppressors for Id1 and Id3 were inserted into two separate cassettes of the same vector followed by establishing cell lines expressing shRNAs against Id1 and Id3 simultaneously through stable transfection. This two-cassette strategy is critical for double knockdown, avoiding additional shRNA vector construction which may double

the transfection time and risk of transfection efficiency.

In this study, three 21 nt sequences within Id1 cDNA with 40-60% GC content were identified using Whitehead tool and used as potential siRNA target against Id1. To minimize the siRNA off-targeting effects, all chosen siRNAs were aligned with the current sequences in NCBI database BLAST. No significant alignment with other sequences was found. The candidate sequences The candidate sequences initially started from the database of an academic institute and were not validated in other studies. Although there were couples of previous studies performed with Id1 siRNAs, these studies all based on the siRNA sequences commercially purchased from either Life Technoligies or Dharmacon (345, 415, 416). The critical step in transient transfection is introduction of siRNA into the mammalian cells. A variety of methods were applied historically including calcium phosphate, lipids, electroporation, ballistics, and a combinations of two or more of these (417). However, no single transfection method is suitable for all types of cells. The cell viability, suppression efficiency can be very different due to different siRNA targets, the amount of siRNAs applied, delivery methods and cell types of interest. In this study, we used a malignant SCLC cell line-N417, which grows in suspension and was regarded as a very difficult cell line to transfect. The reason for low transfection efficiency was due to the fact that the suspension cells have poor capability of taking the transfection complex which consists of transfection reagent and target gene. To transfect target siRNAs to N417 cells efficiently, we used a reverse transfection technique which is a simple and cost-effective delivery system to manipulate the hard-to-transfect cells. Reverse transfection technique was initially described by Mousses *et al* (418) and successfully utilized in large-scale RNAi screens (419). It has been demonstrated that this method

could avoid redundant manipulations (420). Furthermore, siRNA can be introduced into cytoplasm in a high efficiency, low toxicity manner. Accurate delivery of the construct into cytoplasm is a prerequisite for the knockdown of mRNA since siRNA generally performs their biological activities in the cytoplasm (421). With the reverse transfection technique, we have tested three siRNA sequences that could be used against Id1. The silencing effect of three siRNAs was examined by Western blot. We found that they have different efficiency on knockdown Id1 and the second sequence against Id1 (the most efficient silencer) produced 87% reduction of target gene at 48 hours after transfection. A study carried out on 15 human cell lines using reverse transfection technique achieved 46% to 97% suppression of target gene (421). Compared to this previous work on adherent cells, we have achieved relatively good suppression efficiency in transient transfection.

Introduction of siRNAs in mammalian cells induces strong and specific degradation of the target RNA. However, this effect is only transient due to the short lifespan of synthetic siRNAs. This may severely limits the applications and usefulness of siRNAs. To overcome this limitation, plasmid and viral-based expression of shRNA were developed for the long-lived gene silencing effects (422). In this study, we used a strategy to make one single construct that contains both shRNAs and only requires one round of transfection into the recipient cells. In this study, the expression levels of Id1 in N-Id1-1 and N-Id1-5 were reduced to 10% and 45% respectively (Figure 3.4B) compared to the control, whereas the levels of Id3 in those cells were similar to that in the parental cells (Figure 3.4D). This result suggested that suppressing Id1 expression did not change the expression level of Id3, which was in line with our previous study (405). In Id1 and Id3 double knockdown cells, the expression levels of Id1 in

N-Id1-Id3-1 and N-Id1-Id3-2 were reduced to 16% and 35% respectively (Figure 3.4F), the levels of Id3 of those cells were 27% and 44% of that in parental cells (Figure 3.4H). The Id3 silencing efficiencies were similar to that achieved previously (35% and 55%) (405). Thus no cross effect was observed when Id1 and Id3 were suppressed by two separate shRNAs in the same transfectant pool simultaneously. Although complete knockdown of targeting siRNAs was not achieved, we managed to reduce Id1 and Id3 by 90% and 86% respectively in SCLC cells. This suppression was sufficient enough to reduce the levels of Id1 and Id3 in transfectant cells to levels below that in normal epithelial cells of the lung (Beas-2B). Despite the wide applications of plasmid-based shRNA technique, a variety of limitations is obvious. First, most of the current vectors were designed to target a single siRNA. The main shortcoming of a construct encoding single shRNA is that single shRNA molecule may be quickly overwhelmed by the mutations (423). Secondly, two rounds of transfection were prerequisite if a study aimed to test two or more targets simultaneously. Although some previous studies with two rounds of transfection achieved a 90% to 100% reduction of target genes, their studies performed on cells cultured in monolayer (424). For the difficult-to-transfect cells such as cells cultured in suspension, the ideal strategies are the use of single vector consists of multiple cassettes or viral-based shRNAs. A recent study compared three shRNAs co-expression methods which using multiple plasmids and single vector harbouring multiple cassettes. It was found that multiple plasmids were not efficient with more than two shRNAs (425). One study of double knockdown two genes using lentiviral in SCLC showed that 2- to 15- fold differences in gene expression levels between the highest and the lowest expressing cell lines (426). However, the viral-based shRNA

expression system also has its disadvantage because human immune response to viruses not only prevents gene delivery but also has the potential to generate severe complications (427). Compared to the viral-based shRNA expression system, the plasmid-based shRNA expression system may have more widely application for *in vivo* assay. Thus double knockdown of Id1 and Id3 by single plasmid vector containing two shRNAs and with one round of transfection was the most convenient way to minimize the risk during plasmid construction and transfection.

4.2. MTS assay studying the cell growth of SCLC

Although earlier studies have suggested a correlation of Id expression and tumour proliferation, invasiveness and aggressiveness in established cell lines and tissues (357, 360, 428). No investigation was performed to study weather Id1 and Id3 play a synergistic roles in SCLC. Our study is the first to test the functional characteristics of Id1 and Id3 in SCLC tumourigenesis through RNAi technique. We identified that double knockdown of Id1 and Id3 crucially inhibit progression of human SCLC cells N417 in MTS assay. MTS is a novel tetrazolium compound that can only be digested by living cells to produce a formazan product. The quantity of formazan product is measured by the absorbance at 490 nm and the decreased amount of MTS is directly proportional to the number of living cells. Thus MTS assay as an indicator of metabolically active mitochondria is used to reflect the cell viability and proliferation. Results in this study showed that Id1-suppressed cells produced significant reductions in proliferation rate by 1.4- and 2.1-fold comparing with the control (Figure 3.7). Our previous study showed that Id3-suppressed cells reduced cell proliferation by 2.5- and

2.8-fold (405). Thus the efficiency of suppressing Id3 on cell proliferation was 1.3 and 1.8 times of that produced by suppressing Id1. The Id1 and Id3 double knockdown produced 3.9- and 6.4-fold reduction in cell proliferation rate respectively when compared with the control (Figure 3.7). This result showed that the effect produced by joint suppression of Id1 and Id3 on cell proliferation was similar to, or more than the sum of the two effects produced by suppressing Id1 and Id3 separately.

Id1 is most frequently associated with tumourigenesis as it regulates cell proliferation, survival and growth (307, 429). Id1 stimulated survival of esophageal cancer cells through activation of PI3K/Akt/NF kappa B signalling pathway (416) and promoted prostate cancer cell proliferation through inactivation of p16INK4a/pRb pathway (431). In one study of NSCLC, Id1 was reported to induce numerous NSCLC cell lines, primary epithelial and endothelial cells from the lung in response to nAChR as well as EGFR signalling (432). It was found that suppression of Id1 inhibited nicotine- and EGF-induced proliferation and invasion of NSCLC cells. One study showed that Wnt3a induced Id3 expression in a β-catenin-dependent manner and Id3 regulated Wnt3a-induced C2C12 cell proliferation (433). Knockdown of Id3 with siRNA significantly decreased cell viability and proliferation of medulloblastoma cells (434).

4.3. Soft agar assay studying the tumourigenicity of SCLC *in vitro*

Soft agar assay results showed that the number of colonies produced by Id1-suppressed cells was remarkably decreased by more than 13.7-fold compared with

that of the parental cells (Figure 3.8). As showed by our previous work, Id3-suppressed cells produced up to 3.7-fold reduction in number of colonies when compared to parental cells (405). Thus suppression of Id1 produced nearly 4-times reduction on anchorage-dependent growth of the cells than that produced by Id3 suppression. The colony numbers produced by the two Id1 and Id3 double-knockdown transfectant cell lines (1 ± 0.57 and 2 ± 0.57, respectively) were dramatically reduced by 466- and 233-fold respectively when compared with the control (Figure 3.8). The reduction produced by the joint Id1 and Id3 suppression was much larger than the sum of those produced by suppressing Id1 and Id3 separately. Thus the reduced levels of Id1 and Id3 by combined suppression synergistically impaired the colony formation ability of the SCLC cells in soft agar.

4.4. Boyden chamber assay studying the invasiveness of SCLC *in vitro*

The suppression effect was also observed in the invasion assay which showed that Id1-suppressed cells and Id1 and Id3 double knockdown cells produced more than 1.7- and 4.6-fold reduction respectively in relative invasiveness. Therefore, in three bioassays performed *in vitro*, targeting Id1 and Id3 simultaneously produced at least equal or more prominent effect than the sum of that produced by targeting Id1 or Id3 separately. The investigation on suppression of Id3 was performed previously in our group other than the present study (Reference 405 for review).

Id1 induces more aggressive and invasive behavior, as well as a less differentiated

tumour phenotype, and acts as markers of cancer diagnosis and progression in certain types of tumors (430). A number of studies were performed to investigate the effect of double knockdown Id1 and Id3 on cell proliferation and metastasis. Knockdown of Id1 and Id3 hindered metastatic potential of esophageal and pancreatic cancer cells *in vitro* and *in vivo* (435) One study suggested that Id1 and Id3 regulated sustained tumour proliferation during metastatic colonization of the lung (436). Taken together, Id1 and Id3 are important factors in the proliferation and metastasis of tumours.

4.5. Testing the tumourigenesis of SCLC *in vivo*

To study human cancer, plenty of murine models have been established to investigate the factors involved in malignant transformation, invasion and metastasis, as well as to examine response to therapy (61). One of the most widely used models is the human tumour xenograft in which human tumour cells are inoculated, either under the skin or into the organ of immunocompromised mice that do not reject human cells (437). In the field of lung cancer study, spontaneous lung tumours in mice are close to human adenocarcinomas in morphology, histopathology, and molecular characteristics (437). Mouse model for lung cancer can provide a useful tool not only to understand the basic lung tumour biology but also to identify biomarkers for cancer early diagnosis as well as to develop and validate potential new tumour intervention strategies (61). In this study, the human tumour xenograft model was basically used to clarify the possible roles of suppressed genes in tumourigenicity not only *in vitro* but also *in vivo*. To test the effect of suppressing Id1 and Id3 jointly or Id1 alone on tumourigenicity of SCLC *in vivo*, different transfectant cells were inoculated to both flanks of nude mice

testing tumour growth. In the end of the experiment, the average volume of tumours produced by Id1-suppressed groups was significantly reduced by 5-and 7.5-fold, and that in Id1 and Id3 double knockdown groups was reduced by 8.2- and 11.8-fold respectively (Figure 3.11). Similar reduction was also observed by directly weighing the resected tumours at autopsy. The weight of tumour in Id1-suppressed groups was dramatically decreased by 4.1- and 6.6-fold, and that in Id1 and Id3 double knockdown groups was reduced by 6.8- and 10.9-fold respectively (Figure 3.12). Our previous study showed that knockdown Id3 produced a reduction of 2.8- and 2.4-fold in average tumour weight and volume, respectively. Taking all these results together, the greatest tumourigenicty suppression was achieved by the double knockdown of Id1 and Id3 in a joint manner. Although this effect is significantly higher than each of the effects produced by knockdown Id1 and Id3 separately, it is not much more than the sum of those produced by Id1 and Id3 separate knockdown. No significant synergetic effect was observed. Recently, a similar study was performed in NSCLC cells, nude mice were inoculated with Id1-suppressed cells subcutaneously and the tumour growth was compared with corresponding vector controls. The average tumour volume in the knockdown group was significantly reduced by 9.4-fold (438). It seems that the suppressed level of Id1 produced slightly higher reduction in NSCLC than SCLC *in vivo*.

In vivo assay showed that N417 cells with Id1 and Id3 suppression significantly retarded the tumour growth and expansion, which was consistent with the *in vitro* analysis. No significant difference was observed on lengths of latent period as all tumours were visualized 8 days after the inoculation. In N-Id1-1 group, one mouse failed to produce tumours in either of the two flanks; in N-Id1-Id3-1 group, one mouse

failed to produce tumour in the left flank, no significant differences in tumour incidences were tested between the control and testing groups (P=0.48, P=1). Thus it is not certain whether the absence of tumours was due to the suppression effect produced by Id1 and Id3. In a recent study performed in colon cancer cells, it was found reduction of tumour growth achieved by double knockdown Id1 and Id3 was greater than that achieved by Id1- or Id3-suppressed separately. In the Id1 and Id3 double knockdown group, it was identified that 3 out of 20 mice failed to produce any tumour indicating double knockdown Id1 and Id3 can block the tumour formation in the mouse xenografts. From what we observed in our study, although double knockdown Id1 and Id3 did not reduce tumour incidence significantly, it did significantly inhibit malignant progression of the tumour cells.

4.6. Apoptosis and angiogenesis

Our studies showed that expression and function of Id proteins can be inhibited by small interference RNAs and their down-regulation leads to growth arrest of tumour cells. However, the molecular mechanisms responsible for the role of Id1 and Id3 in SCLC are not clear. Our results showed that simultaneous suppression of Id1 and Id3 significantly inhibited tumourigenicity of SCLC by facilitating apoptosis and hindering angiogenesis. In organisms, the increase and decrease of cell numbers are strictly balanced. This balance can be disturbed by excessive proliferation and aberrant apoptosis in the tumourigenesis. Apoptosis is a well-programed way of cell death, and this process is important for balancing cell division and mitosis. Once trigged by death signals, apoptosis program unfolds: membranes are disrupted, the cytoplasmic and

nuclear skeletons are broken down, the cytosol is extruded, the chromosomes are degraded, and the nucleus is fragmented, all in a span of 30 to 120 minutes (439). Evidences have shown that acquired resistance toward apoptosis is one of the hallmarks in tumourigenesis (440).

In this study we investigated the role of Id1 and Id3 in the apoptosis of SCLC induced by cisplatin. Cisplatin is a chemotherapy drug used as the first-line treatment of SCLC. However, cisplatin resistant developed in cancer cells reduces the effectiveness of this agent. The molecular mechanisms underlying the resistance to cisplatin-induced apoptosis was not completely known (347). The results in our study showed that the number of apoptotic cells in Id1-suppressed transfectants increased by 1.6- to 1.8-fold. Our previous work showed that percentage of cells undergoing apoptosis in Id3-suppressed transfectants was 2- to 3-fold higher than that of the control. In Id1 and Id3 double knockdown cells, the percentage of cells undergoing apoptosis increased by 2.5- to 3.5-fold (Figure 3.15). Thus the greatest increment in the percentage of apoptotic cells was achieved through double knockdown of Id1 and Id3 in N417 cells. Our results showed that inhibition of Id1 and Id3 promoted apoptosis of N417 cells in response to cisplatin treatment. While the percentage of apoptotic cells induced by cisplatin was increased in a dose-dependent manner, this increment was facilitated by the suppression of Id1/Id3 (Figure 3.15). This result suggested that Id1 and Id3 may be potential anti-apoptosis molecules whose increased expression may promote tumorigenicity of SCLC through, at least partially, suppressing apoptosis. The discovery in this study that suppression of Id1 and Id3 can increase the sensitivity of SCLC to cisplatin-initiated apoptosis-induction may provide new targets for designing more effective therapies for SCLC treatment.

It was previously observed that Id proteins can induce apoptosis in some cell types (341, 343, 441), they can also function as anti-apoptotic molecules in some other cell types (442). Similarly, the roles of Id proteins are different when studying cisplatin-induced apoptosis under different cancer types. Recently, several investigations were conducted to study the role of Id proteins in cancer cell apoptosis induced by cisplatin. In one study, over-expression of Id1 was necessary for inhibition of the effects of cisplatin-induced apoptosis in gastric-cancer cells (443). In another study, it was showed that high levels of Id3 caused the MG-63 sarcoma cells to be more sensitive to cisplatin-induced apoptosis through activation of reactive oxygen species (ROS) and caspase-3 (347). In SCLC, we found that cisplatin can positively induce apoptosis in Id1 and Id3-suppressed or Id1-suppressed cells in a dose-dependent manner. The experiment was conducted in a period of 24 hours, and after 48 hours the cells may not survive. The high dose of cisplatin or long incubation with cispatin may destroy the factors involved in the energy supply as well as those associated with the apoptosis pathway, hence result in cellular necrosis (444). So far the morphological, biochemical and molecular characteristics in the cisplatin-induced SCLC apoptosis are not clear. Further investigations are needed to fully understand Id protein related apoptosis pathway in SCLC cells.

In human, the diffusion of oxygen through tissues is limited to 100-200 μm to provide all cells a dependable, finely controlled supply of oxygen (445). This system is maintained by angiogenesis which is the process that new blood vessel develop, i.e. endothelial cell division, selective degradation of the basement membrane and the surrounding extracellular matrix, endothelial cell migration, and the formation of a tubular structure (445). Angiogenesis may occur in both physiological and

pathological processes such as tumour growth. The capacity to generate new blood vessels is essential for cells to fully manifest the transformed phenotype (440). Some previous studies demonstrated that Id1 promoted malignant progression of certain types of cancer through facilitating angiogenesis (446, 447), one of the important hallmarks of cancer (440). $Id1^{+/-}Id3^{-/-}$ mice showed poor vascularization and extensive necrosis, and failed to support growth or metastasis of three different tumours (321). One of the most important proangiogenic factors in the angiogenesis process is VEGF.

In this study, it was observed that the level of VEGF was reduced as the decreased levels of Id1 and Id3 in SCLC *in vitro* and *in vivo* (Figure 3.13, Figure 3.16, Figure 3.18). Reduced VEGF secreted by transfectant cells was associated by suppression of angiogenesis (Figure 3.20). Thus Id1 and Id3 up-regulation induced tumourigenicity of SCLC may be achieved, at least in part, by promoting angiogenesis. Our result showed that the angiogenesis activity of the N417 cells was not completely inhibited by the anti-VEGF antibody, indicating that apart from VEGF, there may be some other factors involved in promoting angiogenesis in the SCLC cells. The actual functional roles of Id1 and Id3 may be different and depend on the availability of E-box proteins in a particular cell type (73). Analysing the 5'-UTR of VEGF gene with the Sequence Manipulation Suite, we found that there are eight "CAGCTG" and six "CACCTG" E-boxes in the promoter region. Thus the VEGF gene contains E-boxes. Id proteins preferentially dimerise with Group A members of E proteins and bind to these two E-box regions. The associative molecular events are required to be further explored. Earlier studies showed that not only Id1 and Id3 can affect VEGF, but also VEGF can influence Id1 and Id3, thus there is a feedback loop between Id proteins and VEGF.

The presence of VEGF in the circulation resulted in a marked up-regulation of Id1 and Id3 in the bone marrow, presumably by acting on the progenitor cells that become mobilised (351). Activation of mitogen activated protein kinase (MAPK) pathway by VEGF receptor stimulation can impinge on Id1 and Id3 promoters at the EGR1 site (448). Further study is needed to understand how exactly Id1 and Id3 interact with VEGF to promote the malignant progression of SCLC cells.

4.7. Future work

Our study demonstrated that simultaneous suppression of Id1 and Id3 inhibited the tumourigenicity of SCLC both *in vitro* and *in vivo*. Our results also showed that the tumour-suppression effect was regulated by Id1- and Id3-shRNA through promotion of apoptosis and inhibition of angiogenesis. Further investigation is needed to explore Id1 and Id3 associated apoptosis and angiogenesis pathways which may affect the tumourigenicity of SCLC.

From the apoptosis assay, we found that suppression of Id1 and Id3 can increase the apoptosis rate of SCLC cells when treated with cisplatin. Next step, we may need to investigate the morphologic and molecular characteristics during the apoptosis induced by cisplatin. There are several studies related to the pathways that Id proteins may be involved in. One study showed that the treatment of Id1 overexpressed cells with MEK inhibitor PD098059, resulted in an increased taxol-induced apoptosis rate compared to vector control (401). It was also found that Id1 induced cell proliferation resulted in down-regulation of Bcl-2 and up-regulation of Bax, and thereby suggested that proliferation induced by Id1 is regulated through Raf/MEPK signalling pathways.

Another study indicated, however, the over-expression of Id1 induced apoptosis in T cell lines and primary thymocytes was rescued by inhibition of RORgammat, which is a DNA-binding transcription factor and is a member of the NR1 subfamily of nuclear receptors (449). There was a study on mechanism of Id3 in apoptosis of B lymphocyte progenitors (BLPs). It was demonstrated that Id3 induces apoptosis of both primary and transformed BLPs through a caspase-2-dependent mechanism. It was indicated that this process was P53 independent and cannot be inhibited by Bcl-2 (450). Id1/3-PA7, an inhibitor to both Id1 and Id3 was shown to induce cell-cycle arrest and apoptosis in both ovarian cancer and breast cancer cells (348). Id1/3-PA7 promoted apoptosis by activation of E-box promoter of cyclin-dependent kinase inhibitor (CDKN2A) in both ovarian cancer and breast cancer cells. In SCLC, it is not yet known how Id1 and Id3 induce cisplatin-induced apoptosis and further study is needed to explore the possible pathway.

For further angiogenesis study, the E-box in promoter of VEGF is a potential start. Both “CAGCTG” and “CACCTG” E-boxes in the promoter region of VEGF were detected. Id proteins preferentially dimerise with Group A members of E protein, which bind to these two E-box regions. Therefore we assumed that Id1 and Id3 may be involved in angiogenesis of SCLC by mediating VEGF associated signalling pathway. A study indicated that thrombospondin-1 (TSP-1) is a major target for Id1 in angiogenesis of mouse embryo fibroblasts (352). Another study found that Id1 induced transcriptional activation of VEGF by stabilizing hypoxia-inducible factor-1α (HIF-1α）protein in hepatocellular carcinoma (446). This finding was verified by a recent study in human endothelial and breast cancer cells (451). Id1 was shown to induce VEGF by enhancing the stability and activity of HIF-1α, and activation of

HIF-1α promoters was ERK pathway dependent. These investigations also served as possible angiogenesis pathways and these targets are still waiting to be verified in SCLC.

4.8. Summary and conclusion

Lack of DNA binding domain, Id family members act as the dominant negative regulators of bHLH proteins by forming inactive dimmers with other bHLH transcription factors. Id proteins play a series of roles in cellular functions regarding the cell fate decisions. Deregulation of Id has been identified in numbers of human cancer types. Evidence shows that elevated levels of Id proteins may be sufficient to facilitate neoplastic transformation. Despite the experimental evidence for the connection of Id proteins and tumourigenicity in other tumour cells, crucial data that demonstrate their involvement in SCLC is required due to biology activity varies under different cell type background.

This study bridges the gap of linking Id1 and Id3 proteins to SCLC in Id1 and Id3 suppressed transfectant cells. Our results provide insight into the effect of these proteins on tumourigenicity of SCLC. Using RNAi technique, we first established SCLC cell line N417-derived sublines expressing reduced levels of Id1 and Id3 by transfection of a single vector constructed to co-express two shRNAs simultaneously. We identified that double knockdown of Id1 and Id3 markedly inhibited proliferation rate of N417 cells *in vitro* through MTS assay. Furthermore, anchorage independent assay showed that reduced levels of Id1 and Id3 significantly impaired the colony formation ability in soft agar. In N417 cells, simultaneous inhibition of Id1 and Id3

resulted in almost complete suppression of cell invasion. Thus the *in vitro* assays suggested that Id1 and Id3 inhibition greatly suppressed tumorigenic growth and invasive ability in SCLC cell line N417. We also found that targeting Id1 and Id3 simultaneously produced more prominent tumour-suppression effect than Id1 alone. All above results indicated that Id1 and Id3 play a joint role in promoting tumourigenicity of SCLC. To verify these results, the Id1 and Id3-shRNA and Id1-shRNA transfectant cells were inoculated to nude mice as xenograft tumour model testing tumour growth. *In vivo* assay showed that the volume and weight of the xenograft tumours were significantly reduced in Id1- and Id3-suppressed cells. These results were consistent with those observed in the *in vitro* assays. Id1 and Id3 double knockdown groups exerted more significant effect than Id1 knockdown groups, the effect appeared to be the sum of the inhibition of Id1 and Id3 separately rather than they functioned in a synergistic manner.

We also explored the mechanisms on how Id1 and Id3 function in tumourigenesis of SCLC, and found apoptosis and angiogenesis were two important ways involved in the process. Our results showed that inhibition of Id1 and Id3 promoted apoptosis rate of N417 cells in response to cisplatin treatment in a dose-dependent manner, which was paralleled by the level of Id1 and Id3 suppression. In Western blot and ELISA analysis, it was found that VEGF levels reduced in Id1 and Id3-shRNA transfectant cell lysates and their culture medium. The VEGF produced by different cells was biologically active, and the conditioned medium of Id1 and Id3-suppressed N417 cell blocked the HUVEC cells from forming branching networks. Therefore Id1 and Id3 contribute to the tumourigenesis of SCLC by participating in apoptosis and angiogenesis processes.

In conclusion, this study demonstrated that simultaneous suppression of Id1 and Id3 significantly inhibited tumourigenicity in SCLC cells both *in vitro* and *in vivo*. Our results also found that suppression of Id1 and Id3 allowed N417 cells more sensitive to cisplatin-induced apoptosis. Id1 and Id3 inhibition blocked angiogenesis in N417 cells via down-regulation of VEGF expression. Together, our results suggest that both Id1 and Id3 are important positive regulators in tumourigenicity of SCLC. These results revealed that Id1 and Id3 may promote the malignant progression of SCLC cells through facilitating angiogenesis and suppressing apoptosis.

REFERENCES

1. Maurya P, Meleady P, Dowling P, Clynes M. Proteomic approaches for serum biomarker discovery in cancer. Anticancer Res. 2007;27:1247-55.
2. Collins LG, Haines C, Perkel R, Enck RE. Lung cancer: diagnosis and management. Am Fam Physician. 2007;75:56-63.
3. Jackman DM, Johnson BE. Small-cell lung cancer. Lancet. 2005;366:1385-96.
4. Greenlee RT, Murray T, Bolden S, Wingo PA. Cancer statistics, 2000. CA Cancer J Clin. 2000;50:7-33.
5. Mathers CD, Shibuya K, Boschi-Pinto C, Lopez AD, Murray CJ. Global and regional estimates of cancer mortality and incidence by site: I. Application of regional cancer survival model to estimate cancer mortality distribution by site. BMC Cancer. 2002;2:36.
6. Siegel R, Naishadham D, Jemal A. Cancer statistics, 2012. CA Cancer J Clin. 2012;62:10-29.
7. O'Rourke MA, Feussner JR, Feigl P, Laszlo J. Age trends of lung cancer stage at diagnosis. Implications for lung cancer screening in the elderly. JAMA. 1987;258:921-6.
8. Gridelli C, Perrone F, Monfardini S. Lung cancer in the elderly. Eur J Cancer. 1997;33:2313-4.
9. Jemal A, Siegel R, Ward E, Hao Y, Xu J, Murray T, et al. Cancer statistics, 2008. CA Cancer J Clin. 2008;58:71-96.
10. Kamangar F, Dores GM, Anderson WF. Patterns of cancer incidence, mortality, and prevalence across five continents: defining priorities to reduce cancer disparities in different geographic regions of the world. J Clin Oncol. 2006;24:2137-50.
11. Govindan R, Page N, Morgensztern D, Read W, Tierney R, Vlahiotis A, et al. Changing epidemiology of small-cell lung cancer in the United States over the last 30 years: analysis of the surveillance, epidemiologic, and end results database. J Clin Oncol. 2006;24:4539-44.
12. Ettinger DS, Aisner J. Changing face of small-cell lung cancer: real and artifact. J Clin Oncol. 2006;24:4526-7.
13. Rossi A, Maione P, Colantuoni G, Guerriero C, Ferrara C, Del Gaizo F, et al. Treatment of small cell lung cancer in the elderly. Oncologist. 2005;10:399-411.
14. IARC monograph programme on the evaluation of the carcinogenic risk of chemicals to humans. IARC Monogr Eval Carcinog Risk Chem Hum. 1978;18:15-35.
15. Alberg AJ, Samet JM. Epidemiology of lung cancer. Chest. 2003;123:21S-49S.
16. Boffetta P, Pershagen G, Jockel KH, Forastiere F, Gaborieau V, Heinrich J, et al. Cigar and pipe smoking and lung cancer risk: a multicenter study from Europe. J Natl Cancer Inst. 1999;91:697-701.

17. Parsons A, Daley A, Begh R, Aveyard P. Influence of smoking cessation after diagnosis of early stage lung cancer on prognosis: systematic review of observational studies with meta-analysis. BMJ. 2010;340:b5569.
18. Saha SP, Bhalla DK, Whayne TF, Jr., Gairola C. Cigarette smoke and adverse health effects: An overview of research trends and future needs. Int J Angiol. 2007;16:77-83.
19. Pisick E, Jagadeesh S, Salgia R. Small cell lung cancer: from molecular biology to novel therapeutics. J Exp Ther Oncol. 2003;3:305-18.
20. Rygaard K, Sorenson GD, Pettengill OS, Cate CC, Spang-Thomsen M. Abnormalities in structure and expression of the retinoblastoma gene in small cell lung cancer cell lines and xenografts in nude mice. Cancer Res. 1990;50:5312-7.
21. Sattler M, Salgia R. Molecular and cellular biology of small cell lung cancer. Semin Oncol. 2003;30:57-71.
22. Wistuba, II, Gazdar AF, Minna JD. Molecular genetics of small cell lung carcinoma. Semin Oncol. 2001;28:3-13.
23. Olivier M, Eeles R, Hollstein M, Khan MA, Harris CC, Hainaut P. The IARC TP53 database: new online mutation analysis and recommendations to users. Hum Mutat. 2002;19:607-14.
24. Demirhan O, Tastemir D, Hasturk S, Kuleci S, Hanta I. Alterations in p16 and p53 genes and chromosomal findings in patients with lung cancer: fluorescence in situ hybridization and cytogenetic studies. Cancer Epidemiol. 2010;34:472-7.
25. Ishida T, Chada S, Stipanov M, Nadaf S, Ciernik FI, Gabrilovich DI, et al. Dendritic cells transduced with wild-type p53 gene elicit potent anti-tumour immune responses. Clin Exp Immunol. 1999;117:244-51.
26. Antonia SJ, Mirza N, Fricke I, Chiappori A, Thompson P, Williams N, et al. Combination of p53 cancer vaccine with chemotherapy in patients with extensive stage small cell lung cancer. Clin Cancer Res. 2006;12:878-87.
27. Horn L, Castellanos EL, Johnson DH. Update on new drugs in small cell lung cancer. Expert Opin Investig Drugs. 2011;20:441-5.
28. D'Angelo SP, Pietanza MC. The molecular pathogenesis of small cell lung cancer. Cancer Biol Ther. 2010;10:1-10.
29. Modi S, Kubo A, Oie H, Coxon AB, Rehmatulla A, Kaye FJ. Protein expression of the RB-related gene family and SV40 large T antigen in mesothelioma and lung cancer. Oncogene. 2000;19:4632-9.
30. Wikman H, Kettunen E. Regulation of the G1/S phase of the cell cycle and alterations in the RB pathway in human lung cancer. Expert Rev Anticancer Ther. 2006;6:515-30.
31. Xue Jun H, Gemma A, Hosoya Y, Matsuda K, Nara M, Hosomi Y, et al. Reduced transcription of the RB2/p130 gene in human lung cancer. Mol Carcinog. 2003;38:124-9.

32. Du W, Searle JS. The rb pathway and cancer therapeutics. Current drug targets. 2009;10:581-9.
33. Mori N, Yokota J, Akiyama T, Sameshima Y, Okamoto A, Mizoguchi H, et al. Variable mutations of the RB gene in small-cell lung carcinoma. Oncogene. 1990;5:1713-7Kashii T, Mizushima Y, Monno S, Nakagawa K, Kobayashi M. Gene analysis of K-, H-ras, p53, and retinoblastoma susceptibility genes in human lung cancer cell lines by the polymerase chain reaction/single-strand conformation polymorphism method. J Cancer Res Clin Oncol. 1994;120:143-8.
34. Sekido Y, Fong KM, Minna JD. Molecular genetics of lung cancer. Annu Rev Med. 2003;54:73-87.
35. Rodina A, Vilenchik M, Moulick K, Aguirre J, Kim J, Chiang A, et al. Selective compounds define Hsp90 as a major inhibitor of apoptosis in small-cell lung cancer. Nat Chem Biol. 2007;3:498-507.
36. Picard D, Khursheed B, Garabedian MJ, Fortin MG, Lindquist S, Yamamoto KR. Reduced levels of hsp90 compromise steroid receptor action in vivo. Nature. 1990;348:166-8.
37. Zeng Y, Feng H, Graner MW, Katsanis E. Tumor-derived, chaperone-rich cell lysate activates dendritic cells and elicits potent antitumor immunity. Blood. 2003;101:4485-91.
38. Chiosis G, Vilenchik M, Kim J, Solit D. Hsp90: the vulnerable chaperone. Drug Discov Today. 2004;9:881-8.
39. McDonald E, Workman P, Jones K. Inhibitors of the HSP90 molecular chaperone: attacking the master regulator in cancer. Curr Top Med Chem. 2006;6:1091-107.
40. Chiosis G, Caldas Lopes E, Solit D. Heat shock protein-90 inhibitors: a chronicle from geldanamycin to today's agents. Curr Opin Investig Drugs. 2006;7:534-41.
41. Munster PN, Srethapakdi M, Moasser MM, Rosen N. Inhibition of heat shock protein 90 function by ansamycins causes the morphological and functional differentiation of breast cancer cells. Cancer Res. 2001;61:2945-52.
42. Yip KW, Reed JC. Bcl-2 family proteins and cancer. Oncogene. 2008;27:6398-406.
43. Russell HR, Lee Y, Miller HL, Zhao J, McKinnon PJ. Murine ovarian development is not affected by inactivation of the bcl-2 family member diva. Mol Cell Biol. 2002;22:6866-70.
44. Adams JM, Cory S. The Bcl-2 protein family: arbiters of cell survival. Science. 1998;281:1322-6.
45. Tzifi F, Economopoulou C, Gourgiotis D, Ardavanis A, Papageorgiou S, Scorilas A. The Role of BCL2 Family of Apoptosis Regulator Proteins in Acute and Chronic Leukemias. Adv Hematol. 2012;2012:524308.
46. Kuwana T, Newmeyer DD. Bcl-2-family proteins and the role of mitochondria in apoptosis. Curr Opin Cell Biol. 2003;15:691-9.

47. Ashkenazi A, Dixit VM. Death receptors: signaling and modulation. Science. 1998;281:1305-8.
48. Zou H, Li Y, Liu X, Wang X. An APAF-1.cytochrome c multimeric complex is a functional apoptosome that activates procaspase-9. J Biol Chem. 1999;274:11549-56.
49. Gustafsson AB, Gottlieb RA. Bcl-2 family members and apoptosis, taken to heart. Am J Physiol Cell Physiol. 2007;292:C45-51.
50. Li H, Zhu H, Xu CJ, Yuan J. Cleavage of BID by caspase 8 mediates the mitochondrial damage in the Fas pathway of apoptosis. Cell. 1998;94:491-501.
51. Yin XM, Wang K, Gross A, Zhao Y, Zinkel S, Klocke B, et al. Bid-deficient mice are resistant to Fas-induced hepatocellular apoptosis. Nature. 1999;400:886-91.
52. Jiang SX, Sato Y, Kuwao S, Kameya T. Expression of bcl-2 oncogene protein is prevalent in small cell lung carcinomas. J Pathol. 1995;177:135-8.
53. Azmi AS, Wang Z, Philip PA, Mohammad RM, Sarkar FH. Emerging Bcl-2 inhibitors for the treatment of cancer. Expert Opin Emerg Drugs. 2011;16:59-70.
54. Reed JC, Stein C, Subasinghe C, Haldar S, Croce CM, Yum S, et al. Antisense-mediated inhibition of BCL2 protooncogene expression and leukemic cell growth and survival: comparisons of phosphodiester and phosphorothioate oligodeoxynucleotides. Cancer Res. 1990;50:6565-70.
55. Waters JS, Webb A, Cunningham D, Clarke PA, Raynaud F, di Stefano F, et al. Phase I clinical and pharmacokinetic study of bcl-2 antisense oligonucleotide therapy in patients with non-Hodgkin's lymphoma. J Clin Oncol. 2000;18:1812-23.
56. Rudin CM, Otterson GA, Mauer AM, Villalona-Calero MA, Tomek R, Prange B, et al. A pilot trial of G3139, a bcl-2 antisense oligonucleotide, and paclitaxel in patients with chemorefractory small-cell lung cancer. Ann Oncol. 2002;13:539-45.
57. Rudin CM, Kozloff M, Hoffman PC, Edelman MJ, Karnauskas R, Tomek R, et al. Phase I study of G3139, a bcl-2 antisense oligonucleotide, combined with carboplatin and etoposide in patients with small-cell lung cancer. J Clin Oncol. 2004;22:1110-7.
58. Facchini LM, Penn LZ. The molecular role of Myc in growth and transformation: recent discoveries lead to new insights. FASEB J. 1998;12:633-51.
59. Gazzeri S, Brambilla E, Jacrot M, Chauvin C, Benabid AL, Brambilla C. Activation of myc gene family in human lung carcinomas and during heterotransplantation into nude mice. Cancer Res. 1991;51:2566-71.
60. Nau MM, Brooks BJ, Battey J, Sausville E, Gazdar AF, Kirsch IR, et al. L-myc, a new myc-related gene amplified and expressed in human small cell lung cancer. Nature. 1985;318:69-73.
61. Meuwissen R, Berns A. Mouse models for human lung cancer. Genes Dev. 2005;19:643-64.

62. Akie K, Dosaka-Akita H, Murakami A, Kawakami Y. A combination treatment of c-myc antisense DNA with all-trans-retinoic acid inhibits cell proliferation by downregulating c-myc expression in small cell lung cancer. Antisense Nucleic Acid Drug Dev. 2000;10:243-9.
63. Johnson BE, Ihde DC, Makuch RW, Gazdar AF, Carney DN, Oie H, et al. myc family oncogene amplification in tumor cell lines established from small cell lung cancer patients and its relationship to clinical status and course. J Clin Invest. 1987;79:1629-34.
64. Imai J, Watanabe M, Sasaki M, Yamaguchi R, Tateyama S, Sugano S. Induction of c-met proto-oncogene expression at the metastatic site. Clin Exp Metastasis. 1999;17:457-62.
65. Lengyel E, Prechtel D, Resau JH, Gauger K, Welk A, Lindemann K, et al. C-Met overexpression in node-positive breast cancer identifies patients with poor clinical outcome independent of Her2/neu. Int J Cancer. 2005;113:678-82Liu C, Park M, Tsao MS. Overexpression of c-met proto-oncogene but not epidermal growth factor receptor or c-erbB-2 in primary human colorectal carcinomas. Oncogene. 1992;7:181-5Houldsworth J, Cordon-Cardo C, Ladanyi M, Kelsen DP, Chaganti RS. Gene amplification in gastric and esophageal adenocarcinomas. Cancer Res. 1990;50:6417-22.
66. Wang ZX, Lu BB, Yang JS, Wang KM, De W. Adenovirus-mediated siRNA targeting c-Met inhibits proliferation and invasion of small-cell lung cancer (SCLC) cells. J Surg Res. 2011;171:127-35.
67. Sattler M, Reddy MM, Hasina R, Gangadhar T, Salgia R. The role of the c-Met pathway in lung cancer and the potential for targeted therapy. Ther Adv Med Oncol. 2011;3:171-84.
68. Ma PC, Kijima T, Maulik G, Fox EA, Sattler M, Griffin JD, et al. c-MET mutational analysis in small cell lung cancer: novel juxtamembrane domain mutations regulating cytoskeletal functions. Cancer Res. 2003;63:6272-81.
69. Rolle CE, Kanteti R, Surati M, Nandi S, Dhanasingh I, Yala S, et al. Combination MET inhibition and Topoisomerase I inhibition block cell growth of Small Cell Lung Cancer. Mol Cancer Ther. 2013.
70. Wang C, Curtis JE, Geissler EN, McCulloch EA, Minden MD. The expression of the proto-oncogene C-kit in the blast cells of acute myeloblastic leukemia. Leukemia. 1989;3:699-702Mayrhofer G, Gadd SJ, Spargo LD, Ashman LK. Specificity of a mouse monoclonal antibody raised against acute myeloid leukaemia cells for mast cells in human mucosal and connective tissues. Immunol Cell Biol. 1987;65 (Pt 3):241-50Huizinga JD, Thuneberg L, Kluppel M, Malysz J, Mikkelsen HB, Bernstein A. W/kit gene required for interstitial cells of Cajal and for intestinal pacemaker activity. Nature. 1995;373:347-9.
71. Potti A, Moazzam N, Ramar K, Hanekom DS, Kargas S, Koch M. CD117 (c-KIT) overexpression in patients with extensive-stage small-cell lung carcinoma. Ann Oncol. 2003;14:894-7.

72. Paronetto MP, Farini D, Sammarco I, Maturo G, Vespasiani G, Geremia R, et al. Expression of a truncated form of the c-Kit tyrosine kinase receptor and activation of Src kinase in human prostatic cancer. Am J Pathol. 2004;164:1243-51.
73. Ikeda H, Kanakura Y, Tamaki T, Kuriu A, Kitayama H, Ishikawa J, et al. Expression and functional role of the proto-oncogene c-kit in acute myeloblastic leukemia cells. Blood. 1991;78:2962-8.
74. Tamborini E, Bonadiman L, Negri T, Greco A, Staurengo S, Bidoli P, et al. Detection of overexpressed and phosphorylated wild-type kit receptor in surgical specimens of small cell lung cancer. Clin Cancer Res. 2004;10:8214-9.
75. Johnson BE, Fischer T, Fischer B, Dunlop D, Rischin D, Silberman S, et al. Phase II study of imatinib in patients with small cell lung cancer. Clin Cancer Res. 2003;9:5880-7Dy GK, Miller AA, Mandrekar SJ, Aubry MC, Langdon RM, Jr., Morton RF, et al. A phase II trial of imatinib (ST1571) in patients with c-kit expressing relapsed small-cell lung cancer: a CALGB and NCCTG study. Ann Oncol. 2005;16:1811-6.
76. Heinrich MC, Blanke CD, Druker BJ, Corless CL. Inhibition of KIT tyrosine kinase activity: a novel molecular approach to the treatment of KIT-positive malignancies. J Clin Oncol. 2002;20:1692-703.
77. Burger H, den Bakker MA, Stoter G, Verweij J, Nooter K. Lack of c-kit exon 11 activating mutations in c-KIT/CD117-positive SCLC tumour specimens. Eur J Cancer. 2003;39:793-9.
78. Roskoski R, Jr. Vascular endothelial growth factor (VEGF) signaling in tumor progression. Critical reviews in oncology/hematology. 2007;62:179-213.
79. Tanno S, Ohsaki Y, Nakanishi K, Toyoshima E, Kikuchi K. Human small cell lung cancer cells express functional VEGF receptors, VEGFR-2 and VEGFR-3. Lung Cancer. 2004;46:11-9.
80. Olsson AK, Dimberg A, Kreuger J, Claesson-Welsh L. VEGF receptor signalling - in control of vascular function. Nat Rev Mol Cell Biol. 2006;7:359-71.
81. Fischer B, Marinov M, Arcaro A. Targeting receptor tyrosine kinase signalling in small cell lung cancer (SCLC): what have we learned so far? Cancer Treat Rev. 2007;33:391-406.
82. Spigel DR, Hainsworth JD, Simons L, Meng C, Burris HA, 3rd, Yardley DA, et al. Irinotecan, carboplatin, and imatinib in untreated extensive-stage small-cell lung cancer: a phase II trial of the Minnie Pearl Cancer Research Network. J Thorac Oncol. 2007;2:854-61.
83. Morabito A, Piccirillo MC, Falasconi F, De Feo G, Del Giudice A, Bryce J, et al. Vandetanib (ZD6474), a dual inhibitor of vascular endothelial growth factor receptor (VEGFR) and epidermal growth factor receptor (EGFR) tyrosine kinases: current status and future directions. Oncologist. 2009;14:378-90.
84. Spigel DR, Greco FA, Rubin MS, Shipley D, Thompson DS, Lubiner ET, et al. Phase II study of maintenance sunitinib following irinotecan and carboplatin as first-line treatment for patients

with extensive-stage small-cell lung cancer. Lung Cancer. 2012;77:359-64.
85. Bikfalvi A, Klein S, Pintucci G, Rifkin DB. Biological roles of fibroblast growth factor-2. Endocr Rev. 1997;18:26-45.
86. Ruotsalainen T, Joensuu H, Mattson K, Salven P. High pretreatment serum concentration of basic fibroblast growth factor is a predictor of poor prognosis in small cell lung cancer. Cancer Epidemiol Biomarkers Prev. 2002;11:1492-5.
87. Pardo OE, Wellbrock C, Khanzada UK, Aubert M, Arozarena I, Davidson S, et al. FGF-2 protects small cell lung cancer cells from apoptosis through a complex involving PKCepsilon, B-Raf and S6K2. EMBO J. 2006;25:3078-88.
88. Simms E, Gazdar AF, Abrams PG, Minna JD. Growth of human small cell (oat cell) carcinoma of the lung in serum-free growth factor-supplemented medium. Cancer Res. 1980;40:4356-63.
89. Gazdar AF, Carney DN, Nau MM, Minna JD. Characterization of variant subclasses of cell lines derived from small cell lung cancer having distinctive biochemical, morphological, and growth properties. Cancer Res. 1985;45:2924-30.
90. King R, Wells JR, Krieg P, Snoswell M, Brazier J, Bagley CJ, et al. Production and characterization of recombinant insulin-like growth factor-I (IGF-I) and potent analogues of IGF-I, with Gly or Arg substituted for Glu3, following their expression in Escherichia coli as fusion proteins. J Mol Endocrinol. 1992;8:29-41.
91. Izycki T, Chyczewska E, Naumnik W, Ossolinska M. Serum levels of IGF-I and IGFBP-3 in patients with lung cancer during chemotherapy. Oncol Res. 2006;16:49-54.
92. Yeh J, Litz J, Hauck P, Ludwig DL, Krystal GW. Selective inhibition of SCLC growth by the A12 anti-IGF-1R monoclonal antibody correlates with inhibition of Akt. Lung Cancer. 2008;60:166-74.
93. Camirand A, Pollak M. Co-targeting IGF-1R and c-kit: synergistic inhibition of proliferation and induction of apoptosis in H 209 small cell lung cancer cells. Br J Cancer. 2004;90:1825-9Mitsiades CS, Mitsiades NS, McMullan CJ, Poulaki V, Shringarpure R, Akiyama M, et al. Inhibition of the insulin-like growth factor receptor-1 tyrosine kinase activity as a therapeutic strategy for multiple myeloma, other hematologic malignancies, and solid tumors. Cancer cell. 2004;5:221-30.
94. Herbst RS. Review of epidermal growth factor receptor biology. International journal of radiation oncology, biology, physics. 2004;59:21-6.
95. Akimoto T, Hunter NR, Buchmiller L, Mason K, Ang KK, Milas L. Inverse relationship between epidermal growth factor receptor expression and radiocurability of murine carcinomas. Clin Cancer Res. 1999;5:2884-90.
96. Arteaga CL. Epidermal growth factor receptor dependence in human tumors: more than just

expression? Oncologist. 2002;7 Suppl 4:31-9.
97. Mendelsohn J. The epidermal growth factor receptor as a target for cancer therapy. Endocr Relat Cancer. 2001;8:3-9.
98. Okamoto I, Araki J, Suto R, Shimada M, Nakagawa K, Fukuoka M. EGFR mutation in gefitinib-responsive small-cell lung cancer. Ann Oncol. 2006;17:1028-9.
99. Shiao TH, Chang YL, Yu CJ, Chang YC, Hsu YC, Chang SH, et al. Epidermal growth factor receptor mutations in small cell lung cancer: a brief report. J Thorac Oncol. 2011;6:195-8.
100. Potti A, Willardson J, Forseen C, Kishor Ganti A, Koch M, Hebert B, et al. Predictive role of HER-2/neu overexpression and clinical features at initial presentation in patients with extensive stage small cell lung carcinoma. Lung Cancer. 2002;36:257-61.
101. Micke P, Hengstler JG, Ros R, Bittinger F, Metz T, Gebhard S, et al. c-erbB-2 expression in small-cell lung cancer is associated with poor prognosis. Int J Cancer. 2001;92:474-9.
102. Spindel ER, Gibson BW, Reeve JR, Jr., Kelly M. Cloning of cDNAs encoding amphibian bombesin: evidence for the relationship between bombesin and gastrin-releasing peptide. Proc Natl Acad Sci U S A. 1990;87:9813-7.
103. Cuttitta F, Carney DN, Mulshine J, Moody TW, Fedorko J, Fischler A, et al. Bombesin-like peptides can function as autocrine growth factors in human small-cell lung cancer. Nature. 1985;316:823-6.
104. Brown M, Allen R, Villarreal J, Rivier J, Vale W. Bombesin-like activity: radioimmunologic assessment in biological tissues. Life Sci. 1978;23:2721-8Walsh JH, Wong HC, Dockray GJ. Bombesin-like peptides in mammals. Fed Proc. 1979;38:2315-9Wharton J, Polak JM, Bloom SR, Ghatei MA, Solcia E, Brown MR, et al. Bombesin-like immunoreactivity in the lung. Nature. 1978;273:769-70Yang K, Ulich T, Taylor I, Cheng L, Lewin KJ. Pulmonary carcinoids. Immunohistochemical demonstration of brain-gut peptides. Cancer. 1983;52:819-23Erisman MD, Linnoila RI, Hernandez O, DiAugustine RP, Lazarus LH. Human lung small-cell carcinoma contains bombesin. Proc Natl Acad Sci U S A. 1982;79:2379-83Sorenson GD, Bloom SR, Ghatei MA, Del Prete SA, Cate CC, Pettengill OS. Bombesin production by human small cell carcinoma of the lung. Regul Pept. 1982;4:59-66.
105. Moody TW, Zia F, Venugopal R, Fagarasan M, Oie H, Hu V. GRP receptors are present in non small cell lung cancer cells. J Cell Biochem Suppl. 1996;24:247-56Sun B, Halmos G, Schally AV, Wang X, Martinez M. Presence of receptors for bombesin/gastrin-releasing peptide and mRNA for three receptor subtypes in human prostate cancers. Prostate. 2000;42:295-303Gugger M, Reubi JC. Gastrin-releasing peptide receptors in non-neoplastic and neoplastic human breast. Am J Pathol. 1999;155:2067-76Pansky A, De Weerth A, Fasler-Kan E, Boulay JL, Schulz M, Ketterer S, et al. Gastrin releasing peptide-preferring bombesin receptors mediate growth of human renal cell carcinoma. J Am Soc Nephrol. 2000;11:1409-18.

106. Maruno K, Yamaguchi K, Abe K, Suzuki M, Saijo N, Mishima Y, et al. Immunoreactive gastrin-releasing peptide as a specific tumor marker in patients with small cell lung carcinoma. Cancer Res. 1989;49:629-32.
107. Miyake Y, Kodama T, Yamaguchi K. Pro-gastrin-releasing peptide(31-98) is a specific tumor marker in patients with small cell lung carcinoma. Cancer Res. 1994;54:2136-40.
108. Aoyagi K, Miyake Y, Urakami K, Kashiwakuma T, Hasegawa A, Kodama T, et al. Enzyme immunoassay of immunoreactive progastrin-releasing peptide(31-98) as tumor marker for small-cell lung carcinoma: development and evaluation. Clin Chem. 1995;41:537-43.
109. Carney DN, Marangos PJ, Ihde DC, Bunn PA, Jr., Cohen MH, Minna JD, et al. Serum neuron-specific enolase: a marker for disease extent and response to therapy of small-cell lung cancer. Lancet. 1982;1:583-5.
110. Shibayama T, Ueoka H, Nishii K, Kiura K, Tabata M, Miyatake K, et al. Complementary roles of pro-gastrin-releasing peptide (ProGRP) and neuron specific enolase (NSE) in diagnosis and prognosis of small-cell lung cancer (SCLC). Lung Cancer. 2001;32:61-9.
111. Wojcik E, Kulpa JK, Sas-Korczynska B, Korzeniowski S, Jakubowicz J. ProGRP and NSE in therapy monitoring in patients with small cell lung cancer. Anticancer Res. 2008;28:3027-33.
112. Sang QX. Complex role of matrix metalloproteinases in angiogenesis. Cell research. 1998;8:171-7.
113. Visse R, Nagase H. Matrix metalloproteinases and tissue inhibitors of metalloproteinases: structure, function, and biochemistry. Circ Res. 2003;92:827-39.
114. Michael M, Babic B, Khokha R, Tsao M, Ho J, Pintilie M, et al. Expression and prognostic significance of metalloproteinases and their tissue inhibitors in patients with small-cell lung cancer. J Clin Oncol. 1999;17:1802-8.
115. Ahonen M, Baker AH, Kahari VM. Adenovirus-mediated gene delivery of tissue inhibitor of metalloproteinases-3 inhibits invasion and induces apoptosis in melanoma cells. Cancer Res. 1998;58:2310-5.
116. Pujol JL, Breton JL, Gervais R, Tanguy ML, Quoix E, David P, et al. Phase III double-blind, placebo-controlled study of thalidomide in extensive-disease small-cell lung cancer after response to chemotherapy: an intergroup study FNCLCC cleo04 IFCT 00-01. J Clin Oncol. 2007;25:3945-51.
117. Shepherd FA, Giaccone G, Seymour L, Debruyne C, Bezjak A, Hirsh V, et al. Prospective, randomized, double-blind, placebo-controlled trial of marimastat after response to first-line chemotherapy in patients with small-cell lung cancer: a trial of the National Cancer Institute of Canada-Clinical Trials Group and the European Organization for Research and Treatment of Cancer. J Clin Oncol. 2002;20:4434-9.
118. Johnson CP, Fujimoto I, Perrin-Tricaud C, Rutishauser U, Leckband D. Mechanism of

homophilic adhesion by the neural cell adhesion molecule: use of multiple domains and flexibility. Proc Natl Acad Sci U S A. 2004;101:6963-8.
119. Jensen M, Berthold F. Targeting the neural cell adhesion molecule in cancer. Cancer Lett. 2007;258:9-21.
120. Kim DH, Kwon MS. Role of fine needle aspiration cytology, cell block preparation and CD63, P63 and CD56 immunostaining in classifying the specific tumor type of the lung. Acta Cytol. 2010;54:55-9.
121. Kontogianni K, Nicholson AG, Butcher D, Sheppard MN. CD56: a useful tool for the diagnosis of small cell lung carcinomas on biopsies with extensive crush artefact. J Clin Pathol. 2005;58:978-80.
122. Seidenfaden R, Krauter A, Schertzinger F, Gerardy-Schahn R, Hildebrandt H. Polysialic acid directs tumor cell growth by controlling heterophilic neural cell adhesion molecule interactions. Mol Cell Biol. 2003;23:5908-18.
123. Lynch TJ, Jr. Immunotoxin therapy of small-cell lung cancer. N901-blocked ricin for relapsed small-cell lung cancer. Chest. 1993;103:436S-9S.
124. Fidias P, Grossbard M, Lynch TJ, Jr. A phase II study of the immunotoxin N901-blocked ricin in small-cell lung cancer. Clin Lung Cancer. 2002;3:219-22.
125. Payne G. Progress in immunoconjugate cancer therapeutics. Cancer cell. 2003;3:207-12.
126. Brezicka T, Bergman B, Olling S, Fredman P. Reactivity of monoclonal antibodies with ganglioside antigens in human small cell lung cancer tissues. Lung Cancer. 2000;28:29-36.
127. Nilsson O, Brezicka FT, Holmgren J, Sorenson S, Svennerholm L, Yngvason F, et al. Detection of a ganglioside antigen associated with small cell lung carcinomas using monoclonal antibodies directed against fucosyl-GM1. Cancer Res. 1986;46:1403-7.
128. Brezicka FT, Olling S, Bergman B, Berggren H, Engstrom CP, Hammarstrom S, et al. Coexpression of ganglioside antigen Fuc-GM1, neural-cell adhesion molecule, carcinoembryonic antigen, and carbohydrate tumor-associated antigen CA 50 in lung cancer. Tumour Biol. 1992;13:308-15.
129. Ladisch S, Wu ZL. Detection of a tumour-associated ganglioside in plasma of patients with neuroblastoma. Lancet. 1985;1:136-8.
130. Drake PM, Nathan JK, Stock CM, Chang PV, Muench MO, Nakata D, et al. Polysialic acid, a glycan with highly restricted expression, is found on human and murine leukocytes and modulates immune responses. J Immunol. 2008;181:6850-8.
131. Komminoth P, Roth J, Lackie PM, Bitter-Suermann D, Heitz PU. Polysialic acid of the neural cell adhesion molecule distinguishes small cell lung carcinoma from carcinoids. Am J Pathol. 1991;139:297-304.
132. Slovin SF, Keding SJ, Ragupathi G. Carbohydrate vaccines as immunotherapy for cancer.

Immunol Cell Biol. 2005;83:418-28.
133. Balsara BR, Testa JR. Chromosomal imbalances in human lung cancer. Oncogene. 2002;21:6877-83.
134. Sato M, Shames DS, Gazdar AF, Minna JD. A translational view of the molecular pathogenesis of lung cancer. J Thorac Oncol. 2007;2:327-43.
135. Johnson BE, Sakaguchi AY, Gazdar AF, Minna JD, Burch D, Marshall A, et al. Restriction fragment length polymorphism studies show consistent loss of chromosome 3p alleles in small cell lung cancer patients' tumors. J Clin Invest. 1988;82:502-7.
136. Burbee DG, Forgacs E, Zochbauer-Muller S, Shivakumar L, Fong K, Gao B, et al. Epigenetic inactivation of RASSF1A in lung and breast cancers and malignant phenotype suppression. J Natl Cancer Inst. 2001;93:691-9.
137. Dammann R, Li C, Yoon JH, Chin PL, Bates S, Pfeifer GP. Epigenetic inactivation of a RAS association domain family protein from the lung tumour suppressor locus 3p21.3. Nat Genet. 2000;25:315-9.
138. Agathanggelou A, Cooper WN, Latif F. Role of the Ras-association domain family 1 tumor suppressor gene in human cancers. Cancer Res. 2005;65:3497-508.
139. Hougaard S, Norgaard P, Abrahamsen N, Moses HL, Spang-Thomsen M, Skovgaard Poulsen H. Inactivation of the transforming growth factor beta type II receptor in human small cell lung cancer cell lines. Br J Cancer. 1999;79:1005-11.
140. Zabarovsky ER, Lerman MI, Minna JD. Tumor suppressor genes on chromosome 3p involved in the pathogenesis of lung and other cancers. Oncogene. 2002;21:6915-35.
141. Prudkin L, Behrens C, Liu DD, Zhou X, Ozburn NC, Bekele BN, et al. Loss and reduction of FUS1 protein expression is a frequent phenomenon in the pathogenesis of lung cancer. Clin Cancer Res. 2008;14:41-7.
142. Ji L, Roth JA. Tumor suppressor FUS1 signaling pathway. J Thorac Oncol. 2008;3:327-30.
143. Sozzi G, Veronese ML, Negrini M, Baffa R, Cotticelli MG, Inoue H, et al. The FHIT gene 3p14.2 is abnormal in lung cancer. Cell. 1996;85:17-26.
144. Sard L, Accornero P, Tornielli S, Delia D, Bunone G, Campiglio M, et al. The tumor-suppressor gene FHIT is involved in the regulation of apoptosis and in cell cycle control. Proc Natl Acad Sci U S A. 1999;96:8489-92.
145. Mattei MG, Riviere M, Krust A, Ingvarsson S, Vennstrom B, Islam MQ, et al. Chromosomal assignment of retinoic acid receptor (RAR) genes in the human, mouse, and rat genomes. Genomics. 1991;10:1061-9.
146. Virmani AK, Rathi A, Zochbauer-Muller S, Sacchi N, Fukuyama Y, Bryant D, et al. Promoter methylation and silencing of the retinoic acid receptor-beta gene in lung carcinomas. J Natl Cancer Inst. 2000;92:1303-7.

147. Hiyama K, Hiyama E, Ishioka S, Yamakido M, Inai K, Gazdar AF, et al. Telomerase activity in small-cell and non-small-cell lung cancers. J Natl Cancer Inst. 1995;87:895-902.
148. Counter CM, Avilion AA, LeFeuvre CE, Stewart NG, Greider CW, Harley CB, et al. Telomere shortening associated with chromosome instability is arrested in immortal cells which express telomerase activity. EMBO J. 1992;11:1921-9.
149. Newbold RF. The significance of telomerase activation and cellular immortalization in human cancer. Mutagenesis. 2002;17:539-50.
150. Sarvesvaran J, Going JJ, Milroy R, Kaye SB, Keith WN. Is small cell lung cancer the perfect target for anti-telomerase treatment? Carcinogenesis. 1999;20:1649-51.
151. Zaffaroni N, De Polo D, Villa R, Della Porta C, Collini P, Fabbri A, et al. Differential expression of telomerase activity in neuroendocrine lung tumours: correlation with gene product immunophenotyping. J Pathol. 2003;201:127-33.
152. Kyte JA. Cancer vaccination with telomerase peptide GV1001. Expert Opin Investig Drugs. 2009;18:687-94Taki M, Kagawa S, Nishizaki M, Mizuguchi H, Hayakawa T, Kyo S, et al. Enhanced oncolysis by a tropism-modified telomerase-specific replication-selective adenoviral agent OBP-405 ('Telomelysin-RGD'). Oncogene. 2005;24:3130-40.
153. Bae SS, Cho H, Mu J, Birnbaum MJ. Isoform-specific regulation of insulin-dependent glucose uptake by Akt/protein kinase B. J Biol Chem. 2003;278:49530-6.
154. Strahl T, Thorner J. Synthesis and function of membrane phosphoinositides in budding yeast, Saccharomyces cerevisiae. Biochim Biophys Acta. 2007;1771:353-404.
155. Arboleda MJ, Lyons JF, Kabbinavar FF, Bray MR, Snow BE, Ayala R, et al. Overexpression of AKT2/protein kinase Bbeta leads to up-regulation of beta1 integrins, increased invasion, and metastasis of human breast and ovarian cancer cells. Cancer Res. 2003;63:196-206.
156. Crazzolara R, Cisterne A, Thien M, Hewson J, Baraz R, Bradstock KF, et al. Potentiating effects of RAD001 (Everolimus) on vincristine therapy in childhood acute lymphoblastic leukemia. Blood. 2009;113:3297-306.
157. Engelman JA. Targeting PI3K signalling in cancer: opportunities, challenges and limitations. Nat Rev Cancer. 2009;9:550-62.
158. Kumar CC. Signaling by integrin receptors. Oncogene. 1998;17:1365-73.
159. Shibata T, Kokubu A, Tsuta K, Hirohashi S. Oncogenic mutation of PIK3CA in small cell lung carcinoma: a potential therapeutic target pathway for chemotherapy-resistant lung cancer. Cancer Lett. 2009;283:203-11.
160. Heasley LE. Autocrine and paracrine signaling through neuropeptide receptors in human cancer. Oncogene. 2001;20:1563-9.
161. Pardo OE, Arcaro A, Salerno G, Tetley TD, Valovka T, Gout I, et al. Novel cross talk between MEK and S6K2 in FGF-2 induced proliferation of SCLC cells. Oncogene. 2001;20:7658-67.

162. Moore SM, Rintoul RC, Walker TR, Chilvers ER, Haslett C, Sethi T. The presence of a constitutively active phosphoinositide 3-kinase in small cell lung cancer cells mediates anchorage-independent proliferation via a protein kinase B and p70s6k-dependent pathway. Cancer Res. 1998;58:5239-47.
163. Marinov M, Ziogas A, Pardo OE, Tan LT, Dhillon T, Mauri FA, et al. AKT/mTOR pathway activation and BCL-2 family proteins modulate the sensitivity of human small cell lung cancer cells to RAD001. Clin Cancer Res. 2009;15:1277-87.
164. Krystal GW, Sulanke G, Litz J. Inhibition of phosphatidylinositol 3-kinase-Akt signaling blocks growth, promotes apoptosis, and enhances sensitivity of small cell lung cancer cells to chemotherapy. Mol Cancer Ther. 2002;1:913-22.
165. Pandya KJ, Dahlberg S, Hidalgo M, Cohen RB, Lee MW, Schiller JH, et al. A randomized, phase II trial of two dose levels of temsirolimus (CCI-779) in patients with extensive-stage small-cell lung cancer who have responding or stable disease after induction chemotherapy: a trial of the Eastern Cooperative Oncology Group (E1500). J Thorac Oncol. 2007;2:1036-41.
166. Tarhini A, Kotsakis A, Gooding W, Shuai Y, Petro D, Friedland D, et al. Phase II study of everolimus (RAD001) in previously treated small cell lung cancer. Clin Cancer Res. 2010;16:5900-7.
167. Liu P, Cheng H, Roberts TM, Zhao JJ. Targeting the phosphoinositide 3-kinase pathway in cancer. Nat Rev Drug Discov. 2009;8:627-44.
168. Nusslein-Volhard C, Wieschaus E. Mutations affecting segment number and polarity in Drosophila. Nature. 1980;287:795-801.
169. Watkins DN, Berman DM, Burkholder SG, Wang B, Beachy PA, Baylin SB. Hedgehog signalling within airway epithelial progenitors and in small-cell lung cancer. Nature. 2003;422:313-7.
170. Peacock CD, Watkins DN. Cancer stem cells and the ontogeny of lung cancer. J Clin Oncol. 2008;26:2883-9.
171. Rubin LL, de Sauvage FJ. Targeting the Hedgehog pathway in cancer. Nat Rev Drug Discov. 2006;5:1026-33.
172. Kalderon D. Transducing the hedgehog signal. Cell. 2000;103:371-4.
173. Berman DM, Karhadkar SS, Hallahan AR, Pritchard JI, Eberhart CG, Watkins DN, et al. Medulloblastoma growth inhibition by hedgehog pathway blockade. Science. 2002;297:1559-61.
174. Pepicelli CV, Lewis PM, McMahon AP. Sonic hedgehog regulates branching morphogenesis in the mammalian lung. Curr Biol. 1998;8:1083-6.
175. Varanou A, Page CP, Minger SL. Human embryonic stem cells and lung regeneration. Br J Pharmacol. 2008;155:316-25.
176. Vestergaard J, Pedersen MW, Pedersen N, Ensinger C, Tumer Z, Tommerup N, et al.

Hedgehog signaling in small-cell lung cancer: frequent in vivo but a rare event in vitro. Lung Cancer. 2006;52:281-90.
177. Artavanis-Tsakonas S, Rand MD, Lake RJ. Notch signaling: cell fate control and signal integration in development. Science. 1999;284:770-6.
178. Kunnimalaiyaan M, Chen H. Tumor suppressor role of Notch-1 signaling in neuroendocrine tumors. Oncologist. 2007;12:535-42.
179. Shawber C, Nofziger D, Hsieh JJ, Lindsell C, Bogler O, Hayward D, et al. Notch signaling inhibits muscle cell differentiation through a CBF1-independent pathway. Development. 1996;122:3765-73Lewis J. Notch signalling and the control of cell fate choices in vertebrates. Semin Cell Dev Biol. 1998;9:583-9.
180. Collins BJ, Kleeberger W, Ball DW. Notch in lung development and lung cancer. Semin Cancer Biol. 2004;14:357-64.
181. Bray SJ. Notch signalling: a simple pathway becomes complex. Nat Rev Mol Cell Biol. 2006;7:678-89.
182. Weinmaster G. The ins and outs of notch signaling. Mol Cell Neurosci. 1997;9:91-102.
183. Sriuranpong V, Borges MW, Ravi RK, Arnold DR, Nelkin BD, Baylin SB, et al. Notch signaling induces cell cycle arrest in small cell lung cancer cells. Cancer Res. 2001;61:3200-5.
184. Nusse R, Varmus HE. Many tumors induced by the mouse mammary tumor virus contain a provirus integrated in the same region of the host genome. Cell. 1982;31:99-109.
185. Rijsewijk F, Schuermann M, Wagenaar E, Parren P, Weigel D, Nusse R. The Drosophila homolog of the mouse mammary oncogene int-1 is identical to the segment polarity gene wingless. Cell. 1987;50:649-57.
186. He B, Jablons DM. Wnt signaling in stem cells and lung cancer. Ernst Schering Found Symp Proc. 2006:27-58.
187. Akiyama T. Wnt/beta-catenin signaling. Cytokine Growth Factor Rev. 2000;11:273-82.
188. Veeman MT, Axelrod JD, Moon RT. A second canon. Functions and mechanisms of beta-catenin-independent Wnt signaling. Dev Cell. 2003;5:367-77.
189. De Langhe SP, Reynolds SD. Wnt signaling in lung organogenesis. Organogenesis. 2008;4:100-8.
190. Lemjabbar-Alaoui H, Dasari V, Sidhu SS, Mengistab A, Finkbeiner W, Gallup M, et al. Wnt and Hedgehog are critical mediators of cigarette smoke-induced lung cancer. PLoS One. 2006;1:e93.
191. Konigshoff M, Eickelberg O. WNT signaling in lung disease: a failure or a regeneration signal? Am J Respir Cell Mol Biol. 2010;42:21-31.
192. Park KS, Liang MC, Raiser DM, Zamponi R, Roach RR, Curtis SJ, et al. Characterization of the cell of origin for small cell lung cancer. Cell Cycle. 2011;10:2806-15.

193. Patel AM, Davila DG, Peters SG. Paraneoplastic syndromes associated with lung cancer. Mayo Clin Proc. 1993;68:278-87.
194. Sher T, Dy GK, Adjei AA. Small cell lung cancer. Mayo Clin Proc. 2008;83:355-67.
195. Mason WP, Graus F, Lang B, Honnorat J, Delattre JY, Valldeoriola F, et al. Small-cell lung cancer, paraneoplastic cerebellar degeneration and the Lambert-Eaton myasthenic syndrome. Brain. 1997;120 (Pt 8):1279-300.
196. Chin R, Jr., Cappellari JO, McCain TW, Case LD, Haponik EF. Increasing use of bronchoscopic needle aspiration to diagnose small cell lung cancer. Mayo Clin Proc. 2000;75:796-801Tondini M, Rizzi A. Small-cell lung cancer: importance of fiberoptic bronchoscopy in the evaluation of complete remission. Tumori. 1989;75:266-8.
197. Gibbs AR, Thunnissen FB. Histological typing of lung and pleural tumours: third edition. J Clin Pathol. 2001;54:498-9.
198. Jones AM, Hanson IM, Armstrong GR, O'Driscoll BR. Value and accuracy of cytology in addition to histology in the diagnosis of lung cancer at flexible bronchoscopy. Respir Med. 2001;95:374-8.
199. Hochstenbag MM, Twijnstra A, Wilmink JT, Wouters EF, ten Velde GP. Asymptomatic brain metastases (BM) in small cell lung cancer (SCLC): MR-imaging is useful at initial diagnosis. J Neurooncol. 2000;48:243-8.
200. Bradley JD, Dehdashti F, Mintun MA, Govindan R, Trinkaus K, Siegel BA. Positron emission tomography in limited-stage small-cell lung cancer: a prospective study. J Clin Oncol. 2004;22:3248-54.
201. Voltz R, Carpentier AF, Rosenfeld MR, Posner JB, Dalmau J. P/Q-type voltage-gated calcium channel antibodies in paraneoplastic disorders of the central nervous system. Muscle Nerve. 1999;22:119-22Carpentier AF, Voltz R, DesChamps T, Posner JB, Dalmau J, Rosenfeld MR. Absence of HuD gene mutations in paraneoplastic small cell lung cancer tissue. Neurology. 1998;50:1919.
202. van Meerbeeck JP, Fennell DA, De Ruysscher DK. Small-cell lung cancer. Lancet. 2011;378:1741-55.
203. Lopez-Encuentra A, Bulzebruck H, Feinstein AR, Motta G, Mountain CF, Naruke T, et al. Tumor staging and classification in lung cancer. Summary of the international symposium. Madrid, Spain, 3-4 December 1999. Lung Cancer. 2000;29:79-83.
204. Mountain CF. Clinical biology of small cell carcinoma: relationship to surgical therapy. Semin Oncol. 1978;5:272-9.
205. Johnson BE, Bridges JD, Sobczeck M, Gray J, Linnoila RI, Gazdar AF, et al. Patients with limited-stage small-cell lung cancer treated with concurrent twice-daily chest radiotherapy and etoposide/cisplatin followed by cyclophosphamide, doxorubicin, and vincristine. J Clin Oncol.

1996;14:806-13.
206. Hanna NH, Einhorn LH. Small-cell lung cancer: state of the art. Clin Lung Cancer. 2002;4:87-94.
207. Janne PA, Freidlin B, Saxman S, Johnson DH, Livingston RB, Shepherd FA, et al. Twenty-five years of clinical research for patients with limited-stage small cell lung carcinoma in North America. Cancer. 2002;95:1528-38.
208. Poplin E, Thompson B, Whitacre M, Aisner J. Small cell carcinoma of the lung: influence of age on treatment outcome. Cancer Treat Rep. 1987;71:291-6.
209. Hansen H, Perry M, Arriagada R, Chastang C, Drings P, Osterlind K, et al. Second IASLC Workshop on combined Radiotherapy and Chemotherapy Modalities in Lung Cancer. Treatment evaluation. Lung Cancer. 1994;10 Suppl 1:S7-9.
210. Lad T, Piantadosi S, Thomas P, Payne D, Ruckdeschel J, Giaccone G. A prospective randomized trial to determine the benefit of surgical resection of residual disease following response of small cell lung cancer to combination chemotherapy. Chest. 1994;106:320S-3S.
211. Pignon JP, Arriagada R, Ihde DC, Johnson DH, Perry MC, Souhami RL, et al. A meta-analysis of thoracic radiotherapy for small-cell lung cancer. N Engl J Med. 1992;327:1618-24.
212. Sundstrom S, Bremnes RM, Kaasa S, Aasebo U, Hatlevoll R, Dahle R, et al. Cisplatin and etoposide regimen is superior to cyclophosphamide, epirubicin, and vincristine regimen in small-cell lung cancer: results from a randomized phase III trial with 5 years' follow-up. J Clin Oncol. 2002;20:4665-72.
213. Takada M, Fukuoka M, Kawahara M, Sugiura T, Yokoyama A, Yokota S, et al. Phase III study of concurrent versus sequential thoracic radiotherapy in combination with cisplatin and etoposide for limited-stage small-cell lung cancer: results of the Japan Clinical Oncology Group Study 9104. J Clin Oncol. 2002;20:3054-60.
214. Sculier JP, Paesmans M, Bureau G, Giner V, Lecomte J, Michel J, et al. Randomized trial comparing induction chemotherapy versus induction chemotherapy followed by maintenance chemotherapy in small-cell lung cancer. European Lung Cancer Working Party. J Clin Oncol. 1996;14:2337-44.
215. Beith JM, Clarke SJ, Woods RL, Bell DR, Levi JA. Long-term follow-up of a randomised trial of combined chemoradiotherapy induction treatment, with and without maintenance chemotherapy in patients with small cell carcinoma of the lung. Eur J Cancer. 1996;32A:438-43Byrne MJ, van Hazel G, Trotter J, Cameron F, Shepherd J, Cassidy B, et al. Maintenance chemotherapy in limited small cell lung cancer: a randomised controlled clinical trial. Br J Cancer. 1989;60:413-8.
216. Jeremic B, Shibamoto Y, Acimovic L, Milisavljevic S. Initial versus delayed accelerated

hyperfractionated radiation therapy and concurrent chemotherapy in limited small-cell lung cancer: a randomized study. J Clin Oncol. 1997;15:893-900.
217. Turrisi AT, 3rd, Kim K, Blum R, Sause WT, Livingston RB, Komaki R, et al. Twice-daily compared with once-daily thoracic radiotherapy in limited small-cell lung cancer treated concurrently with cisplatin and etoposide. N Engl J Med. 1999;340:265-71.
218. Breneman JC, Warnick RE, Albright RE, Jr., Kukiatinant N, Shaw J, Armin D, et al. Stereotactic radiosurgery for the treatment of brain metastases. Results of a single institution series. Cancer. 1997;79:551-7.
219. Slevin ML, Clark PI, Joel SP, Malik S, Osborne RJ, Gregory WM, et al. A randomized trial to evaluate the effect of schedule on the activity of etoposide in small-cell lung cancer. J Clin Oncol. 1989;7:1333-40.
220. Skarlos DV, Samantas E, Kosmidis P, Fountzilas G, Angelidou M, Palamidas P, et al. Randomized comparison of etoposide-cisplatin vs. etoposide-carboplatin and irradiation in small-cell lung cancer. A Hellenic Co-operative Oncology Group study. Ann Oncol. 1994;5:601-7.
221. Hanna N, Bunn PA, Jr., Langer C, Einhorn L, Guthrie T, Jr., Beck T, et al. Randomized phase III trial comparing irinotecan/cisplatin with etoposide/cisplatin in patients with previously untreated extensive-stage disease small-cell lung cancer. J Clin Oncol. 2006;24:2038-43.
222. Noda K, Nishiwaki Y, Kawahara M, Negoro S, Sugiura T, Yokoyama A, et al. Irinotecan plus cisplatin compared with etoposide plus cisplatin for extensive small-cell lung cancer. N Engl J Med. 2002;346:85-91.
223. Eckardt JR, von Pawel J, Papai Z, Tomova A, Tzekova V, Crofts TE, et al. Open-label, multicenter, randomized, phase III study comparing oral topotecan/cisplatin versus etoposide/cisplatin as treatment for chemotherapy-naive patients with extensive-disease small-cell lung cancer. J Clin Oncol. 2006;24:2044-51.
224. Loehrer PJ, Sr., Ansari R, Gonin R, Monaco F, Fisher W, Sandler A, et al. Cisplatin plus etoposide with and without ifosfamide in extensive small-cell lung cancer: a Hoosier Oncology Group study. J Clin Oncol. 1995;13:2594-9.
225. Pujol JL, Daures JP, Riviere A, Quoix E, Westeel V, Quantin X, et al. Etoposide plus cisplatin with or without the combination of 4'-epidoxorubicin plus cyclophosphamide in treatment of extensive small-cell lung cancer: a French Federation of Cancer Institutes multicenter phase III randomized study. J Natl Cancer Inst. 2001;93:300-8.
226. Ihde DC, Mulshine JL, Kramer BS, Steinberg SM, Linnoila RI, Gazdar AF, et al. Prospective randomized comparison of high-dose and standard-dose etoposide and cisplatin chemotherapy in patients with extensive-stage small-cell lung cancer. J Clin Oncol. 1994;12:2022-34.
227. Woll PJ, Thatcher N, Lomax L, Hodgetts J, Lee SM, Burt PA, et al. Use of hematopoietic progenitors in whole blood to support dose-dense chemotherapy: a randomized phase II trial in

small-cell lung cancer patients. J Clin Oncol. 2001;19:712-9.
228. Humblet Y, Symann M, Bosly A, Delaunois L, Francis C, Machiels J, et al. Late intensification chemotherapy with autologous bone marrow transplantation in selected small-cell carcinoma of the lung: a randomized study. J Clin Oncol. 1987;5:1864-73.
229. Kristjansen PE, Hansen HH. Prophylactic cranial irradiation in small cell lung cancer--an update. Lung Cancer. 1995;12 Suppl 3:S23-40.
230. Auperin A, Arriagada R, Pignon JP, Le Pechoux C, Gregor A, Stephens RJ, et al. Prophylactic cranial irradiation for patients with small-cell lung cancer in complete remission. Prophylactic Cranial Irradiation Overview Collaborative Group. N Engl J Med. 1999;341:476-84.
231. Fonseca R, O'Neill BP, Foote RL, Grill JP, Sloan JA, Frytak S. Cerebral toxicity in patients treated for small cell carcinoma of the lung. Mayo Clin Proc. 1999;74:461-5.
232. Slotman B, Faivre-Finn C, Kramer G, Rankin E, Snee M, Hatton M, et al. Prophylactic cranial irradiation in extensive small-cell lung cancer. N Engl J Med. 2007;357:664-72.
233. von Pawel J, Schiller JH, Shepherd FA, Fields SZ, Kleisbauer JP, Chrysson NG, et al. Topotecan versus cyclophosphamide, doxorubicin, and vincristine for the treatment of recurrent small-cell lung cancer. J Clin Oncol. 1999;17:658-67.
234. Perez-Soler R, Glisson BS, Lee JS, Fossella FV, Murphy WK, Shin DM, et al. Treatment of patients with small-cell lung cancer refractory to etoposide and cisplatin with the topoisomerase I poison topotecan. J Clin Oncol. 1996;14:2785-90.
235. Ardizzoni A, Manegold C, Debruyne C, Gaafar R, Buchholz E, Smit EF, et al. European organization for research and treatment of cancer (EORTC) 08957 phase II study of topotecan in combination with cisplatin as second-line treatment of refractory and sensitive small cell lung cancer. Clin Cancer Res. 2003;9:143-50.
236. Masuda N, Matsui K, Negoro S, Takifuji N, Takeda K, Yana T, et al. Combination of irinotecan and etoposide for treatment of refractory or relapsed small-cell lung cancer. J Clin Oncol. 1998;16:3329-34Groen HJ, Fokkema E, Biesma B, Kwa B, van Putten JW, Postmus PE, et al. Paclitaxel and carboplatin in the treatment of small-cell lung cancer patients resistant to cyclophosphamide, doxorubicin, and etoposide: a non-cross-resistant schedule. J Clin Oncol. 1999;17:927-32.
237. Ettinger DS, Finkelstein DM, Sarma RP, Johnson DH. Phase II study of paclitaxel in patients with extensive-disease small-cell lung cancer: an Eastern Cooperative Oncology Group study. J Clin Oncol. 1995;13:1430-5Kirschling RJ, Grill JP, Marks RS, Kugler JW, Gerstner JB, Kuross SA, et al. Paclitaxel and G-CSF in previously untreated patients with extensive stage small-cell lung cancer: a phase II study of the North Central Cancer Treatment Group. Am J Clin Oncol. 1999;22:517-22.
238. Bunn PA, Jr., Kelly K. A phase I study of cisplatin, etoposide, and paclitaxel in small cell

lung cancer. Semin Oncol. 1997;24:S12-144-S12-8.
239. Levitan N, Dowlati A, Shina D, Craffey M, Mackay W, DeVore R, et al. Multi-institutional phase I/II trial of paclitaxel, cisplatin, and etoposide with concurrent radiation for limited-stage small-cell lung carcinoma. J Clin Oncol. 2000;18:1102-9.
240. Greco FA, Hainsworth JD. Paclitaxel, carboplatin, and oral etoposide in the treatment of small cell lung cancer. Semin Oncol. 1996;23:7-10.
241. Smyth JF, Smith IE, Sessa C, Schoffski P, Wanders J, Franklin H, et al. Activity of docetaxel (Taxotere) in small cell lung cancer. The Early Clinical Trials Group of the EORTC. Eur J Cancer. 1994;30A:1058-60.
242. Ardizzoni A, Hansen H, Dombernowsky P, Gamucci T, Kaplan S, Postmus P, et al. Topotecan, a new active drug in the second-line treatment of small-cell lung cancer: a phase II study in patients with refractory and sensitive disease. The European Organization for Research and Treatment of Cancer Early Clinical Studies Group and New Drug Development Office, and the Lung Cancer Cooperative Group. J Clin Oncol. 1997;15:2090-6.
243. Negoro S, Fukuoka M, Niitani H, Suzuki A, Nakabayashi T, Kimura M, et al. [A phase II study of CPT-11, a camptothecin derivative, in patients with primary lung cancer. CPT-11 Cooperative Study Group]. Gan To Kagaku Ryoho. 1991;18:1013-9.
244. Masuda N, Fukuoka M, Kusunoki Y, Matsui K, Takifuji N, Kudoh S, et al. CPT-11: a new derivative of camptothecin for the treatment of refractory or relapsed small-cell lung cancer. J Clin Oncol. 1992;10:1225-9.
245. Kudoh S, Fujiwara Y, Takada Y, Yamamoto H, Kinoshita A, Ariyoshi Y, et al. Phase II study of irinotecan combined with cisplatin in patients with previously untreated small-cell lung cancer. West Japan Lung Cancer Group. J Clin Oncol. 1998;16:1068-74.
246. Cormier Y, Eisenhauer E, Muldal A, Gregg R, Ayoub J, Goss G, et al. Gemcitabine is an active new agent in previously untreated extensive small cell lung cancer (SCLC). A study of the National Cancer Institute of Canada Clinical Trials Group. Ann Oncol. 1994;5:283-5.
247. Jassem J, Karnicka-Mlodkowska H, van Pottelsberghe C, van Glabbeke M, Noseda MA, Ardizzoni A, et al. Phase II study of vinorelbine (Navelbine) in previously treated small cell lung cancer patients. EORTC Lung Cancer Cooperative Group. Eur J Cancer. 1993;29A:1720-2.
248. Atchley WR, Fitch WM. A natural classification of the basic helix-loop-helix class of transcription factors. Proc Natl Acad Sci U S A. 1997;94:5172-6.
249. Ledent V, Vervoort M. The basic helix-loop-helix protein family: comparative genomics and phylogenetic analysis. Genome Res. 2001;11:754-70.
250. Massari ME, Murre C. Helix-loop-helix proteins: regulators of transcription in eucaryotic organisms. Mol Cell Biol. 2000;20:429-40.
251. Toledo-Ortiz G, Huq E, Quail PH. The Arabidopsis basic/helix-loop-helix transcription factor

family. Plant Cell. 2003;15:1749-70.
252. Murre C, McCaw PS, Baltimore D. A new DNA binding and dimerization motif in immunoglobulin enhancer binding, daughterless, MyoD, and myc proteins. Cell. 1989;56:777-83.
253. Ferre-D'Amare AR, Pognonec P, Roeder RG, Burley SK. Structure and function of the b/HLH/Z domain of USF. EMBO J. 1994;13:180-9Nair SK, Burley SK. Recognizing DNA in the library. Nature. 2000;404:715, 7-8.
254. Atchley WR, Wollenberg KR, Fitch WM, Terhalle W, Dress AW. Correlations among amino acid sites in bHLH protein domains: an information theoretic analysis. Mol Biol Evol. 2000;17:164-78.
255. Atchley WR, Terhalle W, Dress A. Positional dependence, cliques, and predictive motifs in the bHLH protein domain. J Mol Evol. 1999;48:501-16.
256. Chaudhary J, Skinner MK. Basic helix-loop-helix proteins can act at the E-box within the serum response element of the c-fos promoter to influence hormone-induced promoter activation in Sertoli cells. Mol Endocrinol. 1999;13:774-86.
257. Robinson KA, Koepke JI, Kharodawala M, Lopes JM. A network of yeast basic helix-loop-helix interactions. Nucleic Acids Res. 2000;28:4460-6.
258. Murre C, Bain G, van Dijk MA, Engel I, Furnari BA, Massari ME, et al. Structure and function of helix-loop-helix proteins. Biochim Biophys Acta. 1994;1218:129-35.
259. Murre C, Voronova A, Baltimore D. B-cell- and myocyte-specific E2-box-binding factors contain E12/E47-like subunits. Mol Cell Biol. 1991;11:1156-60Lassar AB, Davis RL, Wright WE, Kadesch T, Murre C, Voronova A, et al. Functional activity of myogenic HLH proteins requires hetero-oligomerization with E12/E47-like proteins in vivo. Cell. 1991;66:305-15Aronheim A, Ohlsson H, Park CW, Edlund T, Walker MD. Distribution and characterization of helix-loop-helix enhancer-binding proteins from pancreatic beta cells and lymphocytes. Nucleic Acids Res. 1991;19:3893-9.
260. Hu JS, Olson EN, Kingston RE. HEB, a helix-loop-helix protein related to E2A and ITF2 that can modulate the DNA-binding ability of myogenic regulatory factors. Mol Cell Biol. 1992;12:1031-42.
261. Caudy M, Grell EH, Dambly-Chaudiere C, Ghysen A, Jan LY, Jan YN. The maternal sex determination gene daughterless has zygotic activity necessary for the formation of peripheral neurons in Drosophila. Genes Dev. 1988;2:843-52Cline TW. Maternal and zygotic sex-specific gene interactions in Drosophila melanogaster. Genetics. 1980;96:903-26.
262. Cline TW. A sex-specific, temperature-sensitive maternal effect of the daughterless mutation of Drosophila melanogaster. Genetics. 1976;84:723-42.
263. Sabourin LA, Rudnicki MA. The molecular regulation of myogenesis. Clin Genet. 2000;57:16-25Naidu PS, Ludolph DC, To RQ, Hinterberger TJ, Konieczny SF. Myogenin and

MEF2 function synergistically to activate the MRF4 promoter during myogenesis. Mol Cell Biol. 1995;15:2707-18.
264. Cabrera CV. The generation of cell diversity during early neurogenesis in Drosophila. Development. 1992;115:893-901Campuzano S, Modolell J. Patterning of the Drosophila nervous system: the achaete-scute gene complex. Trends Genet. 1992;8:202-8.
265. Gostissa M, Ranganath S, Bianco JM, Alt FW. Chromosomal location targets different MYC family gene members for oncogenic translocations. Proc Natl Acad Sci U S A. 2009;106:2265-70.
266. Steingrimsson E, Tessarollo L, Pathak B, Hou L, Arnheiter H, Copeland NG, et al. Mitf and Tfe3, two members of the Mitf-Tfe family of bHLH-Zip transcription factors, have important but functionally redundant roles in osteoclast development. Proc Natl Acad Sci U S A. 2002;99:4477-82.
267. Henthorn PS, Stewart CC, Kadesch T, Puck JM. The gene encoding human TFE3, a transcription factor that binds the immunoglobulin heavy-chain enhancer, maps to Xp11.22. Genomics. 1991;11:374-8.
268. Huan C, Kelly ML, Steele R, Shapira I, Gottesman SR, Roman CA. Transcription factors TFE3 and TFEB are critical for CD40 ligand expression and thymus-dependent humoral immunity. Nat Immunol. 2006;7:1082-91.
269. Ayer DE, Kretzner L, Eisenman RN. Mad: a heterodimeric partner for Max that antagonizes Myc transcriptional activity. Cell. 1993;72:211-22.
270. Zervos AS, Gyuris J, Brent R. Mxi1, a protein that specifically interacts with Max to bind Myc-Max recognition sites. Cell. 1994;79:following 388.
271. Benezra R, Davis RL, Lockshon D, Turner DL, Weintraub H. The protein Id: a negative regulator of helix-loop-helix DNA binding proteins. Cell. 1990;61:49-59.
272. Ellis HM, Spann DR, Posakony JW. extramacrochaetae, a negative regulator of sensory organ development in Drosophila, defines a new class of helix-loop-helix proteins. Cell. 1990;61:27-38.
273. Lasorella A, Rothschild G, Yokota Y, Russell RG, Iavarone A. Id2 mediates tumor initiation, proliferation, and angiogenesis in Rb mutant mice. Mol Cell Biol. 2005;25:3563-74.
274. Garrell J, Modolell J. The Drosophila extramacrochaetae locus, an antagonist of proneural genes that, like these genes, encodes a helix-loop-helix protein. Cell. 1990;61:39-48.
275. Rushlow CA, Hogan A, Pinchin SM, Howe KM, Lardelli M, Ish-Horowicz D. The Drosophila hairy protein acts in both segmentation and bristle patterning and shows homology to N-myc. EMBO J. 1989;8:3095-103.
276. Klambt C, Knust E, Tietze K, Campos-Ortega JA. Closely related transcripts encoded by the neurogenic gene complex enhancer of split of Drosophila melanogaster. EMBO J. 1989;8:203-10.
277. Jones S. An overview of the basic helix-loop-helix proteins. Genome Biol. 2004;5:226.
278. Kewley RJ, Whitelaw ML, Chapman-Smith A. The mammalian basic helix-loop-helix/PAS

family of transcriptional regulators. Int J Biochem Cell Biol. 2004;36:189-204.
279. Zelzer E, Wappner P, Shilo BZ. The PAS domain confers target gene specificity of Drosophila bHLH/PAS proteins. Genes Dev. 1997;11:2079-89.
280. Crews ST. Control of cell lineage-specific development and transcription by bHLH-PAS proteins. Genes Dev. 1998;12:607-20.
281. Dawson SR, Turner DL, Weintraub H, Parkhurst SM. Specificity for the hairy/enhancer of split basic helix-loop-helix (bHLH) proteins maps outside the bHLH domain and suggests two separable modes of transcriptional repression. Mol Cell Biol. 1995;15:6923-31.
282. Landschulz WH, Johnson PF, McKnight SL. The leucine zipper: a hypothetical structure common to a new class of DNA binding proteins. Science. 1988;240:1759-64.
283. Parry DA, Fraser RD, Squire JM. Fifty years of coiled-coils and alpha-helical bundles: a close relationship between sequence and structure. J Struct Biol. 2008;163:258-69.
284. Grandori C, Cowley SM, James LP, Eisenman RN. The Myc/Max/Mad network and the transcriptional control of cell behavior. Annu Rev Cell Dev Biol. 2000;16:653-99.
285. Morgenstern B, Atchley WR. Evolution of bHLH transcription factors: modular evolution by domain shuffling? Mol Biol Evol. 1999;16:1654-63.
286. Staudt LM, Lenardo MJ. Immunoglobulin gene transcription. Annu Rev Immunol. 1991;9:373-98.
287. Ephrussi A, Church GM, Tonegawa S, Gilbert W. B lineage--specific interactions of an immunoglobulin enhancer with cellular factors in vivo. Science. 1985;227:134-40.
288. Nelsen B, Tian G, Erman B, Gregoire J, Maki R, Graves B, et al. Regulation of lymphoid-specific immunoglobulin mu heavy chain gene enhancer by ETS-domain proteins. Science. 1993;261:82-6.
289. Buskin JN, Hauschka SD. Identification of a myocyte nuclear factor that binds to the muscle-specific enhancer of the mouse muscle creatine kinase gene. Mol Cell Biol. 1989;9:2627-40Lassar AB, Buskin JN, Lockshon D, Davis RL, Apone S, Hauschka SD, et al. MyoD is a sequence-specific DNA binding protein requiring a region of myc homology to bind to the muscle creatine kinase enhancer. Cell. 1989;58:823-31.
290. Whelan J, Cordle SR, Henderson E, Weil PA, Stein R. Identification of a pancreatic beta-cell insulin gene transcription factor that binds to and appears to activate cell-type-specific expression: its possible relationship to other cellular factors that bind to a common insulin gene sequence. Mol Cell Biol. 1990;10:1564-72.
291. Ahmad I. Mash-1 is expressed during ROD photoreceptor differentiation and binds an E-box, E(opsin)-1 in the rat opsin gene. Brain Res Dev Brain Res. 1995;90:184-9Bessis A, Salmon AM, Zoli M, Le Novere N, Picciotto M, Changeux JP. Promoter elements conferring neuron-specific expression of the beta 2-subunit of the neuronal nicotinic acetylcholine receptor studied in vitro

and in transgenic mice. Neuroscience. 1995;69:807-19Grant AL, Jones A, Thomas KL, Wisden W. Characterization of the rat hippocalcin gene: the 5' flanking region directs expression to the hippocampus. Neuroscience. 1996;75:1099-115Pepitoni S, Wood IC, Buckley NJ. Structure of the m1 muscarinic acetylcholine receptor gene and its promoter. J Biol Chem. 1997;272:17112-7.

292. Ferre-D'Amare AR, Prendergast GC, Ziff EB, Burley SK. Recognition by Max of its cognate DNA through a dimeric b/HLH/Z domain. Nature. 1993;363:38-45.

293. Ellenberger T, Fass D, Arnaud M, Harrison SC. Crystal structure of transcription factor E47: E-box recognition by a basic region helix-loop-helix dimer. Genes Dev. 1994;8:970-80.

294. Ma PC, Rould MA, Weintraub H, Pabo CO. Crystal structure of MyoD bHLH domain-DNA complex: perspectives on DNA recognition and implications for transcriptional activation. Cell. 1994;77:451-9Shimizu T, Toumoto A, Ihara K, Shimizu M, Kyogoku Y, Ogawa N, et al. Crystal structure of PHO4 bHLH domain-DNA complex: flanking base recognition. EMBO J. 1997;16:4689-97Parraga A, Bellsolell L, Ferre-D'Amare AR, Burley SK. Co-crystal structure of sterol regulatory element binding protein 1a at 2.3 A resolution. Structure. 1998;6:661-72.

295. Walhout AJ, Gubbels JM, Bernards R, van der Vliet PC, Timmers HT. c-Myc/Max heterodimers bind cooperatively to the E-box sequences located in the first intron of the rat ornithine decarboxylase (ODC) gene. Nucleic Acids Res. 1997;25:1493-501.

296. Weintraub H, Dwarki VJ, Verma I, Davis R, Hollenberg S, Snider L, et al. Muscle-specific transcriptional activation by MyoD. Genes Dev. 1991;5:1377-86.

297. Lee JE. Basic helix-loop-helix genes in neural development. Curr Opin Neurobiol. 1997;7:13-20.

298. Srivastava D, Olson EN. Knowing in your heart what's right. Trends Cell Biol. 1997;7:447-53.

299. Begley CG, Aplan PD, Davey MP, Nakahara K, Tchorz K, Kurtzberg J, et al. Chromosomal translocation in a human leukemic stem-cell line disrupts the T-cell antigen receptor delta-chain diversity region and results in a previously unreported fusion transcript. Proc Natl Acad Sci U S A. 1989;86:2031-5.

300. Gowda SD, Koler RD, Bagby GC, Jr. Regulation of C-myc expression during growth and differentiation of normal and leukemic human myeloid progenitor cells. J Clin Invest. 1986;77:271-8.

301. Luscher B, Larsson LG. The basic region/helix-loop-helix/leucine zipper domain of Myc proto-oncoproteins: function and regulation. Oncogene. 1999;18:2955-66.

302. Mathew S, Chen W, Murty VV, Benezra R, Chaganti RS. Chromosomal assignment of human ID1 and ID2 genes. Genomics. 1995;30:385-7Pagliuca A, Bartoli PC, Saccone S, Della Valle G, Lania L. Molecular cloning of ID4, a novel dominant negative helix-loop-helix human gene on chromosome 6p21.3-p22. Genomics. 1995;27:200-3.

303. Deed RW, Hirose T, Mitchell EL, Santibanez-Koref MF, Norton JD. Structural organisation and chromosomal mapping of the human Id-3 gene. Gene. 1994;151:309-14.
304. Heim MA, Jakoby M, Werber M, Martin C, Weisshaar B, Bailey PC. The basic helix-loop-helix transcription factor family in plants: a genome-wide study of protein structure and functional diversity. Mol Biol Evol. 2003;20:735-47.
305. Nehlin JO, Hara E, Kuo WL, Collins C, Campisi J. Genomic organization, sequence, and chromosomal localization of the human helix-loop-helix Id1 gene. Biochem Biophys Res Commun. 1997;231:628-34.
306. Norton JD, Deed RW, Craggs G, Sablitzky F. Id helix-loop-helix proteins in cell growth and differentiation. Trends Cell Biol. 1998;8:58-65.
307. Norton JD. ID helix-loop-helix proteins in cell growth, differentiation and tumorigenesis. J Cell Sci. 2000;113 (Pt 22):3897-905.
308. Perk J, Iavarone A, Benezra R. Id family of helix-loop-helix proteins in cancer. Nat Rev Cancer. 2005;5:603-14.
309.Ruzinova MB, Benezra R. Id proteins in development, cell cycle and cancer. Trends Cell Biol. 2003;13:410-8.
310. Campuzano S. Emc, a negative HLH regulator with multiple functions in Drosophila development. Oncogene. 2001;20:8299-307.
311. Lasorella A, Uo T, Iavarone A. Id proteins at the cross-road of development and cancer. Oncogene. 2001;20:8326-33.
312. Kleeff J, Ishiwata T, Friess H, Buchler MW, Israel MA, Korc M. The helix-loop-helix protein Id2 is overexpressed in human pancreatic cancer. Cancer Res. 1998;58:3769-72.
313. Lin CQ, Singh J, Murata K, Itahana Y, Parrinello S, Liang SH, et al. A role for Id-1 in the aggressive phenotype and steroid hormone response of human breast cancer cells. Cancer Res. 2000;60:1332-40.
314. Lasorella A, Boldrini R, Dominici C, Donfrancesco A, Yokota Y, Inserra A, et al. Id2 is critical for cellular proliferation and is the oncogenic effector of N-myc in human neuroblastoma. Cancer Res. 2002;62:301-6.
315. Lee J, Kim K, Kim JH, Jin HM, Choi HK, Lee SH, et al. Id helix-loop-helix proteins negatively regulate TRANCE-mediated osteoclast differentiation. Blood. 2006;107:2686-93.
316. Norton JD, Atherton GT. Coupling of cell growth control and apoptosis functions of Id proteins. Mol Cell Biol. 1998;18:2371-81.
317. Hara E, Yamaguchi T, Nojima H, Ide T, Campisi J, Okayama H, et al. Id-related genes encoding helix-loop-helix proteins are required for G1 progression and are repressed in senescent human fibroblasts. J Biol Chem. 1994;269:2139-45.
318. Lasorella A, Noseda M, Beyna M, Yokota Y, Iavarone A. Id2 is a retinoblastoma protein

target and mediates signalling by Myc oncoproteins. Nature. 2000;407:592-8.
319. Dyson N. The regulation of E2F by pRB-family proteins. Genes Dev. 1998;12:2245-62.
320. Alani RM, Young AZ, Shifflett CB. Id1 regulation of cellular senescence through transcriptional repression of p16/Ink4a. Proc Natl Acad Sci U S A. 2001;98:7812-6.
321. Lyden D, Young AZ, Zagzag D, Yan W, Gerald W, O'Reilly R, et al. Id1 and Id3 are required for neurogenesis, angiogenesis and vascularization of tumour xenografts. Nature. 1999;401:670-7.
322. Prabhu S, Ignatova A, Park ST, Sun XH. Regulation of the expression of cyclin-dependent kinase inhibitor p21 by E2A and Id proteins. Mol Cell Biol. 1997;17:5888-96.
323. Everly DN, Jr., Mainou BA, Raab-Traub N. Induction of Id1 and Id3 by latent membrane protein 1 of Epstein-Barr virus and regulation of p27/Kip and cyclin-dependent kinase 2 in rodent fibroblast transformation. J Virol. 2004;78:13470-8.
324. Deed RW, Hara E, Atherton GT, Peters G, Norton JD. Regulation of Id3 cell cycle function by Cdk-2-dependent phosphorylation. Mol Cell Biol. 1997;17:6815-21.
325. Hara E, Hall M, Peters G. Cdk2-dependent phosphorylation of Id2 modulates activity of E2A-related transcription factors. EMBO J. 1997;16:332-42.
326. Jan YN, Jan LY. HLH proteins, fly neurogenesis, and vertebrate myogenesis. Cell. 1993;75:827-30.
327. Baonza A, Garcia-Bellido A. Dual role of extramacrochaetae in cell proliferation and cell differentiation during wing morphogenesis in Drosophila. Mech Dev. 1999;80:133-46.
328. Baonza A, de Celis JF, Garcia-Bellido A. Relationships between extramacrochaetae and Notch signalling in Drosophila wing development. Development. 2000;127:2383-93.
329. Sawai S, Campos-Ortega JA. A zebrafish Id homologue and its pattern of expression during embryogenesis. Mech Dev. 1997;65:175-85.
330. Kane DA, Kimmel CB. The zebrafish midblastula transition. Development. 1993;119:447-56.
331. Zhang H, Reynaud S, Kloc M, Etkin LD, Spohr G. Id gene activity during Xenopus embryogenesis. Mech Dev. 1995;50:119-30.
332. Hikasa H, Hori K, Shiokawa K. Structure of aldolase A (muscle-type) cDNA and its regulated expression in oocytes, embryos and adult tissues of Xenopus laevis. Biochim Biophys Acta. 1997;1354:189-203.
333. Wang Y, Benezra R, Sassoon DA. Id expression during mouse development: a role in morphogenesis. Dev Dyn. 1992;194:222-30.
334. Cross JC, Flannery ML, Blanar MA, Steingrimsson E, Jenkins NA, Copeland NG, et al. Hxt encodes a basic helix-loop-helix transcription factor that regulates trophoblast cell development. Development. 1995;121:2513-23.
335. Jen Y, Weintraub H, Benezra R. Overexpression of Id protein inhibits the muscle differentiation program: in vivo association of Id with E2A proteins. Genes Dev. 1992;6:1466-79.

336. Kreider BL, Benezra R, Rovera G, Kadesch T. Inhibition of myeloid differentiation by the helix-loop-helix protein Id. Science. 1992;255:1700-2.
337. Wilson RB, Kiledjian M, Shen CP, Benezra R, Zwollo P, Dymecki SM, et al. Repression of immunoglobulin enhancers by the helix-loop-helix protein Id: implications for B-lymphoid-cell development. Mol Cell Biol. 1991;11:6185-91.
338. Ogata T, Wozney JM, Benezra R, Noda M. Bone morphogenetic protein 2 transiently enhances expression of a gene, Id (inhibitor of differentiation), encoding a helix-loop-helix molecule in osteoblast-like cells. Proc Natl Acad Sci U S A. 1993;90:9219-22.
339. Simonson MS, Rooney A, Herman WH. Expression and differential regulation of Id1, a dominant negative regulator of basic helix-loop-helix transcription factors, in glomerular mesangial cells. Nucleic Acids Res. 1993;21:5767-74.
340. Jen Y, Manova K, Benezra R. Expression patterns of Id1, Id2, and Id3 are highly related but distinct from that of Id4 during mouse embryogenesis. Dev Dyn. 1996;207:235-52.
341. Parrinello S, Lin CQ, Murata K, Itahana Y, Singh J, Krtolica A, et al. Id-1, ITF-2, and Id-2 comprise a network of helix-loop-helix proteins that regulate mammary epithelial cell proliferation, differentiation, and apoptosis. J Biol Chem. 2001;276:39213-9.
342. Tanaka K, Pracyk JB, Takeda K, Yu ZX, Ferrans VJ, Deshpande SS, et al. Expression of Id1 results in apoptosis of cardiac myocytes through a redox-dependent mechanism. J Biol Chem. 1998;273:25922-8.
343. Kee BL, Rivera RR, Murre C. Id3 inhibits B lymphocyte progenitor growth and survival in response to TGF-beta. Nat Immunol. 2001;2:242-7.
344. Andres-Barquin PJ, Hernandez MC, Israel MA. Id4 expression induces apoptosis in astrocytic cultures and is down-regulated by activation of the cAMP-dependent signal transduction pathway. Exp Cell Res. 1999;247:347-55.
345. Zhang X, Ling MT, Wong YC, Wang X. Evidence of a novel antiapoptotic factor: role of inhibitor of differentiation or DNA binding (Id-1) in anticancer drug-induced apoptosis. Cancer Sci. 2007;98:308-14.
346. Ling MT, Wang X, Ouyang XS, Xu K, Tsao SW, Wong YC. Id-1 expression promotes cell survival through activation of NF-kappaB signalling pathway in prostate cancer cells. Oncogene. 2003;22:4498-508Wong YC, Wang X, Ling MT. Id-1 expression and cell survival. Apoptosis. 2004;9:279-89.
347. Koyama T, Suzuki H, Imakiire A, Yanase N, Hata K, Mizuguchi J. Id3-mediated enhancement of cisplatin-induced apoptosis in a sarcoma cell line MG-63. Anticancer Res. 2004;24:1519-24.
348. Mern DS, Hoppe-Seyler K, Hoppe-Seyler F, Hasskarl J, Burwinkel B. Targeting Id1 and Id3 by a specific peptide aptamer induces E-box promoter activity, cell cycle arrest, and apoptosis in

breast cancer cells. Breast Cancer Res Treat. 2010;124:623-33Mern DS, Hasskarl J, Burwinkel B. Inhibition of Id proteins by a peptide aptamer induces cell-cycle arrest and apoptosis in ovarian cancer cells. Br J Cancer. 2010;103:1237-44.

349. Sikder HA, Devlin MK, Dunlap S, Ryu B, Alani RM. Id proteins in cell growth and tumorigenesis. Cancer cell. 2003;3:525-30.

350. Benezra R, Rafii S, Lyden D. The Id proteins and angiogenesis. Oncogene. 2001;20:8334-41.

351. Lyden D, Hattori K, Dias S, Costa C, Blaikie P, Butros L, et al. Impaired recruitment of bone-marrow-derived endothelial and hematopoietic precursor cells blocks tumor angiogenesis and growth. Nat Med. 2001;7:1194-201.

352. Volpert OV, Pili R, Sikder HA, Nelius T, Zaichuk T, Morris C, et al. Id1 regulates angiogenesis through transcriptional repression of thrombospondin-1. Cancer cell. 2002;2:473-83.

353. Fong S, Itahana Y, Sumida T, Singh J, Coppe JP, Liu Y, et al. Id-1 as a molecular target in therapy for breast cancer cell invasion and metastasis. Proc Natl Acad Sci U S A. 2003;100:13543-8.

354. Desprez PY, Lin CQ, Thomasset N, Sympson CJ, Bissell MJ, Campisi J. A novel pathway for mammary epithelial cell invasion induced by the helix-loop-helix protein Id-1. Mol Cell Biol. 1998;18:4577-88.

355. Andres-Barquin PJ, Hernandez MC, Hayes TE, McKay RD, Israel MA. Id genes encoding inhibitors of transcription are expressed during in vitro astrocyte differentiation and in cell lines derived from astrocytic tumors. Cancer Res. 1997;57:215-20.

356. Sablitzky F, Moore A, Bromley M, Deed RW, Newton JS, Norton JD. Stage- and subcellular-specific expression of Id proteins in male germ and Sertoli cells implicates distinctive regulatory roles for Id proteins during meiosis, spermatogenesis, and Sertoli cell function. Cell Growth Differ. 1998;9:1015-24.

357. Langlands K, Down GA, Kealey T. Id proteins are dynamically expressed in normal epidermis and dysregulated in squamous cell carcinoma. Cancer Res. 2000;60:5929-33.

358. Ouyang XS, Wang X, Lee DT, Tsao SW, Wong YC. Over expression of ID-1 in prostate cancer. J Urol. 2002;167:2598-602.

359. Schoppmann SF, Schindl M, Bayer G, Aumayr K, Dienes J, Horvat R, et al. Overexpression of Id-1 is associated with poor clinical outcome in node negative breast cancer. Int J Cancer. 2003;104:677-82.

360. Schindl M, Oberhuber G, Obermair A, Schoppmann SF, Karner B, Birner P. Overexpression of Id-1 protein is a marker for unfavorable prognosis in early-stage cervical cancer. Cancer Res. 2001;61:5703-6.

361. Morrow MA, Mayer EW, Perez CA, Adlam M, Siu G. Overexpression of the Helix-Loop-Helix protein Id2 blocks T cell development at multiple stages. Mol Immunol.

1999;36:491-503.
362. Stighall M, Manetopoulos C, Axelson H, Landberg G. High ID2 protein expression correlates with a favourable prognosis in patients with primary breast cancer and reduces cellular invasiveness of breast cancer cells. Int J Cancer. 2005;115:403-11.
363. Fukuma M, Okita H, Hata J, Umezawa A. Upregulation of Id2, an oncogenic helix-loop-helix protein, is mediated by the chimeric EWS/ets protein in Ewing sarcoma. Oncogene. 2003;22:1-9Nishimori H, Sasaki Y, Yoshida K, Irifune H, Zembutsu H, Tanaka T, et al. The Id2 gene is a novel target of transcriptional activation by EWS-ETS fusion proteins in Ewing family tumors. Oncogene. 2002;21:8302-9.
364. Wilson JW, Deed RW, Inoue T, Balzi M, Becciolini A, Faraoni P, et al. Expression of Id helix-loop-helix proteins in colorectal adenocarcinoma correlates with p53 expression and mitotic index. Cancer Res. 2001;61:8803-10.
365. Tang J, Gordon GM, Muller MG, Dahiya M, Foreman KE. Kaposi's sarcoma-associated herpesvirus latency-associated nuclear antigen induces expression of the helix-loop-helix protein Id-1 in human endothelial cells. J Virol. 2003;77:5975-84.
366. Singh J, Murata K, Itahana Y, Desprez PY. Constitutive expression of the Id-1 promoter in human metastatic breast cancer cells is linked with the loss of NF-1/Rb/HDAC-1 transcription repressor complex. Oncogene. 2002;21:1812-22.
367. Bain G, Cravatt CB, Loomans C, Alberola-Ila J, Hedrick SM, Murre C. Regulation of the helix-loop-helix proteins, E2A and Id3, by the Ras-ERK MAPK cascade. Nat Immunol. 2001;2:165-71.
368. Belletti B, Prisco M, Morrione A, Valentinis B, Navarro M, Baserga R. Regulation of Id2 gene expression by the insulin-like growth factor I receptor requires signaling by phosphatidylinositol 3-kinase. J Biol Chem. 2001;276:13867-74.
369. Langlands K, Yin X, Anand G, Prochownik EV. Differential interactions of Id proteins with basic-helix-loop-helix transcription factors. J Biol Chem. 1997;272:19785-93.
370. Deed RW, Jasiok M, Norton JD. Lymphoid-specific expression of the Id3 gene in hematopoietic cells. Selective antagonism of E2A basic helix-loop-helix protein associated with Id3-induced differentiation of erythroleukemia cells. J Biol Chem. 1998;273:8278-86.
371. Shoji W, Inoue T, Yamamoto T, Obinata M. MIDA1, a protein associated with Id, regulates cell growth. J Biol Chem. 1995;270:24818-25.
372. Yates PR, Atherton GT, Deed RW, Norton JD, Sharrocks AD. Id helix-loop-helix proteins inhibit nucleoprotein complex formation by the TCF ETS-domain transcription factors. EMBO J. 1999;18:968-76.
373. Iavarone A, Garg P, Lasorella A, Hsu J, Israel MA. The helix-loop-helix protein Id-2 enhances cell proliferation and binds to the retinoblastoma protein. Genes Dev. 1994;8:1270-84.

374. Moldes M, Boizard M, Liepvre XL, Feve B, Dugail I, Pairault J. Functional antagonism between inhibitor of DNA binding (Id) and adipocyte determination and differentiation factor 1/sterol regulatory element-binding protein-1c (ADD1/SREBP-1c) trans-factors for the regulation of fatty acid synthase promoter in adipocytes. Biochem J. 1999;344 Pt 3:873-80.
375. Neuman T, Keen A, Zuber MX, Kristjansson GI, Gruss P, Nornes HO. Neuronal expression of regulatory helix-loop-helix factor Id2 gene in mouse. Dev Biol. 1993;160:186-95Ellmeier W, Weith A. Expression of the helix-loop-helix gene Id3 during murine embryonic development. Dev Dyn. 1995;203:163-73.
376. Riechmann V, van Cruchten I, Sablitzky F. The expression pattern of Id4, a novel dominant negative helix-loop-helix protein, is distinct from Id1, Id2 and Id3. Nucleic Acids Res. 1994;22:749-55.
377. Cooper CL, Newburger PE. Differential expression of Id genes in multipotent myeloid progenitor cells: Id-1 is induced by early-and late-acting cytokines while Id-2 is selectively induced by cytokines that drive terminal granulocytic differentiation. J Cell Biochem. 1998;71:277-85Cooper CL, Brady G, Bilia F, Iscove NN, Quesenberry PJ. Expression of the Id family helix-loop-helix regulators during growth and development in the hematopoietic system. Blood. 1997;89:3155-65.
378. Murphy JJ, Norton JD. Cell-type-specific early response gene expression during plasmacytoid differentiation of human B lymphocytic leukemia cells. Biochim Biophys Acta. 1990;1049:261-71Christy BA, Sanders LK, Lau LF, Copeland NG, Jenkins NA, Nathans D. An Id-related helix-loop-helix protein encoded by a growth factor-inducible gene. Proc Natl Acad Sci U S A. 1991;88:1815-9.
379. Tournay O, Benezra R. Transcription of the dominant-negative helix-loop-helix protein Id1 is regulated by a protein complex containing the immediate-early response gene Egr-1. Mol Cell Biol. 1996;16:2418-30.
380. Littlewood TD, Evan GI. Transcription factors 2: helix-loop-helix. Protein Profile. 1995;2:621-702.
381. Biggs JR, Zhang Y, Murphy EV. Repression of the Id2 (inhibitor of differentiation) gene promoter during exit from the cell cycle. J Cell Physiol. 1995;164:249-58.
382. Kurabayashi M, Jeyaseelan R, Kedes L. Doxorubicin represses the function of the myogenic helix-loop-helix transcription factor MyoD. Involvement of Id gene induction. J Biol Chem. 1994;269:6031-9.
383. Saisanit S, Sun XH. A novel enhancer, the pro-B enhancer, regulates Id1 gene expression in progenitor B cells. Mol Cell Biol. 1995;15:1513-21.
384. Saisanit S, Sun XH. Regulation of the pro-B-cell-specific enhancer of the Id1 gene involves the C/EBP family of proteins. Mol Cell Biol. 1997;17:844-50.

385. Einarson MB, Chao MV. Regulation of Id1 and its association with basic helix-loop-helix proteins during nerve growth factor-induced differentiation of PC12 cells. Mol Cell Biol. 1995;15:4175-83.
386. Hollnagel A, Oehlmann V, Heymer J, Ruther U, Nordheim A. Id genes are direct targets of bone morphogenetic protein induction in embryonic stem cells. J Biol Chem. 1999;274:19838-45.
387. Nakashima K, Takizawa T, Ochiai W, Yanagisawa M, Hisatsune T, Nakafuku M, et al. BMP2-mediated alteration in the developmental pathway of fetal mouse brain cells from neurogenesis to astrocytogenesis. Proc Natl Acad Sci U S A. 2001;98:5868-73.
388. Dorai H, Sampath TK. Bone morphogenetic protein-7 modulates genes that maintain the vascular smooth muscle cell phenotype in culture. J Bone Joint Surg Am. 2001;83-A Suppl 1:S70-8.
389. Massague J. TGF-beta signal transduction. Annu Rev Biochem. 1998;67:753-91.
390. Yanagisawa M, Takizawa T, Ochiai W, Uemura A, Nakashima K, Taga T. Fate alteration of neuroepithelial cells from neurogenesis to astrocytogenesis by bone morphogenetic proteins. Neurosci Res. 2001;41:391-6.
391. Korchynskyi O, ten Dijke P. Identification and functional characterization of distinct critically important bone morphogenetic protein-specific response elements in the Id1 promoter. J Biol Chem. 2002;277:4883-91.
392. Lopez-Rovira T, Chalaux E, Massague J, Rosa JL, Ventura F. Direct binding of Smad1 and Smad4 to two distinct motifs mediates bone morphogenetic protein-specific transcriptional activation of Id1 gene. J Biol Chem. 2002;277:3176-85.
393. Lilja H, Kamohara Y, Neuman T, Demetriou AA, Rozga J. Transforming growth factor beta1 helps maintain differentiated functions in mitogen-treated primary rat hepatocyte cultures. Mol Cell Biol Res Commun. 1999;1:188-95.
394. Sugai M, Gonda H, Kusunoki T, Katakai T, Yokota Y, Shimizu A. Essential role of Id2 in negative regulation of IgE class switching. Nat Immunol. 2003;4:25-30.
395. Kang Y, Chen CR, Massague J. A self-enabling TGFbeta response coupled to stress signaling: Smad engages stress response factor ATF3 for Id1 repression in epithelial cells. Mol Cell. 2003;11:915-26.
396. Goumans MJ, Valdimarsdottir G, Itoh S, Rosendahl A, Sideras P, ten Dijke P. Balancing the activation state of the endothelium via two distinct TGF-beta type I receptors. EMBO J. 2002;21:1743-53.
397. Zhang W, Liu HT. MAPK signal pathways in the regulation of cell proliferation in mammalian cells. Cell research. 2002;12:9-18.
398. Ohtani N, Zebedee Z, Huot TJ, Stinson JA, Sugimoto M, Ohashi Y, et al. Opposing effects of Ets and Id proteins on p16INK4a expression during cellular senescence. Nature.

2001;409:1067-70.
399. Ling MT, Wang X, Ouyang XS, Lee TK, Fan TY, Xu K, et al. Activation of MAPK signaling pathway is essential for Id-1 induced serum independent prostate cancer cell growth. Oncogene. 2002;21:8498-505.
400. Wang X, Xu K, Ling MT, Wong YC, Feng HC, Nicholls J, et al. Evidence of increased Id-1 expression and its role in cell proliferation in nasopharyngeal carcinoma cells. Mol Carcinog. 2002;35:42-9.
401. Cheung HW, Ling MT, Tsao SW, Wong YC, Wang X. Id-1-induced Raf/MEK pathway activation is essential for its protective role against taxol-induced apoptosis in nasopharyngeal carcinoma cells. Carcinogenesis. 2004;25:881-7.
402.Nagata Y, Shoji W, Obinata M, Todokoro K. Phosphorylation of helix-loop-helix proteins ID1, ID2 and ID3. Biochem Biophys Res Commun. 1995;207:916-26.
403. Bounpheng MA, Dimas JJ, Dodds SG, Christy BA. Degradation of Id proteins by the ubiquitin-proteasome pathway. FASEB J. 1999;13:2257-64.
404. Deed RW, Armitage S, Norton JD. Nuclear localization and regulation of Id protein through an E protein-mediated chaperone mechanism. J Biol Chem. 1996;271:23603-6.
405. Kamalian L, Forootan SS, Bao ZZ, Zhang Y, Gosney JR, Foster CS, et al. Inhibition of tumourigenicity of small cell lung cancer cells by suppressing Id3 expression. Int J Oncol. 2010;37:595-603.
406. Napoli C, Lemieux C, Jorgensen R. Introduction of a Chimeric Chalcone Synthase Gene into Petunia Results in Reversible Co-Suppression of Homologous Genes in trans. Plant Cell. 1990;2:279-89.
407. Hui SW, Langner M, Zhao YL, Ross P, Hurley E, Chan K. The role of helper lipids in cationic liposome-mediated gene transfer. Biophys J. 1996;71:590-9.
408. Karra D, Dahm R. Transfection techniques for neuronal cells. J Neurosci. 2010;30:6171-7.
409. Pheiffer BH, Zimmerman SB. Polymer-stimulated ligation: enhanced blunt- or cohesive-end ligation of DNA or deoxyribooligonucleotides by T4 DNA ligase in polymer solutions. Nucleic Acids Res. 1983;11:7853-71.
410. Compton SJ, Jones CG. Mechanism of dye response and interference in the Bradford protein assay. Anal Biochem. 1985;151:369-74.
411. Rygaard K, Spang-Thomsen M. Quantitation and gompertzian analysis of tumor growth. Breast Cancer Res Treat. 1997;46:303-12.
412. Folkman J. Tumor angiogenesis: therapeutic implications. N Engl J Med. 1971;285:1182-6.
413. Nishida N, Yano H, Nishida T, Kamura T, Kojiro M. Angiogenesis in cancer. Vasc Health Risk Manag. 2006;2:213-9.
414. Kamalian L, Gosney JR, Forootan SS, Foster CS, Bao ZZ, Beesley C, et al. Increased

expression of Id family proteins in small cell lung cancer and its prognostic significance. Clin Cancer Res. 2008;14:2318-25.

415. Swarbrick A, Akerfeldt MC, Lee CS, Sergio CM, Caldon CE, Hunter LJ, et al. Regulation of cyclin expression and cell cycle progression in breast epithelial cells by the helix-loop-helix protein Id1. Oncogene. 2005;24:381-9.

416. Li B, Cheung PY, Wang X, Tsao SW, Ling MT, Wong YC, et al. Id-1 activation of PI3K/Akt/NFkappaB signaling pathway and its significance in promoting survival of esophageal cancer cells. Carcinogenesis. 2007;28:2313-20.

417. Aoki M, Ishii T, Kanaoka M, Kimura T. RNA interference in immune cells by use of osmotic delivery of siRNA. Biochem Biophys Res Commun. 2006;341:326-33Borawski J, Lindeman A, Buxton F, Labow M, Gaither LA. Optimization procedure for small interfering RNA transfection in a 384-well format. Journal of biomolecular screening. 2007;12:546-59Chiu YL, Ali A, Chu CY, Cao H, Rana TM. Visualizing a correlation between siRNA localization, cellular uptake, and RNAi in living cells. Chemistry & biology. 2004;11:1165-75Simeoni F, Morris MC, Heitz F, Divita G. Insight into the mechanism of the peptide-based gene delivery system MPG: implications for delivery of siRNA into mammalian cells. Nucleic Acids Res. 2003;31:2717-24.

418. Mousses S, Caplen NJ, Cornelison R, Weaver D, Basik M, Hautaniemi S, et al. RNAi microarray analysis in cultured mammalian cells. Genome Res. 2003;13:2341-7.

419. Aza-Blanc P, Cooper CL, Wagner K, Batalov S, Deveraux QL, Cooke MP. Identification of modulators of TRAIL-induced apoptosis via RNAi-based phenotypic screening. Mol Cell. 2003;12:627-37Chanda SK, White S, Orth AP, Reisdorph R, Miraglia L, Thomas RS, et al. Genome-scale functional profiling of the mammalian AP-1 signaling pathway. Proc Natl Acad Sci U S A. 2003;100:12153-8.

420. LaPan P, Zhang J, Pan J, Haney S. Quantitative optimization of reverse transfection conditions for 384-well siRNA library screening. Assay and drug development technologies. 2008;6:683-91.

421. Fujita S, Ota E, Sasaki C, Takano K, Miyake M, Miyake J. Highly efficient reverse transfection with siRNA in multiple wells of microtiter plates. Journal of bioscience and bioengineering. 2007;104:329-33.

422. Bantounas I, Phylactou LA, Uney JB. RNA interference and the use of small interfering RNA to study gene function in mammalian systems. J Mol Endocrinol. 2004;33:545-57.

423. Boden D, Pusch O, Lee F, Tucker L, Ramratnam B. Human immunodeficiency virus type 1 escape from RNA interference. J Virol. 2003;77:11531-5.

424. Imai-Nishiya H, Mori K, Inoue M, Wakitani M, Iida S, Shitara K, et al. Double knockdown of alpha1,6-fucosyltransferase (FUT8) and GDP-mannose 4,6-dehydratase (GMD) in antibody-producing cells: a new strategy for generating fully non-fucosylated therapeutic

antibodies with enhanced ADCC. BMC biotechnology. 2007;7:84Wang W, Di X, D'Agostino RB, Jr., Torti SV, Torti FM. Excess capacity of the iron regulatory protein system. J Biol Chem. 2007;282:24650-9.

425. McIntyre GJ, Arndt AJ, Gillespie KM, Mak WM, Fanning GC. A comparison of multiple shRNA expression methods for combinatorial RNAi. Genetic vaccines and therapy. 2011;9:9.

426. Grzelinski M, Pinkenburg O, Buch T, Gold M, Stohr S, Kalwa H, et al. Critical role of G(alpha)12 and G(alpha)13 for human small cell lung cancer cell proliferation in vitro and tumor growth in vivo. Clin Cancer Res. 2010;16:1402-15.

427. Guo X, Wang W, Hu J, Feng K, Pan Y, Zhang L, et al. Lentivirus-mediated RNAi knockdown of NUPR1 inhibits human nonsmall cell lung cancer growth in vitro and in vivo. Anat Rec (Hoboken). 2012;295:2114-21.

428. Polsky D, Young AZ, Busam KJ, Alani RM. The transcriptional repressor of p16/Ink4a, Id1, is up-regulated in early melanomas. Cancer Res. 2001;61:6008-11.

429. Tang J, Gordon GM, Nickoloff BJ, Foreman KE. The helix-loop-helix protein id-1 delays onset of replicative senescence in human endothelial cells. Lab Invest. 2002;82:1073-9Suh HC, Leeanansaksiri W, Ji M, Klarmann KD, Renn K, Gooya J, et al. Id1 immortalizes hematopoietic progenitors in vitro and promotes a myeloproliferative disease in vivo. Oncogene. 2008;27:5612-23.

430. Israel MA, Hernandez MC, Florio M, Andres-Barquin PJ, Mantani A, Carter JH, et al. Id gene expression as a key mediator of tumor cell biology. Cancer Res. 1999;59:1726s-30s.

431. Ouyang XS, Wang X, Ling MT, Wong HL, Tsao SW, Wong YC. Id-1 stimulates serum independent prostate cancer cell proliferation through inactivation of p16(INK4a)/pRB pathway. Carcinogenesis. 2002;23:721-5.

432. Pillai S, Rizwani W, Li X, Rawal B, Nair S, Schell MJ, et al. ID1 facilitates the growth and metastasis of non-small cell lung cancer in response to nicotinic acetylcholine receptor and epidermal growth factor receptor signaling. Mol Cell Biol. 2011;31:3052-67.

433. Zhang L, Shi S, Zhang J, Zhou F, ten Dijke P. Wnt/beta-catenin signaling changes C2C12 myoblast proliferation and differentiation by inducing Id3 expression. Biochem Biophys Res Commun. 2012;419:83-8.

434. Phi JH, Choi SA, Lim SH, Lee J, Wang KC, Park SH, et al. ID3 contributes to cerebrospinal fluid seeding and poor prognosis in medulloblastoma. BMC Cancer. 2013;13:291.

435. Shuno Y, Tsuno NH, Okaji Y, Tsuchiya T, Sakurai D, Nishikawa T, et al. Id1/Id3 knockdown inhibits metastatic potential of pancreatic cancer. J Surg Res. 2010;161:76-82.

436. Gupta GP, Perk J, Acharyya S, de Candia P, Mittal V, Todorova-Manova K, et al. ID genes mediate tumor reinitiation during breast cancer lung metastasis. Proc Natl Acad Sci U S A. 2007;104:19506-11.

437. Morton CL, Houghton PJ. Establishment of human tumor xenografts in immunodeficient mice. Nature protocols. 2007;2:247-50.
438. Cheng YJ, Tsai JW, Hsieh KC, Yang YC, Chen YJ, Huang MS, et al. Id1 promotes lung cancer cell proliferation and tumor growth through Akt-related pathway. Cancer Lett. 2011;307:191-9.
439. Wyllie AH, Kerr JF, Currie AR. Cell death: the significance of apoptosis. International review of cytology. 1980;68:251-306.
440. Hanahan D, Weinberg RA. The hallmarks of cancer. Cell. 2000;100:57-70.
441. Kim D, Peng XC, Sun XH. Massive apoptosis of thymocytes in T-cell-deficient Id1 transgenic mice. Mol Cell Biol. 1999;19:8240-53.
442. Sato AY, Antonioli E, Tambellini R, Campos AH. ID1 inhibits USF2 and blocks TGF-beta-induced apoptosis in mesangial cells. Am J Physiol Renal Physiol. 2011;301:F1260-9Shin DH, Jang SH, Kang BC, Kim HJ, Oh SH, Kong G. Constitutive overexpression of Id-1 in mammary glands of transgenic mice results in precocious and increased formation of terminal end buds, enhanced alveologenesis, delayed involution. J Cell Physiol. 2011;226:1340-52.
443. Li W, Zhang CH, Hong YL, Li J, Hu YM, Zhao CF. Inhibitor of DNA-binding-1/inhibitor of differentiation-1 (ID-1) is implicated in various aspects of gastric cancer cell biology. Molecular biology reports. 2012;39:3009-15.
444. Gonzalez VM, Fuertes MA, Alonso C, Perez JM. Is cisplatin-induced cell death always produced by apoptosis? Molecular pharmacology. 2001;59:657-63.
445. Hoeben A, Landuyt B, Highley MS, Wildiers H, Van Oosterom AT, De Bruijn EA. Vascular endothelial growth factor and angiogenesis. Pharmacological reviews. 2004;56:549-80.
446. Lee TK, Poon RT, Yuen AP, Ling MT, Wang XH, Wong YC, et al. Regulation of angiogenesis by Id-1 through hypoxia-inducible factor-1alpha-mediated vascular endothelial growth factor up-regulation in hepatocellular carcinoma. Clin Cancer Res. 2006;12:6910-9.
447. Ling MT, Lau TC, Zhou C, Chua CW, Kwok WK, Wang Q, et al. Overexpression of Id-1 in prostate cancer cells promotes angiogenesis through the activation of vascular endothelial growth factor (VEGF). Carcinogenesis. 2005;26:1668-76Maw MK, Fujimoto J, Tamaya T. Role of inhibitor of DNA binding-1 protein is related to angiogenesis in the tumor advancement of uterine endometrial cancers. Experimental and therapeutic medicine. 2010;1:351-6.
448. Mechtcheriakova D, Wlachos A, Holzmuller H, Binder BR, Hofer E. Vascular endothelial cell growth factor-induced tissue factor expression in endothelial cells is mediated by EGR-1. Blood. 1999;93:3811-23.
449. Yang Y, Wang HC, Sun XH. Id1 induces apoptosis through inhibition of RORgammat expression. BMC immunology. 2008;9:20.

450. Kee BL. Id3 induces growth arrest and caspase-2-dependent apoptosis in B lymphocyte progenitors. J Immunol. 2005;175:4518-27.
451. Kim HJ, Chung H, Yoo YG, Kim H, Lee JY, Lee MO, et al. Inhibitor of DNA binding 1 activates vascular endothelial growth factor through enhancing the stability and activity of hypoxia-inducible factor-1alpha. Molecular cancer research : MCR. 2007;5:321-9.

APPENDIX I. RECIPES OF SOLUTIONS AND REAGENTS

Tissue culture

Complete culture medium

RPMI-1640 500ml
FCS 50ml
L-glutamine(2 mmol/l) 5ml
Penicillin and streptomycin (100 U/ml) 5ml

Trypsin/versene

Trypsin 2.5ml
Versene 100ml

Cryomedium

DMSO 1ml
Complete culture medium 9ml

Molecular cloning

RF1

Potassium chloride 7.456g
Manganese chloride 9.9g
Potassium acetate 2.94g
Calcium chloride 1.5g
Glycerol 150g
Dissolve in 1 liter distil water, adjust pH to 5.8, filter through 0.22u Nalgene.

RF2

MOPS 2.1g
Potassium chloride 0.745g
Calcium chloride 11g
Glycerol 150g
Dissolve in 1 liter distil water, adjust pH to 6.8, filter through 0.22u Nalgene.

2M Magnesium salt solution

1M Magnesium sulphate 2.465g
1M Magnesium chloride 2.033g
Distil water 10ml, filter through 0.22u Nalgene.

SOB medium

Tryptone 20g
Yeast extract 5g
Sodium chloride 0.5g
Potassium chloride 0.186g
Autoclave

2M Magnesium salt solution 10ml
Filter sterilized

SOC medium
SOB medium 4.85ml
2M Magnesium salt solution 50 µl
20% Glucose 100 µl
Filter sterilized

Agar solution preparation
In order to make agar plates containing Zeocin, X-gal, and IPTG, the following stocks should be made up, as well as L-Broth and L-Agar.
X-gal in DMSO
X-gal (40 mg/mL) 10ml
DMSO 10ml
Store at -20 ℃ in 1ml aliquots at foil wrapped tubes, use 40 µl on each plate.

100 mM IPGT
IPTG 238 mg
Sterile distilled water 10ml
Filter sterilized.
Store at -20 ℃ in 1ml aliquots, use 40 µl on each plate.

LB-Broth
Tryptone 5 g
Yeast extract 2.5 g
Sodium chloride 2.5 g
Distilled water to 500 ml
Autoclaved for 30 minutes

LB-Agar
Tryptone 5g
Yeast extract 2.5 g
Sodium chloride 2.5 g
1.5 % Agar 7.5g
Distiled water up to 500 ml.
Autoclaved for 30 minutes

DNA gel electrophoresis
EDTA(0.5M)
EDTA 46.525g
Water to 250 ml
Adjust pH to 8.0, autoclaved
TBE(10X)
Tris 108g
Boric acid 55g
0.5M EDTA 40ml

Water up to 1 liter
Autoclaved

6 × DNA loading buffer
0.5% bromophenol blue
0.5% xylene cyanol
60% glycerol in distilled water 1ml
Store at 4 ℃.

SDS gel electrophoresis
SDS-PAGE gel
12.5% NEXT GEL® 10ml
10%APS 60μl
TEMED 6μl

10%APS
APS 100mg
Distilled water up to 1ml

Running buffer
20 ×NEXT GEL® running buffer 25ml
Distilled water up to 500ml

2 × sample loading buffer
0.5M Tris-HCI pH 6.8 1.25ml
10% SDS 2ml
0.05% bromophenol blue 200μl
Glycerol 2.5ml
Distilled water 3.55ml
2-beta-mercaptoethanol 100μl/ml
(added freshly before experiment)

10% SDS
SDS 10g
Distilled water 80ml
Add distilled water to make 100ml total solution

0.5M Tris-HCI (pH 6.8)
Tris base 6g
Distilled water 60ml
Adjust pH to 6.8, add distilled water to make 100ml total solution

10 × TBS buffer
Tris base 60.55g
Sodium chloride 87.66g
Distilled water 800ml
Adjust pH to 7.5, add distilled water to make 1liter total solution

5% TBST
1 ×TBS buffer 1liter
Tween-20 0.5ml

Immunohistochemistry
10 mM Sodium Citrate Solution buffer (pH 6.0)
Tris sodium citrate (dihydrate) 29.41 g
Distilled water 10 up to liters
Adjust pH to 6.0

Tris-buffered saline with 0.05% Tween 20 (TBST, pH 7.6)
Tris base 60.72g
Sodium chloride 87.66g
Tween 20 5ml
Adjust pH to 7.6,
Distilled water 10 up to liters

APPENDIX II. LIST OF CHEMICALS AND BIOLOGICS

Abnova
Mouse anti-Id1,Id3 monoclonal antibody (WB)

Amresco
12.5% NEXT GEL
NEXT GEL running buffer

BD
BioCoat™ Matrigel™ Invasion Chamber
Extracellular matrix

Bio-RAD
Coomassie Blue

Biosera
FCS

Bios Europe
DPX synthetic resin

BioVision
Annexin V-PE detection kit

Dako
Rabbit anti-mouse HRP immunoglubolin
DAB
Anti-rabbit HRP-conjugated polymer

Fisher Scientific
Methanol
Xylene
Ethanol
Yeast extract
Tryptone

GE Healthcare
PVDF membrane
ECL

Gibco
Trypsin
Versene

InvivoGen

psiRNA-DUO vector

Kodak
Developer
Fixer
Kodak films

Life Technologies
RPMI-1640
A Silencer® Select Negative Control
Opti-MEM I Reduced Medium
Zeocin
siRNA oligonucleotide

Lonza
L-glutamine
Penicillin
Streptomycin
ProSieve colour protein marker

Mayer's
Hematoxylin

Millipore
EndoGRO reduced-serum medium
In Vitro Angiogenesis Assay Kit

NBS Biologicals
Safeview

New England BioLabs
100 × BSA
10 × buffer 2
*Acc*65I restriction enzyme
*Hin*dIII restriction enzyme
*Bbs*I restriction enzyme
T4 ligase
*Cla*I restriction enzyme
*Nde*I restriction enzyme
*Psp*1406I restriction enzyme
*Nsi*I restriction enzyme

Promega
PCR cleanup kit
Bovine serum albumin
CellTiter 96® AQueous One Solution Reagent

QIAGEN
plasmid mini-prep kit

RayBio
Human VEGF ELISA kit

Roche
X-tremeGENE siRNA Transfection Reagent
X-treme GENE HP DNA transfection reagent

Santa Cruz
Rabbit anti-Id1 polyclonal antibody (IHC)
Rabbit anti-Id3 polyclonal antibody (IHC)

Sigma
LB Agar powder
DMSO
CelLytic-M
Protein inhibitor
APS
TEMED
2-beta-mercaptoethanol
Ponceau S
Monse beta-actin monoclonal antibody
Low melting temperature agarose
Tween-20
MTT
Cisplatin
EDTA
Agarose
Protein standard
Glycerol
LB broth
SDS
Tri-sodium citrate
Tris base
Sodium chloride
Potassium chloride
Manganese chloride
Potassium acetate
Calcium chloride
MOPS
Glucose
Boric acid
Bromophenol blue

StemCell Technologies
ClonaCell-TSC

Thermo Scientific
Mouse anti-VEGF monoclonal antibody

APPENDIX III. LIST OF EQUIPMENTS

Aperio Technologies
ScanScope

BD biosciences
FACS Calibur
Syringes
Needles

Bio-Rad
Mini-PROTEAN 3
Mini Trans-Blot Electrophoretic Transfer Cell
DNA gel electrophoresis rig

BioTek
Spectrophotometer

Leica
Microtome

Nikon
Multiple-headed microscope

Nunc
Filter cap flasks
Cryotubes
Petri dishes

Oxford Optronix Gelcount
Soft agar automated scanner

Shandon
Sequenza casstte

Star Lab
Micorotubes
Pipett tips

Whatman
Filter paper

APPENDIX IX. RELEVANT PUBLICATIONS

- Chen D, Forootan SS, Gosney JR, Forootan FS, Ke Y. Increased expression of Id1 and Id3 promotes tumourigenicity by enhancing angiogenesis and suppressing apoptosis in small cell lung cancer (Preliminary accepted for publication)
- Bao ZZ, Malki MI, Forootan SS, Adamson J, Forootan FS, Chen D, Foster CS, Rudland PS, Ke Y. A novel cutaneous fatty acid-binding protein-related signaling pathway leading to malignant progression in prostate cancer cells. Genes and Cancer 2013 vol 4 pp 297-314
- Forootan FS, Forootan SS, Malki MI, Chen D, Li G, Lin K, Rudland PS, Foster CS, Ke Y. The expression of C-FABP and PPARγ and their prognostic significance in prostate cancer. International Journal of Oncology pp DOI: 10.3892/ijo.2013.2166